U.S.NRC
United States Nuclear Regulatory Commission
Protecting People and the Environment

NUREG/CR-7217
ANL-11/60

Application of Automated Analysis Software to Eddy Current Inspection Data from Steam Generator Tube Bundle Mock-up

Office of Nuclear Regulatory Research

AVAILABILITY OF REFERENCE MATERIALS IN NRC PUBLICATIONS

NRC Reference Material

As of November 1999, you may electronically access NUREG-series publications and other NRC records at NRC's Library at www.nrc.gov/reading-rm.html. Publicly released records include, to name a few, NUREG-series publications; *Federal Register* notices; applicant, licensee, and vendor documents and correspondence; NRC correspondence and internal memoranda; bulletins and information notices; inspection and investigative reports; licensee event reports; and Commission papers and their attachments.

NRC publications in the NUREG series, NRC regulations, and Title 10, "Energy," in the *Code of Federal Regulations* may also be purchased from one of these two sources.

1. **The Superintendent of Documents**
   U.S. Government Publishing Office
   Mail Stop IDCC
   Washington, DC 20402-0001
   Internet: bookstore.gpo.gov
   Telephone: (202) 512-1800
   Fax: (202) 512-2104

2. **The National Technical Information Service**
   5301 Shawnee Rd., Alexandria, VA 22312-0002
   www.ntis.gov
   1-800-553-6847 or, locally, (703) 605-6000

A single copy of each NRC draft report for comment is available free, to the extent of supply, upon written request as follows:

Address: **U.S. Nuclear Regulatory Commission**
Office of Administration
Publications Branch
Washington, DC 20555-0001
E-mail: distribution.resource@nrc.gov
Facsimile: (301) 415-2289

Some publications in the NUREG series that are posted at NRC's Web site address www.nrc.gov/reading-rm/doc-collections/nuregs are updated periodically and may differ from the last printed version. Although references to material found on a Web site bear the date the material was accessed, the material available on the date cited may subsequently be removed from the site.

Non-NRC Reference Material

Documents available from public and special technical libraries include all open literature items, such as books, journal articles, transactions, *Federal Register* notices, Federal and State legislation, and congressional reports. Such documents as theses, dissertations, foreign reports and translations, and non-NRC conference proceedings may be purchased from their sponsoring organization.

Copies of industry codes and standards used in a substantive manner in the NRC regulatory process are maintained at—

The NRC Technical Library
Two White Flint North
11545 Rockville Pike
Rockville, MD 20852-2738

These standards are available in the library for reference use by the public. Codes and standards are usually copyrighted and may be purchased from the originating organization or, if they are American National Standards, from—

American National Standards Institute
11 West 42nd Street
New York, NY 10036-8002
www.ansi.org
(212) 642-4900

Legally binding regulatory requirements are stated only in laws; NRC regulations; licenses, including technical specifications; or orders, not in NUREG-series publications. The views expressed in contractorprepared publications in this series are not necessarily those of the NRC.

The NUREG series comprises (1) technical and administrative reports and books prepared by the staff (NUREG–XXXX) or agency contractors (NUREG/CR–XXXX), (2) proceedings of conferences (NUREG/CP–XXXX), (3) reports resulting from international agreements (NUREG/IA–XXXX), (4) brochures (NUREG/BR–XXXX), and (5) compilations of legal decisions and orders of the Commission and Atomic and Safety Licensing Boards and of Directors' decisions under Section 2.206 of NRC's regulations (NUREG–0750).

U.S.NRC
United States Nuclear Regulatory Commission
Protecting People and the Environment

NUREG/CR-7217
ANL-11/60

Application of Automated Analysis Software to Eddy Current Inspection Data from Steam Generator Tube Bundle Mock-up

Manuscript Completed: January 2012
Date Published: September 2016

Prepared by:
S. Bakhtiari, W.J. Shack and T.W. Elmer
Argonne National Laboratory
Argonne, IL 60439

M. Rossi, NRC Project Manager

NRC Job Code Y6582

Office of Nuclear Regulatory Research

ABSTRACT

This report documents the results of evaluations of computerized data screening software used for analyzing eddy current data obtained during the inspection of steam generator tubes. The work was performed at Argonne National Laboratory (ANL) as part of on-going activities under the International Steam Generator Tube Integrity Program (ISG-TIP) sponsored by the U.S. Nuclear Regulatory Commission (NRC). Following the initial review of the available literature, a software-based tool widely used by industry for in-service inspection applications was acquired and used to automatically analyze bobbin probe data collected previously from the ANL-NRC steam generator tube bundle mock-up. A subset of that data was initially used to establish data screening parameters. The results of those tests were used to iteratively adjust the data screening parameters to further evaluate their influence on the detection and classification of signals. Alternative configurations of the data screening parameters for different regions of the SG mock-up were further examined. The detection probability and false call rate were evaluated to help determine the influence of selected data screening parameters on the performance of automated data analysis software. The data in each chosen configuration was sorted out using special-purpose algorithms generated at Argonne with standard spreadsheet software. The results of analyses performed on eddy current inspection data from different elevations of the SG mock-up are discussed in this report. Comparisons are made between the detection probability results based on automated analysis with that based on manual analysis of data from a previous round-robin exercise. Some general remarks are finally provided regarding advantages and limitations of conventional automated data analysis programs for in-service inspection of steam generator tubes based on bobbin probe examinations.

FOREWORD

This report documents a study conducted by Argonne National Laboratory (ANL) under contract with the U.S. Nuclear Regulatory Commission (NRC), to study licensee inspection programs that utilize automated analysis of eddy current signal data. Inspection reliability is important to properly assess the condition of steam generator tubes.

Steam generator tubes, which are a few millimeters thick, comprise the thinnest portion of the primary coolant boundary in pressurized water reactors. Therefore, regular inspection for flaws or defects is required. Eddy current analysis is the industry standard method for in-service inspection of these tubes. During an outage, hundreds or thousands of tubes may be tested by a certified inspector. Automated analysis software, which processes and evaluates eddy current data is sometimes used in combination with or in place of manual (human) analysis. However, use of this software in lieu of human inspectors may lead to difficulty in detection of new degradation modes or other issues, such as movement of physical supports during operation.

This NUREG/CR documents an evaluation of a widely used commercial software product that industry utilizes for analyzing eddy current signals. Argonne National Laboratory performed this evaluation on a mock-up steam generator tube assembly. This mock-up was constructed prior to this study and inspected with bobbin coil and motorized rotating pancake probes. The mock-up bundle contained artifacts that would be encountered in an operating steam generator, such as support structures and geometric tube variations. Hundreds of flaws were added to the bundle to simulate the types of flaws commonly observed in the field. For instance, the bundle contained corrosion deposits, dents, wear, and stress-corrosion cracks. An expert task group with members from industry, ANL, and the NRC reviewed the eddy current signals from the mock-up flaws to ensure realistic simulation of flaws found in the field.

This report documents the research findings with regard to the use of automated analysis of eddy current inspection signals. A discussion of the detection probability of automated analysis compared to those based on manual analysis of data from a previous round-robin exercise is included. This report also includes discussion regarding advantages and limitations of conventional automated data analysis programs for in-service inspection of steam generator tubes based on bobbin probe examinations. The information in this report is of value for NRC regional inspectors, because at the time of publication several US licensees are making use of these automated analysis software programs to analyze their steam generator tube inspection data.

TABLE OF CONTENTS

LIST OF FIGURES

LIST OF TABLES

EXECUTIVE SUMMARY

Automated data analysis software may be employed in field applications as a replacement for the primary, secondary, or both human analyst teams. The use of automated analysis (AA) tools can help to significantly improve the efficiency and consistency of data analysis during in-service inspection (ISI) of steam generator (SG) tubes. Reliable application of such tools that commonly employ threshold based detection and rule-based classification algorithms require access to an extensive database of representative signals encountered during field application. Optimization of the setup parameters of these tools in general is a tradeoff between detection probability and false call rate. Better understanding of the algorithms and the associated setup parameters as well as the intrinsic limitations of AA tools in general can help improve ISI reliability.

This report documents the results of evaluations of computerized data screening software used for analyzing eddy current (EC) data obtained during the inspection of SG tubes. The work was performed at Argonne National Laboratory (ANL) as part of on-going activities under the International Steam Generator Tube Integrity Program (ISG-TIP) sponsored by the U.S. Nuclear Regulatory Commission. Following the initial review of the available literature, a prominent software-based tool, the Computer Data Screening (CDS™) module of the EC data analysis software Eddynet®Suite, from Zetec Inc., was acquired and used to automatically analyze bobbin probe data collected previously from the ANL-NRC steam generator tube bundle mock-up. A subset of the mock-up data was initially used to establish data screening parameters. The results of those tests were used to iteratively adjust the data screening parameters to further evaluate their influence on the detection and classification of signals. Alternative configurations of the data screening parameters for different regions of the SG mock-up were further examined. The detection probability and false call rate were evaluated to help determine the influence of selected data screening parameters on the performance of AA software.

Bobbin probe inspection data from all elevations (free-span, tube support plate, tubesheet) of the SG mock-up were analyzed using the CDS program. Data from all free-span and TSP elevations were subsequently used for comparative probability of detection (POD) studies. Comparisons were made between the detection probability results based on automated analysis with that based on manual analysis of data from a previous round-robin exercise. Unlike the free-span and the TSP elevations, analysis of bobbin probe inspection data from the TS region was deemed unreliable due to excessive level of EC noise associated with the mechanical expansion of the tubes. It is worth noting that bobbin probe techniques are not generally considered reliable for detection and characterization of flaws in the TS region. As such, the CDS results for TS elevations of the SG mock-up were evaluated only in a qualitative manner. The data in each flaw location was sorted out using the special-purpose algorithms generated by Argonne, with standard spreadsheet software. In general, the results of analyses based on EC inspection data from the free-span and TSP elevations suggest that automated data screening tools can provide comparable or better detection capability than that achieved by manual analysis when comparatively higher false call rates are tolerated. The higher POD values by AA software were achieved through incorporation of multiple data screening setups for the same region of tubing. The results also suggest that, in comparison with other elevations of the SG mock-up, flaws near the tube-to-tubesheet region may be detected with comparable probability to other elevations but with significantly higher false call rates.

Some general remarks are also provided in this report regarding advantages and limitations of conventional automated data analysis tools used in the evaluation of SG tube bobbin probe EC data. Although AA algorithms could be optimized to provide improved detection capability over manual analysis, the possibility exists for visually discernable signals to go undetected using automated data screening tools. A number of factors that could affect the performance of conventional AA programs include inadequate or overly constrained algorithms, modification of previously qualified setup parameters, data quality issues, influence of noise (low S/N), incomplete tube coverage, incorrect identification of support structures (landmarks), and inherent limitations of a particular NDE technique. Intrinsic to the rule-based nature of expert system algorithms, the possibility of missing new or unexpected forms of degradation exists when representative signals are not included in the qualification database used for optimization of the software. As such, direct application of a generic setup provided by an examination technique specification sheet (ETSS) and qualified for particular test conditions may not be applicable for field applications. Furthermore, inclusion of manual analysis as part of the data analysis process or as oversight for automated data analysis results can help improve the detection probability of potential flaw signals with atypical probe responses. This is particularly important when AA tools are employed as replacement for both the primary and the secondary analyst team. Inclusion of manual analysis as an integral part of the ISI data analysis process can both help resolve potential discrepancies between independent AA tools and between reported redundant entries by alternative or overlapping data screening configurations of the same AA tool. Incorporation of adjustments to the measured signals by AA algorithms may also be necessary particularly when alternate repair criteria are implemented.

ACKNOWLEDGMENTS

This work was sponsored by the Office of Nuclear Regulatory Research, U.S. Nuclear Regulatory Commission (NRC), under Job Code N6582. The NRC Project Manager is M. Rossi. The authors thank K. Karwoski and E. Murphy for their useful guidance in the performance of this work. The authors also wish to acknowledge C. Mathison (Zetec, Inc.) for providing technical support and C. Smith (EPRI), for providing helpful suggestions. The staff at Zetec is also thanked for their assistance and valuable comments.

ABBREVIATIONS AND ACRONYMS

AA	automated analysis
ANL	Argonne National Laboratory
AAPDD	automated analysis performance demonstration database
ASME	American Society of Mechanical Engineers
BC	bobbin coil
CDS	Computer Data Screening
EC	eddy current
EDM	electro-discharge machine
EPRI	Electric Power Research Institute
ETSS	examination technique specification sheet
FBH	flat-bottom hole
ID	inner diameter
IDSCC	inner diameter stress corrosion crack/cracking
IGA	intergranular attack
ISG-TIP	International Steam Generator Tube Integrity Program
ISI	in-service inspection
NDE	nondestructive examination/evaluation
NRC	U.S. Nuclear Regulatory Commission
OD	outer diameter
ODSCC	outer-diameter stress corrosion crack/cracking
POD	probability of detection
POPCD	probability of prior cycle detection
PTW	percent throughwall
ROI	region of interest
RR	round robin
SCC	stress corrosion crack/cracking
SG	steam generator
S/N	signal-to-noise ratio
SSPD	site-specific performance demonstration
TS	tubesheet
TSP	tube support plate
TTS	top of the tube sheet
TW	throughwall

1 INTRODUCTION

Manual analysis of multi-frequency EC inspection data collected during shutdown periods is a challenging and laborious process. Computerized data analysis tools have been routinely employed during SG ISI to help improve the process efficiency and the reliability of data analysis. Since bobbin probe examinations have historically served as the primary EC inspection method for full-length examination of SG tubes, software development in this area has revolved mostly around automated analysis of data acquired with bobbin probes.

Computerized or AA software has been employed as replacement for the primary analyst, the secondary analyst, or both. Initial adjustment of variables that determine the performance of AA tools is performed by a skilled analyst familiar with the software. Depending on the extent of examinations and the types of degradation mechanisms of concern, the complexity of data screening setups can vary significantly among different sites. Intrinsic to the rule-based nature of the majority of such algorithms, variable settings are applicable to a specific set of test conditions. Readjustment of the variables may be necessary if the test conditions vary. The degree of conservatism in setting the data screening variables determines the probability of detection and in turn the number of false calls.

The primary objective of this work was to assess the capability of conventional automated EC data analysis tools used in the review of SG tube EC inspection data. The efforts were carried out as part of on-going activities under the ISG-TIP sponsored by the NRC. Initial studies at ANL focused on gaining a better understanding of the important features of such algorithms including the critical parameters for detecting and classifying a wide range of degradation and non-degradation signals. Subsequently, a commercially prominent data screening software was acquired. Vendor-supplied information and other accessible literature on this subject were reviewed. The software was first tested on representative EC inspection data collected with a bobbin probe from the ANL-NRC SG tube bundle mock-up containing tubes with primarily laboratory-produced flaws (a small number contained machined flaws). These initial tests helped determine the proper setting of variables for screening of data at different locations (elevations) and for different flaw types present in the SG mock-up. Following optimization of the data screening parameters, the software was used to evaluate all of the EC inspection data from the mock-up. The effect of changing the screening parameters on the detection and classification of indications in the SG mock-up was examined. Their influence on detection as a function of flaw type and location was also evaluated.

In the subsequent sections, a general description of AA tools used for SG ISI applications is provided. The basic structure of common data screening software including the type of algorithms and test logic is first described. The design of the SG tube bundle mock-up and the type of flaws present is then provided. Application of commercial AA software to bobbin probe data collected from the SG mock-up is subsequently described. The results of comparative assessments on the effect of setup parameters and screening configurations on POD are presented. Finally, some general remarks are provided regarding the results of studies as well as a discussion on advantages and limitations of automated data analysis tools.

2 AUTOMATED DATA ANALYSIS TOOLS FOR STEAM GENERATOR TUBE EXAMINATIONS

Analysis of eddy current inspection data has traditionally been performed in a manual fashion by teams of qualified analysts. Software-based tools for automatic analysis of EC examination data from SG tubes have been in use since the early 1980s and have helped to speed up the analysis process for the large amount of data collected during an ISI. Since bobbin probe inspections have historically served as the primary nondestructive examination (NDE) method for the full-length examination of SG tubing, software development in this area has predominantly revolved around tools for data acquired with bobbin probes. Computerized or automated analysis software has been used in the field as replacement for the primary analyst, the secondary analyst, or both. Initial adjustment of variables that determine the performance of AA tools is performed by a skilled analyst familiar with the software. Depending on the extent of examinations and the types of degradation mechanisms of concern, the complexity of data screening setups can vary significantly among different sites. Intrinsic to the rule-based nature of the majority of such algorithms, the data screening parameters are established for a specific set of test conditions. As such, readjustment of the variables may be necessary if the test conditions vary. The degree of conservatism used in setting the data screening variables influences the probability of detection and in turn the number of false calls (overcall rate). Among other factors, the number of overcalls is also dependent on the type of damage or degradation and its location in the SG.

Automated data analysis software for SG tube examinations are provided by a number of vendors in the U.S. including AREVA (US-AIDA™), Corestar (AutoVISION™), Westinghouse (ADS™), and Zetec (CDS™). An AA module is typically available as an integrated feature of a commercial software package, which commonly includes data acquisition, analysis, and management components. Depending on the vendor, the software product may run under the Windows or the HP-UX operating system. Because of the significant improvements in capabilities of personal computers, the general trend on the preferred environment for future software development is toward the Windows operating system. Software development in this area has focused primarily on the processing of data acquired with bobbin probes. Conventional AA tools can be broadly categorized as expert system algorithms employing amplitude threshold schemes and rule-based logic to detect and classify signals. Differences among such tools may be associated with the EC signal features used by the detection and identification algorithms and the number of steps applied for classifying discontinuities at different elevations within the SG. Options are typically provided to operate in an interactive or in a fully automated mode. In the latter mode of operation, the AA software automatically performs the analysis and the final results are generated without human intervention. In the interactive mode, recorded signals by the AA software may be reviewed during the process and the results may be reviewed by a human analyst prior to their final acceptance.

Detection and classification of EC signals by AA algorithms is done using a combination of threshold-based routines and rule-based algorithms (logic statements) that partly emulate the process followed by a human data analyst for interpreting EC probe response. Automatic calibration of data is often recommended to help ensure consistency of the analysis results. Pre-defined landmark tables specific to each particular SG design are used to automatically locate different regions of the SG that may then be screened for known degradation or non-degradation modes of interest. The landmark table maps the expected location of tube support structures and transitions to the position of their associated signals in EC data. A low-frequency

channel with strong probe response from extraneous discontinuities is commonly employed by landmark detection algorithms to locate the position of support structures and transitions. The probe speed and digitization rate are used to locate the approximate location of a known landmark. More accurate positional information is determined through application of a series of rules and thresholds by landmark detection algorithms. Adjustment of detection variables is often necessary for proper identification of all landmarks.

A series of signal preprocessing routines (filters) are first applied to data from specific analysis channels to help suppress unwanted signals and in turn improve the signal-to-noise ratio (S/N). The initial detection of signals of potential interest is commonly based on an amplitude (voltage) threshold criterion. Depending on the expected signal characteristics at a particular test frequency and probe excitation mode, different peak detection algorithms may be selected to identify the signals of interest. Detected signals above a user-defined threshold are marked for further evaluation. Subsequently, signals that conform to a set of predetermined criteria (rules) for a particular mode of degradation are classified accordingly. The final classification may be based on satisfying one or a number of criteria that are sequentially tested on a signal. The expert system rules for characterizing signals could vary significantly depending on the complexity of the signal and its location in the SG.

A number of measurement options are thus provided to deal with differences in probe response at different test frequencies. A fixed or a variable measurement window length can be chosen, depending on the expected probe response to a flaw at a particular location in the SG. Signal features such as the expected range in variation of phase angle and its impedance plane response that are captured by the prescribed measurement type are used as the main criteria for classifying signals. In certain cases a nested series of conditions have to be met before an indication is positively identified. The degree of conservatism in setting up the rules is application dependent and could be site-specific. The extent and complexity of computerized data screening settings for detection and classification of EC indications often follows a parallel path as that used for manual analysis of data, which depends on the SG operating history and in turn on degradation and non-degradation mechanisms of potential concern. As such, the level of EC noise present in a particular SG will have a direct influence on the adjustment of data screening parameters.

Field experience with automated data analysis tools over the years has demonstrated that they can provide comparable or better detection performance to that achieved by manual analysis of EC inspection data. In theory, the detection sensitivity of AA software may be adjusted to flag low-amplitude signals that may not be readily detectable by manual analysis. However, the tradeoff for improving the POD is an increase in the number of false calls. Another limitation of conventional AA tools used in evaluating data collected with the bobbin probe is associated with the detection capability of the probe itself. The underlying assumption for all rule-based algorithms is that the signal characteristics associated with a particular mode of degradation is relatively well defined. This may not always hold true particularly in presence of high levels of noise and interfering signals from extraneous discontinuities. Furthermore, while there is no minimum amplitude threshold for reporting of flaw-like signals during manual analysis of ISI data, reporting of signals by AA algorithms is dependent on a globally applied minimum threshold. Thus, the possibility exists that visually discernible signals which do not conform to the characteristic probe response from a particular flaw type could go undetected when the data is analyzed in an automated manner. Finally, it is worth noting that analyst expertise in setting up the AA algorithms for site-specific applications will influence the performance of the software.

Performance demonstration requirements for automated data analysis tools are defined by the EPRI PWR steam generator examination guidelines **(Ref. 1)**. Generic qualification of AA software products is based on the automated analysis performance demonstration database (AAPDD). The type of damage mechanisms included in the AAPDD is listed in the Appendix G of the EPRI guidelines. Appendix G also defines the procedure for demonstrating the performance capability of AA software for site-specific performance demonstration (SSPD) applications. The types of damage mechanisms included in the database used for qualification of AA software are similar to those used for qualification of human analyst. The initial qualification using AAPDD is done to demonstrate the capability of AA software to detect and characterize (i.e., classification and sizing) known types of damage mechanisms. The generic qualification on the AAPDD is commonly performed by the software vendor. Acceptable performance demonstration of AA software involves achieving a minimum POD of 80 percent at a 90 percent confidence level for all flaw categories included in the AAPDD. The number of false calls, while recorded, does not influence the generic qualification process. Acceptability of the number of false calls by a particular AA algorithm may be taken into consideration on a site-specific basis. Analogous to training and testing of a human analyst, the dataset used for site-specific qualification of AA software is expected to include a sufficient number of plant-specific signals associated with active and potentially latent degradation mechanisms. Accordingly, information about the SG design and operating history for a particular site as well as that from similar plants is included in the SSPD for qualification of AA software. Automated analysis software that satisfies both AAPDD and SSPD requirements may then be implemented in the field. Performance demonstration may not be required for application of AA software to detect signals associated with non-degradation mechanisms such as tube deformations and deposits. According to the EPRI guidelines for automated data analysis, independent software systems should be used when AA tools are employed as replacement for both the primary and the secondary analyst teams. Independence in this context refers to the type of algorithms incorporated into the software for detecting and characterizing signals. As noted in the EPRI guidelines, AA software products from different vendors that employ similar detection algorithms may not be considered as independent systems. It is also recommended by the EPRI guidelines for AA that the signal characterization from the AA systems be manually reviewed by at least one human analyst team to verify proper operation of the data analysis algorithms.

Following the performance demonstration process, a qualified examination technique specification sheet (ETSS) may be implemented during the ISI at a particular site. The number of applicable ETSSs depends on the number of active and potential degradation and non-degradation mechanisms in the SGs at that site. The ETSS document applicable to the site-qualified AA software commonly provides instructions for setting up and analyzing EC inspection data. This includes information about the calibration procedure (manual or automatic), location of SG support structures (landmarks), mode of analysis (interactive or fully automated), manual review procedure, reporting requirements, and applicable AA algorithms for screening of data from different SG elevations. The setup parameters are also provided in the ETSS for each data screening algorithm and include the threshold values and test logic for locating, detecting, and characterizing signals associated with each degradation and non-degradation mechanism of interest. To assist with implementation of AA tools, drawings are commonly included in the site-specific data analysis guidelines that identify the SG regions covered by each data screening setup. While supplementary NDE techniques are used in regions of the SG tube where bobbin probe examinations are not qualified, AA algorithms for bobbin probe data are typically set to provide complete coverage of the entire tube length. Identification of landmarks is the first stage of AA process and is critical to proper operation of

the software. Data is analyzed manually when all the landmarks for a tube cannot be automatically located. Setting up the site-qualified AA software configurations for implementation at a particular plant is commonly carried out by a designated EC analyst. The same analyst may also be responsible for verifying, and if necessary validating (through SSPD), of any modifications made to the data screening configurations. Modifications made to the AA data screening configurations needs to be reviewed and approved by an independent qualified data analyst to conform to SSPD requirements.

Improving the efficiency and reliability of computerized data analysis tools has been an active area of research and development during the past two decades. Improving the performance of data analysis results has been a major focus of the emerging AA software. More accurate characterization of flaw signals is also of great importance. Availability of automated data analysis tools is particularly important for more widespread deployment of array probe technology. In view of limitations with computational resources, employment of more computationally efficient AA algorithms is necessary to extract information from the large amount of NDE data collected from full-length examination of SG tubes with array probes. A viable approach for improving the effectiveness of bobbin probe AA software is to incorporate information from complementary EC examination techniques. Versatile AA algorithms that include the review of EC inspection data from different probe types could help increase the POD and the accuracy in classifying indications in SG tubes. Emerging AA software packages employ more elaborate signal processing and data analysis algorithms which could help improve the performance of AA systems. The use of advanced filtering schemes can help increase the POD while keeping the number of false calls to an acceptable level. Such filters can provide significant improvement in S/N in certain cases, thus improving the capability to detect difficult signals. Incorporation of enhanced feature extraction and classification algorithms could help better discriminate between flaw signals and inconsequential signals. Modern AA software tools are expected to employ more reliable automatic file recognition and tracking capabilities, thus helping to reduce the possibility of unintentional errors caused by human intervention. The performance of the AA software products being developed by the industry will ultimately be determined through field trials following their qualification in accordance with the EPRI guidelines.

In the following section, a description of the SG tube bundle mock-up design and the type of flaws present in the mock-up is provided. In the succeeding section, application of a commercially available automated data screening tool to EC inspection data from the SG mock-up is provided. The initial generic setups and the tests carried out to optimize AA screening configurations on a subset of tubes from the available database are first presented. The results on the application of the AA software to all the EC inspection data from the SG tube bundle mockup are subsequently discussed.

3 STEAM GENERATOR TUBE BUNDLE MOCK-UP

Eddy current bobbin probe inspection data collected previously from the SG tube bundle mock-up at Argonne was used to assess the capability of conventional AA software. As will be discussed in the following section, AA tools employ location-dependent data analysis algorithms. Correct identification of landmarks (hot/cold leg tube ends, tube support structures, dimensional/geometry transitions, etc.) in a particular SG design is therefore critical to their proper operation. A detailed description of the SG mock-up design and the types of flaws present in the tubes is provided in other reports **(Refs. 2, 3)**. For the purpose of completeness, a brief description of the tube bundle mockup is again presented here.

A schematic drawing of the SG tube bundle mockup is shown in Fig. 3.1. It consists of 400 full-length straight tubes which include multiple test sections each. The test sections are Alloy 600 tubing material with nominal 22.2-mm (0.875-in.) diameter and 1.27-mm (0.05-in.) wall thickness. Each full-length tube consists of 9 test sections, each 0.3 m (12 in.) long and a 0.91-m (36-in.)-long probe run-out section at the top. The test sections are denoted as level A through I in Fig. 3.1. The center-to-center spacing of the tubes is 3.25 cm (1.28 in.). Tube sections are butted end-to-end to form a continuous tube, held together by 19-mm (0.75-in)-thick high-density polyethylene plates. The lowest level (A) in the mock-up simulates the tube-sheet (TS) section with the tubes being fully expanded inside a 30.5-cm (6-in.) -long carbon steel-collar. A few tubes in the TS level are only partially expanded. Levels 4 (D), 7 (G), and 9 (I) simulate drilled hole tube support plate (TSP) intersections. The TSPs are 19-mm (0.75-in.) -thick carbon-steel plates. The other five levels (B, C, E, F and H) of the mock-up simulate SG tube free-span regions.

The majority of test sections in the SG mock-up contain laboratory-produced flaws. A small number of test sections contain machined flaws (EDM notches and laser-cut slots). The distribution of flaw types present in the mock-up is provided in Table 3.1 **(Ref. 2)**. The flaw types include intergranular attack (IGA), outer-diameter stress corrosion cracking (ODSCC), primary-water or inner-diameter stress corrosion cracking (PWSCC), wear/wastage, fatigue, and machined flaws. The TSP sections of the mock-up contain stress corrosion cracks (SCCs) of both OD and ID origin. Cracks in the TSP region may be associated with dents. Dents were also produced in flaw-free tube sections. The crevice region of some TSP intersections is covered with magnetic tape or a ferromagnetic fluid to simulate magnetite deposits. Axial and circumferential outer diameter (OD) and inner diameter (ID) SCCs were produced for the TS expansion transition region. In some elevations, a mixture of magnetite and copper bonded with epoxy simulating sludge deposits was placed above the expansion transition region and TSP intersection. Simulated deposits were also placed at a number flaw-free tube sections. Flaws in the free-span regions are mostly axial ODSCC, both planar and segmented. A small number of other flaw types such as IGA and wear were also placed in various locations in the tube bundle.

In reference to Table 3.1, the depths of flaws in the mock-up are distributed into three ranges, 0–50 percent throughwall (PTW), 51–80 PTW, and 81–100 PTW with the distribution intentionally skewed toward deeper flaws **(Ref. 2)**. This distribution is expected to increase confidence in the POD values for deep flaws. Also, the mock-up contains short sections of discontinuous tubes. The EC probe response from tube-end discontinuities resembles the signal from a through-wall 360° circumferential notch. The use of short tube sections was necessary to generate realistic flaws and to further allow reconfiguration of the tube bundle as

needed. As will be noted in the following section, the large EC probe response from discontinuities in the mock-up that are not representative of those observed in the field could create a challenge when data is to be analyzed in an automated manner.

The EC inspection data from the mock-up were collected with magnetically biased ("mag-biased") bobbin probes. Magnetically biased probes were used so that the signals from sensitized and non-sensitized test sections would have similar EC responses. Because of the wider use of non–magbiased probes in the field, equivalency was demonstrated between the two probe types.

A detailed description of the EC data acquisition parameters for examination of tubes in the mock-up is presented in Ref. 2. The ETSS for acquisition with a bobbin probe is also provided in that report. In summary, bobbin probe inspection data were taken at 400, 200, 100, and 20 kHz in both differential and absolute mode. Data were collected on the pull with a probe speed of ~53 cm/s (21 in./s) and a digitization rate of 800 samples/s, thus maintaining a sampling rate of around 15 samples/cm (38 samples/in). Data were calibrated using an ASME standard with 100, 80, 60, 40 and 20 PTW flat-bottom holes, and a 10 PTW OD and a 20 PTW ID circumferential groove. A 1.9-cm (0.75-in.) carbon steel collar on the calibration standard was used for simulating the probe response from TSPs. Calibration of amplitude was based on setting the peak-to-peak voltage reading at 400 kHz primary test channel to 4.0v and normalized to all other channels. The phase angle for all test channels was set to 40 degrees. The phase angle rotation for the 20 kHz locator channel was set so that the probe response from the TSP was at 270°. In accordance with the site-qualified ETSS, three process channels were additionally generated. The process channels consisted of 400|100 kHz differential TSP suppression mix (P1), 400|100 kHz absolute TSP suppression mix (P2), and 200|400|100 kHz differential TTS expansion mix (P3). The three-frequency mix (Eddynet™ "turbo mix") was implemented for suppressing the probe response from TSP and TTS expansion transition. Phase-based calibration curves were also generated using as-built dimensions of the 100, 60, and 20 PTW holes to estimate flaw depths.

Table 3.1 Distribution of flaw types in the SG tube bundle mock-up.

Max. Depth Range (PTW)	EDM & Laser-cut Slots	IGA	ODSCC @ TS	ODSCC @ TSP	ODSCC @ Free–span	PWSCC @ TS	PWSCC @TSP	PWSCC @ Free–span	Wear/ Wastage	Fatigue
0–50	7	2	3	14	15	4	8	1	6	0
51–80	13	9	2	14	26	8	16	0	6	0
81–100	1	2	16	41	49	35	7	3	0	3

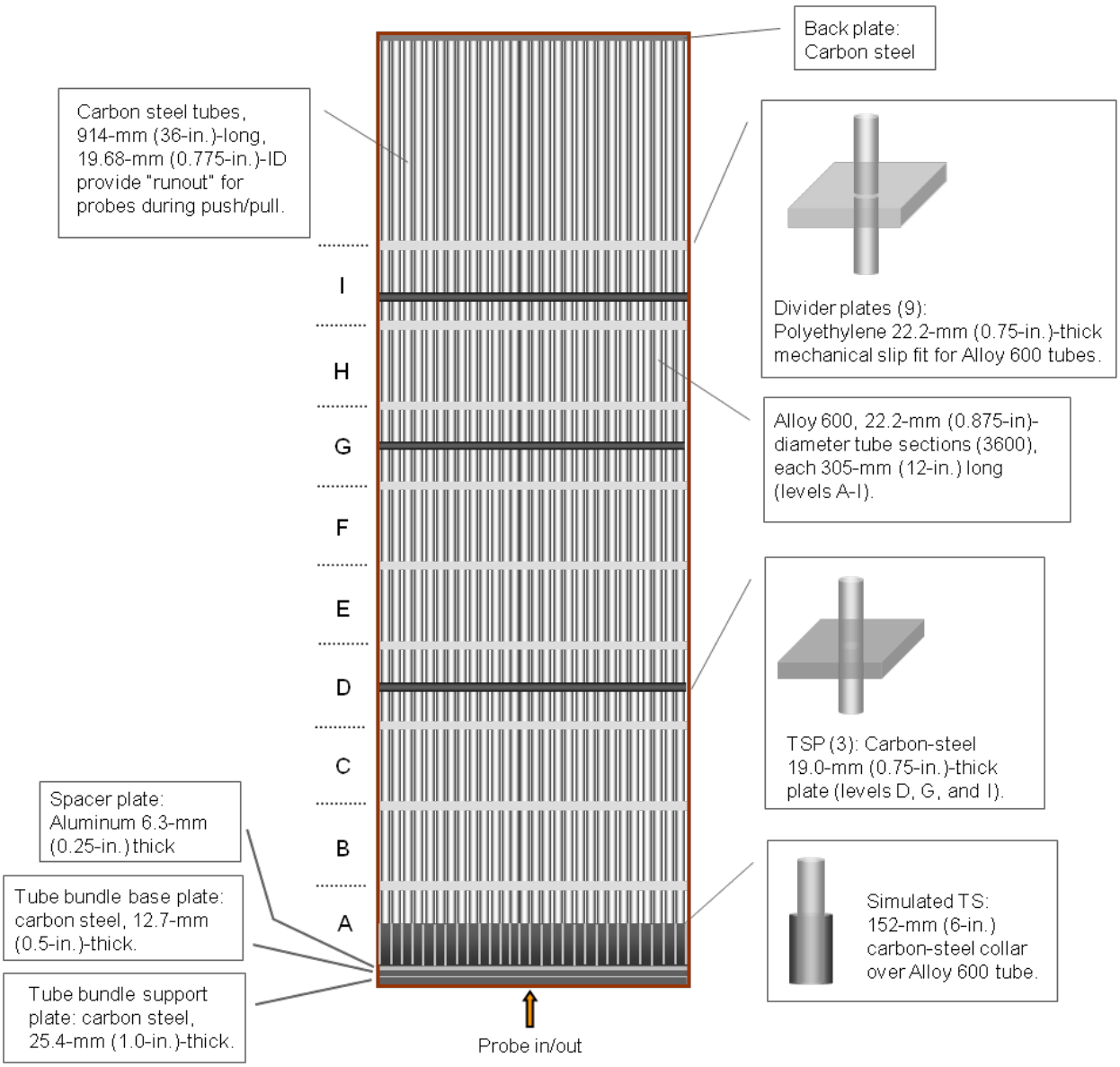

Figure 3.1 Schematic drawing of the SG tube bundle mock-up.

4 APPLICATION OF COMPUTERIZED DATA SCREENING TO SG TUBE BUNDLE MOCK-UP

Following the initial review of the literature on conventional automated data analysis tools for SG tube examinations, a prominent AA tool that is routinely employed for ISI applications was selected for the planned studies at Argonne. The latest version of the commercially available EC data analysis software Eddynet®Suite, from Zetec Inc., was acquired and installed on a HP-UX workstation. The software package provides various tools for manual analysis and automatic screening of EC inspection data including the Computer Data Screening (CDS™) module. Bobbin probe inspection data collected previously from the SG tube bundle mock-up was used for all the tests conducted in this work. Data from a subset of tubes in the training data set from the NDE round-robin exercise was initially used to set the data screening parameters for detecting and classifying the type of flaws present in the mock-up. Following optimization of the setup parameters for a number of location-specific algorithms using the entire training data set, CDS was used to analyze the EC inspection data for all the test sections in the mock-up.

In the following sections, a general description of the AA software used in the studies is presented. The main components of the software including algorithms for locating, detecting, and classifying signals are briefly described. The results of the initial performance evaluations of the algorithms using generic setups and their subsequent optimization for generating a set of mock-up-specific data screening configurations are then discussed. Subsequently, the results from application of the optimized CDS configurations to bobbin probe inspection data from the entire SG mock-up are presented.

4.1 Basic Structure of Computer Data Screening (CDS) Tool

The CDS program is comprised of a number of algorithms that employ threshold-based schemes and rule-based test logic to detect and classify EC signals. A general overview of the main components of the CDS is presented here. A detailed description of the CDS software with a complete list of embedded algorithms and the associated setup parameters is provided elsewhere **(Ref. 4)**.

The CDS module of the Zetec Eddynet™ data analysis software can be accessed through a user interface window which allows implementation of a wide range of user-defined screening criteria for automatic processing of EC data collected with bobbin probes. As noted in Ref. 4, CDS does not independently evaluate EC inspection data. Rather, data screening criteria are based specifically on user-defined parameters and acceptance criteria. Single or multiple data screening configurations (“sorts”) can be developed to analyze data from various regions of the SG tubing. The parameters of a sort for a particular region along the tube include the algorithms and test logic for locating, detecting, and classifying EC signals. A signal is reported when it meets all the prescribed criteria defined by that sort.

Conventional automated data analysis tools commonly employ location-dependent algorithms to identify signals. Proper operation of such AA tools is therefore dependent on the availability of a landmark table with accurate information about known structures in a particular SG. Landmark tables for a number of standard SG designs with default positional information for tube support structures and transitions are provided under the Eddynet™ environment. Modifications may be made to those tables as necessary for application to modified SG designs. Development of the

landmark table for the SG tube bundle mock-up and the use of the table for identifying mock-up specific structures and discontinuities are discussed in the next section.

Three different modes of operation are available for running CDS. In the two interactive modes, the process is halted each time a signal is detected along a tube or after the data over the entire length of a tube is processed. In the automated mode, unless a discrepancy causes the process to abort, the process will terminate once all the tubes in the current directory (calibration group) have been analyzed. The analysis results will be sequentially entered into the *Report Editor* file after completing the process for each tube. The reported information for signals that meet the data screening criteria typically includes the tube (row and column), voltage, phase, depth, reporting channel, flaw location (with respect to nearest landmark), classification code, analyst identifier code, and data file name.

The user-defined input parameters for a sort configuration in the CDS editor window are associated with *region*, *location*, *detection*, and *classification* setups. Under the *region* menu one defines the positional information for the length of SG tube to be examined and a list of sorts to be applied to selected regions over that length. The positional input parameters must be consistent with the labeling and the relative locations listed in the landmark table. Multiple sort configurations may be generated under each *region* menu. Multiple *regions* with separate set of sorts may also be created. The *location* parameters define the range for the regions of interest where the detection and classification processes will be applied. It is worth noting that the sorts under the *region* menu use *OR* logic while the detection and classification stages use *AND* logic. This simply implies that a signal will be reported if it meets the criteria set by any one of the sort configurations defined under *region* menu. A signal must, however, meet all the criteria set under the *detection* and the *classification* test logic to be reported.

The *detection* setup parameters include measurement channel (test frequency), measurement type, detection algorithm, measurement window size, and amplitude threshold values. Selection of the measurement channel for detection will depend on the region of SG tube (free-span, TSP, TS, TTS, etc.) to be screened by the sort. Qualified test frequencies are commonly defined in the applicable ETSS. The measurement type can be based on the vertical component of the signal, the horizontal component of the signal, or both. A class of peak detection algorithms is available under the *detection* algorithm menu. Selection of an appropriate detection algorithm depends on the region of interest defined by the sort and the expected EC signal characteristics for the degradation or non-degradation mode of concern. Detection of a potential signal may be based on simple amplitude threshold schemes or based on more elaborate peak detection schemes. For example, a commonly used algorithm, *Filtered Peaks*, detects the maximum value of the signal away from the null value and identifies that as a true peak when the impedance plane trajectory predictably traverses across two quadrants. The algorithm applies a cross-correlation filter to the data from the measurement channel in order to minimize the influence of unwanted signals. Detected signals that fall within the lower and upper limit of the prescribed amplitude (voltage) threshold will be kept for subsequent processing by the classification test logic.

The *classification* setup parameters include measurement channel, test channel, measurement algorithm, measurement window size, amplitude threshold values, phase angle window, and depth range. The measurement channel for classification is the channel used for initial measurement of signals passed on from the previous detection stage. The test channel is subsequently used for the evaluation of classification test logic using the measurement points

on the signal obtained by the measurement channel. When activated, the test channel is used for reporting of the signals that satisfy the classification test logic. Selection of the optimum measurement and test frequency once again depends on the region of interest defined by the sort and the expected EC signal characteristics for the degradation or non-degradation mode of concern. As with the detection stage, qualified measurement and test channels are commonly defined by the applicable ETSSs. The same channel may be also used for both measurement and testing. A class of measurement algorithms is available for examination of signals by the classification test logic. Classification measurement algorithms may simply locate the peak-to-peak points on a signal or employ more elaborate schemes. For example, a commonly used algorithm, *Transition Amplitude Volts Peak-To-Peak*, is employed when closely spaced signals need to be identified individually. To identify a signal, the algorithm searches over the transition regions on both sides of the peak position and stops when the signal amplitude no longer varies. The window size, when applicable, determines the number of data points to search around the peak position of the signal by the classification measurement algorithm. Once the signal is identified, amplitude threshold, phase angle window, and depth range conditions defined in each classification logic line are used to ultimately accept or reject the signal. Any number of classification logic lines may be created for sequential application to the data. A signal will be reported by CDS if it satisfies the acceptance criteria set by all the classification logic lines. It is worth noting that more elaborate classification test logic with a larger number of data screening parameters normally translates to more stringent criteria for reporting of potential signals and in turn results in a lower number of false calls.

4.2 Implementation of Generic Setups for Performance Evaluations

Initial studies on the application of CDS to bobbin probe inspection data from the SG tube bundle mock-up were associated with the examination of different setup parameters for detection and classification of flaws. The setup parameters include those for locating, detecting, and classifying different degradation and non-degradation types of interest. A general description of those parameters was provided in the previous section. As noted earlier, because CDS employs location-dependent algorithms, proper identification of SG structures (tube ends, TSP, TTS, etc.) through a *Landmarks Table* is vital to the operation of the program. As a prerequisite to the application of CDS, a landmark table for the SG mock-up was first created. A series of generic data screening configurations were initially used to review the EC bobbin probe data from a subset of SG mock-up tubes. The results of those studies are discussed below.

A description of the SG tube bundle mock-up design and the type of degradation and artifacts present in the mock-up was discussed in Sec. 3. As noted earlier, each full-length tube in the mock-up is made up of nine 12-in. sections that are butted end-to-end to form a continuous tube. The lowest elevation simulates the TS section with each tube fitted with a 6-in. carbon-steel collar. Also present are drilled carbon-steel tube support plates at three different elevations in the mock-up. The mock-up does not conform to any standard SG design, so generic files in the available list of landmark tables under the Eddynet™ environment could not be used. Additionally, the spacing between the tube end sections, resembling a 360°, 100 PTW notch, generates large flaw-like signals that must be taken into account during automatic screening of data.

A mock-up-specific landmark table was generated at Argonne for automatic identification of structures and discontinuities at different SG mock-up elevations. To allow CDS to bypass flaw-

like signals associated with the tube end sections, a number of approaches including separate region designation for each tube section were examined. Ultimately, the approach taken was to label the intersections as one type of landmark. The landmark table (in inches) generated for the mock-up is shown in Fig. 4.1, with the labels denoting the bottom tube end (TEH), TTS (TSH), three TSP levels (01H, 02H, and 03H), and nine tube-end sections (TE1-TE9). The three-letter codes for the type of landmark being used were selected from the available list of standard landmark types. Also provided in that table is the location (elevation) of each landmark in inches with respect to the lower tube end. The *Locating Selectables* dialog box was next used to adjust the detection parameters associated with the landmark labels. Figure 4.2(a) displays the setup variables in that window, which includes the locator type, detection channel, probe speed, and threshold values for the signals from the different support structures. A number of *Locator* algorithms are available for detecting and identifying extraneous structures. Depending on the *Locator* type, either amplitude or phase of the signal may be used to identify support structures. The probe speed is also used by certain locator algorithms. Other important setup parameters include the search limits (in number of data points) around the pre-defined landmark positions and, when applicable, the threshold values for detecting signals from different types of structures. Selection of the optimum algorithm is mainly dependent on the EC probe response from the type of structures present in a particular SG, which in turn influences the selection of *Landmark Channel* (locator channel/frequency). Although any absolute or differential channel may be used for locating landmarks, the most viable frequency is typically the lowest test frequency that generates a large probe response from extraneous discontinuities and has low sensitivity to flaws within the tube wall.

Different *Locator* types were examined for automatic identification of landmarks in the mock-up. A type-5 *Locator* which employs a threshold-based algorithm for detection of intersections was eventually used. The 20 kHz absolute channel was selected as the *Landmark Channel*. It is worth noting that attaining an optimal set of threshold values for the entire data set is typically a recursive process that requires inclusion of data files that represent the possible range of variation in probe response from each landmark. Validity of the setup parameters for detection and identification of landmarks may also be examined more closely using the *Landmark Location Output* window shown in Fig. 4.2(b), which lists the landmark locations identified by the *Locator* algorithm and their positional deviations from the nominal values listed in the *Landmarks Table*. Application of the automatic landmark detection algorithm to bobbin probe data from a representative SG mock-up tube is shown in Fig. 4.3. The automatically added labels representing landmarks identified along the tube length are displayed in the landmark column on the left hand side of the analysis window. All the discontinuities and support structures in this case were correctly detected and labeled.

It should be noted that threshold-based automatic landmark detection algorithms may not always correctly identify all the landmarks in a tube. In addition to such factors as tubing anomalies, variability in the geometry of interfaces between tube sections and in turn the probe response from those locations could necessitate occasional variable adjustments to ensure proper landmark detection. In those cases, either the detection thresholds may need to be adjusted or the landmarks may have to be placed manually. Other minor variable adjustments performed later for the SG mock-up included the number of points that determine the zone for each landmark; i.e., lead/lag (+/-), which is made in the *Locating Selectables* dialog box. Although this adjustment did not influence the results of analysis with regard to detection and classification of signals, it resulted in a more accurate reporting of the positional information for signals located in close proximity to the support plates.

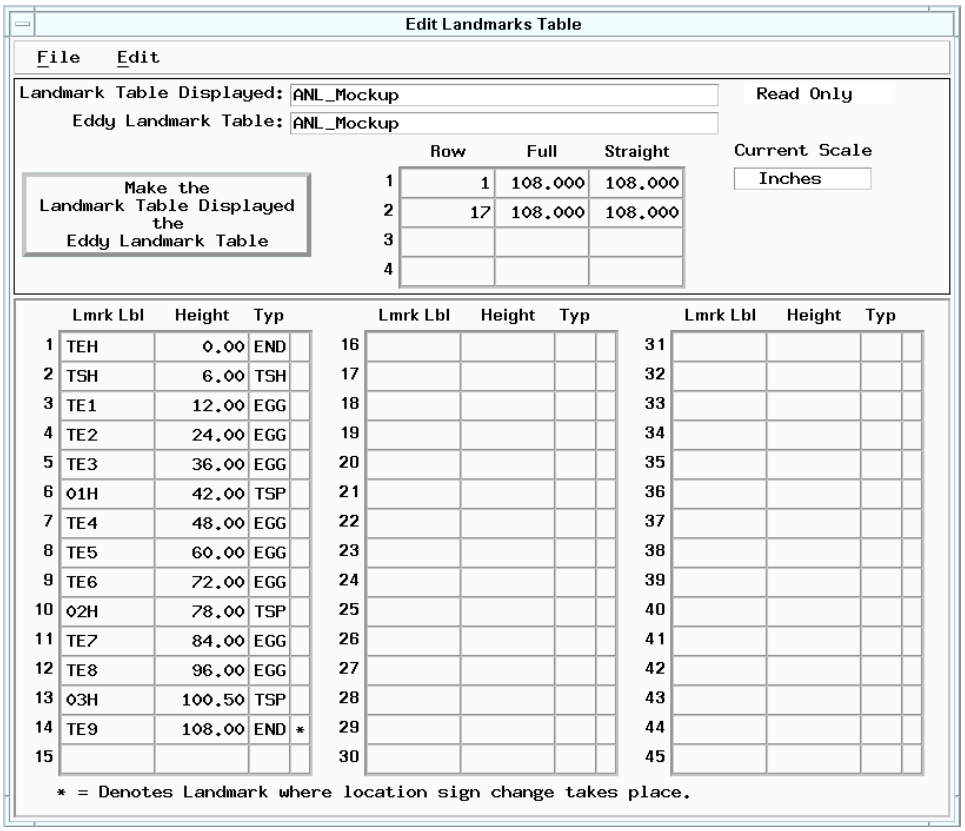

Figure 4.1 Display of *Landmark Table* generated for identification of discontinuities and structures in the tube bundle mock-up.

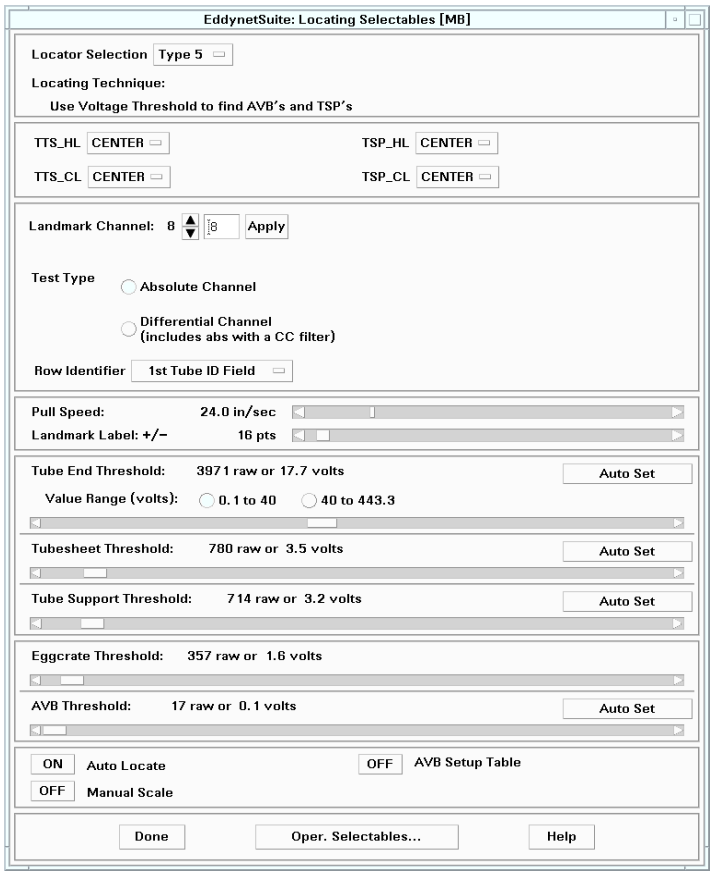

(a)

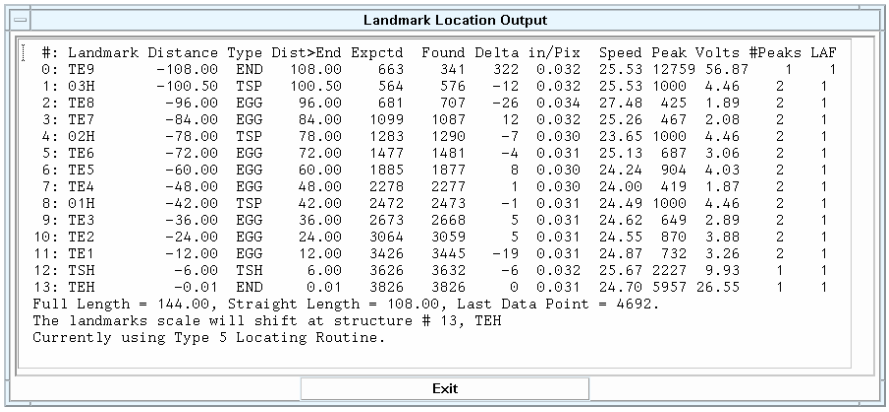

(b)

Figure 4.2 Display of setup parameters from (a) *Locating Selectables* dialog box used for the adjustment of landmark detection parameters, and (b) *Landmark Location Output* window for more detailed examination of the locating parameters.

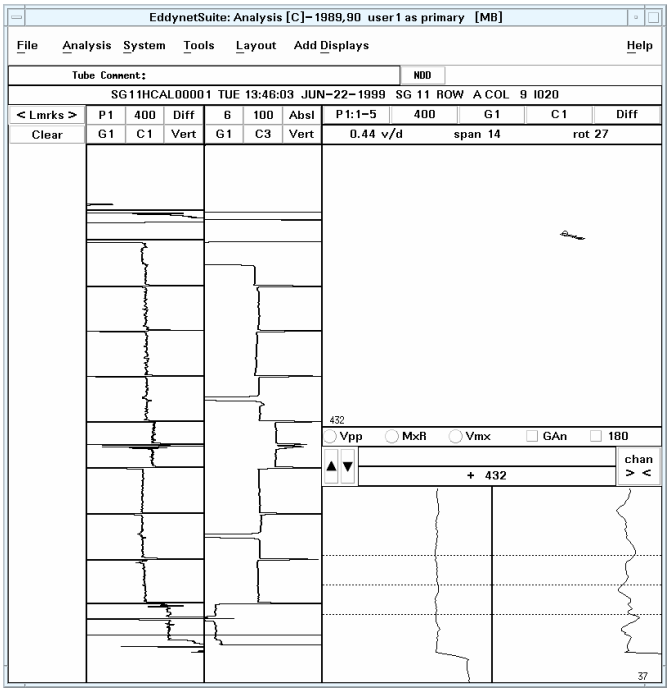

(a)

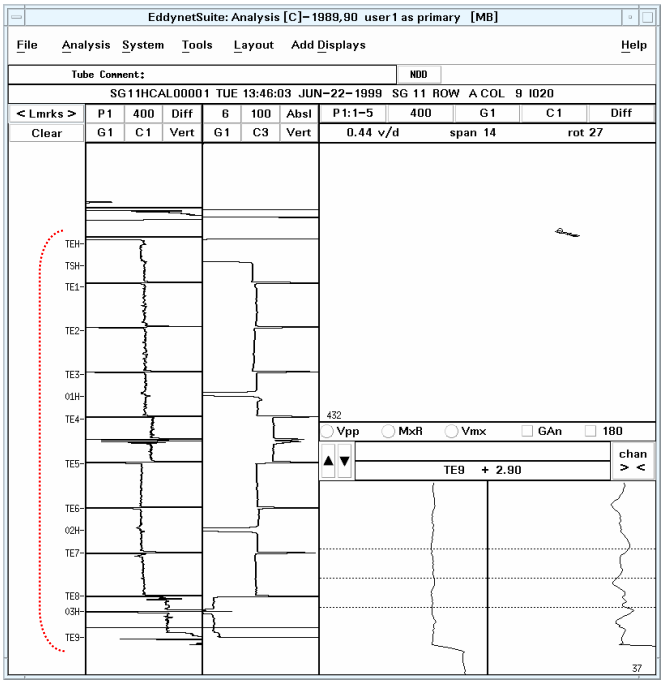

(b)

Figure 4.3 Display of representative bobbin probe data for a full-length mock-up tube (a) before and (b) after application of the automatic landmark locator.

The *CDS Editor* was subsequently used to create location-specific sort configurations for locating, detecting, and classifying flaw signals in the SG mock-up tubes from the training data set. Evaluations of generic data screening parameters were carried out by initially running the CDS in an interactive mode. As noted earlier, this function allows the user to step through the data and examine each detection call on potential indications. This operating mode is particularly useful when iterative adjustments to the sort parameters need to be made. Bobbin probe inspection data from a subset of mock-up tubes designated as the training data set were used for the initial assessments. The setups used typical values suggested by the CDS reference material for detection and classification of potential indications in those particular regions. Based on these initial tests, preliminary generic setups for the type of flaws present in the training data set were created and subsequently applied to all the tubes included in the training data set.

Figure 4.4 displays the CDS editor window with the preliminary settings for the analysis of data at two different regions of the tube bundle mock-up. The data screening configuration for indications in the free-span region is shown in Fig. 4.4(a). Also marked on that figure are the setup areas for defining the sort configurations (*Regions* and *Indications* list) and the associated parameters for locating, detecting, and classifying indications. The *location* setup for the free-span screens the entire length of each tube excluding the landmark zones. The free-span (Region 1) includes the entire length of the tube excluding the landmark zones. Activation of the *Not* logic in that line causes the search routine to bypass landmark regions within the prescribed window size. The peak detection algorithm selected for this region is defined as *Filtered Peaks*, which automatically applies a first-order cross correlation filter primarily to eliminate baseline fluctuations in the data. To emulate the manual analysis procedure, the measurement channel for detection of signals was selected as the 400|100 kHz differential TSP suppression mix (P1). An amplitude threshold of 0.3v was used for detection of potential signals. Two separate logic lines were created for the classification of signals. The first test logic line uses the 200 kHz differential channel for both measurement and testing. Because the sorts are associated with free-span region of the tube, the classification measurement and reporting channels used in the second test logic are the 200 kHz differential and the P1 channel, respectively. In both cases, the measurement algorithm used is *Transition Amplitude VPP*, which was described in the previous section. Figure 4.4(b) shows the setup for the analysis of signals at TSP elevations. The TSP suppression channel in this case was used for both detection and classification of signals. For the preliminary evaluations, the screening zone for each TSP was extended by 1 inch on both sides of the intersection to overlap the free-span region. In combination, the two regions cover the entire length of each tube.

Bobbin probe data from a subset of tubes in the training data set were screened automatically using the CDS setups described above. Representative test cases are presented next that demonstrate the results of the initial evaluations. An intermediate and the final stage of the analysis process are shown in Fig. 4.5(a) and (b), respectively. The tube in this case contains single and multiple cracks at different free-span elevations. With the current sort settings, all free-span indications were detected in this particular tube. As displayed in Fig. 4.5(b), the locations of detected signals are marked with an arrow in the landmark column of the analysis window. Similar results are shown in Fig. 4.6 for another tube identified previously as having fatigue cracking at the highest TSP elevation. Once again, the indications in this case were detected using the preliminary CDS setup.

The data screening sorts for the free-span and the TSP regions of the mock-up were subsequently applied to all the tubes included in the training data set. Although the majority of free-span and TSP indications were detected by CDS, some indications went undetected using the initial setup variables. Figures 4.7 to 4.10 show the signals, identified through manual analysis of data, which went undetected using the preliminary setups.

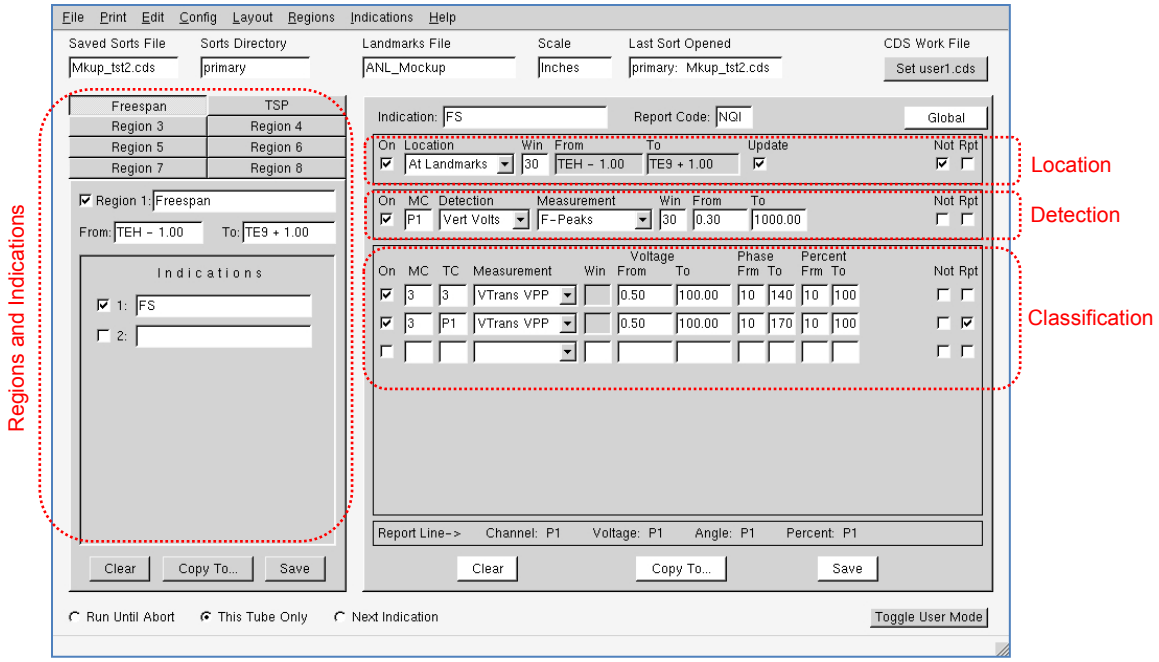

(a)

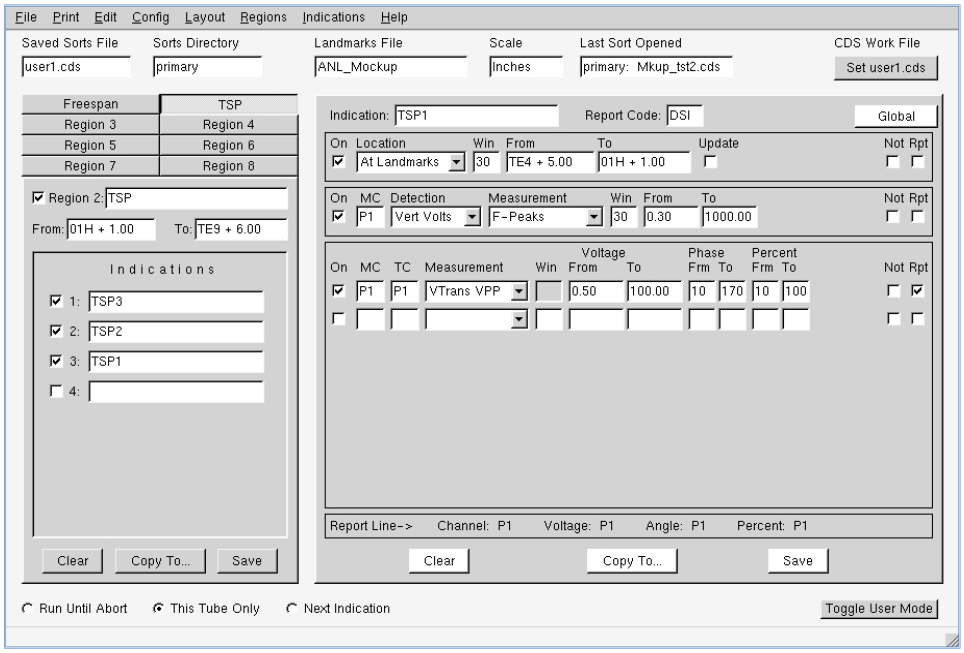

(b)

Figure 4.4 Display of CDS Editor window for setting up the *location*, *detection*, and *classification* parameters for different regions of the tube bundle mock-up. Shown here are the initial settings for the (a) free-span and (b) TSP elevations of the mock-up.

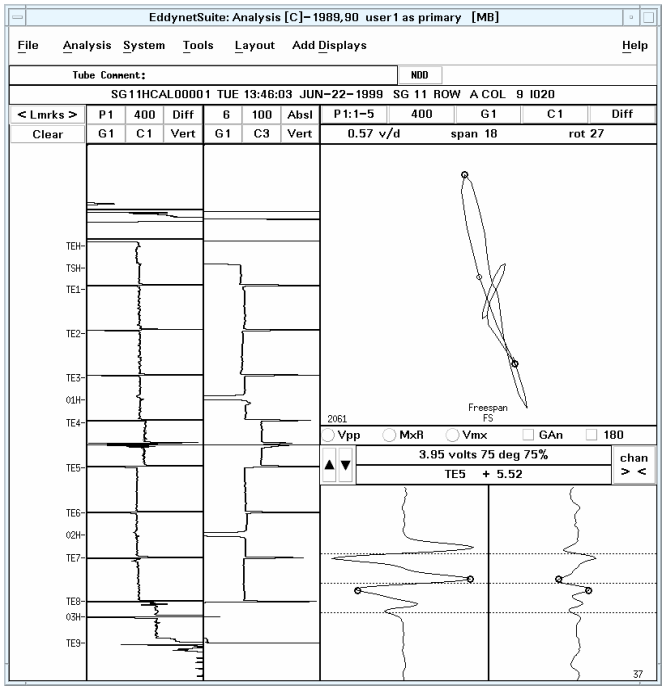

(a)

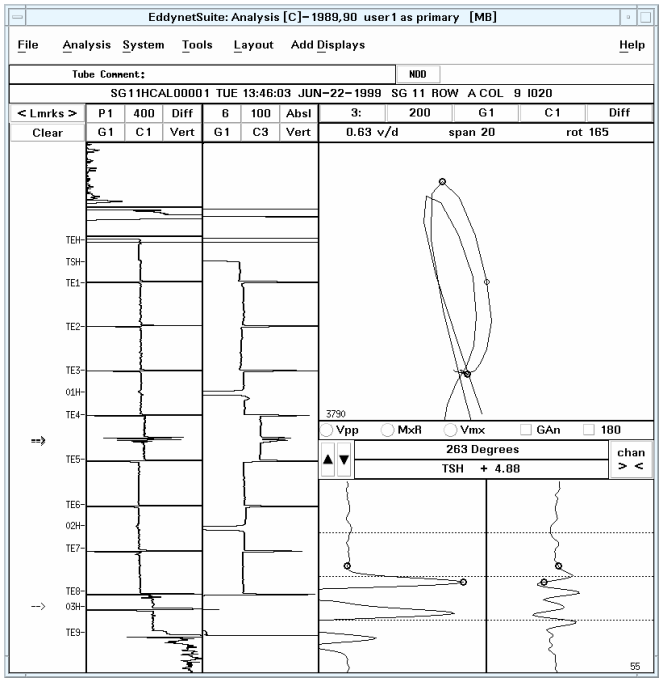

(b)

Figure 4.5 Display of different stages of the CDS process for representative bobbin probe data from a mock-up tube with single and multiple SCC indications at two separate free-span elevations for the (a) intermediate and (b) final stage of analysis with the detected indications marked (arrows) in the landmark column of the analysis window.

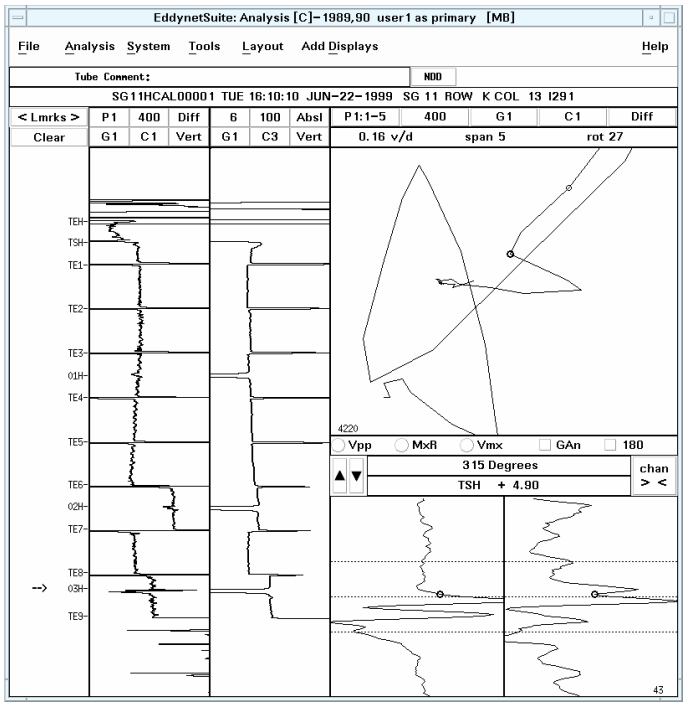

(a)

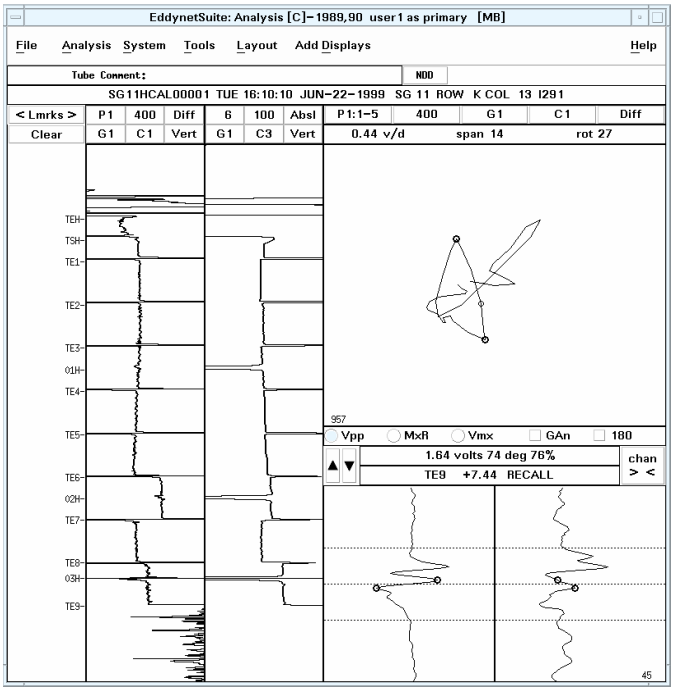

(b)

Figure 4.6 Display of different stages of the CDS process for representative bobbin probe data from a mock-up tube with fatigue cracking at a TSP for the (a) intermediate stage of analysis, and (b) recall of the indication following termination of the analysis process.

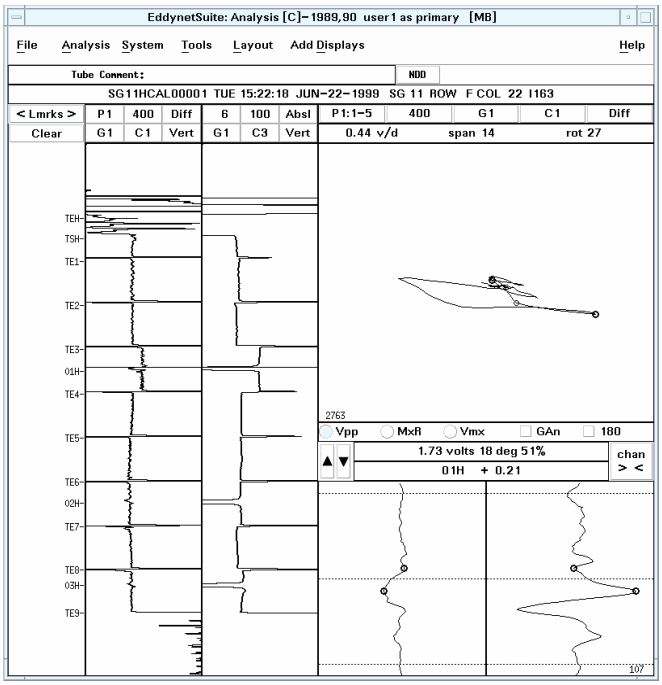

Figure 4.7 Manual analysis of bobbin probe signal displayed in the main analysis window for an ID indication at a dented TSP intersection.

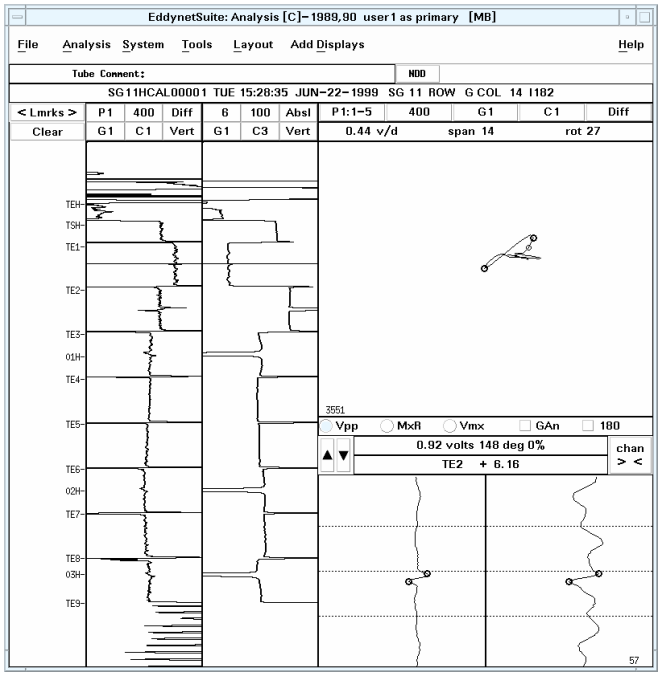

Figure 4.8 Manual analysis of bobbin probe signal displayed in the main analysis window for a free-span indication.

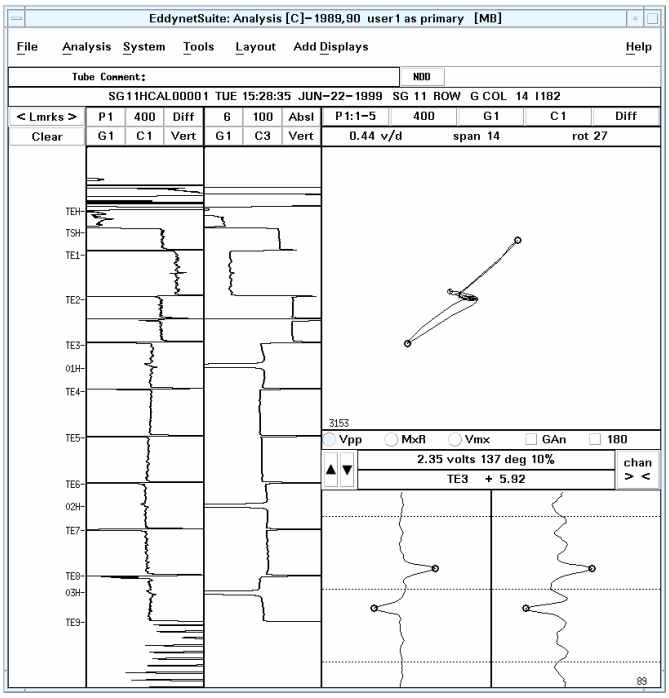

Figure 4.9 Manual analysis of bobbin probe signal displayed in the main analysis window for a free-span indication.

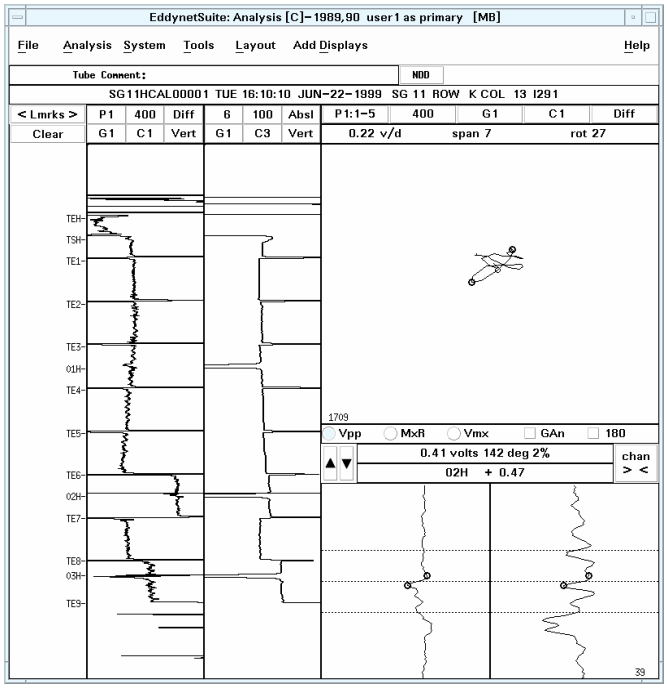

Figure 4.10 Manual analysis of bobbin probe signal displayed in the main analysis window for a small OD indication at a TSP intersection.

In Figs. 4.7-4.10, the flaw signal was not detected with the initial CDS setting for the TSP sort. The probable causes for omission of these signals was attributed to the detection measurement type (Fig. 4.7), lower limit on the percent depth value for reporting with the classification logic (Figs. 4.8, 4.9) and lower voltage limit of the detection threshold (Fig. 4.10).

Modifications were subsequently made to the existing free-span and TSP sorts to help detect the signals that were missed during the initial screening of tubes in the training data set. The modifications included lowering of the voltage threshold for detection of low amplitude signals and selection of an alternative detection algorithm for flaw signals in the TSP region. Additional sorts were also generated for screening of the TS elevation of the SG mock-up (special interest). As a result of high false call rate in the TS region, defined as the number of false calls divided by the number of unflawed test sections, the tube sections inside the TS were excluded from screening by CDS. Only the sort generated for the analysis of data over a small zone at the top of the tube-sheet (TTS) was activated. Figures 4.11(a) and (b) display the CDS editor window for the free-span and the TSP sorts, respectively. The free-span (Region 1) includes the entire length of the tube excluding the landmark regions. Three separate sorts were created under Region 2 for examination of TSP level indications. The CDS editor windows for TTS and TS regions are displayed in Fig. 4.12(a) and (b), respectively. Analogous to manual analysis of bobbin probe data from the mock-up, the detection and classification of signals at the TS elevations was based on examination of the process channels consisting of two- and three-frequency mixes, which suppress the probe response from the TS and the TTS transition, respectively. In comparison to the previous setup, the voltage threshold values for TTS sort were increased in order to reduce the number of false calls in that region.

Bobbin probe data for all tubes in the training data set was analyzed automatically using the modified sorts described above. Figures 4.13 and 4.14 show screen captures of the CDS results for three indications missed using the initial setups for the free-span and TSP regions. In Fig. 4.13, the previously missed signal in the TSP region of the fourth tube section was detected following modification of the TSP screening sort. In Fig. 4.14, the previously missed free-span indications in the second and third tube sections were detected following modification of the free-span screening sort. All three indications were subsequently detected using the modified sorts shown in Fig. 4.11. Figure 4.15 shows the final results of the processing by CDS for all tubes in the training data set in the *Report Editor* dialog box. With the exception of the signal shown in Fig. 4.10, all free-span and TSP indications were detected using the modified sorts. With only a small number of false calls, all TTS indications were also detected using the newly generated sort for that particular region of the mock-up. Following the termination of the CDS process, the reported entries associated with the flaw depth (column 6), the three-letter indication code (column 11), and the flaw origin (column 12) were manually edited to match the format prescribed for manual analysis of bobbin probe data from the SG mock-up.

Following the initial evaluations based on the training data set, bobbin probe inspection data from a subset of mock-up tubes designated as the analyst testing/qualification data were used to further assess the CDS sort configurations. The sorts generated for three different regions of the tube bundle, namely, free-span, TSP, and TTS were subsequently applied to all twelve tubes included in the qualification data set. Screen capture of the CDS results for representative tubes in that data set are shown in Figs. 4.16 through 4.20. Figure 4.16(a) shows the CDS results over the full length of a tube with detected signals (marked by arrows) at the free-span, TSP, and TTS elevations. In reference to Figs. 4.16(b) and (c), the free-span indication near the second TSP was correctly detected while the signal from a dent at the first

TSP elevation was incorrectly identified as a flaw. Although the latter reported signal may be eliminated by adjusting the lower limit of the phase angle in the classification logic line, it can potentially result in elimination of calls associated with shallow ID originated flaws. Examples of shallow ID flaws that could be affected in this manner are provided below. As noted previously, the challenge is to determine the optimum settings for the classification logic lines to best maintain a balance between conservatism in detection of potential indications and an acceptable false call rate.

Figure 4.17 shows the CDS results for another tube with flaws in different TSP elevations. Figure 4.17(a) shows screen capture of the final analysis results with all detected indications marked in the landmark column of the analysis window. Figure 4.17(b) shows a large ODSCC flaw detected in the first TSP. An indication identified as IGA at the second TSP elevation was not detected with the current settings of the TSP sort. Three other examples of CDS analysis results on tubes from the test data set are provided in Figs. 4.18 to 4.20. An example of a low-amplitude signal associated with a shallow ODSCC flaw in the free-span region of the tube is shown in Fig. 4.18. Examples of IDSCC signals detected at a dented TSP and in the free-span region of the tube are shown in Figs. 4.19 and 4.20. In all cases, the flaws were properly detected and identified using the modified settings of the sort parameters.

The final result of the processing by CDS for all tubes in the test data set is shown in Fig. 4.21. All the entries made in the *Report Editor* dialog box are listed. The columns associated with the estimated flaw depth (column 6), reporting code (column 11), and flaw origin (column 12) were manually edited to more closely match with the report entry format prescribed for manual analysis of bobbin probe data from the mock-up. Based on the results of the analysis here, the free-span and TSP indications in all tubes from the test data set were detected with a high detection probability and with a low false call rate. The false call rate for the TTS indications, however, is rather excessive.

Subsequent efforts were aimed at further optimization of the setup parameters based on the signals present in the training and the testing data sets. Alternative detection algorithms for reducing the number of double calls on long indications were also further evaluated. Examples of signals from the qualification data set which were reported twice by CDS are shown in Fig. 4.22, as seen in the screening results in Fig. 4.21(a) and (b) from the report editor, where both flaws were called twice. This may be attributed to the detection algorithm used here, which is optimized for detection of closely spaced signals. Also, examples of ferromagnetic markers identified by CDS as flaw indications are shown in Fig. 4.23. The markers, which were placed within one inch of the tube end, were intended for more accurate reporting of positional information for rotating probes. The markers in a small number of tubes can produce a large probe response that could be misinterpreted as shallow ID indications. Although such signals do not pose a major problem with regard to the evaluation of EC detection capability for the SG mock-up data, they can increase the number of false calls if the entries are kept as reported. These false calls can be eliminated through implementation of more detailed sorts that would examine additional channels for characterization of such signals. Specifically, possible options for minimizing the number of such false calls include incorporation of additional logic lines in the free-span sort and creation of a separate sort for classification of such signals. A more elaborate sort may include classification logic that uses information from the lower frequency absolute channels and/or uses the three-frequency TTS mix channel for suppression of probe response associated with permeability variations.

As noted earlier, detection of EC signals is strongly dependent on the setting of amplitude threshold values that are used by both the detection and classification algorithms. These thresholds are initially set based on the level of noise present in the inspection data. The ability to detect a particular signal is therefore dependent on its S/N. The primary challenge is to optimize the threshold values to provide an acceptable tradeoff between detection and the overcall rate. To further evaluate the test logic for the free-span and TSP regions of the mock-up, the voltage threshold values were slightly reduced to assess their effect on detection. Based on feedback from the earlier tests, the amplitude threshold values for the TTS signals were also significantly increased. In general, the adjusted threshold values for the free-span and TSP regions did not influence the detection of flaw signals in this data set. However, the slight reduction of amplitude threshold values resulted in a measurable increase in the number of overcalls particularly at the TSP elevations. Screen capture of the CDS results for a representative tube with overcalls at two TSP elevations is displayed in Fig. 4.24(a). The signal for one of the two overcalls is shown in Fig. 4.24(b).

An example of a signal that was not detected with the current sort configuration is shown in Fig. 4.25. The degradation is IGA at a TSP intersection. It should be noted that detection of IGA with bobbin probes, using either manual or automatic analysis procedures, can be challenging. The difficulty is attributed to the complex morphology of the flaw which results in atypical phase angle response that cannot be properly characterized based on the conventional analysis logic for crack-like or volumetric indications. A separate sort may have to be generated for detection of such signals in the mock-up. Potential indicators of the flaw in this case are the relatively large amplitude of the TSP mix residual signal and subtle changes in probe response at other test frequencies in comparison to the probe response from a clean TSP (i.e., a TSP elevation with no flaws in the tube). This test case demonstrates the potential difficulty in characterizing IGA using bobbin probe.

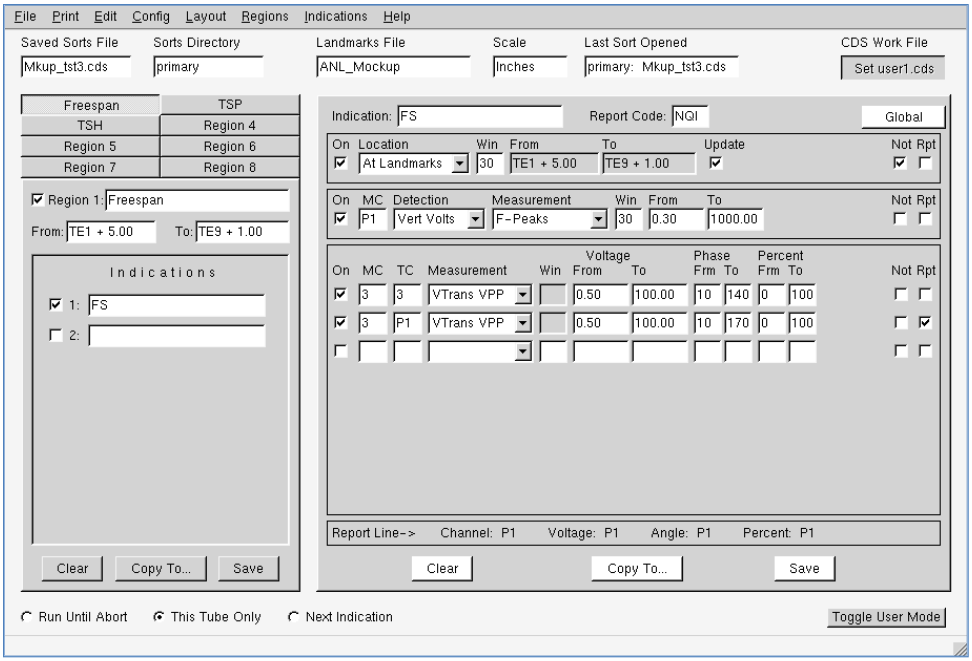

(a)

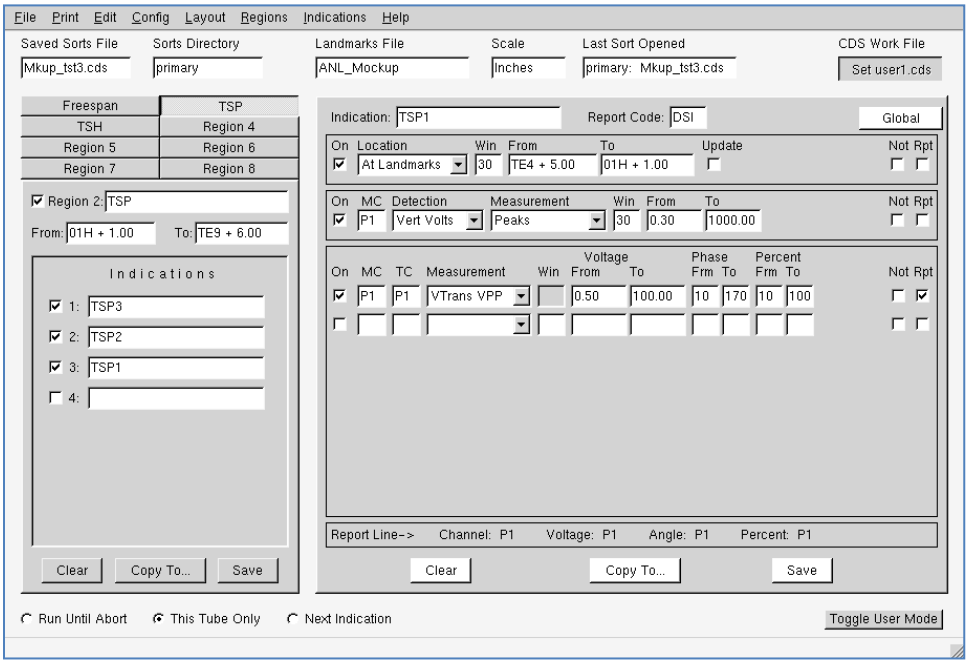

(b)

Figure 4.11 Display of CDS Editor window for setting up the location, detection, and classification sorts for different regions of the tube bundle mock-up settings for the (a) free-span and (b) TSP elevations of the mock-up.

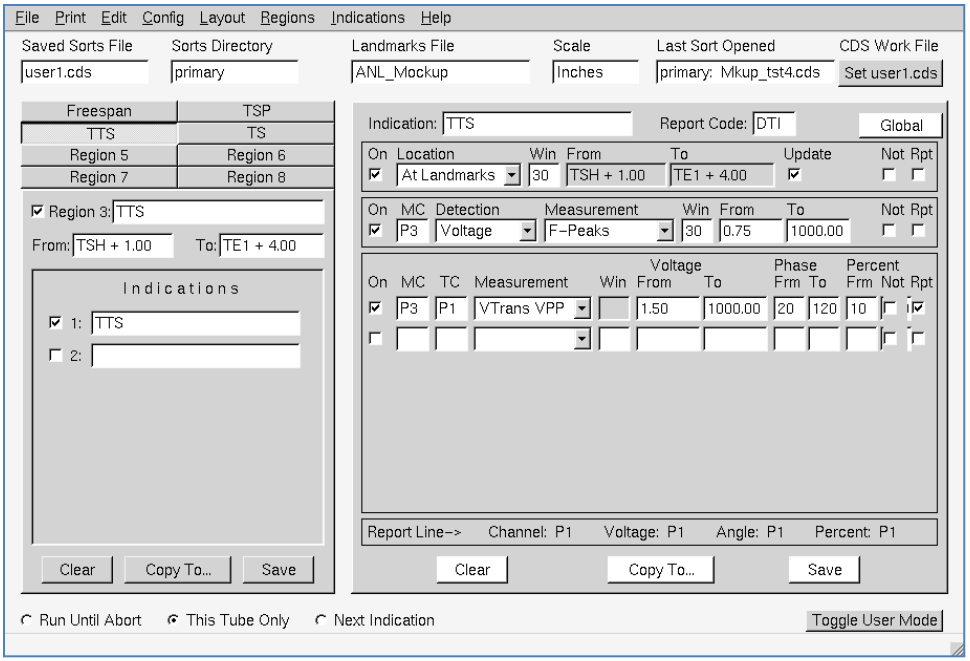

(a)

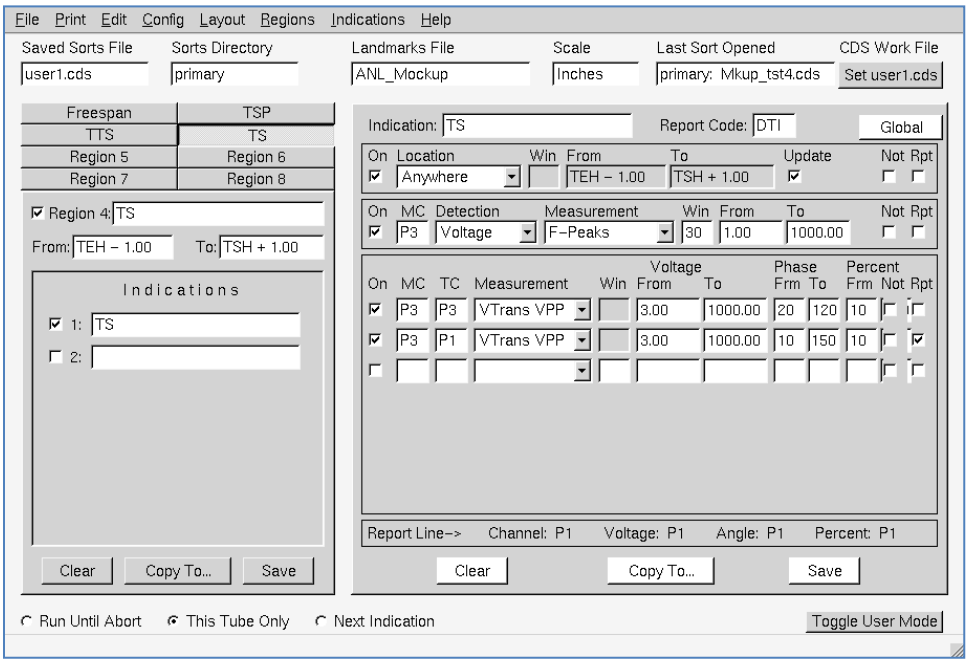

(b)

Figure 4.12 Display of the CDS Editor window used for setting up the parameters associated with the location, detection, and classification algorithms. Shown here are the sorts for the (a) TTS and (b) the TS elevations of the SG mock-up.

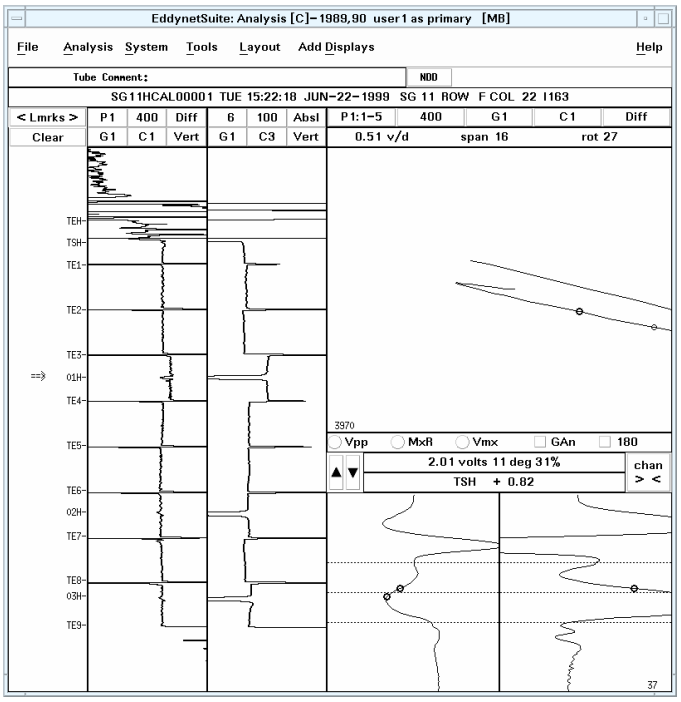

Figure 4.13 Display of the CDS results for the same tube shown in Fig. 4.7 with the detected indications marked with arrows in the landmark column of the analysis window.

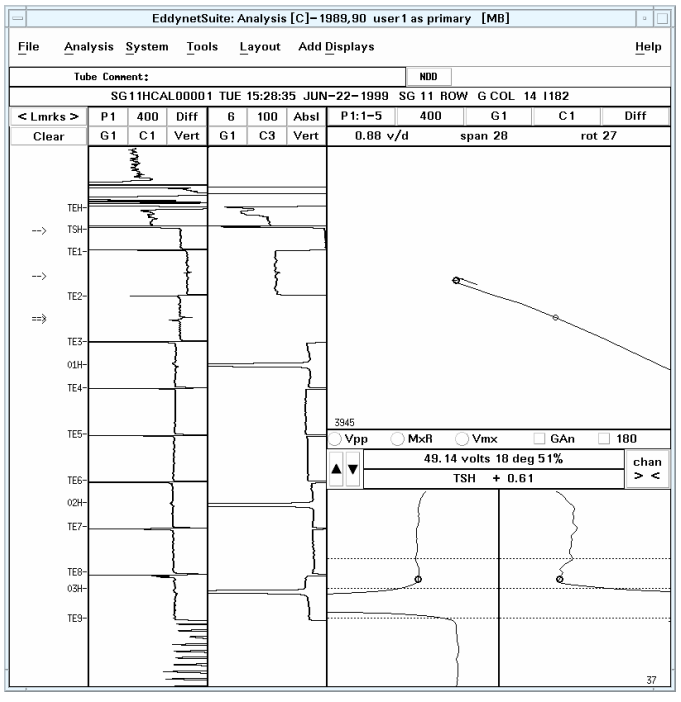

Figure 4.14 Display of the CDS results for the same tube shown in Figs. 4.8 and 4.9 with the detected indications marked with arrows in the landmark column of the analysis window.

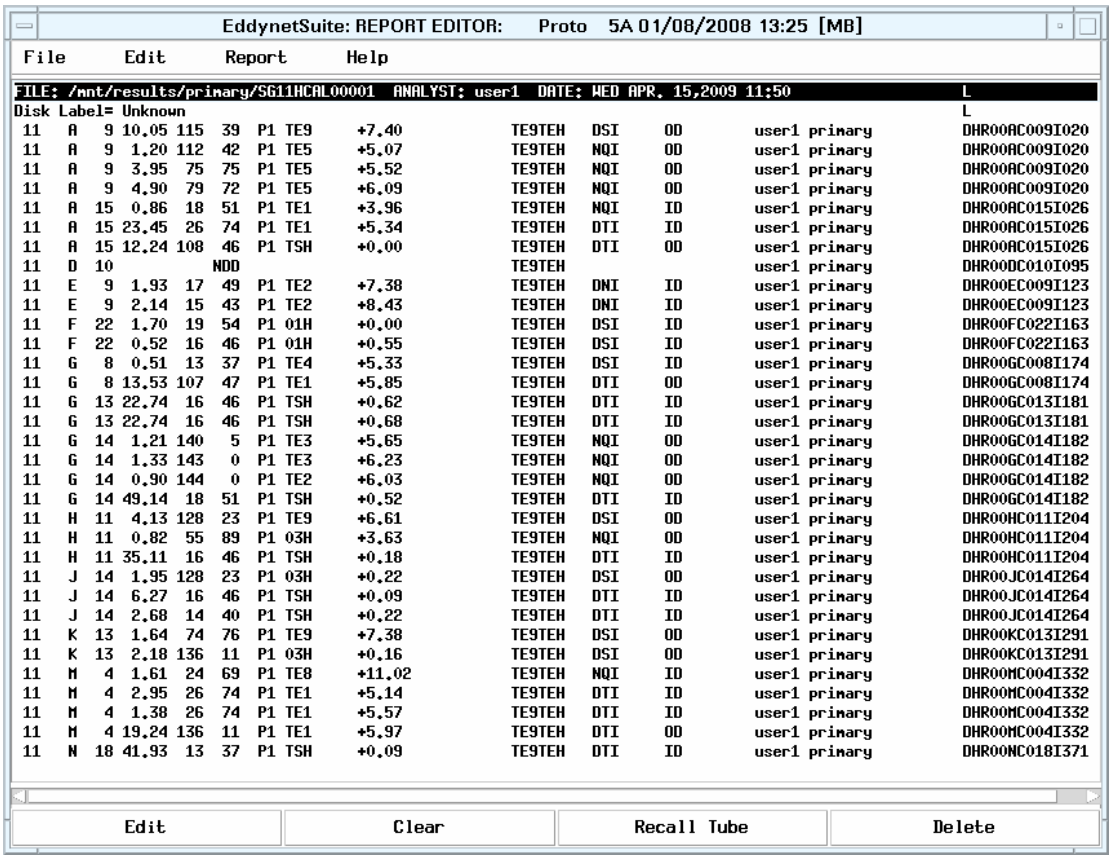

Figure 4.15 Results of the CDS analysis displayed by the *Report Editor* dialog box for all thirteen tubes in the training data set.

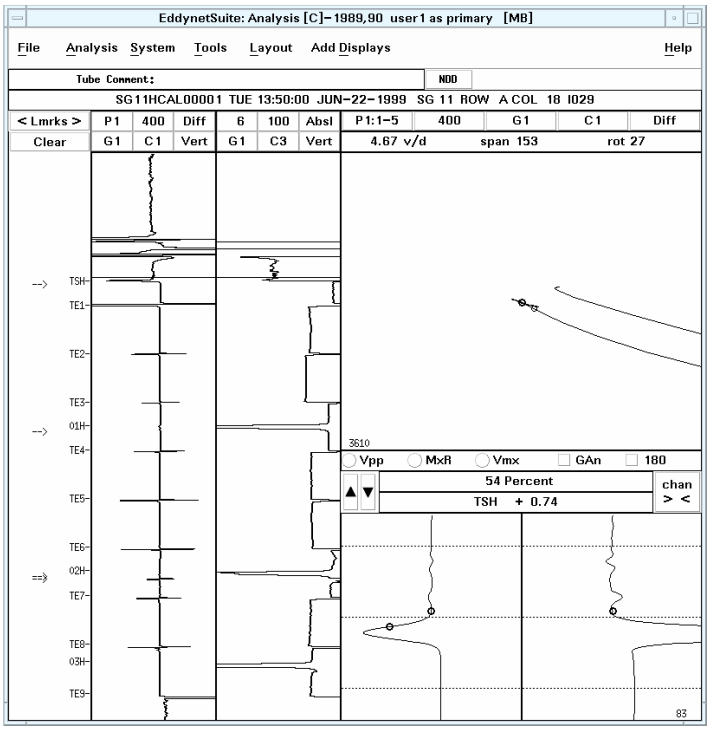

(a)

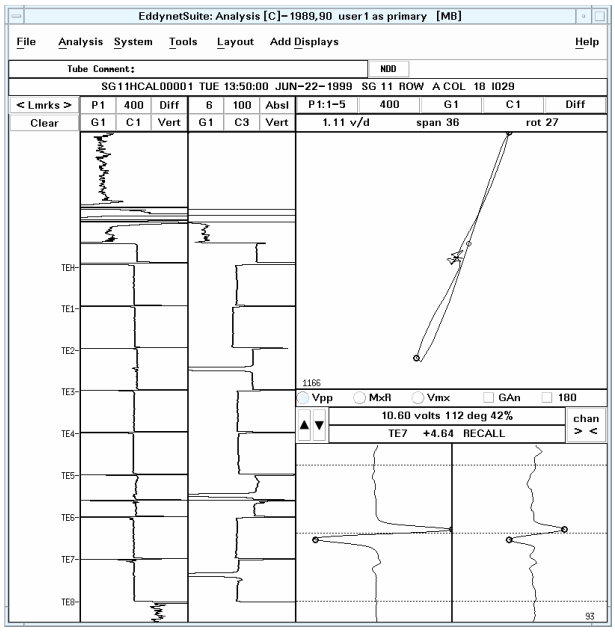

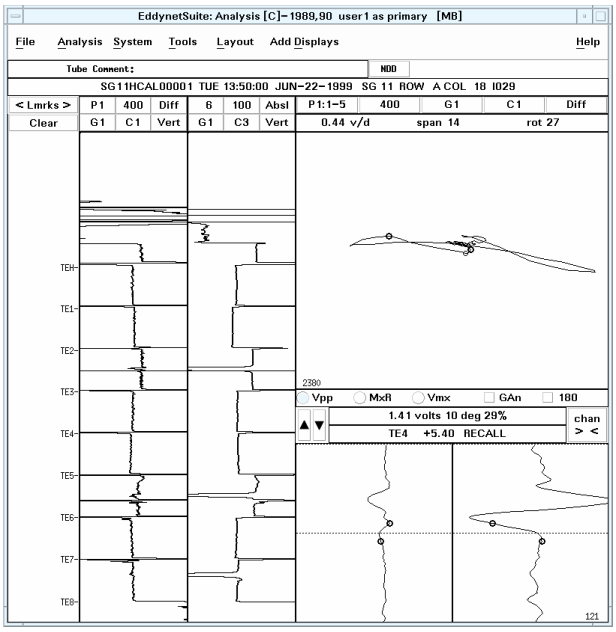

(b) (c)

Figure 4.16 Display of the CDS results for the entire length of a mock-up tube from the test data set for the (a) final CDS results with the detected signals marked with arrows in the landmark column of the analysis window, (b) a large ODSCC signal near the second TSP intersection, and (c) a dent signal at the first TSP intersection.

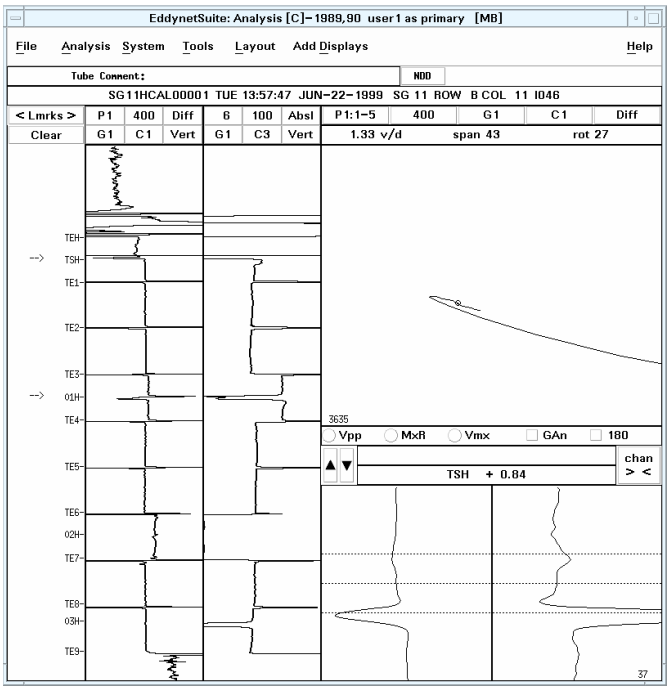

(a)

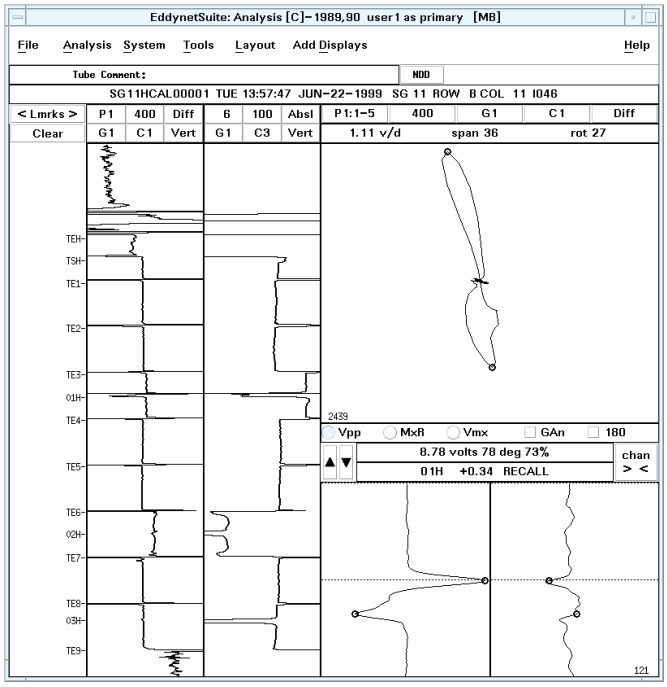

(b)

Figure 4.17 Display of the CDS results for the entire length of a mock-up tube from the test data set for the (a) final CDS results with the detected signals marked with arrows in the landmark column of the analysis window and (b) an ODSCC signal at the first TSP intersection.

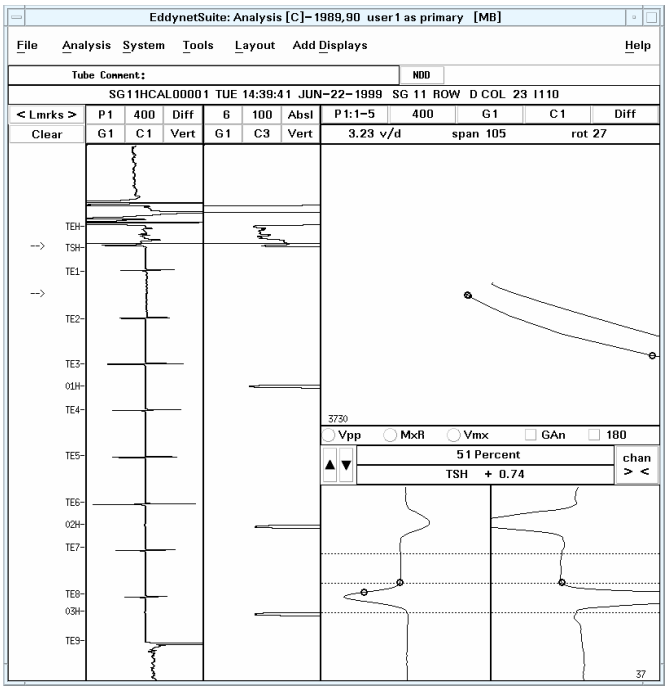

(a)

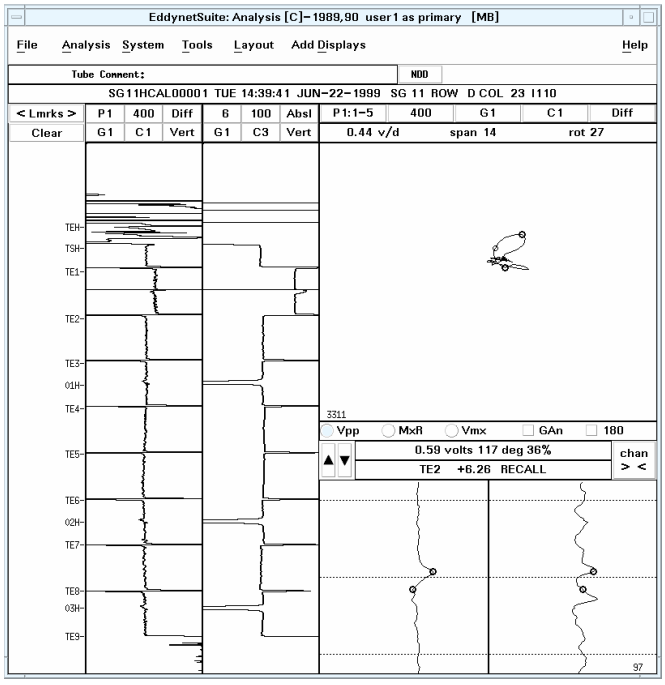

(b)

Figure 4.18 Display of the CDS results for the entire length of a mock-up tube from the test data set. Shown here are (a) final CDS results with the detected signals marked with arrows in the landmark column of the analysis window and (b) signal from a shallow ODSCC flaw located in the free-span region of the tubing.

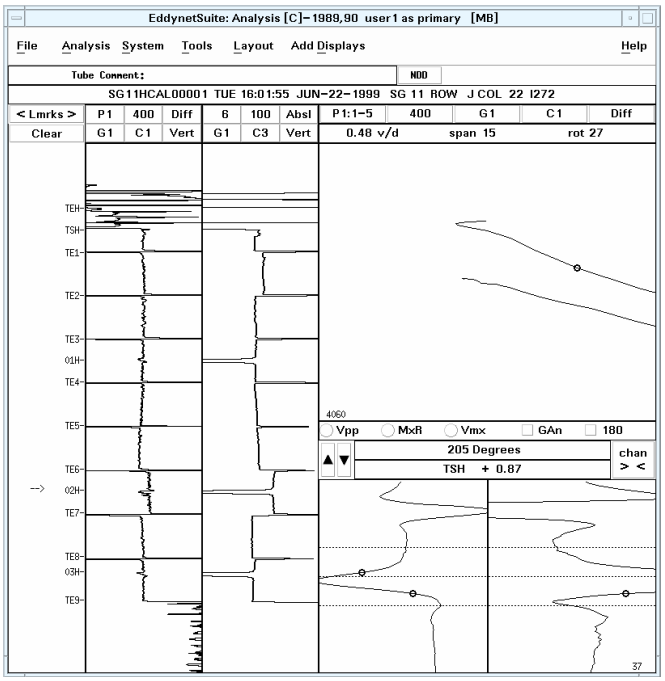

(a)

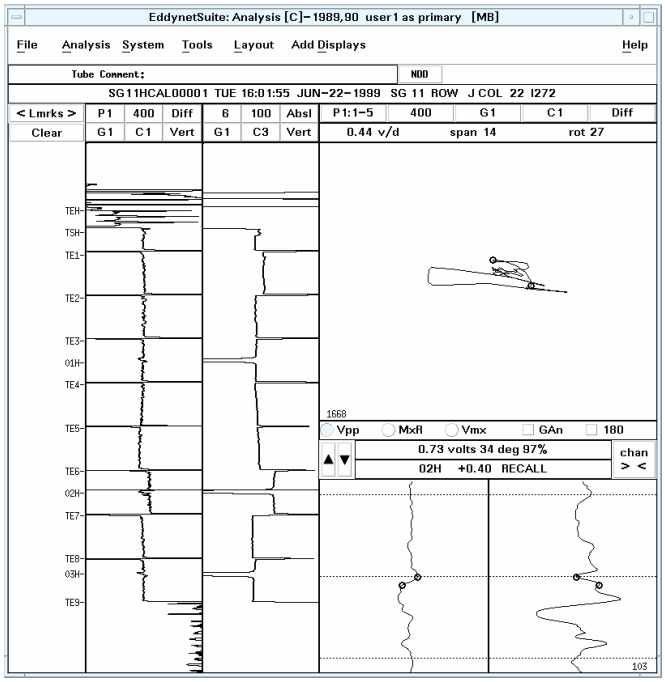

(b)

Figure 4.19 Display of the CDS results for the entire length of a mock-up tube from the test data set. Shown here are (a) final CDS results with the detected signals marked with arrows in the landmark column of the analysis window and (b) signal from an IDSCC flaw at a dented tube support region.

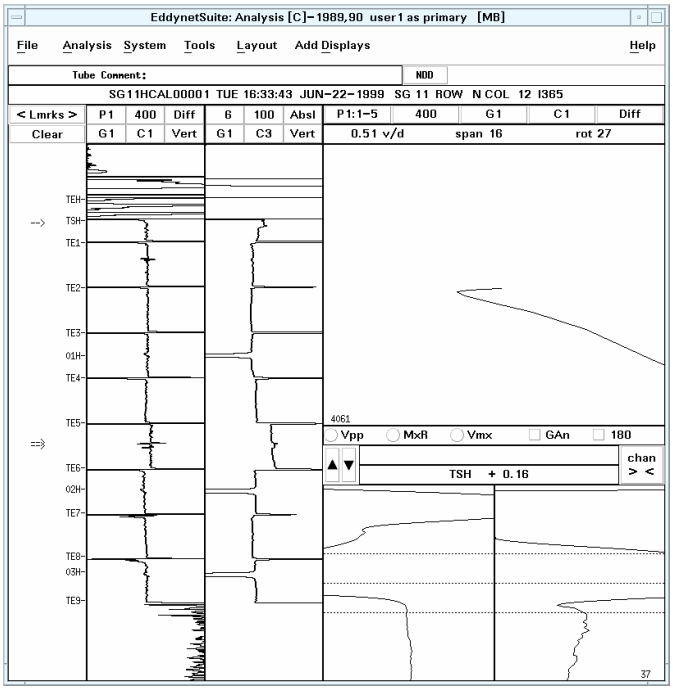

(a)

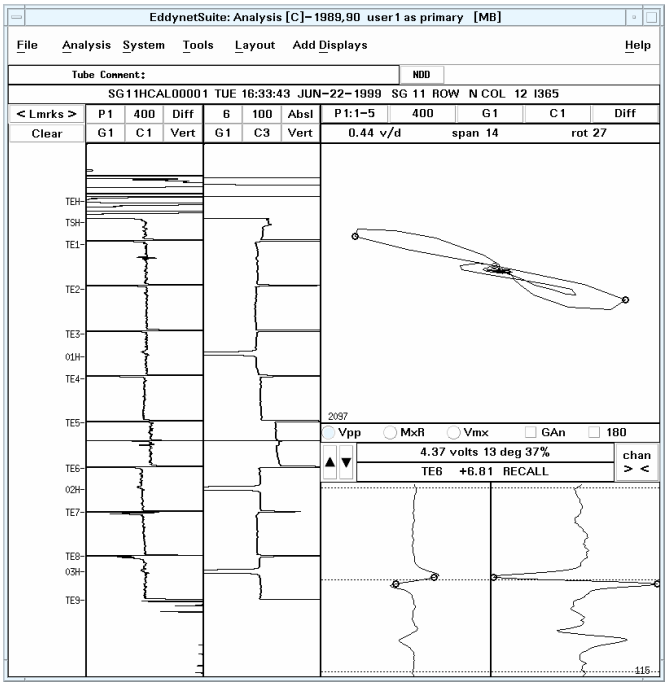

(b)

Figure 4.20 Display of the CDS results for the entire length of a mock-up tube from the test data set. Shown here are (a) final CDS results with the detected signals marked with arrows in the landmark column of the analysis window and (b) signal from one of two closely spaced axial IDSCC flaws in the free-span region of the tube.

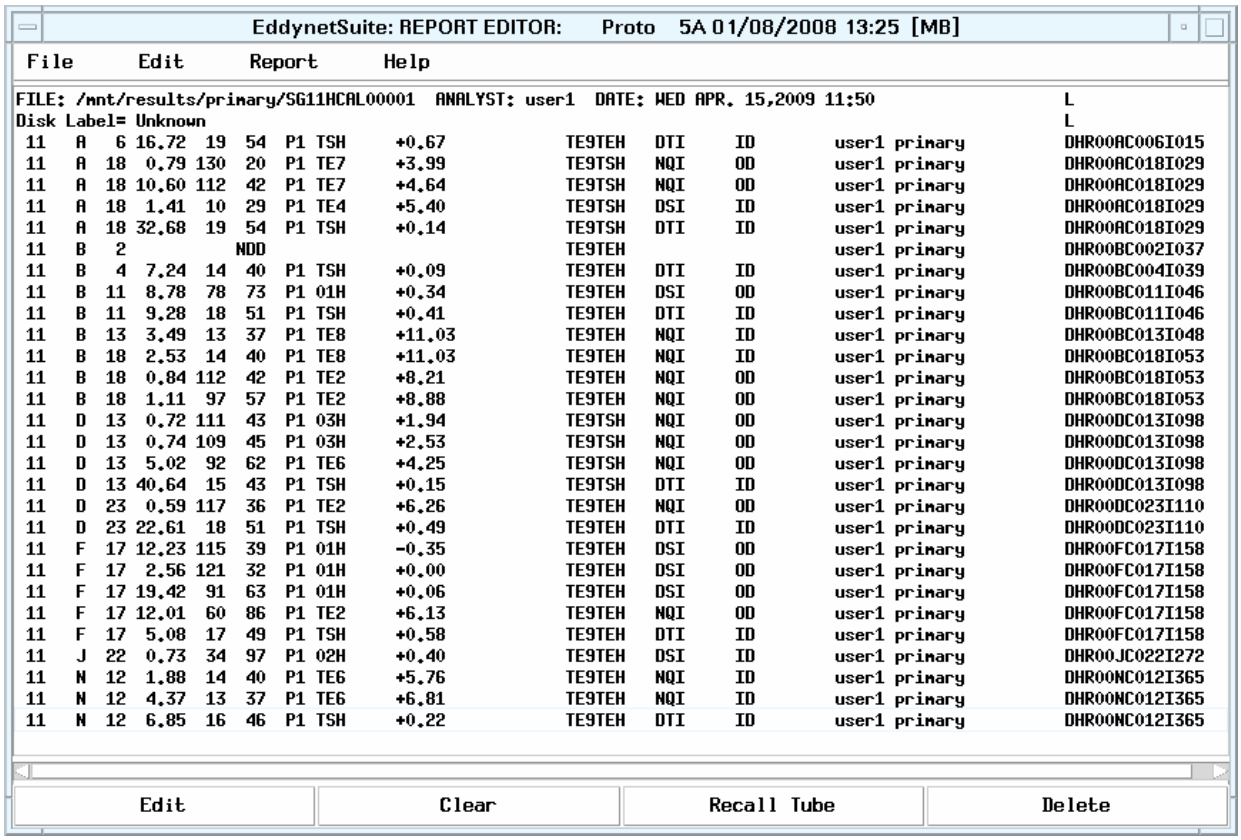

Figure 4.21 Results of the CDS analysis displayed by the *Report Editor* dialog box for all twelve tubes in the testing data set.

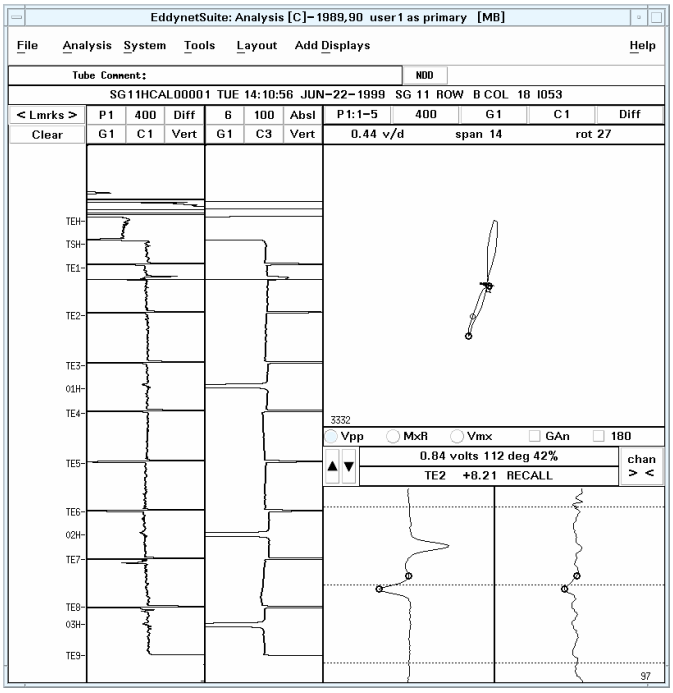

(a)

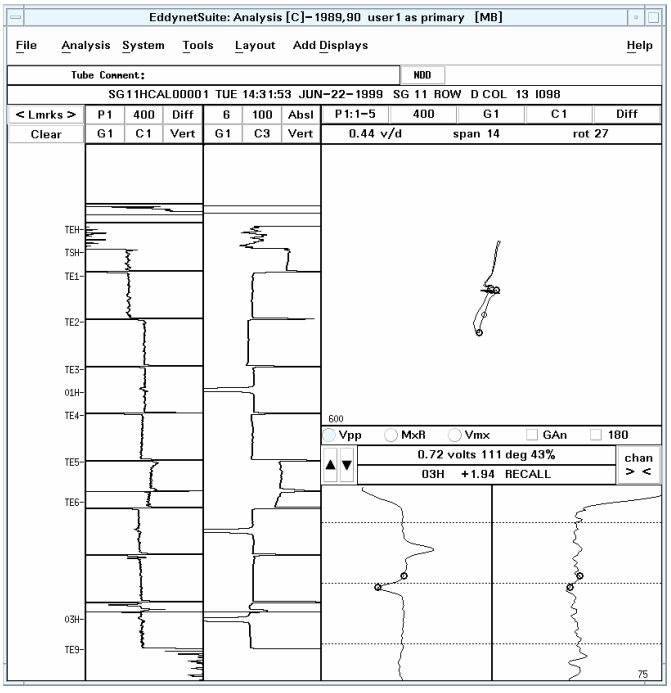

(b)

Figure 4.22 Display of the CDS results for two free-span ODSCC indications.

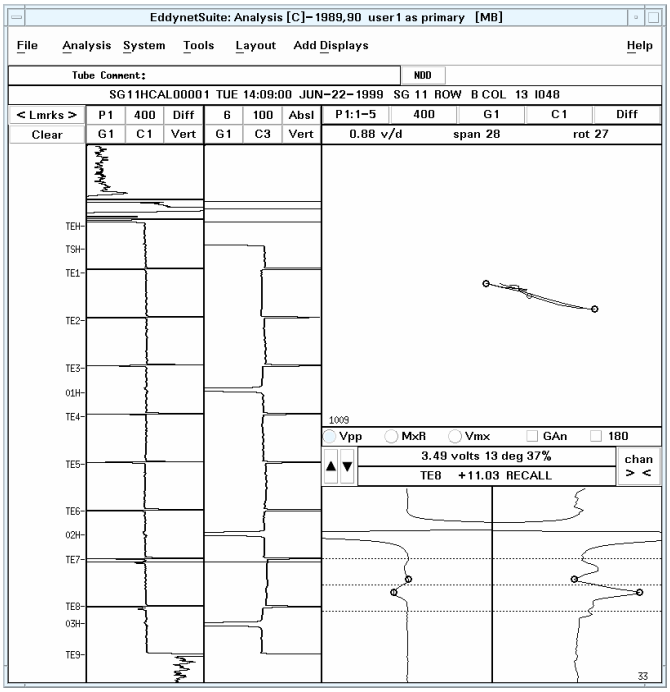

(a)

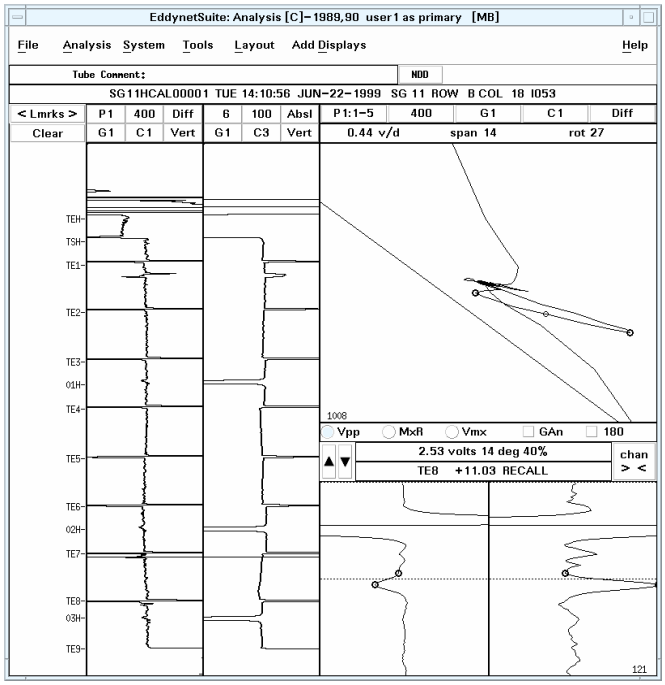

(b)

Figure 4.23 Examples of ferromagnetic markers near the tube end identified as indications by CDS.

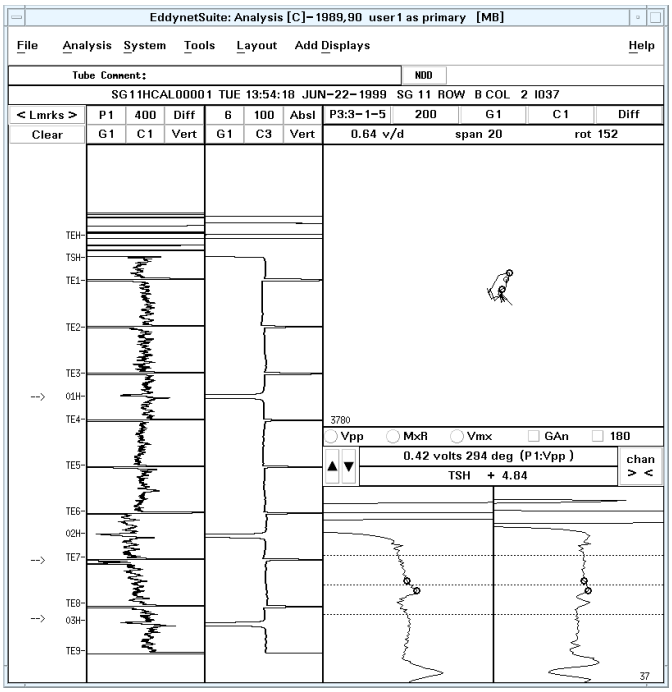

(a)

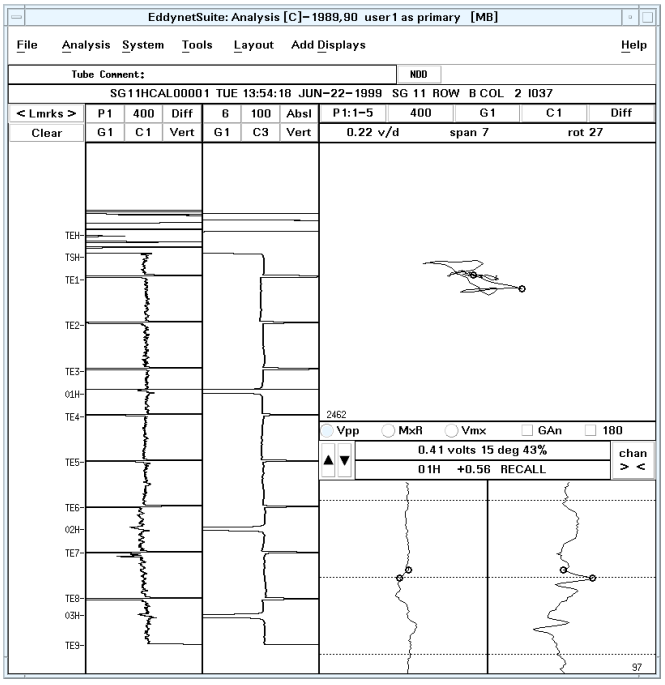

(b)

Figure 4.24 Display of the CDS results for the entire length of a mock-up tube from the test data set. Shown here are (a) final CDS results with the detected signals marked with arrows in the landmark column of the analysis window and (b) an example of a false call at a TSP elevation due to a low voltage threshold.

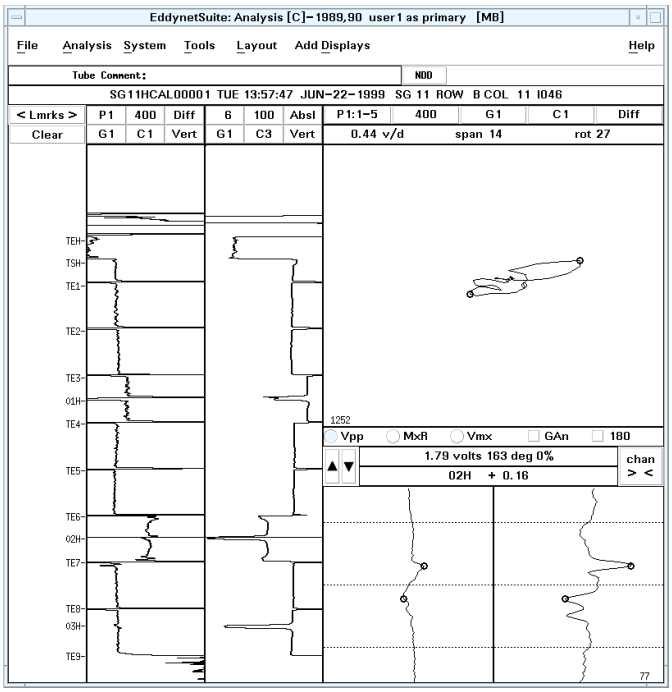

(a)

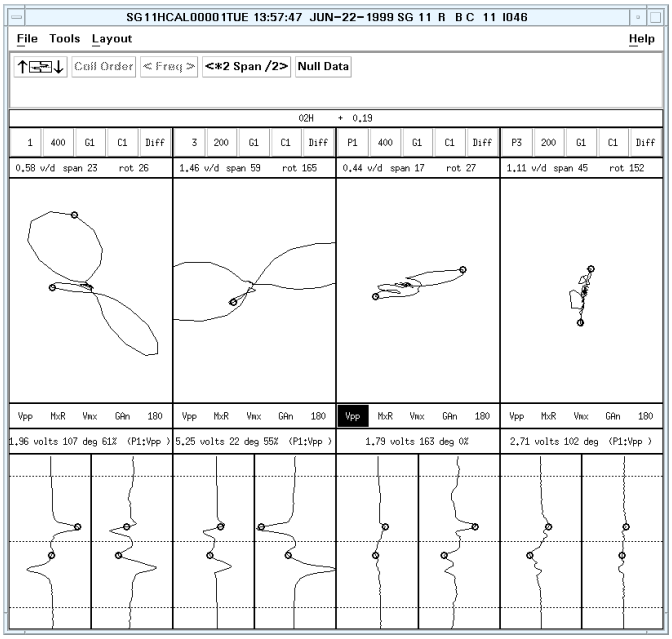

(b)

Figure 4.25 An example of a missed call for IGA at a TSP intersection. Shown here are the signals measured manually from (a) the 400|100 kHz TSP mix channel and (b) multiple Lissajous with expanded strip chart display of the same signal from four different channels.

A number of CDS sorts were generated and tested for the analysis of data from different regions of the tube bundle mock-up. To verify the results of analyses using the CDS sort configurations generated at Argonne and to further seek consultation on optimization of CDS setup parameters on alternative configurations, Argonne staff attended a two-day workshop at Zetec. Following consultation with the vendor, modifications were made to the aforementioned CDS setups and complementary data screening configurations were additionally generated. Further evaluations were subsequently carried out on alternative data screening setups that could help improve the detection probability of signals present in the SG mock-up and to further determine the possibility of overcoming some known limitations in dealing with difficult flaw types. The results of evaluations using the modified sort configurations are discussed below.

The preliminary investigations suggest in general that the latest set of sorts in most parts provide redundancy checks for screening different regions of the mock-up. Other sorts included in this latest set are those for detection and classification of dent (non-degradation mechanisms) signals at TSPs and for generating single calls on long axial indications. It is worth noting that while increasing the number of sorts for screening the same region of tubing generally improves the detection probability, increasing the number of classification logic tests for a given sort could lead to less conservative detection results. As mentioned earlier, this is because the *Indications* definition list follows an *OR* logic while the sort test logic follows an *AND* logic.

The CDS Editor window for representative sort configurations associated with different regions of the mock-up is displayed in Figs. 4.26-4.29. Two separate *Indication* identification regions defined for screening of free-span elevations are displayed in Fig. 4.26. The primary sort in Fig. 4.26(a) employs a differential channel (200 kHz measurement channel) while the secondary sort employs an absolute channel (100 kHz measurement channel) for detection. As it was noted earlier, the detection and classification test logic of the configuration shown in Fig. 4.26(a) is better suited for identifying closely spaced signals while the complementary sort shown in Fig. 4.26(b) is set specifically for the measurement and reporting of relatively long axial signals. The detection algorithm shown in Fig. 4.26(b) employs a lower frequency absolute channel with a larger measurement window size in order to better capture such signals. Except for the difference in measurement class and window size, similar classification test logic is used in both cases. The main difference between the two sorts is the use of a lower frequency absolute channel with a larger window size for detection of long axial signals.

Representative setups for the sorts used to screen TSP elevations are shown in Figs. 4.27 and 4.28. Four separate sort configurations under the *Indications* list were defined for detection and classification of signals at TSP elevations. Three of those are associated with detection of flaw signals and one is associated with detection of dent signals over the same region of tubing. Figures 4.27(a) and (b) display a two sort configuration for detection of flaw signals at the third TSP elevation. The main difference between the two setups is the use of 200 kHz differential channel (channel 3) in Fig. 4.27(a) and the use of TSP suppression mix (P1) in Fig. 4.27(b) as the test channel in the classification logic. Other detection and classification parameters for the two TSP sorts are similar to those described earlier. Duplicate sets of sorts are created for all three TSP elevations in the mock-up. Additional setups for reporting of flaws and geometry deformations at dented TSP regions are shown in Fig. 4.28. The sort configuration shown in Fig. 4.28(a) is based on the TTS suppression mix (P3) that was created to specifically detect flaw signals in dented regions. The setup displayed in Fig. 4.28(b) on the other hand is intended for reporting of dents at TSP elevations. In this case the horizontal component of the signal is used in the detection logic as the EC probe response from tube geometry change is

expected to produce a large horizontal component. A duplicate set of sort configurations were created for screening the three TSP elevations in the SG mock-up.

The CDS editor window for setting up the sorts to detect indications at or near the top of the tube-sheet (TTS) is shown in Fig. 4.29. The measurement channel for both the detection and the classification test logic in this case uses the three-frequency TTS mix (P3) for measurement and testing of signals in that region. Unlike the earlier setups in which the two-frequency TSP suppression mix was used for reporting of signals, the same three-frequency mix channel is used in the modified setup for both measurement and reporting of signals. The text boxes for percent depth values were deactivated in this case because a viable calibration curve cannot be created for P3. It should also be noted that, when a calibration curve does not exist for the test channel used in the classification test logic, the text boxes for percent depth values need to be deactivated. Failure to deactivate the depth range in such cases could result in bypassing of the logic line and in turn missing potentially relevant signals.

The latest CDS setup parameters were evaluated on the qualification data set from the SG mock-up. Representative results following the analysis of all tubes in that data set are shown in Figs. 4.30-4.32. An example of detection of a long axial indication at a TSP elevation by two separate sort configurations is shown in Fig. 4.30. While two individual signals were reported by the fist setup, the second complementary setup for screening the same TSP region resulted in only one reported entry. Another example of multiple calls for the same indication is provided in Fig. 4.31. In this case, a relatively long signal in the free-span region was identified as two separate signals by one sort and as one continuous signal by another sort. It is worth noting that, the setup shown in Fig. 4.26(b) may not be used as an alternative to that shown in Fig. 4.26(a). This is because the detection algorithm in Fig. 4.26(b) is not optimized for capturing flaw signals that are in close proximity to other relevant or non-relevant signals. Figure 4.32 provides an example of signals detected at a dented TSP region with separate calls generated for the dent signal (non-degradation mechanism) and the potential flaw signal at the same intersection by two different sort configurations.

The final results of analysis for all tubes in the test data set with the modified CDS sort parameters are shown in Fig. 4.33. The columns associated with the estimated flaw depth (column 6), reporting code (column 11), and flaw origin (column 12) were manually edited to more closely match with the report entry format prescribed for manual analysis of the bobbin probe data from the SG mock-up. Calls associated with markers near the end of tube sections were also removed from the original list. The analysis results in general show comparable detection capability to the previous sort settings for flaw signals in the free-span and the TSP regions. As expected, inclusion of the additional sorts resulted in a larger number of redundant calls. The number of calls in the TTS region of the mock-up was minimized by intentionally setting a large detection threshold. As noted earlier, while EC inspection data from the TTS region of the SG mock-up were analyzed, because of the high level of noise associated with mechanically expanded tubes, application of CDS to data from the TTS level may not in general be justified in view of the large number of overcalls.

Additional tests were next carried out to further examine the utility of applying multiple CDS sort configuration to the same region of tubing. A larger data set composed of both the training and the performance test data was used in this study. Data analysis results associated with the application of CDS to bobbin probe data from a subset of 25 tubes from the SG mock-up using the sort configurations shown in Figs. 4.26-4.29 are provided in Table 4.1. The columns

associated with the estimated flaw depth (column 6), reporting code (column 11), and flaw origin (column 12) were manually edited to more closely match with the report entry format prescribed for manual analysis of the bobbin probe data from the SG mock-up. Calls associated with markers near the end of tube sections were removed from the original list. The results were exported from the *Report Editor* dialog box and converted to text format for further evaluation outside the Eddynet™ environment. The sort configuration for screening of data within the TS region of the mock-up was deactivated. As described previously, this was done to eliminate the large number of false calls associated with the excessive level of EC noise from the mechanical expansion of the tubes in the TS region. The reported data analysis results were again manually edited to more closely match the report entry format prescribed for manual analysis of the bobbin probe data from the SG mock-up. In addition, entries associated with markers near the end of tube sections were removed from the original list. Examination of the analysis results listed in the table indicates that while nearly all flaws were detected, the number of redundant calls associated with the same signal and the total number of overcalls increased using multiple configurations.

Figures 4.34-4.38 show examples of typical signals that were reported either multiple times by different sorts covering the same region of the tube or were determined later to be false calls. Figure 4.34 displays a potential indication at a dented TSP region, which was called as a 1.19v ID indication by one sort and as a 0.77v OD indication by another sort. In both cases the flaw depth was estimated to be relatively deep. Figure 4.35 displays the CDS results for another tube with an indication at a dented TSP intersection. Separate calls were reported for the dent and the flaw signal by different sorts. In this particular case the location of the flaw signal did not match with that identified through manual analysis of data. Examples of representative false calls reported in the free-span regions of the tube associated with the ferromagnetic marker near the tube end and with baseline noise are presented in Fig. 4.36. A typical example of multiple detections made by separate sorts for the same region of the tube is shown in Fig. 4.37(a), (b). In this case, three separate entries were made for the same signal by different sorts due to overlapping regions. The measured signal amplitude varies between (a) 2.59v by free-span sort and (b) 4.13v by TSP sort. Another example of multiple calls for the same flaw signal is presented in Fig. 4.38. In this case, five separate entries were made for the same signal by different TSP sorts with the measured signal amplitude varying between 0.54v and 1.95v. The tests here generally indicate that, while inclusion of multiple sorts for screening of the same region of tubing can produce more conservative data analysis results, it can also lead to increased number of redundant calls. Also, depending on the type of detection and classification algorithm being used, the reported signal amplitudes can in some cases vary significantly.

Follow-on tests using the data screening configurations shown in Figs. 4.26-4.29 included comparison of the CDS results from different combination of sorts. The purpose of this study was to find an acceptable trade-off between detection probability and overcall rate using multiple sort configurations. To reduce the number of redundant calls a number of tests were conducted to identify the minimum number of sort configurations that would provide comparable detection probability while keeping the number of redundant and overcalls to an acceptable level. Other tests were also carried out to assess the effect of detection thresholds and other data screening parameters on the automated data analysis results. A brief description of the results based on a reduced number of data screening configurations is presented here.

For the next series of tests the number of sort configurations was reduced to one for the screening of free-span and TSP regions of the tube bundle mock-up. This was done by deactivating the previously-generated configurations from the *Indications* list in the *CDS Editor* dialog box and keeping only the most conventional setups for each region. The only data screening configurations kept were the ones shown in Fig. 4.26(a) for the free-span region and in Fig. 4.27(b) for the TSP region, respectively. The CDS results using the modified set of sorts for the data set of 25 tubes composed of the training and testing data set is shown in Table 4.2. The final results were once again exported from the *Report Editor* dialog box and converted to text format for subsequent evaluations. The columns associated with the estimated flaw depth (column 6), reporting code (column 11), and flaw origin (column 12) were manually edited to more closely match with the report entry format prescribed for manual analysis of the bobbin probe data from the SG mock-up. Most calls associated with the markers near the end of tube sections were also removed from the original list. Comparison of the results between the complete set of sorts shown in Table 4.1 and the modified sort list shown in Table 4.2 indicates that with the exception of one indication all the previously reported signals were reported using the modified settings. The primary difference between the two screening configurations is the number of redundant calls. A total of 61 calls were reported using the previous settings for the free-span and TSP regions. While nearly all flaws were detected, the total number of reported entries was reduced to 35 calls with the modified CDS configuration.

Examples of the false calls using the latest sort configuration are shown in Figs. 4.39 and 4.40. The signal associated with a dented TSP region identified as a false call is shown in Fig. 4.39(a). An example of a false call associated with baseline noise in the free-span region of the tube is shown in Fig. 4.39(b). Another set of false calls associated with a dent at a TSP elevation is shown in Fig. 4.40. Examples of missed indications at a dented TSP zone are shown in Fig. 4.41. In those cases, the flaw signal was missed due to elimination of a sort for that region of tubing. The results of these tests suggest that it is possible to achieve comparable detection probability using a smaller number of sorts. However, it should be noted that because of the statistically small number of tubes included in this study, the results may not apply to that for the entire SG mock-up.

The reduced set of sorts discussed above was next used to assess the effect of threshold values on detection. In this series of tests, the screening parameters were adjusted to simulate the influence of higher level of baseline noise on the detection and classification of signals. The *CDS Editor* dialog box for the modified sort configurations for screening of the free-span and TSP elevations of the SG mock-up are displayed in Fig. 4.42. Only the detection and classification threshold values were adjusted for these tests. As noted previously, the CDS employs separate threshold variables for the detection and the classification stages. Although reporting of a signal is commonly based on satisfying the conditions for both test logics, a signal may be reported based on the detection logic alone. The option to independently define the threshold variables thus provides more freedom with regard to adjusting the level of conservatism in reporting of signals. Figure 4.42(a) displays the modified *CDS Editor* dialog box for the free-span sort. In reference to the previous setup, the classification voltage threshold for all test channels was increased to 0.75v from its previous value of 0.5v. The parameter setting for the TSP elevations is displayed in Fig. 4.42(b). For the TSP regions the detection threshold was raised to 0.4v from its previous value of 0.2v. All other variables were kept unchanged. From a practical standpoint, the threshold values are often adjusted to compensate for changes in the level of noise present in EC inspection data and in order to achieve an acceptable balance between the detection probability and the number of false calls.

The CDS results using the modified set of sorts for the data set of 25 tubes composed of the training and testing data set is shown in Table 4.3. The columns associated with the estimated flaw depth (column 6), reporting code (column 11), and flaw origin (column 12) were manually edited to more closely match with the report entry format prescribed for manual analysis of the bobbin probe data from the SG mock-up. Most calls associated with the markers near the end of tube sections were also removed from the original list. As in the past, the final results were exported from the *Report Editor* dialog box and converted to text format. Representative cases of missed signals due to modification of the threshold values for the free-span and TSP sort configurations are shown next. Figure 4.43 shows examples of missed indications at two different TSP elevations in connection with the higher classification threshold value. The signals were measured manually following the application of CDS. The low-amplitude signal shown in Fig. 4.43(a) is associated with a shallow ODSCC near a TSP edge. The signal in Fig. 4.43(b) is associated with an ID indication at a dented TSP region with only the dent signal reported by CDS in that region. Examples of missed free-span signals are shown in Fig. 4.44. Finally, an example of a false call which was eliminated because of using the higher threshold value is shown in Fig. 4.45. In all cases the signals were missed because of using a higher threshold value for reporting of indications in the classification stage.

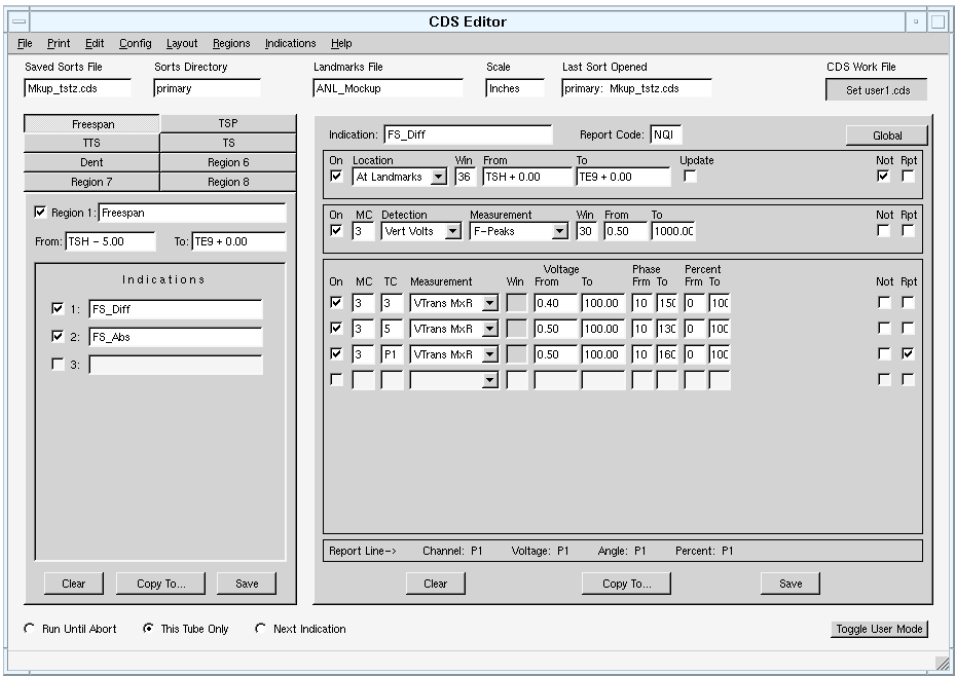

(a)

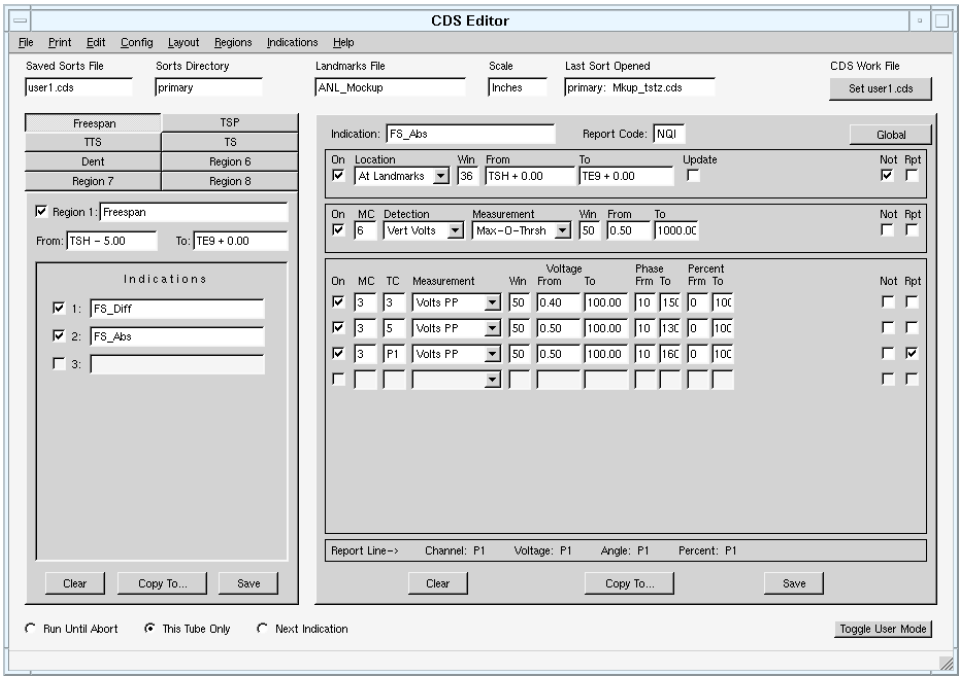

(b)

Figure 4.26 Display of the CDS Editor window used for setting up the parameters associated with the location, detection, and classification of free-span signal sorts for detection of (a) closely-spaced signals and (b) long axial signals.

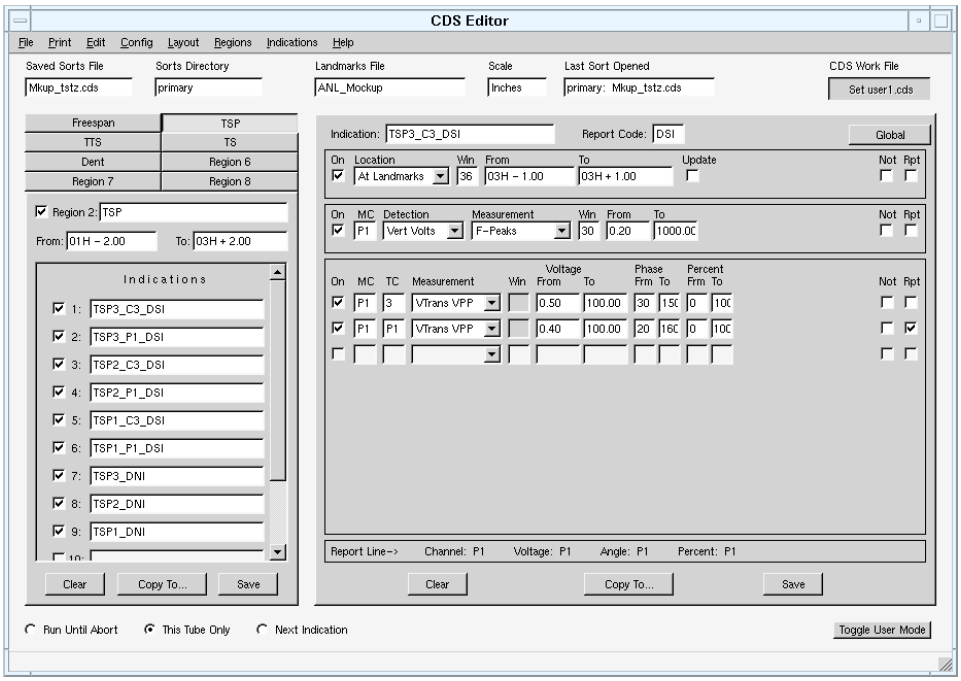

(a)

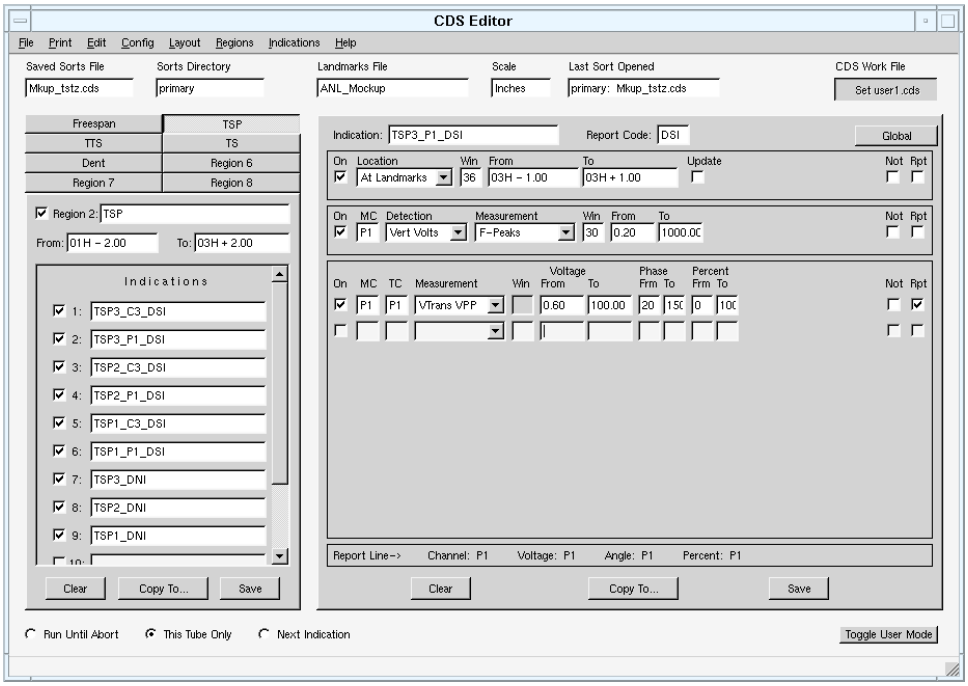

(b)

Figure 4.27 Display of the CDS Editor window used for setting up the parameters associated with the location, detection, and classification of indications at TSP elevations. Shown here are the sorts for detection of closely-spaced flaw signals at TSPs using (a) 200 kHz (channel 3) and (b) TSP suppression mix (P1) as the test channel.

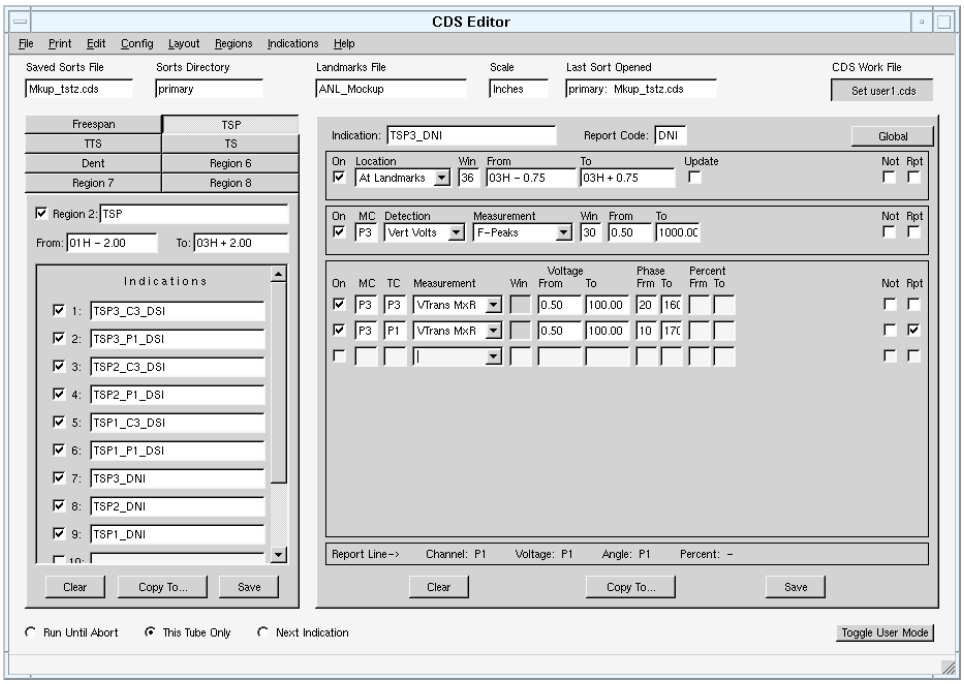

(a)

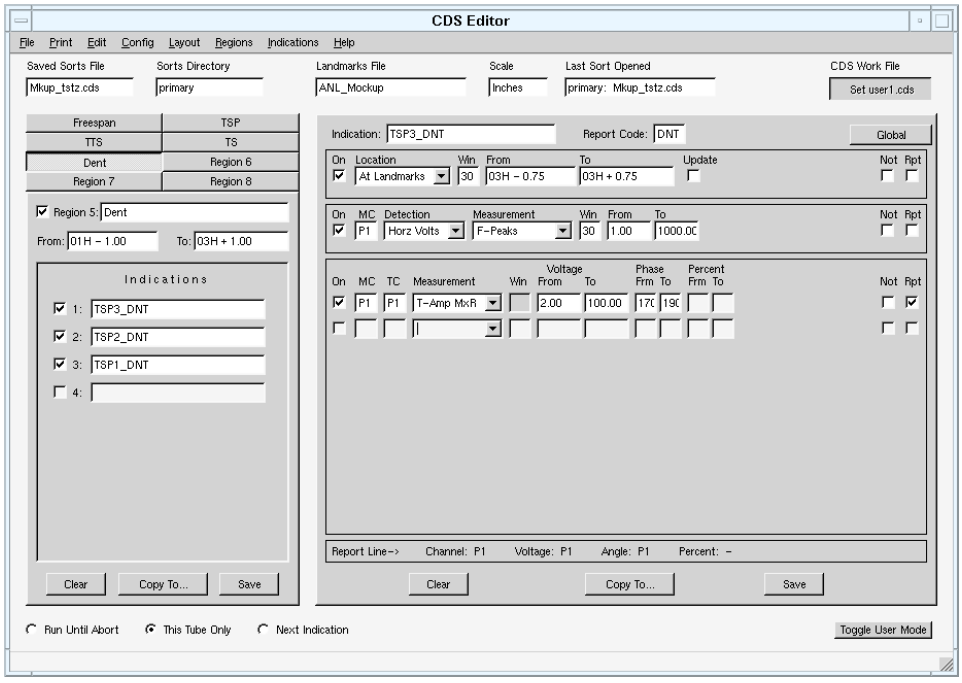

(b)

Figure 4.28 Display of the CDS Editor window used for setting up the parameters associated with the location, detection, and classification of flaw and non-flaw-like signals at TSP elevations. Shown here are the sorts for detection of (a) flaw signals at a dented TSP using TTS suppression mix (P3) for detection and (b) tube geometry change associated with denting.

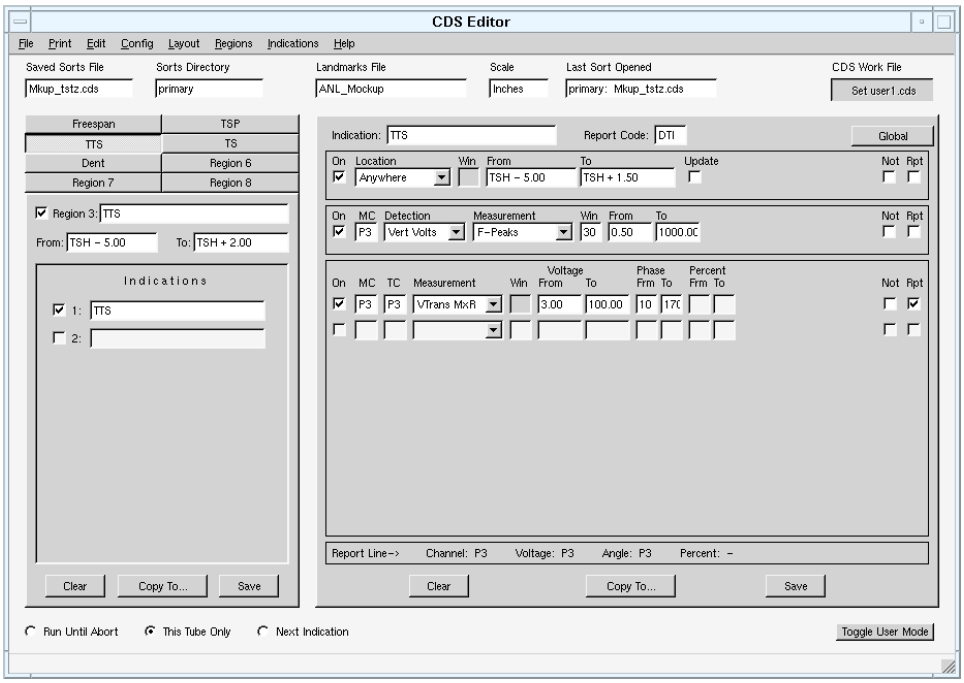

Figure 4.29 Display of the CDS Editor window used for setting up the parameters associated with the location, detection, and classification of flaw signals at or near the top of the tube-sheet.

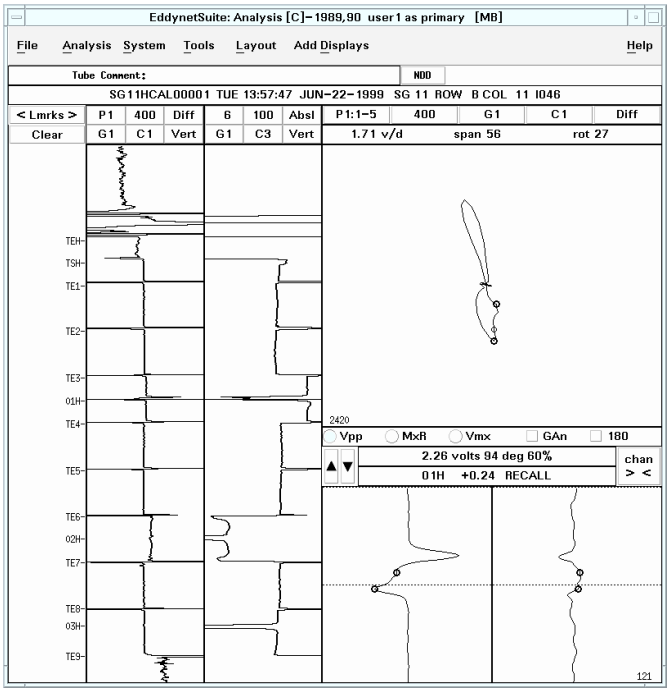

(a)

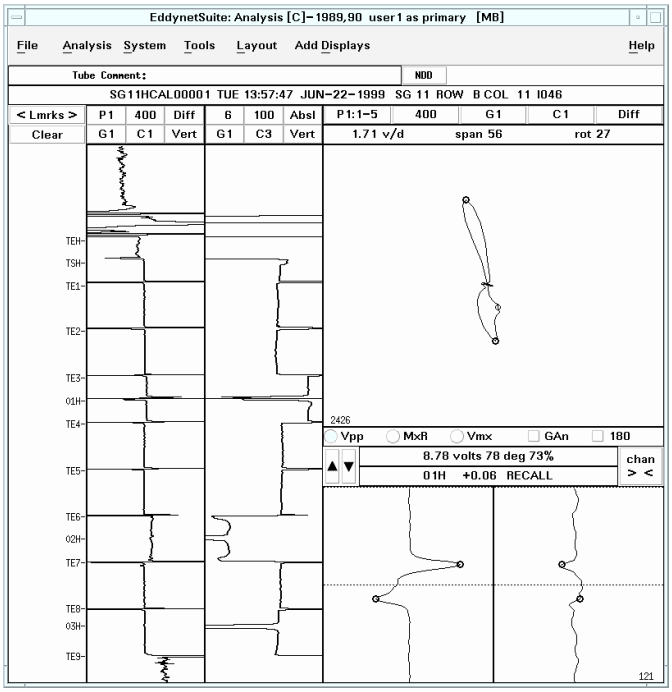

(b)

Figure 4.30 Display of the CDS results for the entire length of a mock-up tube from the test data set of a relatively long indication at the first TSP elevation, which was identified (a) as two separate signals by one sort and (b) as one signal by another sort.

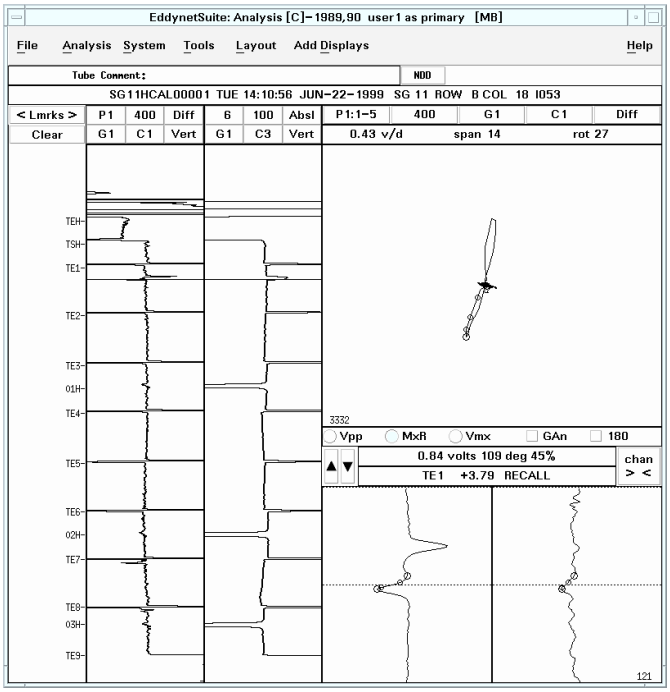

(a)

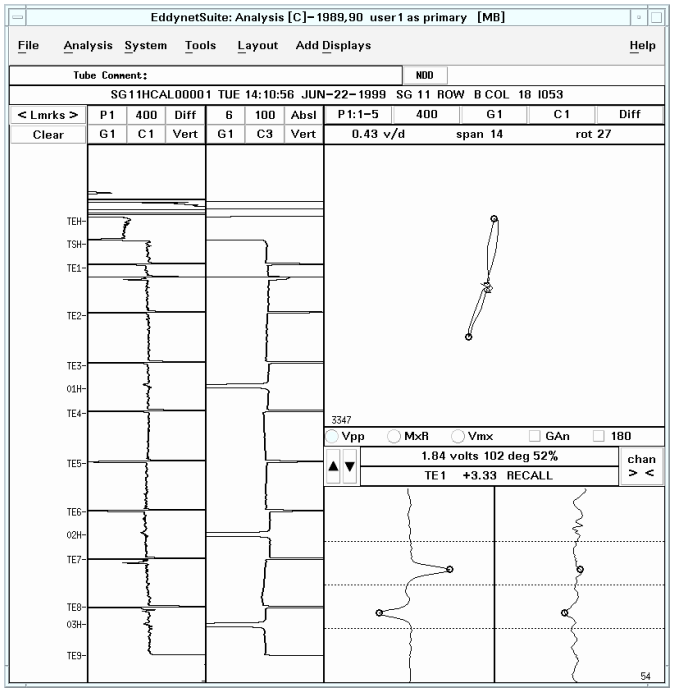

(b)

Figure 4.31 Display of the CDS results for the entire length of a mock-up tube from the test data set of a relatively long indication in the free-span, which was identified (a) as two separate signals by one sort and (b) as one signal by another sort.

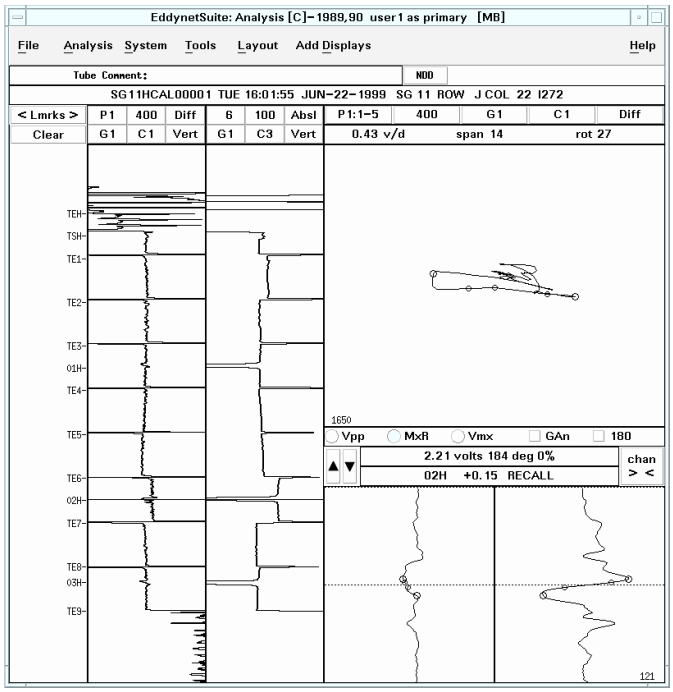

(a)

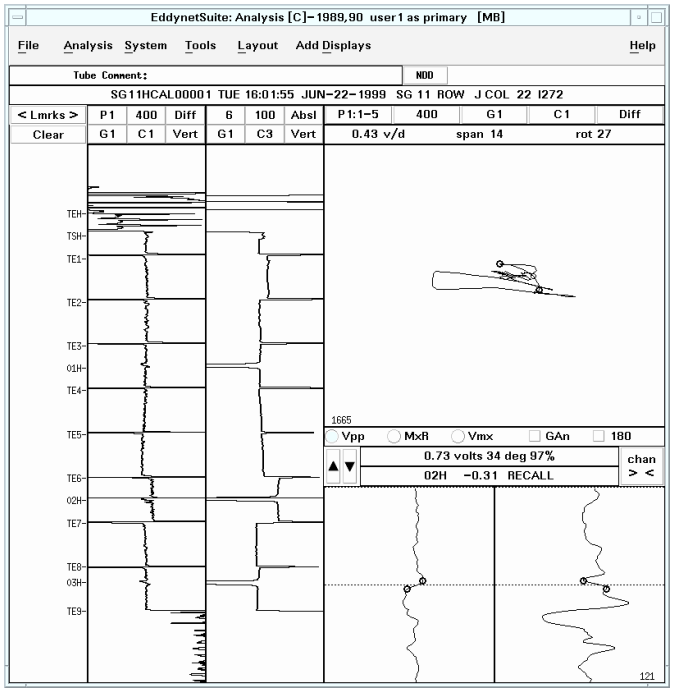

(b)

Figure 4.32 Display of the CDS results for the entire length of a mock-up tube from the test data set example of a dented TSP region with separate calls for the (a) dent by one sort and (b) potential flaw signal by another sort at the second TSP elevation.

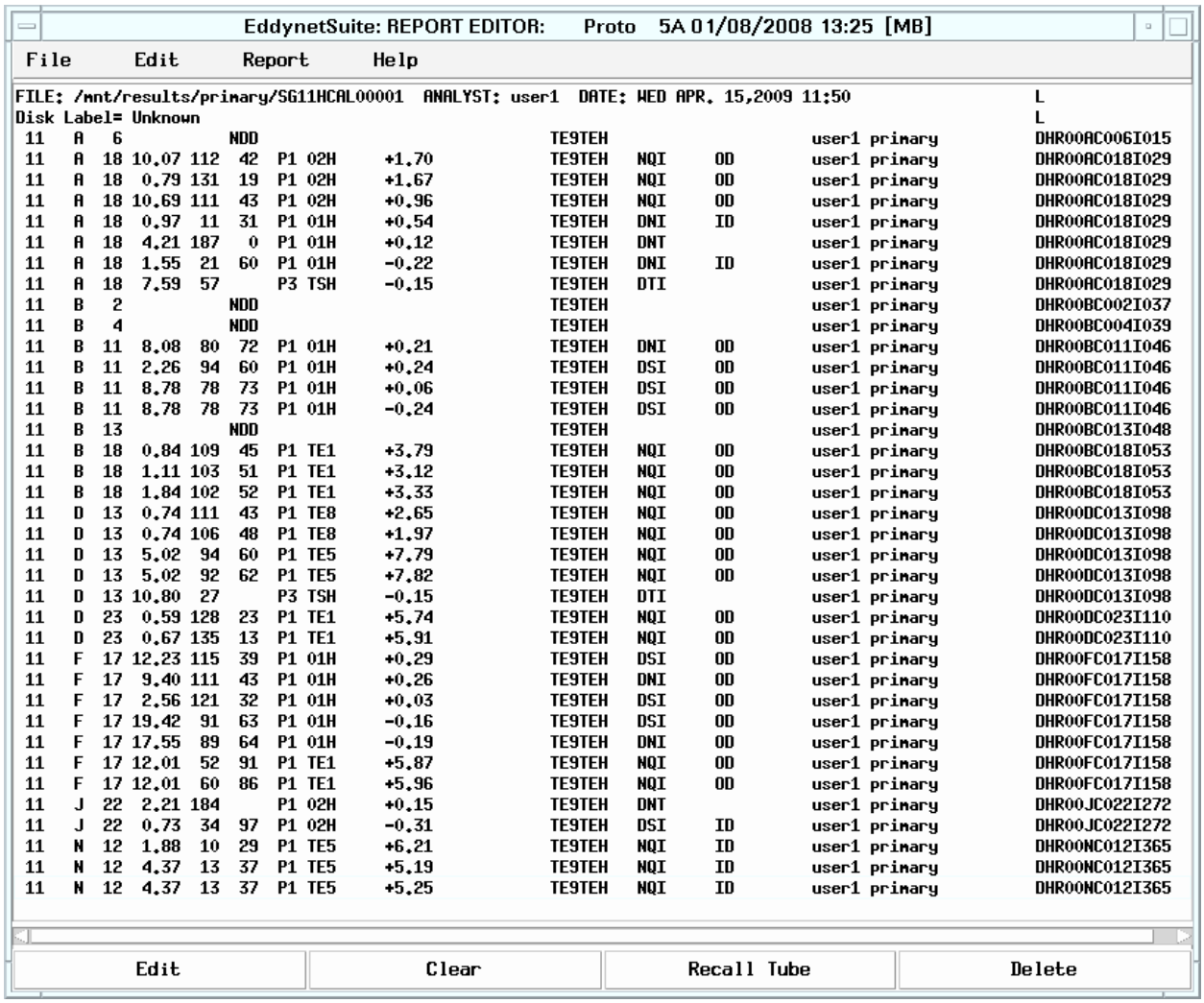

Figure 4.33 Results of the CDS process displayed by the *Report Editor* dialog box for all twelve tubes in the testing data set using the modified sorts.

Table 4.1 Tabulated results of the CDS process for combined training and testing data sets that was exported from the Eddynet™ *Report Editor* dialog box.

11	A	6			NDD				TE9TEH			user1	primary	DHR00AC006I015
11	A	9	9.22	113	41	P1	03H	-0.03	TE9TEH	DNI	OD	user1	primary	DHR00AC009I020
11	A	9	10.05	115	39	P1	03H	0	TE9TEH	DSI	OD	user1	primary	DHR00AC009I020
11	A	9	1.2	112	42	P1	TE4	6.93	TE9TEH	NQI	OD	user1	primary	DHR00AC009I020
11	A	9	3.95	75	75	P1	TE4	6.48	TE9TEH	NQI	OD	user1	primary	DHR00AC009I020
11	A	9	4.9	79	72	P1	TE4	6.54	TE9TEH	NQI	OD	user1	primary	DHR00AC009I020
11	A	9	4.9	75	75	P1	TE4	5.91	TE9TEH	NQI	OD	user1	primary	DHR00AC009I020
11	A	15	2.17	185		P1	01H	0.09	TE9TEH	DNT		user1	primary	DHR00AC015I026
11	A	15	1.19	30	86	P1	01H	-0.24	TE9TEH	DSI	ID	user1	primary	DHR00AC015I026
11	A	15	0.77	63	84	P1	01H	-0.27	TE9TEH	DNI	OD	user1	primary	DHR00AC015I026
11	A	15	14.69	33		P3	TSH	0.66	TE9TEH	DTI		user1	primary	DHR00AC015I026
11	A	15	24.64	44		P3	TSH	0	TE9TEH	DTI		user1	primary	DHR00AC015I026
11	A	18	10.07	112	42	P1	02H	1.7	TE9TEH	NQI	OD	user1	primary	DHR00AC018I029
11	A	18	0.79	131	19	P1	02H	1.67	TE9TEH	NQI	OD	user1	primary	DHR00AC018I029
11	A	18	10.69	111	43	P1	02H	0.96	TE9TEH	NQI	OD	user1	primary	DHR00AC018I029
11	A	18	0.97	11	31	P1	01H	0.54	TE9TEH	DNI	ID	user1	primary	DHR00AC018I029
11	A	18	4.21	187	0	P1	01H	0.12	TE9TEH	DNT		user1	primary	DHR00AC018I029
11	A	18	1.55	21	60	P1	01H	-0.22	TE9TEH	DNI	ID	user1	primary	DHR00AC018I029
11	A	18	7.59	57		P3	TSH	-0.15	TE9TEH	DTI		user1	primary	DHR00AC018I029
11	B	2			NDD				TE9TEH			user1	primary	DHR00BC002I037
11	B	4			NDD				TE9TEH			user1	primary	DHR00BC004I039
11	B	11	8.08	80	72	P1	01H	0.21	TE9TEH	DNI	OD	user1	primary	DHR00BC011I046
11	B	11	2.26	94	60	P1	01H	0.24	TE9TEH	DSI	OD	user1	primary	DHR00BC011I046
11	B	11	8.78	78	73	P1	01H	0.06	TE9TEH	DSI	OD	user1	primary	DHR00BC011I046
11	B	11	8.78	78	73	P1	01H	-0.24	TE9TEH	DSI	OD	user1	primary	DHR00BC011I046
11	B	13			NDD				TE9TEH			user1	primary	DHR00BC013I048
11	B	18	0.84	109	45	P1	TE1	3.79	TE9TEH	NQI	OD	user1	primary	DHR00BC018I053
11	B	18	1.11	103	51	P1	TE1	3.12	TE9TEH	NQI	OD	user1	primary	DHR00BC018I053
11	B	18	1.84	102	52	P1	TE1	3.33	TE9TEH	NQI	OD	user1	primary	DHR00BC018I053
11	D	10			NDD				TE9TEH			user1	primary	DHR00DC010I095
11	D	13	0.74	111	43	P1	TE8	2.65	TE9TEH	NQI	OD	user1	primary	DHR00DC013I098
11	D	13	0.74	106	48	P1	TE8	1.97	TE9TEH	NQI	OD	user1	primary	DHR00DC013I098
11	D	13	5.02	94	60	P1	TE5	7.83	TE9TEH	NQI	OD	user1	primary	DHR00DC013I098
11	D	13	5.02	92	62	P1	TE5	7.86	TE9TEH	NQI	OD	user1	primary	DHR00DC013I098
11	D	13	10.8	27		P3	TSH	-0.15	TE9TEH	DTI		user1	primary	DHR00DC013I098
11	D	23	0.59	128	23	P1	TE1	5.74	TE9TEH	NQI	OD	user1	primary	DHR00DC023I110
11	D	23	0.67	135	13	P1	TE1	5.91	TE9TEH	NQI	OD	user1	primary	DHR00DC023I110
11	E	9			NDD				TE9TEH			user1	primary	DHR00EC009I123
11	F	17	12.23	115	39	P1	01H	0.29	TE9TEH	DSI	OD	user1	primary	DHR00FC017I158
11	F	17	9.4	111	43	P1	01H	0.26	TE9TEH	DNI	OD	user1	primary	DHR00FC017I158
11	F	17	2.56	121	32	P1	01H	0.03	TE9TEH	DSI	OD	user1	primary	DHR00FC017I158
11	F	17	19.42	91	63	P1	01H	-0.16	TE9TEH	DSI	OD	user1	primary	DHR00FC017I158
11	F	17	17.55	89	64	P1	01H	-0.19	TE9TEH	DNI	OD	user1	primary	DHR00FC017I158
11	F	17	12.01	52	91	P1	TE1	5.87	TE9TEH	NQI	OD	user1	primary	DHR00FC017I158
11	F	17	12.01	60	86	P1	TE1	5.96	TE9TEH	NQI	OD	user1	primary	DHR00FC017I158
11	F	22	3.17	181		P1	01H	0.11	TE9TEH	DNT		user1	primary	DHR00FC022I163
11	F	22	0.52	20	57	P1	TE3	5.36	TE9TEH	DNI	ID	user1	primary	DHR00FC022I163
11	G	8	1.19	12	34	P1	TE3	2.37	TE9TEH	NQI	ID	user1	primary	DHR00GC008I174
11	G	8	28.75	70		P3	TSH	0.18	TE9TEH	DTI		user1	primary	DHR00GC008I174
11	G	8	53.82	62		P3	TSH	-0.15	TE9TEH	DTI		user1	primary	DHR00GC008I174
11	G	13	5.21	26		P3	TEH	5.37	TE9TEH	DTI		user1	primary	DHR00GC013I181
11	G	13	5.21	26		P3	TEH	5.31	TE9TEH	DTI		user1	primary	DHR00GC013I181
11	G	13	4.12	19		P3	TEH	1.3	TE9TEH	DTI		user1	primary	DHR00GC013I181
11	G	14	1.21	149	0	P1	TE2	6.32	TE9TEH	NQI	OD	user1	primary	DHR00GC014I182
11	G	14	1.33	139	7	P1	TE2	5.77	TE9TEH	NQI	OD	user1	primary	DHR00GC014I182
11	G	14	2.35	137	10	P1	TE2	5.95	TE9TEH	NQI	OD	user1	primary	DHR00GC014I182
11	G	14	0.92	148	0	P1	TE1	6	TE9TEH	NQI	OD	user1	primary	DHR00GC014I182
11	G	14	0.9	142	2	P1	TE1	5.97	TE9TEH	NQI	OD	user1	primary	DHR00GC014I182
11	G	14	9.26	27		P3	TSH	-0.52	TE9TEH	DTI		user1	primary	DHR00GC014I182
11	H	11	4.13	128	23	P1	03H	1.01	TE9TEH	DSI	OD	user1	primary	DHR00HC011I204
11	H	11	4.13	128	23	P1	03H	0.83	TE9TEH	DSI	OD	user1	primary	DHR00HC011I204
11	H	11	2.59	122	30	P1	03H	1.07	TE9TEH	NQI	OD	user1	primary	DHR00HC011I204
11	H	11	5.83	33		P3	TSH	-0.18	TE9TEH	DTI		user1	primary	DHR00HC011I204
11	J	14	0.98	146	0	P1	03H	0.73	TE9TEH	DSI	OD	user1	primary	DHR00JC014I264
11	J	14	0.82	165	0	P1	03H	0.67	TE9TEH	DNI	OD	user1	primary	DHR00JC014I264
11	J	14	0.54	158	0	P1	03H	0.38	TE9TEH	DSI	OD	user1	primary	DHR00JC014I264
11	J	14	1.95	128	23	P1	03H	-0.13	TE9TEH	DSI	OD	user1	primary	DHR00JC014I264
11	J	14	1.88	141	4	P1	03H	-0.16	TE9TEH	DNI	OD	user1	primary	DHR00JC014I264
11	J	22	2.21	184		P1	02H	0.15	TE9TEH	DNT		user1	primary	DHR00JC022I272
11	J	22	0.73	34	97	P1	02H	-0.31	TE9TEH	DSI	ID	user1	primary	DHR00JC022I272
11	K	13	1.64	74	76	P1	03H	0.03	TE9TEH	DSI	OD	user1	primary	DHR00KC013I291
11	K	13	1.48	74	76	P1	03H	0	TE9TEH	DNI	OD	user1	primary	DHR00KC013I291
11	K	13	2.18	136	11	P1	03H	-0.24	TE9TEH	DSI	OD	user1	primary	DHR00KC013I291
11	K	13	1.94	133	16	P1	03H	-0.27	TE9TEH	DNI	OD	user1	primary	DHR00KC013I291
11	K	13	0.4	139	7	P1	TE6	5.47	TE9TEH	DSI	OD	user1	primary	DHR00KC013I291
11	M	4	3.42	22		P3	TSH	0.86	TE9TEH	DTI		user1	primary	DHR00MC004I332
11	M	4	32.47	50		P3	TSH	0.03	TE9TEH	DTI		user1	primary	DHR00MC004I332
11	N	12	1.88	10	29	P1	TE5	6.21	TE9TEH	NQI	ID	user1	primary	DHR00NC012I365
11	N	12	4.37	13	37	P1	TE5	5.19	TE9TEH	NQI	ID	user1	primary	DHR00NC012I365
11	N	12	4.37	13	37	P1	TE5	5.25	TE9TEH	NQI	ID	user1	primary	DHR00NC012I365
11	N	18	5.36	26		P3	TSH	-0.09	TE9TEH	DTI		user1	primary	DHR00NC018I371

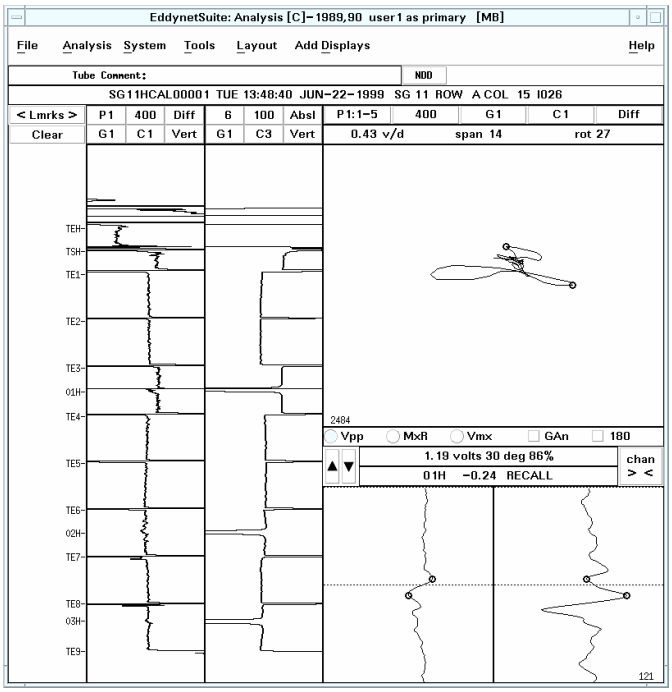

(a)

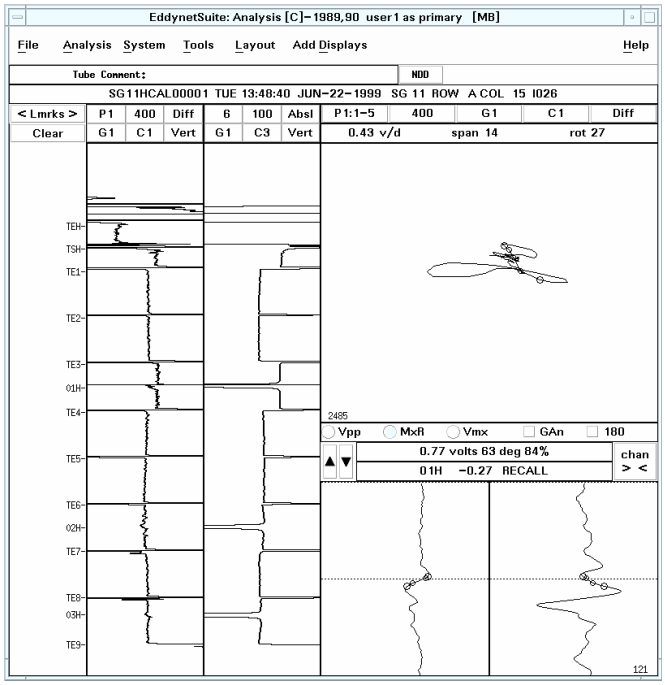

(b)

Figure 4.34 Display of the CDS results for a mock-up tube with an indication at a dented TSP region, which was classified as (a) a 1.19v ID indication by one sort and (b) a 0.77v OD indication by another sort.

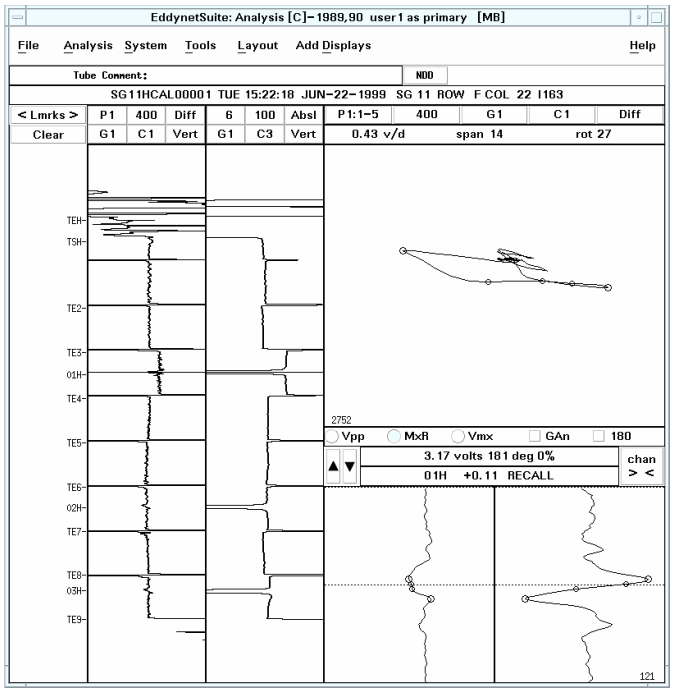

(a)

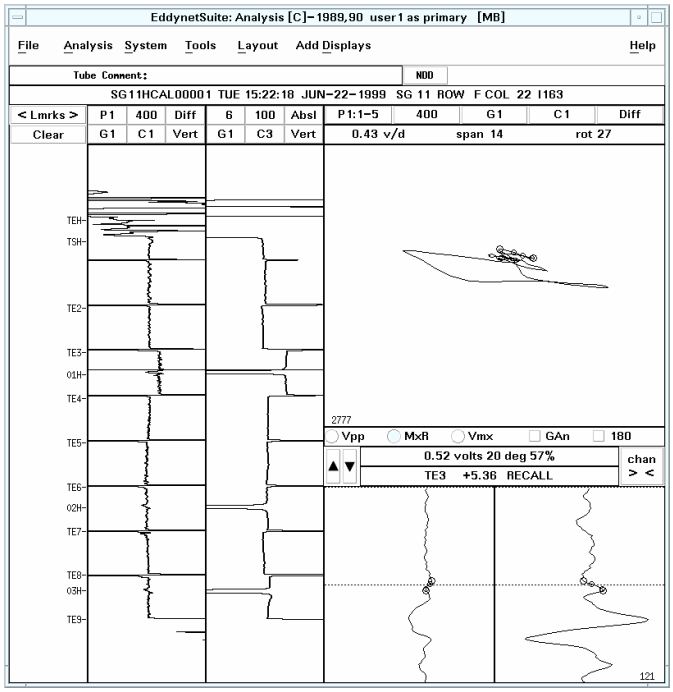

(b)

Figure 4.35 Display of the CDS results for a mock-up tube with an indication at a dented TSP region with separate calls for the (a) dent by one sort and (b) an ID flaw signal by another sort.

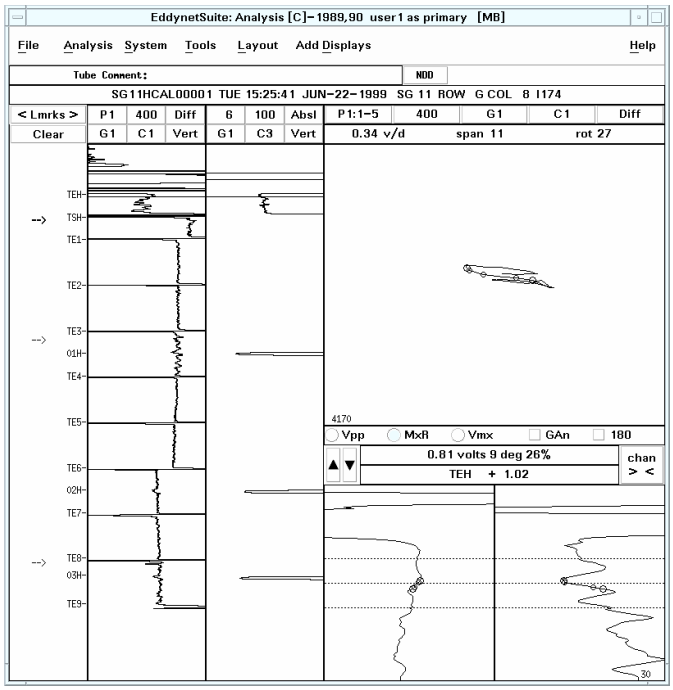

(a)

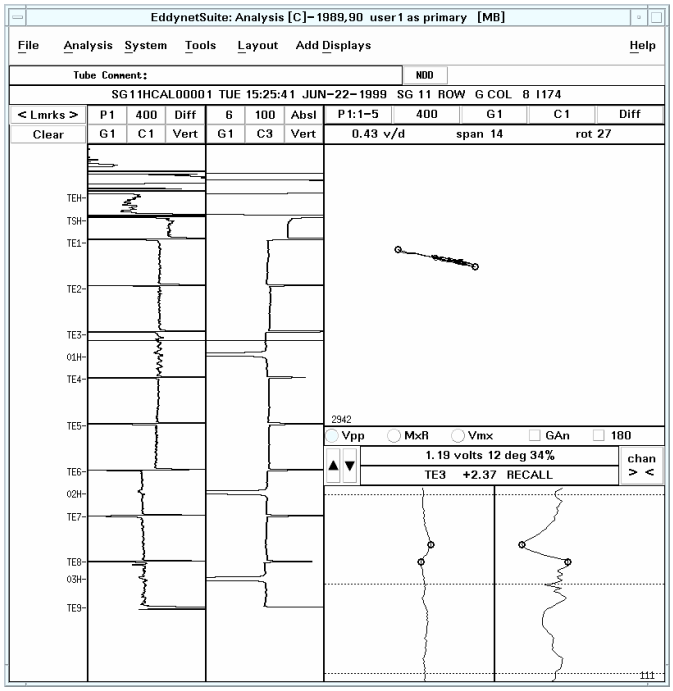

(b)

Figure 4.36 Display of (a) the CDS results for the entire length of a mock-up tube and (b) baseline noise at the fourth tube section.

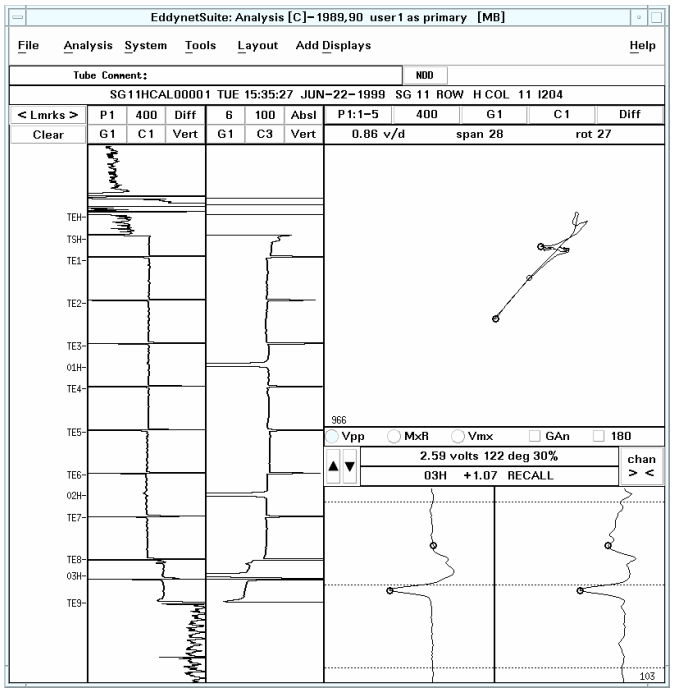

(a)

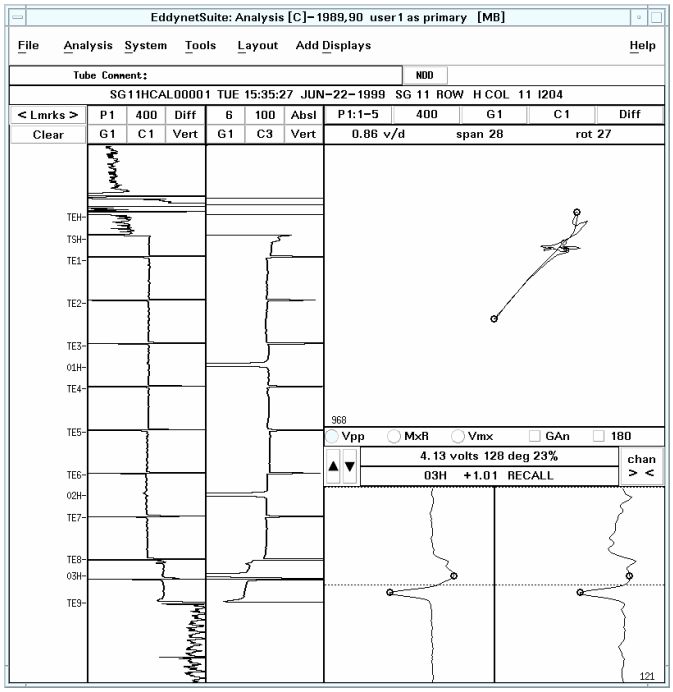

(b)

Figure 4.37 Display of the CDS results for a mock-up tube with an indication near a TSP edge. The measured signal amplitude varies between (a) 2.59v by free-span sort and (b) 4.13v by TSP sort.

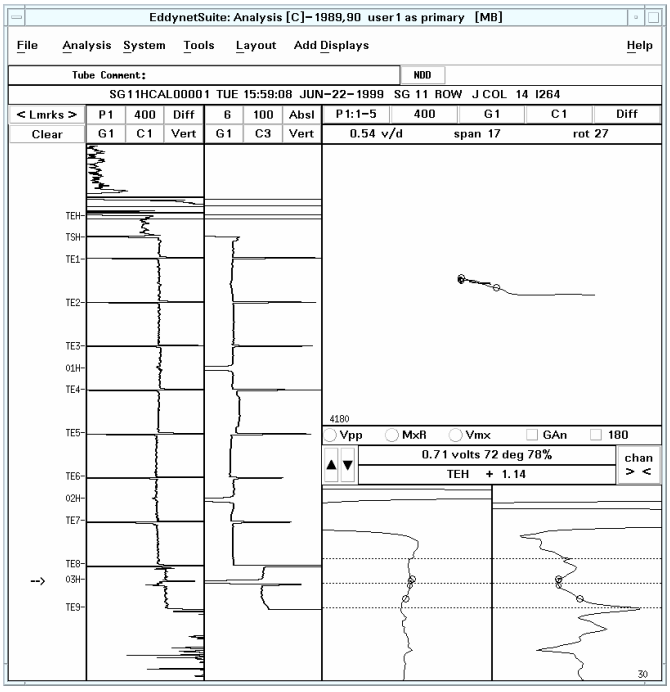

(a)

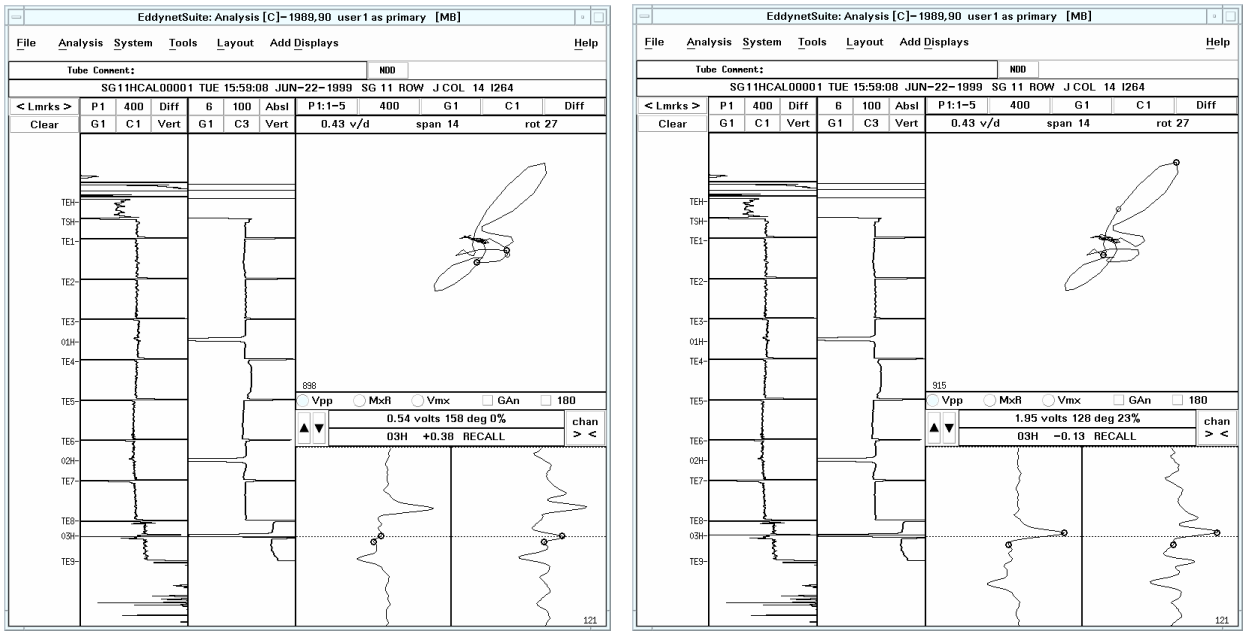

(b)

Figure 4.38 (a) Display of the CDS results for the entire length of a mock-up tube (b) Five separate entries were made for the same signal associated with an indication near a TSP edge by different sorts with the measured signal amplitude varying between 0.54v and 1.95v.

Table 4.2 Results of the CDS process using the modified sorts for the combined training and testing data sets.

11	A	6	3.17	32		P3	TEH	5.32	TE9TEH	DTI		user1	primary	DHR00AC006I015
11	A	9	10.05	115	39	P1	03H	0	TE9TEH	DSI	OD	user1	primary	DHR00AC009I020
11	A	9	1.2	112	42	P1	TE4	6.93	TE9TEH	NQI	OD	user1	primary	DHR00AC009I020
11	A	9	3.95	75	75	P1	TE4	6.48	TE9TEH	NQI	OD	user1	primary	DHR00AC009I020
11	A	9	4.9	75	75	P1	TE4	5.91	TE9TEH	NQI	OD	user1	primary	DHR00AC009I020
11	A	15	2.17	185		P1	01H	0.09	TE9TEH	DNT		user1	primary	DHR00AC015I026
11	A	15	1.19	30	86	P1	01H	-0.24	TE9TEH	DSI	ID	user1	primary	DHR00AC015I026
11	A	15	14.69	33		P3	TSH	0.66	TE9TEH	DTI		user1	primary	DHR00AC015I026
11	A	15	24.64	44		P3	TSH	0	TE9TEH	DTI		user1	primary	DHR00AC015I026
11	A	18	0.79	131	19	P1	02H	1.85	TE9TEH	NQI	OD	user1	primary	DHR00AC018I029
11	A	18	10.6	109	45	P1	02H	1.17	TE9TEH	NQI	OD	user1	primary	DHR00AC018I029
11	A	18	4.21	187	0	P1	01H	0.12	TE9TEH	DNT		user1	primary	DHR00AC018I029
11	A	18	7.59	57		P3	TSH	-0.15	TE9TEH	DTI		user1	primary	DHR00AC018I029
11	B	2			NDD				TE9TEH			user1	primary	DHR00BC002I037
11	B	4			NDD				TE9TEH			user1	primary	DHR00BC004I039
11	B	11	2.26	94	60	P1	01H	0.24	TE9TEH	DSI	OD	user1	primary	DHR00BC011I046
11	B	11	8.78	78	73	P1	01H	-0.24	TE9TEH	DSI	OD	user1	primary	DHR00BC011I046
11	B	13			NDD				TE9TEH			user1	primary	DHR00BC013I048
11	B	18	0.84	109	45	P1	TE1	3.79	TE9TEH	NQI	OD	user1	primary	DHR00BC018I053
11	B	18	1.11	103	51	P1	TE1	3.12	TE9TEH	NQI	OD	user1	primary	DHR00BC018I053
11	D	10			NDD				TE9TEH			user1	primary	DHR00DC010I095
11	D	13	0.74	111	43	P1	TE8	2.67	TE9TEH	NQI	OD	user1	primary	DHR00DC013I098
11	D	13	0.74	106	48	P1	TE8	1.99	TE9TEH	NQI	OD	user1	primary	DHR00DC013I098
11	D	13	5.02	94	60	P1	TE5	7.77	TE9TEH	NQI	OD	user1	primary	DHR00DC013I098
11	D	13	10.8	27		P3	TSH	-0.12	TE9TEH	DTI		user1	primary	DHR00DC013I098
11	D	23	0.59	128	23	P1	TE1	5.67	TE9TEH	NQI	OD	user1	primary	DHR00DC023I110
11	D	23	4.42	29		P3	TEH	5.36	TE9TEH	DTI		user1	primary	DHR00DC023I110
11	E	9			NDD				TE9TEH			user1	primary	DHR00EC009I123
11	F	17	12.23	115	39	P1	01H	0.32	TE9TEH	DSI	OD	user1	primary	DHR00FC017I158
11	F	17	2.56	121	32	P1	01H	0.06	TE9TEH	DSI	OD	user1	primary	DHR00FC017I158
11	F	17	19.42	91	63	P1	01H	-0.13	TE9TEH	DSI	OD	user1	primary	DHR00FC017I158
11	F	17	12.01	52	91	P1	TE1	5.87	TE9TEH	NQI	OD	user1	primary	DHR00FC017I158
11	F	22	3.17	181		P1	01H	0.11	TE9TEH	DNT		user1	primary	DHR00FC022I163
11	G	8	28.75	70		P3	TSH	0.18	TE9TEH	DTI		user1	primary	DHR00GC008I174
11	G	8	53.82	62		P3	TSH	-0.15	TE9TEH	DTI		user1	primary	DHR00GC008I174
11	G	13	5.21	26		P3	TEH	5.37	TE9TEH	DTI		user1	primary	DHR00GC013I181
11	G	13	5.21	26		P3	TEH	5.31	TE9TEH	DTI		user1	primary	DHR00GC013I181
11	G	13	4.12	19		P3	TEH	1.3	TE9TEH	DTI		user1	primary	DHR00GC013I181
11	G	14	1.21	149	0	P1	TE2	6.32	TE9TEH	NQI	OD	user1	primary	DHR00GC014I182
11	G	14	1.33	139	7	P1	TE2	5.77	TE9TEH	NQI	OD	user1	primary	DHR00GC014I182
11	G	14	0.9	142	2	P1	TE1	5.97	TE9TEH	NQI	OD	user1	primary	DHR00GC014I182
11	G	14	9.26	27		P3	TSH	-0.52	TE9TEH	DTI		user1	primary	DHR00GC014I182
11	H	11	4.13	128	23	P1	03H	1.01	TE9TEH	DSI	OD	user1	primary	DHR00HC011I204
11	H	11	4.08	133	16	P1	03H	1.07	TE9TEH	NQI	OD	user1	primary	DHR00HC011I204
11	H	11	5.83	33		P3	TSH	-0.18	TE9TEH	DTI		user1	primary	DHR00HC011I204
11	J	14	0.98	146	0	P1	03H	0.73	TE9TEH	DSI	OD	user1	primary	DHR00JC014I264
11	J	14	1.95	128	23	P1	03H	-0.13	TE9TEH	DSI	OD	user1	primary	DHR00JC014I264
11	J	22	2.21	184		P1	02H	0.15	TE9TEH	DNT		user1	primary	DHR00JC022I272
11	J	22	0.73	34	97	P1	02H	-0.31	TE9TEH	DSI	OD	user1	primary	DHR00JC022I272
11	K	13	1.64	74	76	P1	03H	0.03	TE9TEH	DSI	OD	user1	primary	DHR00KC013I291
11	K	13	2.18	136	11	P1	03H	-0.24	TE9TEH	DSI	OD	user1	primary	DHR00KC013I291
11	M	4	3.42	22		P3	TSH	0.86	TE9TEH	DTI		user1	primary	DHR00MC004I332
11	M	4	32.47	50		P3	TSH	0.03	TE9TEH	DTI		user1	primary	DHR00MC004I332
11	N	12	1.88	10	29	P1	TE5	6.18	TE9TEH	NQI	ID	user1	primary	DHR00NC012I365
11	N	12	4.37	13	37	P1	TE5	5.16	TE9TEH	NQI	ID	user1	primary	DHR00NC012I365
11	N	18	5.36	26		P3	TSH	-0.09	TE9TEH	DTI		user1	primary	DHR00NC018I371

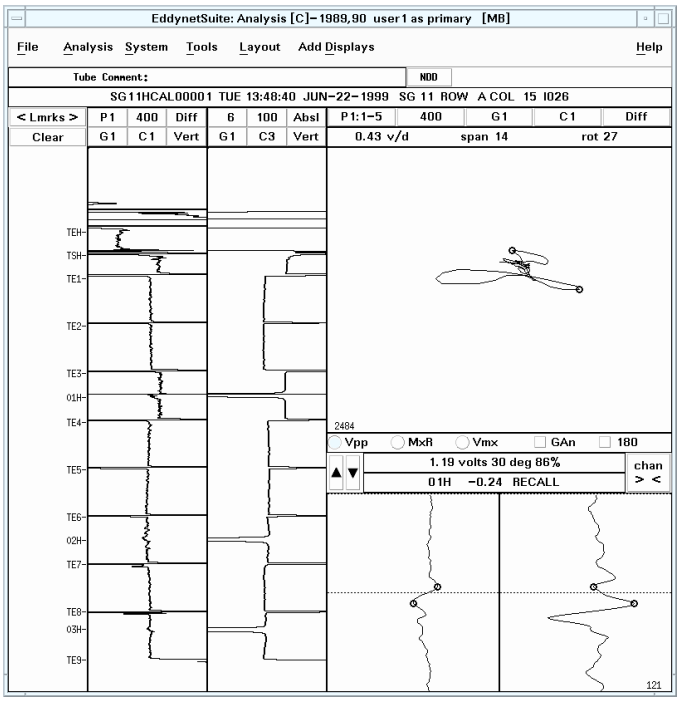

(a)

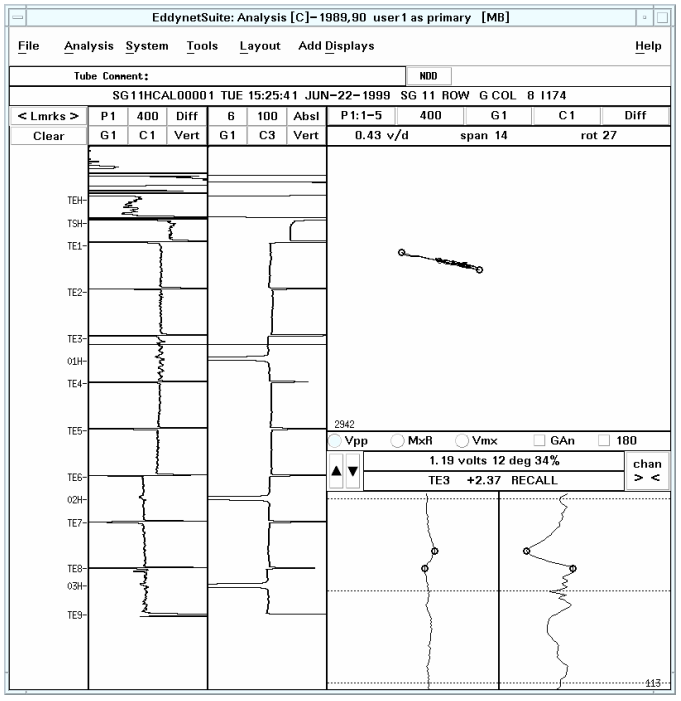

(b)

Figure 4.39 Display of the CDS results for (a) dented TSP and (b) baseline noise in the free-span region of the tube.

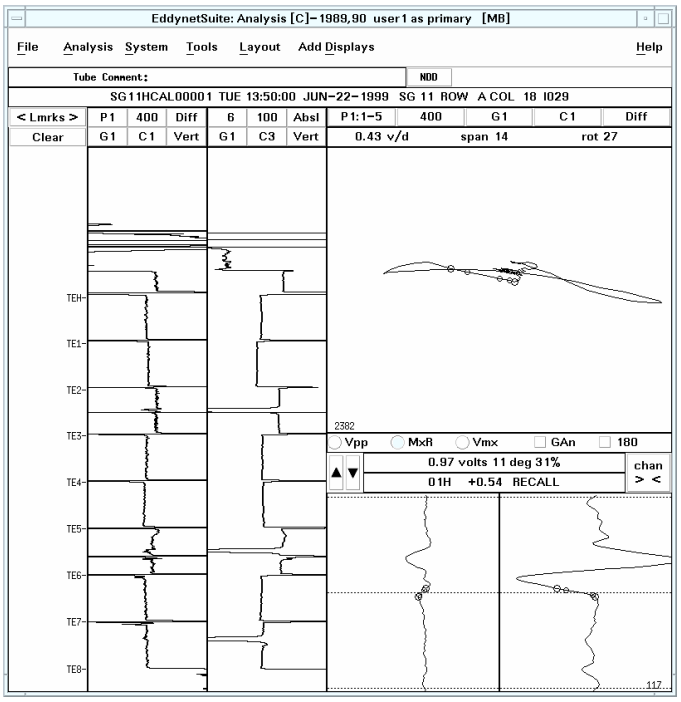

(a)

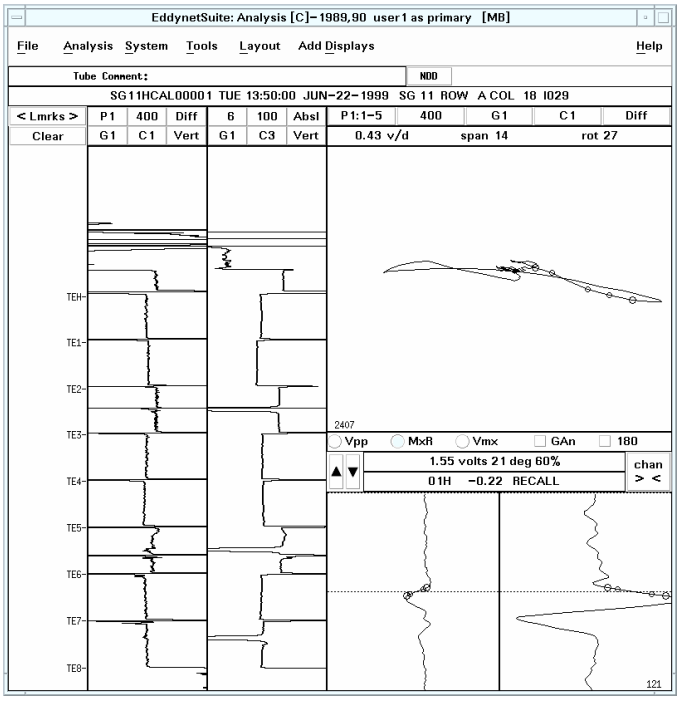

(b)

Figure 4.40 Display of the CDS results for (a) the left excursion and (b) the right excursion of a differential signal associated with a dent at a TSP elevation.

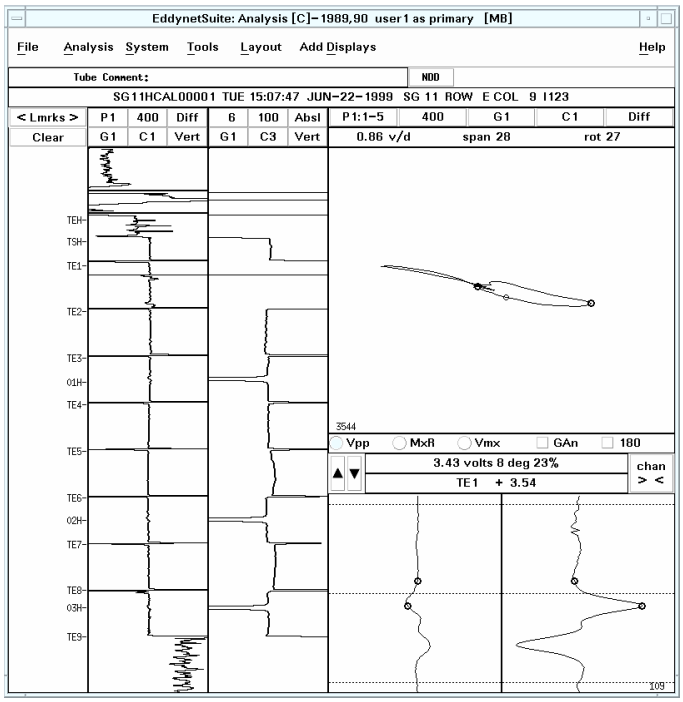

(a)

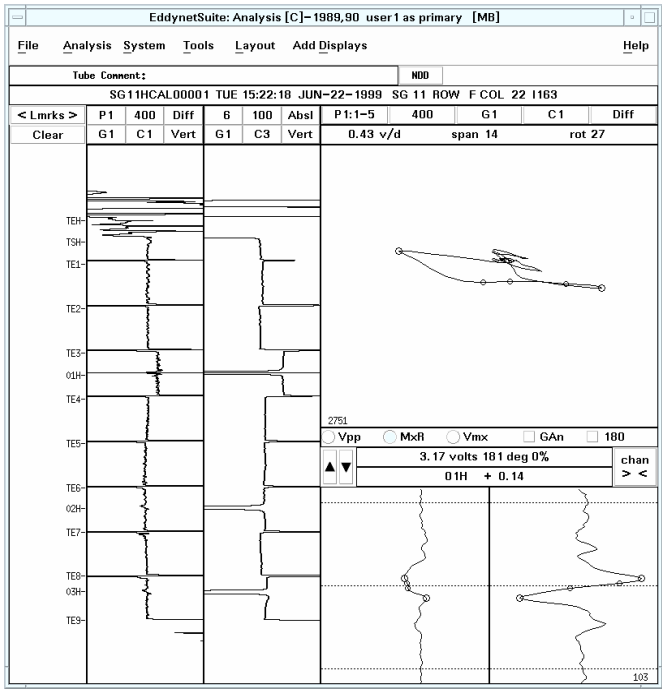

(b)

Figure 4.41 Display of manual data analysis results of ID indications at (a) dented free-span (ding) and (b) dented TSP elevation.

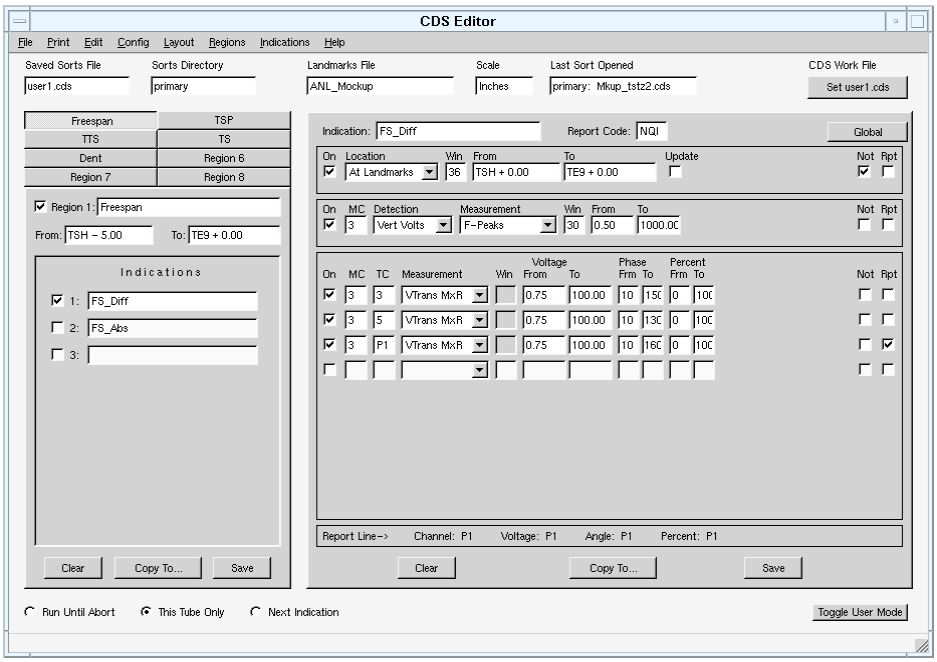

(a)

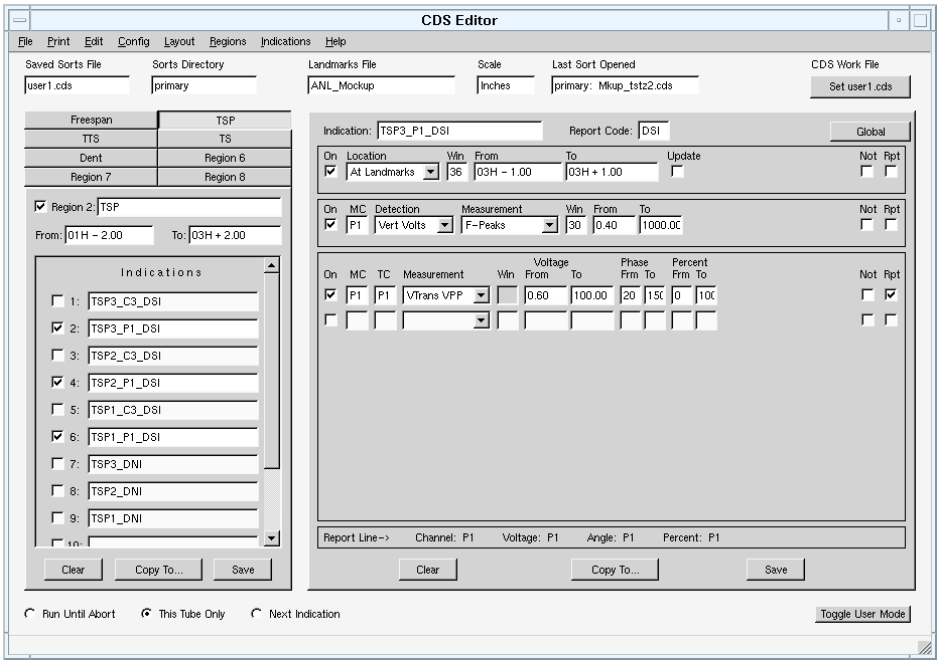

(b)

Figure 4.42 Display of the CDS Editor dialog box used for setting up the parameters associated with the location, detection, and classification of flaws in the tube bundle mock-up. Shown here are the modified (a) free-span and (b) TSP sorts with a reduced number of successive screening configurations for the same region of the tube.

Table 4.3 Results of the CDS process using the modified sorts for the combined training and testing data sets, which was exported from the *Report Editor* dialog box and converted to text format.

11	A	6	3.17	32	DTI	P3	TEH	5.32	TE9TEH	user1	primary	DHR00AC006I015
11	A	9	10.05	115	DSI	P1	03H	0	TE9TEH	user1	primary	DHR00AC009I020
11	A	9	1.2	112	NQI	P1	TE4	6.93	TE9TEH	user1	primary	DHR00AC009I020
11	A	9	3.95	75	NQI	P1	TE4	6.48	TE9TEH	user1	primary	DHR00AC009I020
11	A	9	4.9	75	NQI	P1	TE4	5.91	TE9TEH	user1	primary	DHR00AC009I020
11	A	15	2.17	185	DNT	P1	01H	0.09	TE9TEH	user1	primary	DHR00AC015I026
11	A	15	14.69	33	DTI	P3	TSH	0.66	TE9TEH	user1	primary	DHR00AC015I026
11	A	15	24.64	44	DTI	P3	TSH	0	TE9TEH	user1	primary	DHR00AC015I026
11	A	18	0.79	131	NQI	P1	02H	1.67	TE9TEH	user1	primary	DHR00AC018I029
11	A	18	10.69	111	DSI	P1	02H	0.96	TE9TEH	user1	primary	DHR00AC018I029
11	A	18	4.21	187	DNT	P1	01H	0.12	TE9TEH	user1	primary	DHR00AC018I029
11	A	18	7.59	57	DTI	P3	TSH	-0.12	TE9TEH	user1	primary	DHR00AC018I029
11	B	2			NDD				TE9TEH	user1	primary	DHR00BC002I037
11	B	4			NDD				TE9TEH	user1	primary	DHR00BC004I039
11	B	11	2.26	94	DSI	P1	01H	0.24	TE9TEH	user1	primary	DHR00BC011I046
11	B	11	8.78	78	DSI	P1	01H	-0.24	TE9TEH	user1	primary	DHR00BC011I046
11	B	13			NDD				TE9TEH	user1	primary	DHR00BC013I048
11	B	18	0.84	109	NQI	P1	TE1	3.79	TE9TEH	user1	primary	DHR00BC018I053
11	B	18	1.11	103	NQI	P1	TE1	3.12	TE9TEH	user1	primary	DHR00BC018I053
11	D	10			NDD				TE9TEH	user1	primary	DHR00DC010I095
11	D	13	5.02	94	NQI	P1	TE5	7.77	TE9TEH	user1	primary	DHR00DC013I098
11	D	13	10.8	27	DTI	P3	TSH	-0.15	TE9TEH	user1	primary	DHR00DC013I098
11	D	23	4.42	29	DTI	P3	TSH	-0.49	TE9TEH	user1	primary	DHR00DC023I110
11	E	9			NDD				TE9TEH	user1	primary	DHR00EC009I123
11	F	17	12.23	115	DSI	P1	01H	0.29	TE9TEH	user1	primary	DHR00FC017I158
11	F	17	2.56	121	DSI	P1	01H	0.03	TE9TEH	user1	primary	DHR00FC017I158
11	F	17	19.42	91	DSI	P1	01H	-0.16	TE9TEH	user1	primary	DHR00FC017I158
11	F	17	12.01	52	NQI	P1	TE1	5.87	TE9TEH	user1	primary	DHR00FC017I158
11	F	22	3.17	181	DNT	P1	01H	0.12	TE9TEH	user1	primary	DHR00FC022I163
11	G	8	28.75	70	DTI	P3	TSH	0.15	TE9TEH	user1	primary	DHR00GC008I174
11	G	8	53.82	62	DTI	P3	TSH	-0.18	TE9TEH	user1	primary	DHR00GC008I174
11	G	13	5.21	26	DTI	P3	TEH	5.37	TE9TEH	user1	primary	DHR00GC013I181
11	G	13	5.21	26	DTI	P3	TEH	5.31	TE9TEH	user1	primary	DHR00GC013I181
11	G	13	4.12	19	DTI	P3	TEH	1.3	TE9TEH	user1	primary	DHR00GC013I181
11	G	14	1.21	149	NQI	P1	TE2	6.32	TE9TEH	user1	primary	DHR00GC014I182
11	G	14	1.33	139	NQI	P1	TE2	5.77	TE9TEH	user1	primary	DHR00GC014I182
11	G	14	0.9	142	NQI	P1	TE1	5.97	TE9TEH	user1	primary	DHR00GC014I182
11	G	14	9.26	27	DTI	P3	TSH	-0.52	TE9TEH	user1	primary	DHR00GC014I182
11	H	11	4.13	128	DSI	P1	03H	0.86	TE9TEH	user1	primary	DHR00HC011I204
11	H	11	5.83	33	DTI	P3	TSH	-0.18	TE9TEH	user1	primary	DHR00HC011I204
11	J	14	0.98	146	DSI	P1	03H	0.73	TE9TEH	user1	primary	DHR00JC014I264
11	J	14	1.95	128	DSI	P1	03H	-0.13	TE9TEH	user1	primary	DHR00JC014I264
11	J	22	2.21	184	DNT	P1	02H	0.15	TE9TEH	user1	primary	DHR00JC022I272
11	K	13	1.64	74	DSI	P1	03H	0.06	TE9TEH	user1	primary	DHR00KC013I291
11	K	13	2.18	136	DSI	P1	03H	-0.22	TE9TEH	user1	primary	DHR00KC013I291
11	M	4	3.42	22	DTI	P3	TSH	0.86	TE9TEH	user1	primary	DHR00MC004I332
11	M	4	32.47	50	DTI	P3	TSH	0.03	TE9TEH	user1	primary	DHR00MC004I332
11	N	12	1.88	10	NQI	P1	TE5	6.21	TE9TEH	user1	primary	DHR00NC012I365
11	N	12	4.37	13	NQI	P1	TE5	5.19	TE9TEH	user1	primary	DHR00NC012I365
11	N	18	5.36	26	DTI	P3	TSH	-0.09	TE9TEH	user1	primary	DHR00NC018I371

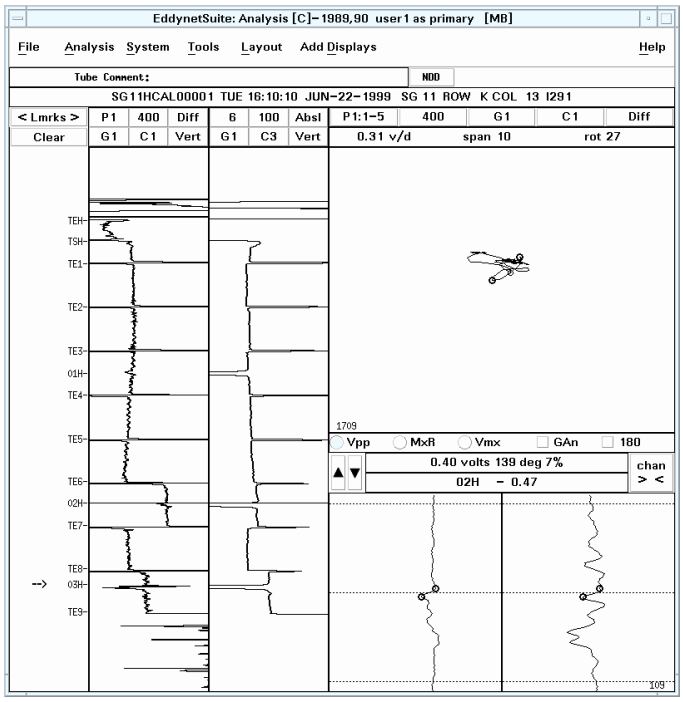

(a)

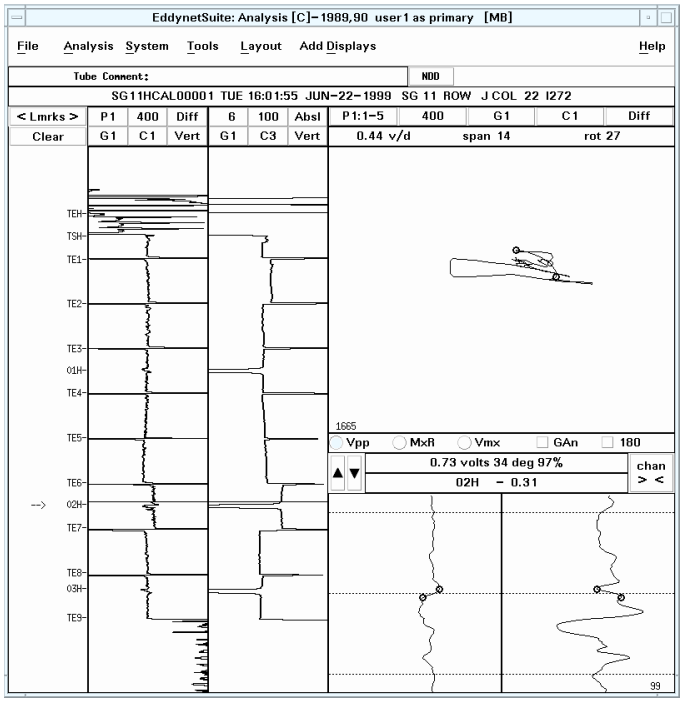

(b)

Figure 4.43 Display of the CDS results for representative SG mock-up tubes with missed calls at TSP elevations due to an increase in the detection threshold. The displayed signals, measured manually, are associated with (a) a shallow OD and (b) an ID indication at different TSP elevations.

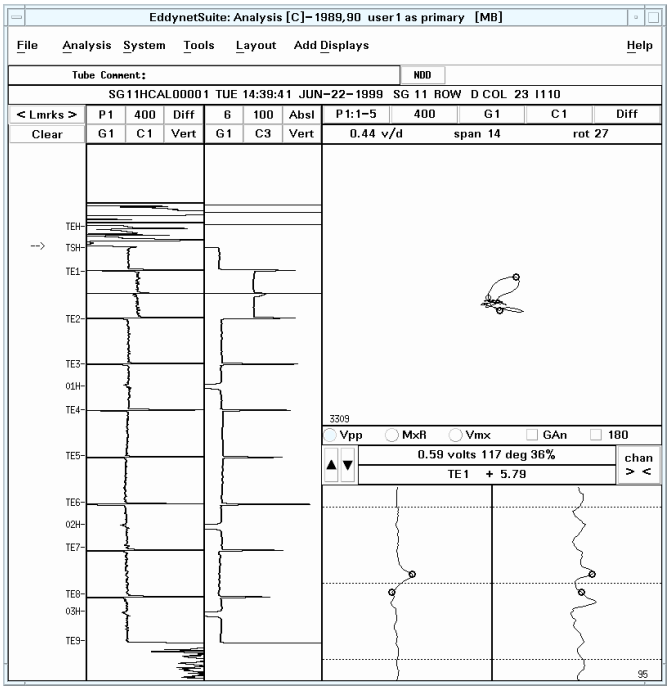

(a)

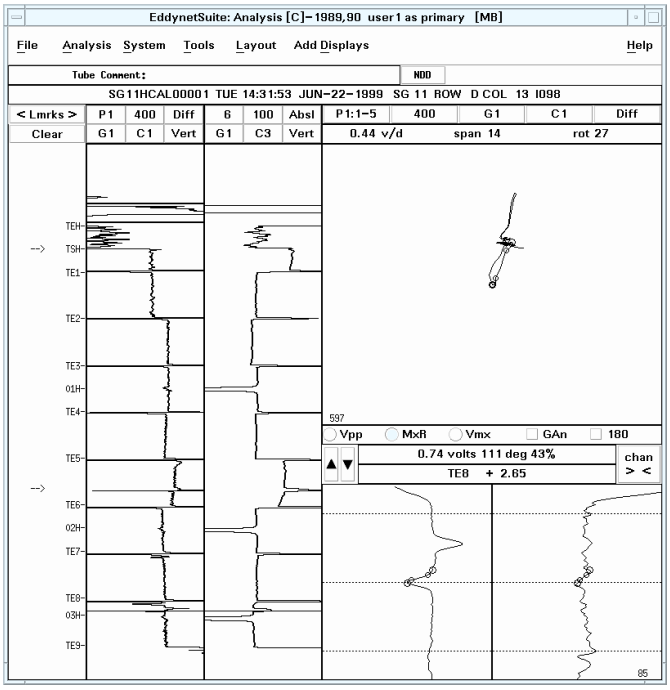

(b)

Figure 4.44 Display of the CDS results for representative SG mock-up tubes with missed calls at free-span regions due to increase in detection and classification thresholds. The displayed signals, measured manually, were identified as OD indications at the (a) second and (b) ninth tube section.

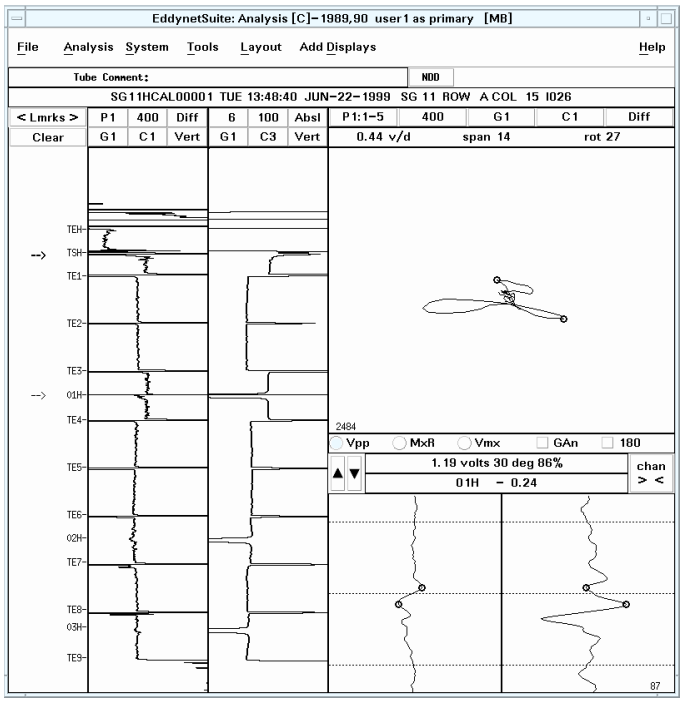

Figure 4.45 The displayed signal, reported as an indication by the previous sort settings, was not reported as a result of modifying the detection threshold value for the TSP sort. The signal in this SG mock-up tube was later identified as a false indication.

4.3 Automated Analysis of EC Inspection Data from the Entire Mock-up

Following the initial optimization and testing of the data screening configurations discussed in the previous section, CDS was next applied to the bobbin probe data collected previously from the entire SG tube bundle mock-up. Various configurations of the setup parameters and combination of sorts tested earlier on the training and qualification data sets were also applied to the SG mock-up EC inspection database. The optimal set of sorts was compared against alternative configurations to help determine the effect of critical data screening parameters on the detection probability and false call rate. The results from analyses of data from different elevations of the mock-up are discussed below.

As noted previously, the CDS *Report Editor* provides the positional information for the reported signal entries in reference to the nearest landmark location. Independent evaluation of the data analysis results, however, requires availability of the positional information in terms of data point values. When dealing with large data sets, manual inclusion of this information into the analysis report file would be impractical. To get around this issue, the *epri_scan3* program was used to automatically perform conversion of relative positional information of the CDS results to data point values. The program is readily available as a separate utility outside the Eddynet™ environment. The output text file generated by the *epri_scan3* program may subsequently be read and manipulated by other application software.

Additionally, a number of data manipulation routines were implemented under the spreadsheet software Microsoft Excel™ to allow efficient sorting and grading of the analysis results for POD calculations. Two separate *Macros* written in Visual Basic language were created for manipulation of the data analysis results. An Excel *Macro* was generated to initially sort, in ascending order, all the entries in the analysis results file based on the tube's row and column position within the SG and the elevation of each reported entry. A sample spreadsheet file containing a subset of SG mock-up tubes that was processed by the sort *Macro* is shown in Table 4.4. A second *Macro* was implemented to read the sorted data and grade the results based on a user-generated truth table. In its current form, EC data analysis results may be graded for detection, signal amplitude (voltage range), flaw origin (ID/OD), depth, and phase angle range. Table 4.5 displays the sample truth table that was used to grade the analysis results shown in Table 4.4. Also listed in that table is the detection result for each flaw as well as the total number of detected signals and overcalls, which were automatically generated by the *Macro*. In reference to Table 4.5, the grading algorithm also marks the false call entries in the analysis results file. The *Macro* is used to automatically calculate the number of detected and missed calls based on the information provided in the truth table spreadsheet.

4.3.1 Analyses of Data for Tube Support Plate (TSP) Elevations

Eddy current inspection data from all TSP elevations of the mock-up were analyzed by using the optimized set of CDS sorts described earlier. Flaws in tube sections which were located outside the TSP grading zone were eliminated from the list. Data screening configurations of Figs. 4.27 and 4.28, which employ multiple setups for screening of all TSP elevations were initially used. The results generally indicate a high POD value for all flaws present at the TSP elevations of the SG mock-up. The small number of missed indications in this case is associated mostly with low-amplitude indications and those with atypical signal characteristics. False calls in this particular data set were associated mostly with dented intersections.

Representative signals pertaining to undetected flaws are shown in Figs. 4.46-4.48. Eddy current probe response from two test sections with indications located near the edge of the TSP is shown in Figs. 4.46(a) and 4.46(b). The flaws in this case were identified as a shallow ID crack at a dented TSP region and a low-amplitude OD crack at the edge of the TSP, respectively. Only that part of the probe response associated with the dent was reported by CDS in this case. Undetected signals associated with a shallow OD crack and a volumetric OD flaw at two different TSP regions is displayed in Figs. 4.47(a) and 4.47(b), respectively. Finally, undetected signals associated with IGA are shown in Fig. 4.48. The signals shown in Figs. 4.47 and 4.48 were missed because of the uncharacteristic nature of the probe response for those particular flaw types. As noted previously, automated algorithms such as CDS rely on consistent signal behavior including proper initial excursion and phase response to correctly classify potential indications. Significant distortion of signals caused by such factors as tube geometry variations and conducting or magnetic deposits in close proximity to the flaw could lead to the mischaracterization of signals. The complex structure of degradation types such as IGA could also result in mischaracterization of potential flaw signals since the probe response from such degradation types do not conform to the expected probe response from either crack-like or volumetric flaws. Although the test logic of the data screening algorithm may be adjusted to report such signals as flaws, the reduction of constraints for improving the detection probability will in turn result in an increased number of false calls. Nevertheless, a conservative approach when using automated data analysis tools is to periodically evaluate and adjust the test logic to ensure proper detection of unexpected degradation types with signal characteristics that may be different from those present in the training data set.

Comparative tests were subsequently performed to determine the effect of different sort configurations on detection and classification of flaws in the TSP region. A subset of the multiple sort configurations comprised of only one sort was subsequently used to analyze the TSP data. The CDS Editor dialog box for the alternative screening configurations was shown in Fig. 4.27(b). Only three data screening configurations for detection of flaw signals were activated (one for each TSP elevation) in this case. As noted previously, the test logic of the selected sort here can be considered as the most common setup for detection of flaw signals at the TSP elevations. Also used was the sort configuration to report the dent (non-degradation) signals at TSP elevations.

Bobbin probe data for all TSP elevations of the SG mock-up were subsequently analyzed using the optimized data screening setups. To conduct comparative assessments, the analysis results in each case were converted by using the *epri_scan3* program and subsequently sorted and graded automatically by using the Excel *Macros* generated for this purpose. Although the *Macros* allow grading to be done based on different reporting parameters (e.g., signal amplitude, estimated depth, flaw origin), the grading of bobbin probe data here is based on detection alone. A variable grading unit, defined in terms of the number of data points, is used to set the detection zone for signals. Multiple hits within a grading unit are treated as one detection call in that zone. It should be noted that counting of the number of overcalls is not currently based on any grading unit (i.e., all calls are counted even if they are potentially redundant calls). This can lead to slight over-estimation of the false call rate, particularly when a combination of sorts is used to screen the same region of the tube.

In terms of the total number of entries made by CDS for TSP level indications, a total of 404 calls were reported by the first configuration (multiple sort setups) and 204 calls by the second configuration shown (single sort setup), respectively. Based on the truth table for flaws present

at the TSP elevations, application of the first configuration resulted in 12 missed signals and 93 overcalls, while the second configuration resulted in 23 missed signals and 49 overcalls.

Data analysis results for all unreported indications as a result of applying the second configuration with reduced number of sorts are shown in Figs. 4.49-4.55. The use of the first configuration resulted in a small number of missed indications at the TSPs with most of those being associated with either low-amplitude signals or with atypical signal characteristics. As expected, the number of missed signals using the second configuration was larger and the number of overcalls was smaller. Comparison of the two data analysis results indicates that nearly all the additional missed indications from the second configuration are associated with flaw signals at dented TSPs. Inclusion of the complementary sorts (in the first configuration), however, resulted in a noticeably higher overcall rate.

Assessments of the CDS results were conducted next by comparing the probability of detection (POD) for different flaw types at the TSP elevations of the SG mock-up. Data analysis results on the application of CDS to the analysis of bobbin probe inspection data from TSP elevations using two separate sets of configurations were presented above. The first configuration for those tests consisted of multiple sorts, which were optimized for detection of all flaw signals at TSP elevations of the SG mock-up. The second configuration, which was a subset of the first one and may be considered as a more common setup, consisted of a single sort for screening of the same elevations. The CDS analysis results using the two configurations noted above were first sorted and graded using a set of Excel *Macros* generated for this purpose. The detection results were then used to generate POD curves for flaws present at the TSP elevations of the SG mock-up. For these comparative studies, manual analysis results from the round-robin (RR) exercise were used to help better assess the POD results with the automated data screening software.

Figure 4.56 shows the POD curves for the CDS detection results at TSP elevations using the configuration composed of multiple sorts. A subset of TSP flaws identified as longitudinal inner-diameter stress corrosion cracking (LIDSCC) was used for the initial calculations. For comparison both linear-logistic and log-logistic fits to the same data are plotted with the flaw depth as the independent variable. Detailed description of the two fitting methods have been provided in a number of past technical reports on the evaluation of RR data analyses results from SG mock-up **(Refs. 2, 3)**. In brief, these past studies performed by the industry on the probability of detection suggest that the log-logistic curve is a more appropriate choice when the signal amplitude (voltage) is used as the independent variable. Conservatism of that approach, however, is not clear when the flaw depth is taken as the independent variable. The linear-logistic fit on the other hand is expected to produce a more conservative estimate of detection probability. It is worth noting that the flaw size distribution and in turn the statistical acceptability of a database can influence the fitting results and the confidence on the POD results. The graph shown in Fig. 4.56 displays the typical behavior when the same data was fitted with the two curves mentioned above. In general, the log-logistic fit provides a higher POD at smaller flaw depths and the linear-logistic fit provides a higher POD at larger flaw depths. Although the POD curves with both fitting methods have been generated, it should be noted that for these comparative studies either one of the two logistic curves may be used to assess the detection results. It should also be noted that the POD results so far have all been generated using fixed values for the false call rate near the tail end (zero depth) of the logistic fits to the data. The small false call rate values used in these preliminary evaluations were chosen based on the results from the manual analysis of the RR data.

Figures 4.57 and 4.58 display the POD curves for the TSP level flaws using the two data screening configurations noted above. The CDS detection results for the multiple sort configuration (denoted as TSP2) and the single sort configuration (denoted as TSP1) are plotted along with the composite RR results and the results by an expert analyst (not a fully blind test). Separate sets of curves were generated for the LIDSCC and the LODSCC flaws at the TSP elevations. The POD curves for flaws identified as LIDSCC are shown in Figs. 4.57(a) and 4.57(b) using log-logistic and linear-logistic fits, respectively. The POD results for LODSCC flaws using the same approach are shown in Fig. 4.58. In general, the CDS detection results using the multiple sort configuration provides the highest POD values in all cases. The single sort configuration on the other hand provided the lowest POD values. Based on the spread of the POD results from all teams that took part in manual analysis of the RR data (not shown here), the differences among the POD curves shown in Figs. 4.57 and 4.58 seem to be relatively small for this particular data set.

Table 4.4 Sample Excel spreadsheet containing the analysis results for a subset of SG mock-up tubes, which were sorted using a *Macro* generated for this purpose.

SG	Row	Col	Ampl (V)	Ph (deg)	Depth (%T	Channel	Location	Charac. Code			Is Flaw	Overcalls
11	A	6	3.17	32		P3	3648	DTI	5.32	TEH	1	OC - 2
11	A	9	10.05	115		P1	576	DSI	0	03H	1	
11	A	9	1.2	112		P1	2046	NQI	6.93	TE4	1	
11	A	9	3.95	75		P1	2061	NQI	6.48	TE4	1	
11	A	9	4.9	75		P1	2080	NQI	5.91	TE4	1	
11	A	15	2.17	185		P1	2473	DNT	0.09	01H	0	
11	A	15	14.69	33		P3	3650	DTI	0.66	TSH	1	
11	A	15	24.64	44		P3	3672	DTI	0	TSH	1	
11	A	18	0.79	131		P1	1144	NQI	1.67	02H	1	OC - 1
11	A	18	10.69	111		P1	1166	DSI	0.96	02H	1	OC - 1
11	A	18	4.21	187		P1	2396	DNT	0.12	01H	0	
11	A	18	7.59	57		P3	3589	DTI	-0.12	TSH	1	OC - 1
11	B	2					3740	NDD	0		0	
11	B	4					2469	NDD	0		0	
11	B	11	2.26	94		P1	2420	DSI	0.24	01H	1	
11	B	11	8.78	78		P1	2436	DSI	-0.24	01H	1	
11	B	13					2436	NDD	0		0	
11	B	18	0.84	109		P1	3332	NQI	3.79	TE1	1	
11	B	18	1.11	103		P1	3354	NQI	3.12	TE1	1	
11	D	10					2474	NDD	0		0	
11	D	13	5.02	94		P1	1614	NQI	7.77	TE5	1	
11	D	13	10.8	27		P3	3659	DTI	-0.15	TSH	1	OC - 2
11	D	23	4.42	29		P3	3722	DTI	-0.49	TSH	1	OC - 1
11	E	9					3820	NDD	0		0	
11	F	17	12.23	115		P1	2249	DSI	0.29	01H	1	
11	F	17	2.56	121		P1	2258	DSI	0.03	01H	1	
11	F	17	19.42	91		P1	2264	DSI	-0.16	01H	1	
11	F	17	12.01	52		P1	3049	NQI	5.87	TE1	1	
11	F	22	3.17	181		P1	2752	DNT	0.12	01H	0	
11	G	8	28.75	70		P3	4003	DTI	0.15	TSH	1	
11	G	8	53.82	62		P3	4014	DTI	-0.18	TSH	1	
11	G	13	5.21	26		P3	3909	DTI	5.37	TEH	1	OC - 2
11	G	13	5.21	26		P3	3911	DTI	5.31	TEH	1	OC - 2
11	G	13	4.12	19		P3	4046	DTI	1.3	TEH	1	OC - 2
11	G	14	1.21	149		P1	3145	NQI	6.32	TE2	1	
11	G	14	1.33	139		P1	3163	NQI	5.77	TE2	1	
11	G	14	0.9	142		P1	3547	NQI	5.97	TE1	1	
11	G	14	9.26	27		P3	3942	DTI	-0.52	TSH	1	OC - 1
11	H	11	4.13	128		P1	966	DSI	0.86	03H	1	
11	H	11	5.83	33		P3	4124	DTI	-0.18	TSH	1	OC - 1
11	J	14	0.98	146		P1	886	DSI	0.73	03H	1	
11	J	14	1.95	128		P1	915	DSI	-0.13	03H	1	
11	J	22	2.21	184		P1	1650	DNT	0.15	02H	0	
11	K	13	1.64	74		P1	957	DSI	0.06	03H	1	
11	K	13	2.18	136		P1	966	DSI	-0.22	03H	1	
11	M	4	3.42	22		P3	3818	DTI	0.86	TSH	1	
11	M	4	32.47	50		P3	3845	DTI	0.03	TSH	1	
11	N	12	1.88	10		P1	2063	NQI	6.21	TE5	1	
11	N	12	4.37	13		P1	2097	NQI	5.19	TE5	1	
11	N	18	5.36	26		P3	4053	DTI	-0.09	TSH	1	
											41	11

Table 4.5 Graded results for the sample data set shown in Table 4.4 using an Excel™ *Macro* generated for this purpose.

FLAW ID			FLAW TYPE	ORIENT	BC	BC	ID/OD	Beginning	End of	MAX DEPTH	AVE DEPTH	LENGTH	Expert	TRUE	CIRC POS	FLAW ID				
tow,Col,Leve	TS	Special			VOLTS	PHASE	ACTUAL	of flaw	flaw	%TW	%TW	mm	BC Call	STATE	REL to					
Axial Position	Location	Interest												CALL	MARKER (°)			POD	ID/OD	Depth
(data point)		Location																		
A09I 0576		80273	WASTAGE	X	10.08	114	OD	561	593	60	NA	21.0	DSI	MVI	NA	A090576	1	1	0	0
A09E 2046		52118	LODSCC	L	1.21	112	OD	2036	2051	88	NA	12.7	NQI	SAI	NA	A092046	1	1	0	0
A09E 2060		53681	LODSCC	L	4.04	75	OD	2051	2071	88	NA	16.9	NQI	SAI	NA	A092060	1	1	0	0
A09E 2080		54803	LODSCC	L	4.9	75	OD	2071	2090	88	NA	16.1	NQI	SAI	NA	A092080	1	1	0	0
A15D 2484		19999	DENT	X	1.2	30	X	2474	2490	0	NA	13.5	DSI	DNT	NA	A152484	0			
A15A 3648	19270		LIDSCC	L	24.93	26	ID	3640	3654	99	NA	11.9	NQI	SCI	NA	A153648	1	1	0	0
A18G 1165		26254	DENT	X	10.73	110	OD	1137	1179	0	NA	35.6	NQI	DNT	NA	A181165	0			
A18D 2395		19999	DENT	X	4.21	186	X	2377	2412	0	NA	29.6	DNT	DNT	NA	A182395	0			
B11G 1250		19999	IGA	X	0	0	OD	1229	1267	60	NA	32.2	NDD	MMI	NA	B111250	1	0	0	0
B11D 2431		20163	LODSCC	L	8.78	70	OD	2410	2447	90	NA	31.3	DSI	SAI	NA	B112431	1	1	0	0
B18B 3348		13403	LODEDM	L	1.84	102	OD	3320	3367	60	NA	21.0	NQI	SAI	NA	B183348	1	1	0	0
D13I 0610		73523	LODEDM	L	1.47	104	OD	593	626	66	NA	20.0	NQI	SAI	NA	D130610	1	0	0	0
D13F 1614		88520	CODSCC	C	5.03	94	OD	1608	1619	73	NA	7.0	NQI	SCI	NA	D131614	1	1	0	0
D13A 3600	18124 - 20034		CODSCC	C	0	0	OD	3595	3605	98	NA	35.0	NDD	MCI	NA	D133600	1	0	0	0
D23B 3310		50050	LODSCC	L	0.59	133	OD	3297	3316	78	NA	16.1	NQI	MAI	NA	D233310	1	0	0	0
E09B 3544		46160	LIDSCC	L	3.47	8	ID	3503	3548	23	NA	38.1	DNI	MAI	NA	E093544	1	0	0	0
F17D 2263		19712	LODSCC	L	19.84	90	OD	2234	2282	97	NA	40.6	DSI	MMI	NA	F172263	1	1	0	0
F17B 3049		50704	LODSCC	L	12.19	60	OD	3028	3069	95	NA	34.7	NQI	MAI	NA	F173049	1	1	0	0
F22D 2765		21416	LIDSCC	L	1.72	19	ID	2735	2783	49	NA	40.6	DNI	SAI	NA	F222765	1	0	0	0
G08A 4013	19550 - 22749		LODSCC	L	40.6	138	OD	3990	4031	88	NA	34.7	DTI	MMI	NA	G084013	1	1	0	0
G13F 1968		79999	DNG	X	2.01	190	X	1958	1981	0	NA	19.5	DNG	NOF	NA	G131968	0			
G14C 3163		79999	LODSCC	L	0	0	OD	3150	3180	10	NA	22.0	NDD	SAI	NA	G143163	1	1	0	0
G14B 3547		51974	CODSCC	C	2.52	139	OD	3530	3560	55	NA	27.0	NQI	SCI	NA	G143547	1	1	0	0
H11I 0967		86698	IGA	X	4.36	132	OD	953	984	38	NA	26.2	NQI	SVI	NA	H110967	1	1	0	0
J14I 0915		83174	LODSCC	L	2.02	131	OD	874	930	55	NA	47.4	DSI	SAI	NA	J140915	1	1	0	0
J22G 1665		23541	LIDSCC	L	0.99	18	ID	1624	1675	83	NA	43.2	DSI	SAI	NA	J221665	1	0	0	0
K13I 0966		78589	LODSCC	L	2.21	140	OD	941	979	86	NA	32.2	DSI	SAI	NA	K130966	1	1	0	0
K13G 1709		17285	FATIGUE	C	0.42	146	OD	1508	1880	99	NA	20.0	DSI	SCI	NA	K131709	1	0	0	0
M04A 3817	20019 - 23097		CIDSCC	C	3.51	24	ID	3803	3874	80	NA	60.1	NQI	MMI	NA	M043817	1	1	0	0
N12F 2097		24532	LIDSCC	L	4.38	13	ID	2084	2106	47	NA	18.6	NQI	SAI	NA	N122097	1	1	0	0
N12B 3707		59999	NOF	X	4.6	188	OD	3688	3718	0	NA	25.4	DNG	NOF	NA	N123707	0			
N18A 4052	20550		CODSCC	C	54.47	13	OD	4032	4062	82	NA	27.0	DTI	MCI	NA	N184052	1	1	0	0
																	27	19	0	0

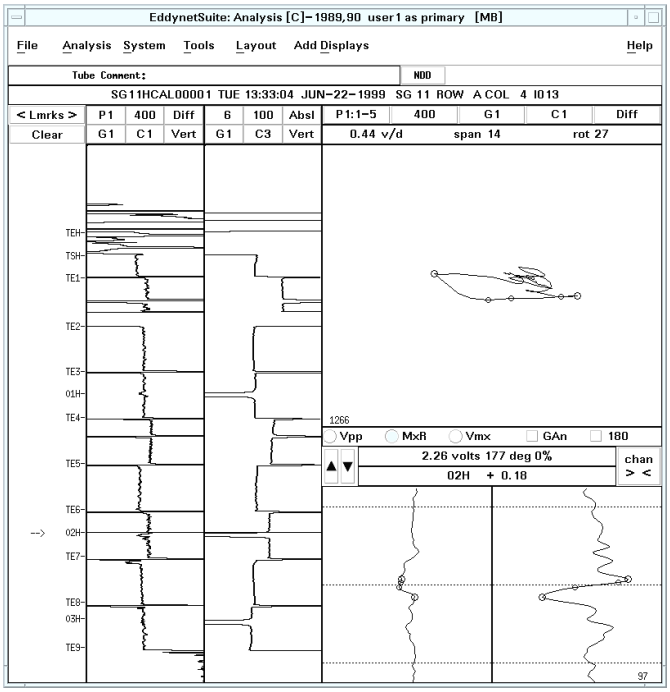

(a)

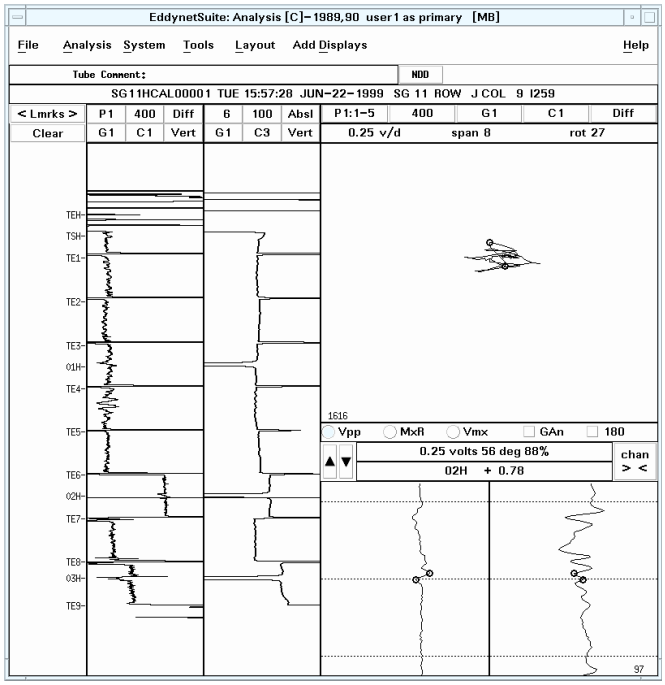

(b)

Figure 4.46 Display of the CDS results for representative manually measured missed signals associated with (a) the dent part of the probe response detected by CDS in a TSP zone also containing shallow ID cracking and (b) a low amplitude OD flaw identified as fatigue cracking.

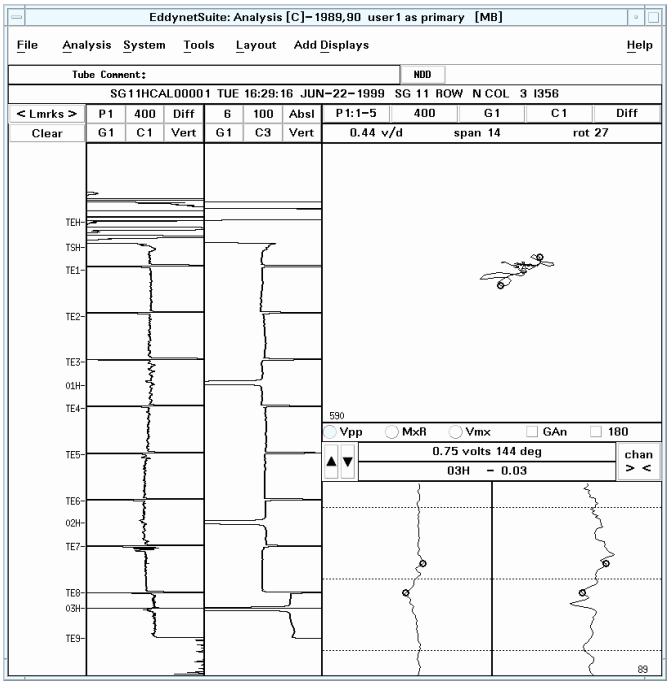

(a)

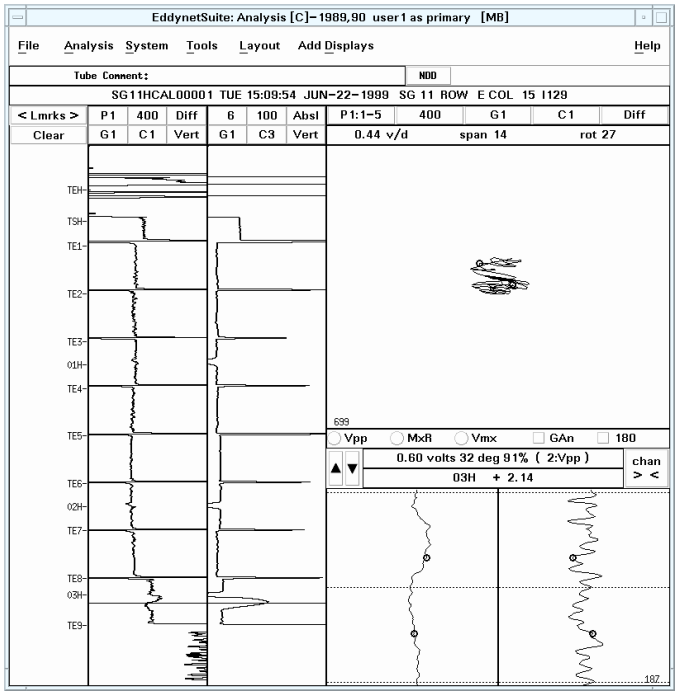

(b)

Figure 4.47 Display of the CDS results for manually measured missed signals, identified as shallow (a) ODSCC and (b) volumetric OD flaw at the TSP region.

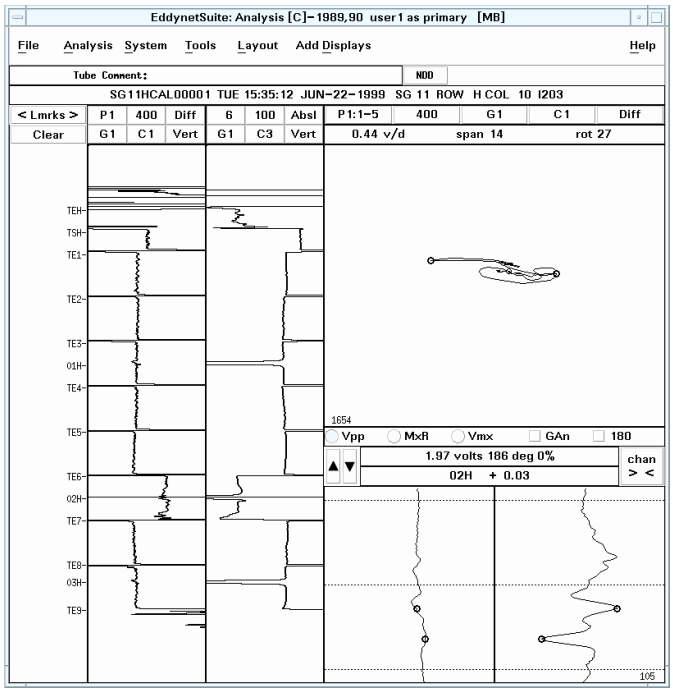

(a)

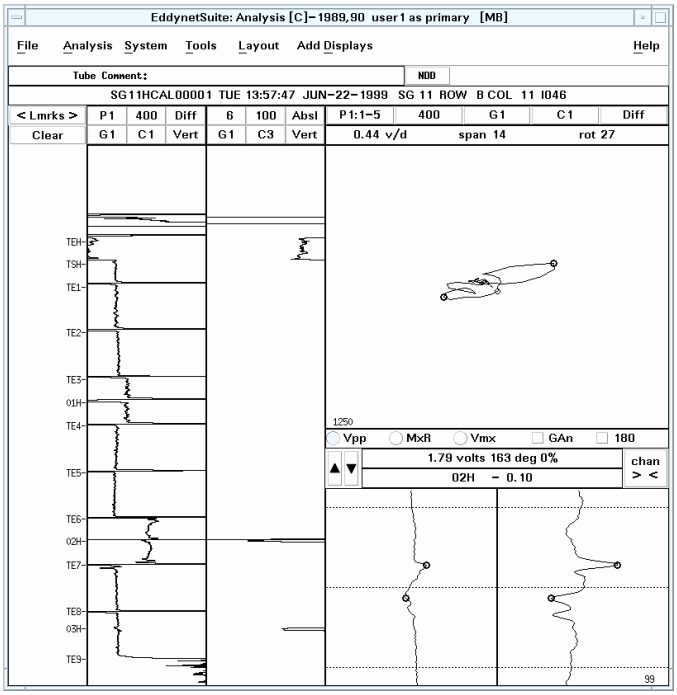

(b)

Figure 4.48 Display of the CDS results for manually measured missed signals at TSP regions, both identified as IGA.

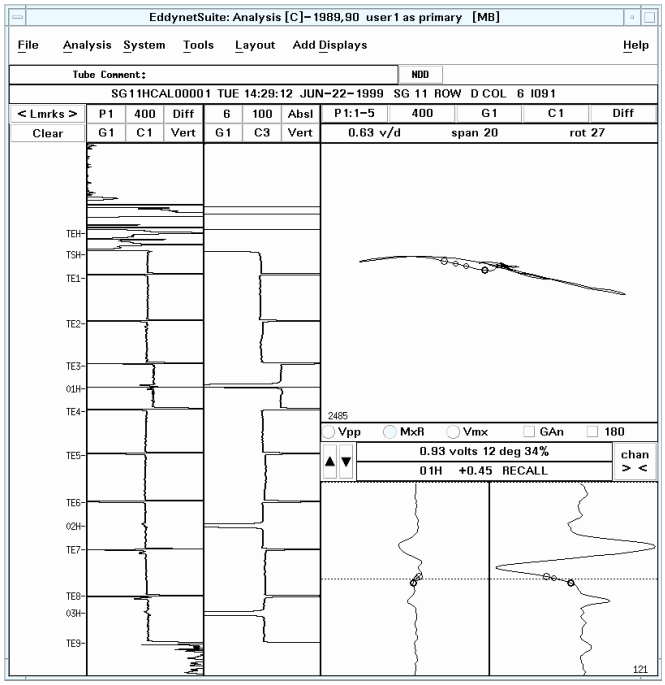

(a)

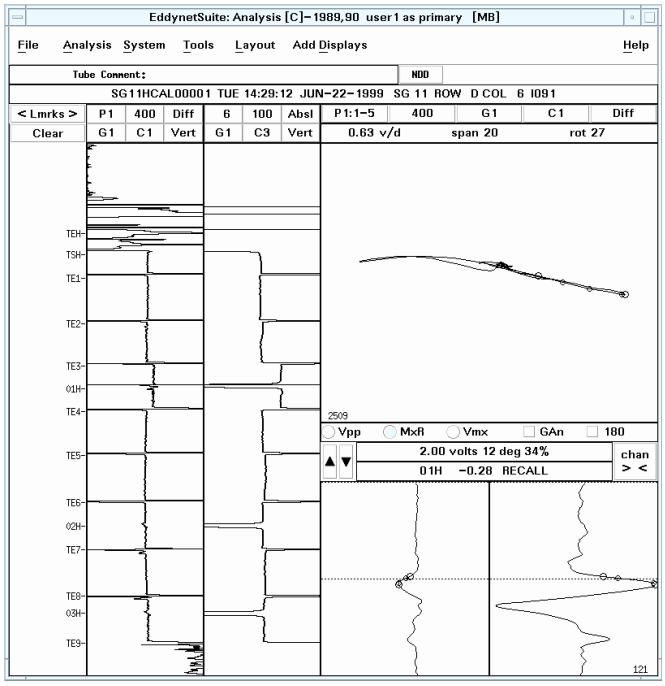

(b)

Figure 4.49 Display of the CDS results for a signal at a dented TSP elevation of the SG mock-up. Shown above are two separate detection calls made using the multiple sort configuration.

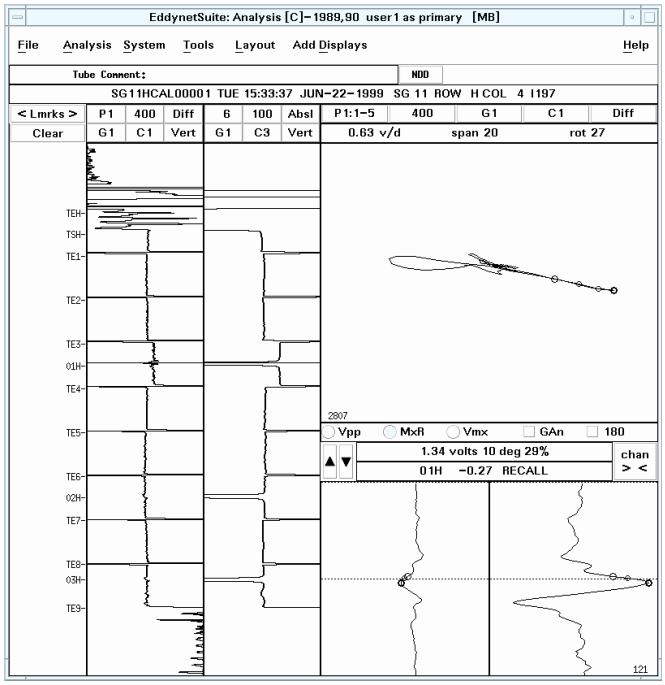

(a)

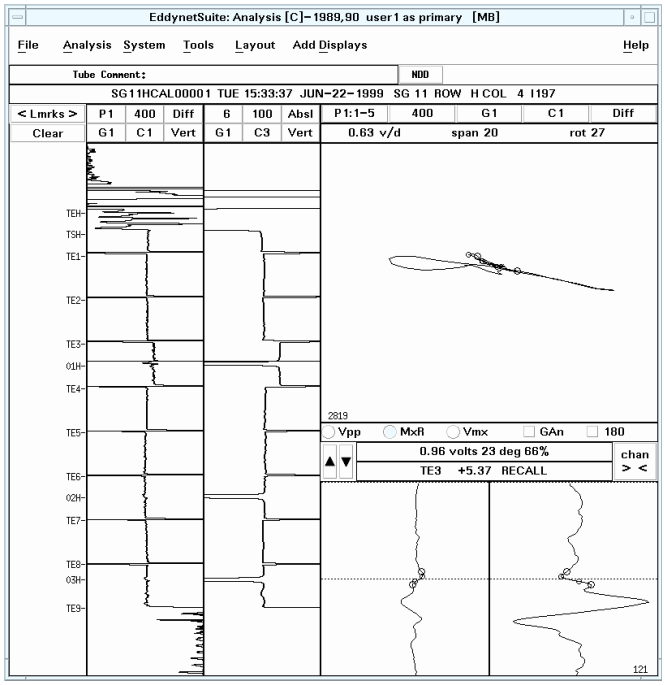

(b)

Figure 4.50 Display of the CDS results for a signal at a dented TSP elevation of the SG mock-up. Shown above are two separate detection calls made using the multiple sort configuration.

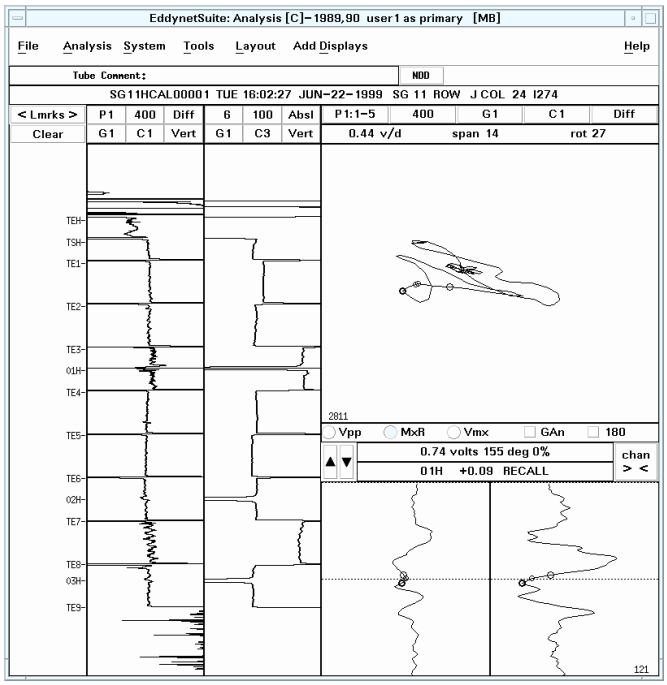

(a)

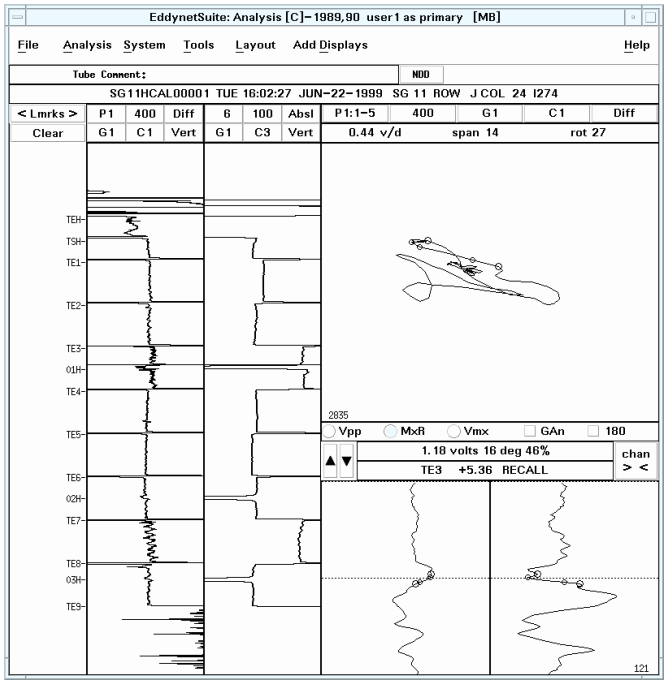

(b)

Figure 4.51 Display of the CDS results for a signal at a dented TSP elevation of the SG mock-up. Shown above are two separate detection calls made using the multiple sort configuration.

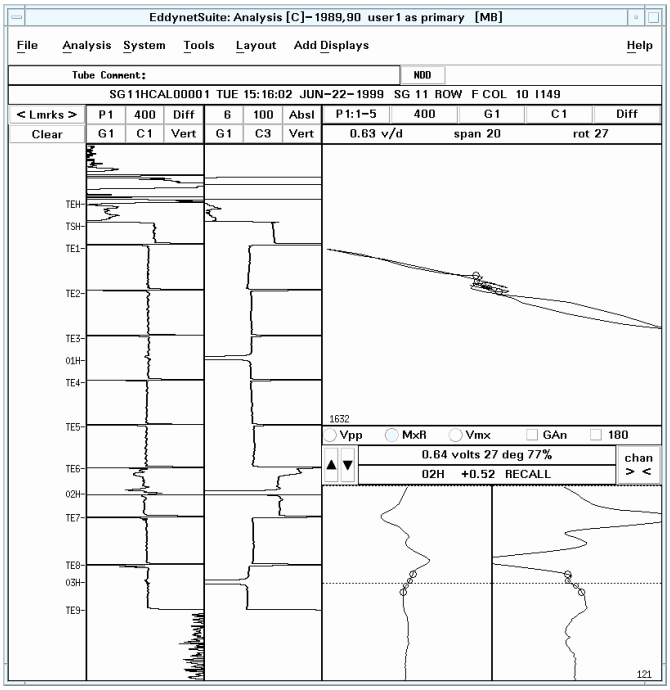

(a)

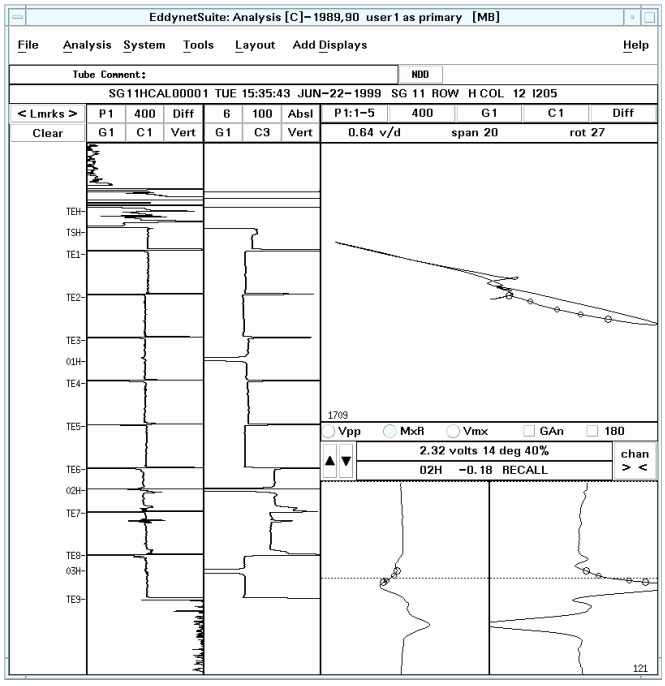

(b)

Figure 4.52 Display of the CDS results for two separate signals at a dented TSP elevation of the SG mock-up. Shown above are the detection calls made using the multiple sort configuration.

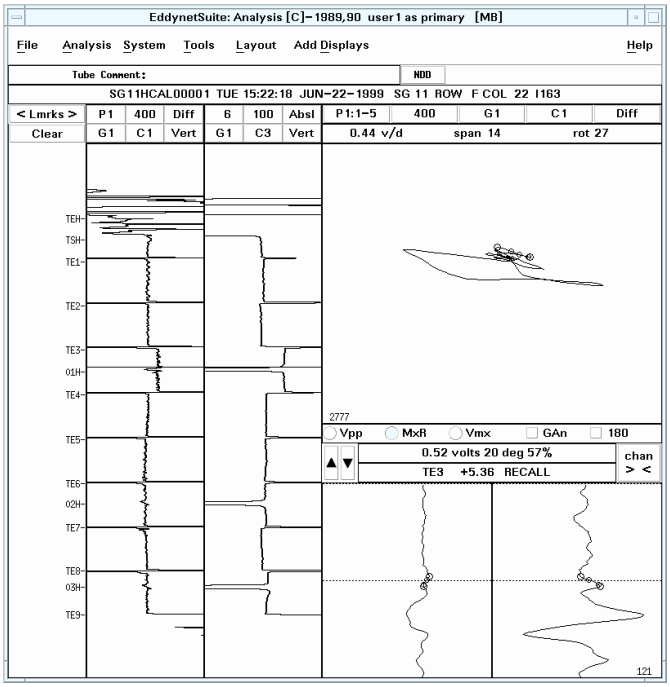

(a)

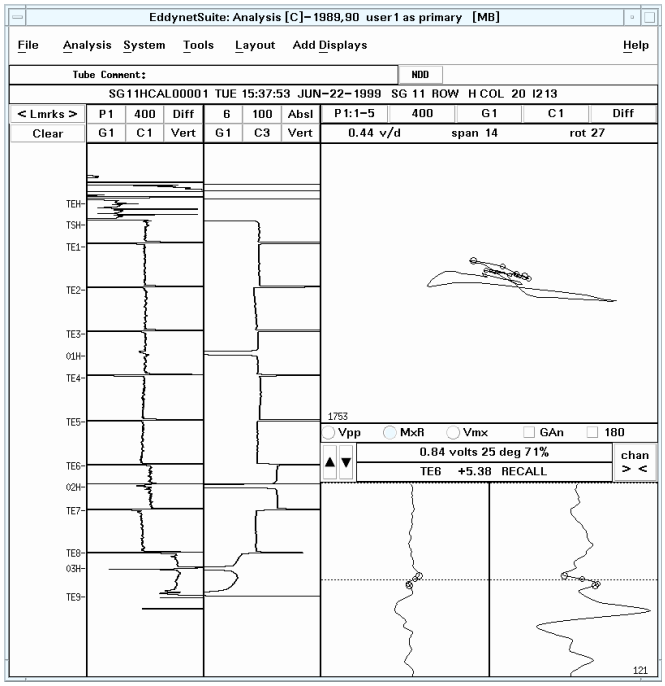

(b)

Figure 4.53 Display of the CDS results for two separate signals at dented TSP elevations of the SG mock-up. Shown above are the detection calls made using the multiple sort configuration.

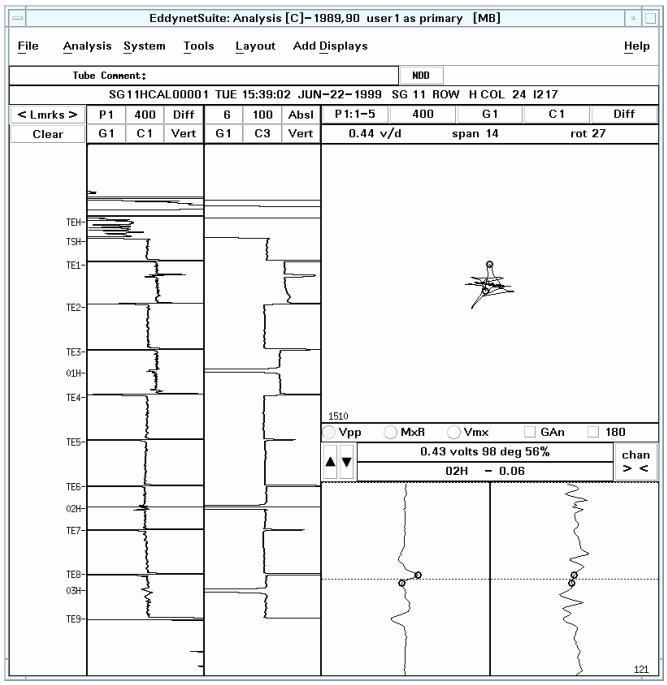

(a)

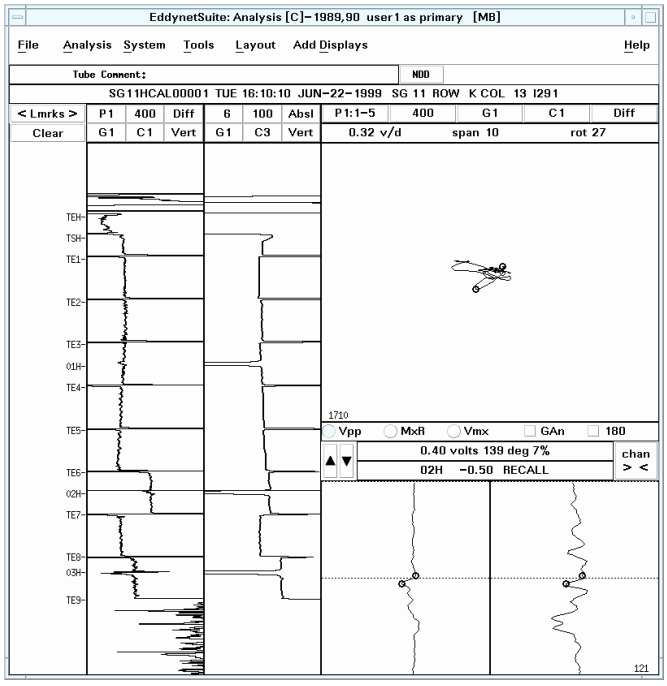

(b)

Figure 4.54 Display of the CDS results for two separate low-amplitude signals at TSP elevations of the SG mock-up. Shown above are the detection calls made using the multiple sort configuration.

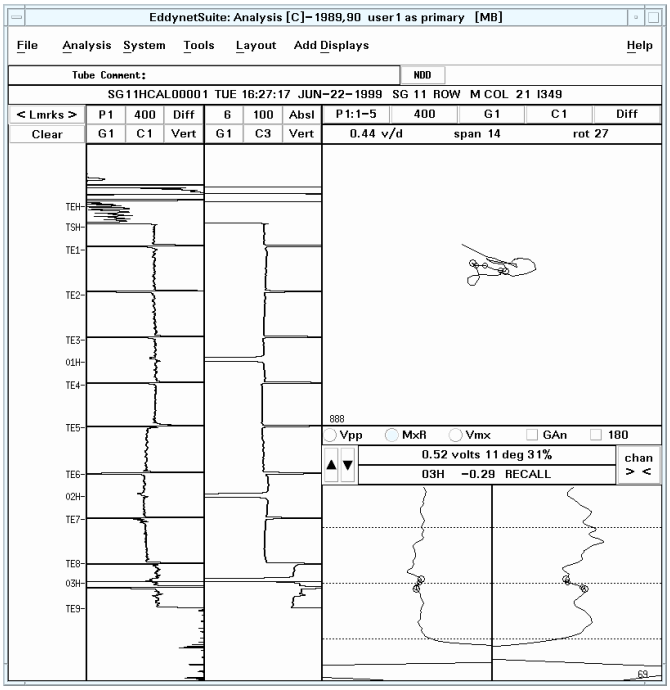

(a)

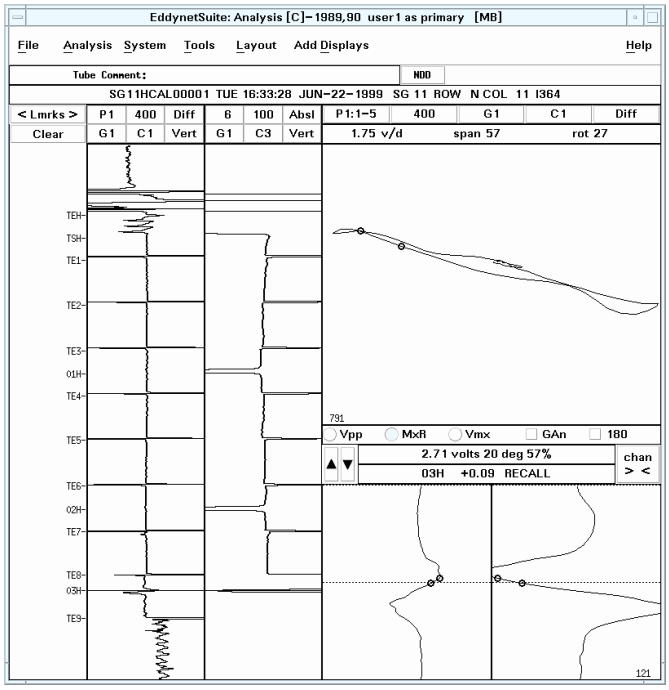

(b)

Figure 4.55 Display of the CDS results for two separate signals at TSP elevations of the SG mock-up. Shown above are the detection calls at (a) a non-dented and (b) a dented TSP elevation made using the multiple sort configuration.

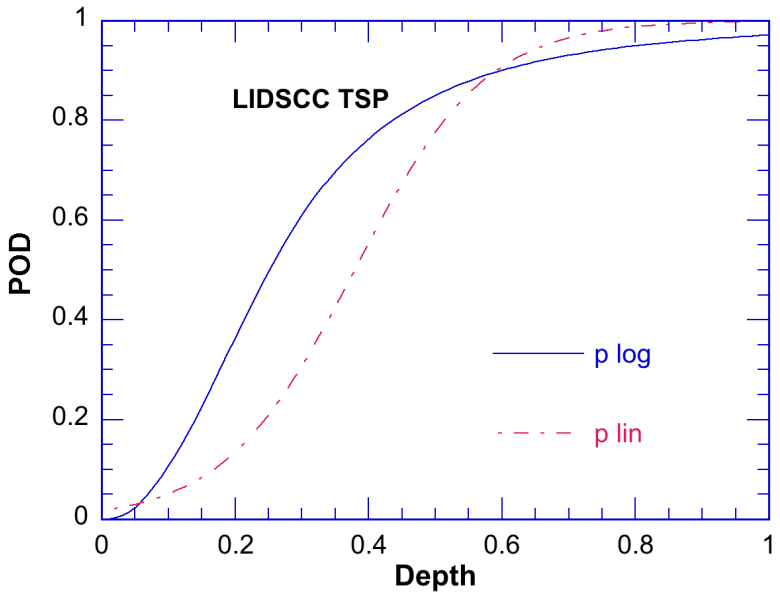

Figure 4.56 Representative POD curves as a function of depth for flaws at the TSP elevations identified as LIDSCC using the CDS configuration with multiple sorts.

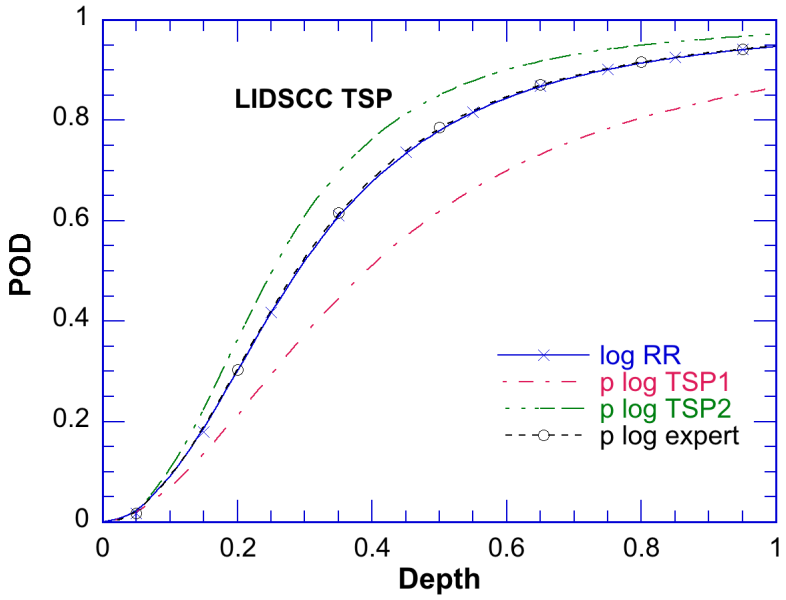

(a)

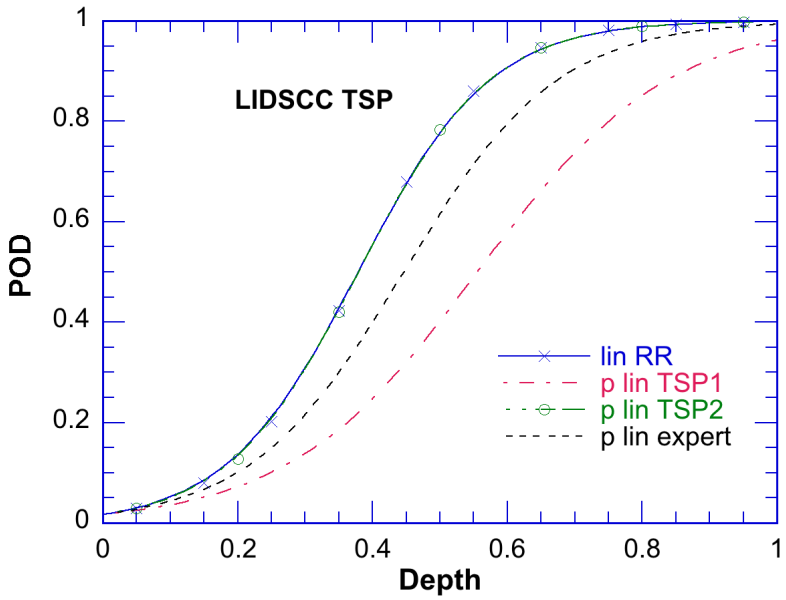

(b)

Figure 4.57 POD curves for flaws at the TSP elevations identified as LIDSCC using the CDS configuration with multiple sorts (TSP2), CDS configuration with single sort (TSP1), composite round-robin manual analysis (RR), and expert analyst (expert) results.

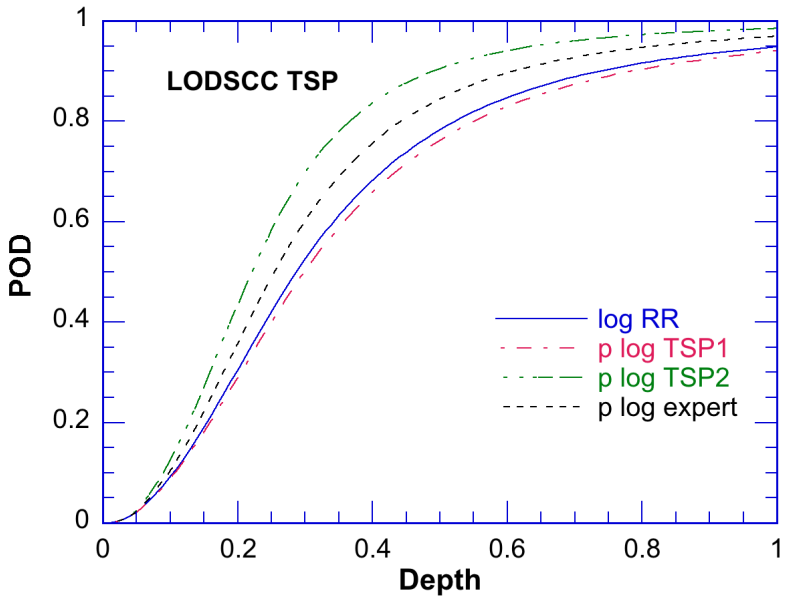

(a)

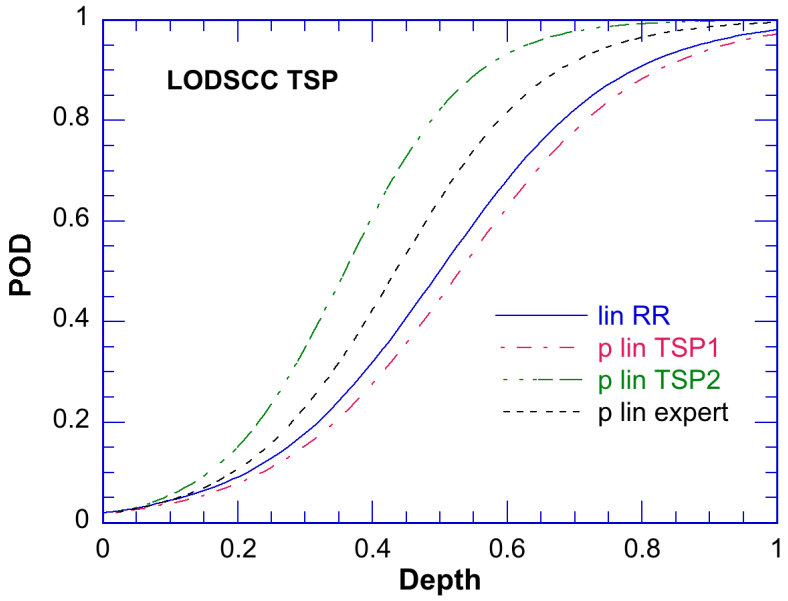

(b)

Figure 4.58 POD curves for flaws at the TSP elevations identified as LODSCC using the CDS configuration with multiple sorts (TSP2), CDS configuration with single sort (TSP1), composite round-robin manual analysis (RR), and expert analyst (expert) results.

4.3.2 Analyses of Data for Free-span Elevations

The results of analyses associated with automated screening of bobbin probe inspection data collected from free-span elevations of the SG tube bundle mock-up is discussed next. Comparative tests were once again performed to determine the effect of different data screening setups on detection and classification of flaws. The POD results using multiple and single sort configurations are presented first. The effect on the POD for free-span flaw signals of adjusting some key setup parameters is also discussed.

Bobbin probe inspection data from the free-span region of the SG mock-up was analyzed next by using the two complementary data screening configurations in Fig. 4.26 and displayed again in Fig. 4.59. The first data screening configuration consisted of two separate sort setups for detection and classification of flaw signals in the free-span. A description of the two data screening configurations, displayed under the *Indications* menu of the *CDS Editor* window, was provided earlier. In reference to Fig. 4.59(a) and (b), the primary sort employed a differential channel (200 kHz) while the secondary sort employed an absolute channel (100 kHz) for detection. Different detection algorithms were also employed in the two setups. The detection algorithm for the primary sort is better suited for detection of closely-spaced signals whereas the one used for the secondary sort is better suited for detection of longer signals. To permit adjustment of the measurement window size for the classification stage, a peak-to-peak measurement method was used in the secondary sort configuration. The inclusion of the secondary sort was done mainly to provide a more accurate measurement of the signal amplitude (voltage) for long axial indications.

Bobbin probe data from the free-span regions was first analyzed by activating both sorts shown in Fig. 4.59. For both sorts, the *location* test logic was slightly modified to minimize the number of potential entries associated with detection of signals near the expansion transition region. This was done by defining the beginning of the free-span screening region to start at ~12.5 mm (0.5 in.) above the TTS. As in the past, the CDS analysis results using the two aforementioned screening configurations were sorted and graded using the *Excel* spread-sheet *Macros* described earlier. The detection results were then used to generate POD curves for flaws present in the free-span of the SG mock-up. The manual analysis results from an earlier RR exercise and the results generated by an expert analyst were once again used to help better assess the POD results obtained using the automated data screening software.

Data analysis results for representative signals identified either as a missed indication or as a false call using the sort configurations displayed in Fig. 4.59 are presented next. The majority of the missed indications by CDS in the free-span region of the SG mock-up were associated with low-amplitude signals present either by themselves or in conjunction with tube deformation (ding). Nearly all missed indications exhibiting relatively large signal amplitudes were associated with IGA type flaws. As noted previously, this is attributed to the characteristically unpredictable nature of the bobbin probe response from such indications. Figures 4.60–4.62 display a series of low-amplitude signals identified as free-span ODSCC, which were not reported by CDS. In all cases, the indications were missed because of their low signal amplitude which was below the voltage threshold defined in the characterization test logic. Data analysis results for another missed indication identified as ODSCC in the free-span region is displayed in Fig. 4.63. Figure 4.63(a) shows the probe response in the main Eddynet™ analysis window. The probe response at different test frequencies is shown in Fig. 4.63(b) in multiple Lissajous display format. Although the flaw signal in this case is clearly detectable in the

measurement channel, this indication was missed because of the out-of-range phase response in the test channel. It is worth noting that although the peak-to-peak voltages measured manually for some of the signals shown here are above the prescribed detection threshold, the measured values may not be identical to those made by the CDS algorithms. Any discrepancies between the automated and manually measured signal amplitudes are in general associated with the type of detection algorithm employed, which may use either a fixed or a user-defined measurement window size, and the background suppression method. Such measurement variability is more likely to occur for low amplitude signals and for complex flaws where the signal is not clearly discernible.

Data analysis results for representative missed indications in conjunction with tube deformation (free-span dent/ding) are displayed in Figs. 4.64 and 4.65. In all those cases, the signal from the ODSCC flaw was masked by the larger probe response (change in fill-factor) associated with the tube deformation. Another example of a missed indication attributed in part to tube geometry change is shown in Fig. 4.66. The flaw present in that zone was identified as IGA (volumetric degradation). Figure 4.66(a) shows the probe response at the primary analysis channel in the main Eddynet™ analysis window. The probe response at different test frequencies, in multiple Lissajous display format, is shown in Fig. 4.66(b). Improper EC phase response attributed to IGA is plausibly the main factor for missing or mischaracterizing this particular signal.

Data analysis results for representative missed indications in the free-span region identified as IGA type flaws are shown in Figs. 4.67 and 4.68. In all cases, missing of the flaw signal by CDS was once again attributed to improper phase angle response at the primary test frequency. As noted earlier, no viable data classification screening configurations have been identified in this study for reliable detection or classification of IGA based on bobbin probe inspection data. The test logic of the classification stage may be bypassed (i.e., report on detection alone) or relaxed in order to report such signals. This approach for detection of flaws with unpredictable probe response, however, could result in unacceptably high overcall rates.

An example of a long axial indication in the free-span with separate report entries for each lobe of the differential signal is shown in Fig. 4.69. The use of a larger window size by the secondary sort in this case resulted in reporting of an additional entry based on the total length of the signal. Two separate entries, Fig 4.69(a), (b) were made by the primary sort shown in Fig. 4.59(a). An additional entry was reported by the secondary sort shown in Fig. 4.59(b) based on the total length of the signal. The true peak-to-peak amplitude of the signal, however, was not captured by the measurement window. Examples of false calls associated with ferromagnetic tube-end markers and with high level of baseline noise are presented in Figs. 4.70(a) and 4.70(b), respectively. The signals were reported by CDS as flaws because they satisfy all the conditions set by the classification test logic (i.e., fall within prescribed amplitude threshold and phase range) for all the test channels. As discussed previously, elimination of such calls through incorporation of more exclusive criteria into the characterization test logic could reduce the conservatism in reporting of relevant signals.

The bobbin probe data from the free-span regions was next analyzed by activating only the primary CDS sort displayed in Fig. 4.59(a). As expected, this resulted in a small number of additional missed indications in comparison with the previous configuration employing both sorts. Examples of signals not reported as a result of deactivating the secondary sort are shown in Fig. 4.71. The signal associated with an ODSCC indication in the free-span of the SG

mock-up is shown in Fig 4.71(a). The reason for missing the signal in this case was attributed to its close proximity to the end of the tube section. Although no flaws are expected to be present in the mockup within 25 mm (1 in.) of the tube-end, variations in probe speed and in turn the acquisition sampling rate could lead to small variations in axial scaling of data. This can consequently result in small variations in locating the landmarks using the automatic landmark detection algorithm. Data analysis result for another missed indication is shown in Fig. 4.71(b). In this case, missing of the signal was attributed to the size of the measurement window used by the primary sort. This signal was detected using the previous screening configuration because of the larger measurement window used by the secondary sort configuration. The use of a larger window size resulted in capturing the entire signal which allowed proper measurement of its peak-to-peak amplitude which was above the voltage threshold for reporting by the classification test logic.

The POD results for the free-span of the SG mock-up using the two data screening configurations discussed above are presented in Fig. 4.72. Separate POD curves were generated for the automated analysis results using the two-sort configuration (denoted as FS2) and the single sort configuration (denoted as FS1). To help better assess the results, the POD curves for CDS are once again plotted along with the previously established composite POD curve from the manual analysis of the data by the RR team (denoted as RR) and that from an expert analyst (denoted as expert). As noted previously, unlike the CDS and the manual analysis of RR data, the analysis by an expert was not performed in a totally blind test fashion, which may have influenced the corresponding POD results. The analysis results were fitted using both linear-logistic and log-logistic curves. The linear-logistic is expected to produce more conservative estimates of the detection probability. The POD curves were generated only for flaws identified as LODSCC in the free-span region of the SG mock-up. Separate POD curves for other flaw types present in that region were not generated because the database did not include a statistically acceptable number of flaws. Once again a small false call rate value was used to generate the POD curves in these studies. The fixed value was chosen based on the results from manual analysis of the EC inspection data by the RR teams.

The POD curves for free-span ODSCC flaws using a linear-logistic fit is shown in Fig. 4.72(a). The results based on a log-logistic fit are shown in Fig. 4.72(b). As expected, the deviation between the POD results for the two automated screening configurations was small. However, the number of false calls was significantly different for the two data screening configurations. The number of overcalls using the first (multiple sorts) and the second (single sort) configuration were 175 and 81, respectively. The small increase in POD as a result of incorporating a secondary sort resulted in a measurably larger overcall rate. In reference to Fig. 4.72, the detection probability with CDS is higher than that from the composite RR analysis results and closer to the POD curve for the expert analyst results.

Bobbin probe inspection data collected from all the free-span regions of the SG mock-up was next used to further assess the influence of some key CDS setup parameters on the detection of flaw signals. The POD results were then compared to those obtained using the CDS configurations discussed previously. Inspection data from the free-span was chosen for this study because the data screening configurations for those regions employ a smaller number of setup parameters compared to those used for the TSP elevations. Modification of the setup parameters included increasing of the amplitude threshold (T), reduction of phase depth window (D), and a combination of both (TD). Thus, for the free span region two-sort, modified amplitude threshold, a notation of FS2_T is used, and so on. The modifications were included in the

classification test logic for reporting of signals. The modified sort configurations were then applied to the entire dataset.

Figure 4.73 displays the CDS editor window for the first modified setup, which includes two sort configurations for screening of bobbin probe data from the free-span elevations. The setup shown in Fig. 4.73(a) incorporates a differential channel and the one in Fig. 4.73(b) incorporates an absolute channel in its detection logic line, respectively. In comparison with the original setup examined previously, the detection threshold in the classification test logic was increased by 0.1v (from 0.5v to 0.6v) in the first configuration and by 0.2v (from 0.5v to 0.7v) in the second configuration. The small increase in the threshold values here is analogous to the modification of setup parameters for site-specific applications to compensate for higher level of noise present in the EC inspection data **(Ref. 5)**. The second modified setup used for the comparative assessments here is shown in Fig. 4.74. The lower limit of the depth window for reporting of flaw signals in this case was changed to ten percent, from its original value of zero percent, in the classification logic line. It should be noted that with the depth and the phase angle being dependent parameters, increasing the lower limit of the depth window is equivalent to reducing of the phase window defined in the classification logic line. As such, the depth adjustment will affect the detection of both shallow OD and shallow ID indications. Based on the phase calibration curve for the classification test channel (P1:400|100 kHz mix), changing the lower limit of the depth parameter here to 10 percent translates to a reduction of approximately 7° in the upper bound of the phase window (affecting detection of OD originated signals) and approximately 7° in lower bound of the phase window (affecting detection of ID originated signals).

The CDS configurations discussed above were sequentially applied to the screening of bobbin probe inspection data collected from free-span regions of the SG mock-up. The analysis results for representative signals, which were missed as a result of modifying one or more of the test logic parameters, is displayed in Figs. 4.75 to 4.77. Figure 4.75 shows two previously detected flaw signals which were not reported by the modified CDS setups displayed in Fig. 4.73. Per Fig. 4.73, as indicated by the results, slight changes in voltage threshold or phase limits may result in missing of indications. The flaw signals in Figs. 4.75(a) and (b), both identified as axial ODSCC, were missed as a result of using a higher detection threshold in the classification test logic. Figure 4.76 shows representative missed indications using the CDS setup displayed in Fig. 4.74. The flaw signals, identified as circumferential and axial ODSCC, were not reported because their phase angle lies outside the prescribed flaw reporting window. Two other examples of missed indications attributed to the modified setup parameters are shown in Fig. 4.77. The signal displayed in Fig. 4.77(a) was not reported because of its phase response. The signal displayed in Fig. 4.77(b) on the other hand was not reported by either one of the modified sort configurations shown in Figs. 4.73 and 4.74.

A set of POD curves was subsequently generated using the results of analyses on the entire free-span data set with the optimized and the modified CDS configurations discussed above. Once again, the optimized configuration here is in reference to the CDS setup shown in Fig. 4.59 and the modified configurations are in reference to those shown in Figs. 4.73 and 4.74. It is worth noting that incorporation of a larger number of samples in the available database, particularly shallow indications, is expected to improve the reliability of POD calculations. To assess the viability of combining data from different flaw types, POD curves were first generated based on the detection results with the optimized sort configurations. Figure 4.78 shows the POD curve generated using the detection results for all flaws identified as SCC (axial and

circumferential SCC of both OD and ID origin) and that generated using only the detection results for axial SCC (LODSCC) flaws. Figures 4.78(a) and 4.78(b) display the POD curves using log-logistic and linear-logistic fits, respectively. The results here indicate a negligible shift in the detection probability using different combinations of SCC flaws. Subsequently, composite POD curves were generated using the detection results for all the SCC flaws available in the database. The POD curve using the optimized CDS setup parameters and those using the modified setup parameters are presented in Fig. 4.79. The three modified configurations included the setups shown in Figs. 4.73, the setups shown in Fig. 4.74 and a combination of both. While the POD curves for all modified setups exhibit a shift to the right (reduction in detection probability), the largest shift is associated with the CDS setup with combined amplitude threshold and depth window adjustment. The results of comparative tests here generally indicate that relatively small adjustments of the test logic parameters can have measurable effects on the detection probability. It is also worth noting that the statistical distribution of the flaw sizes in a database will influence the level of change in the POD results.

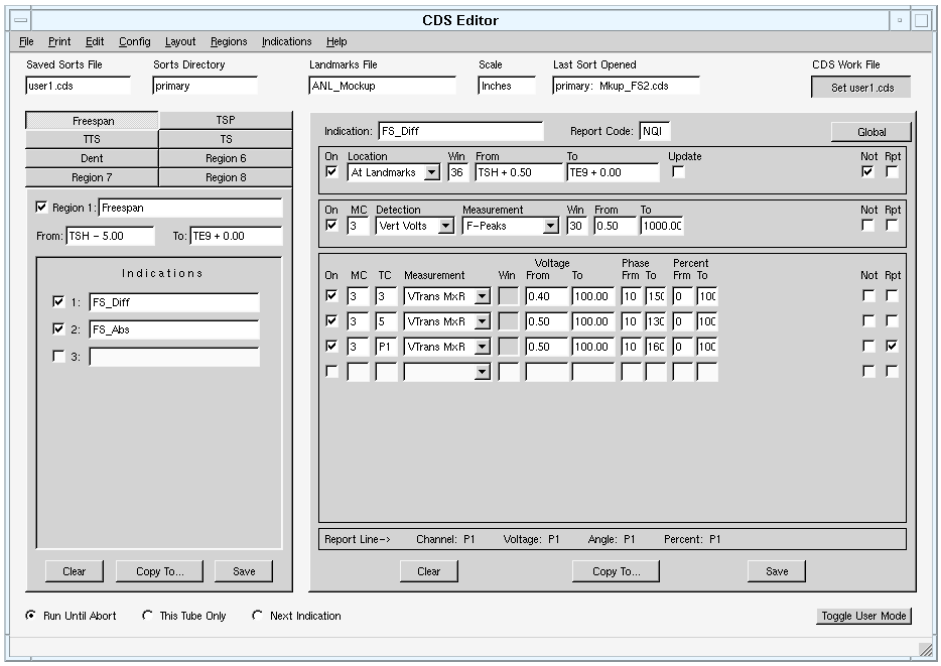

(a)

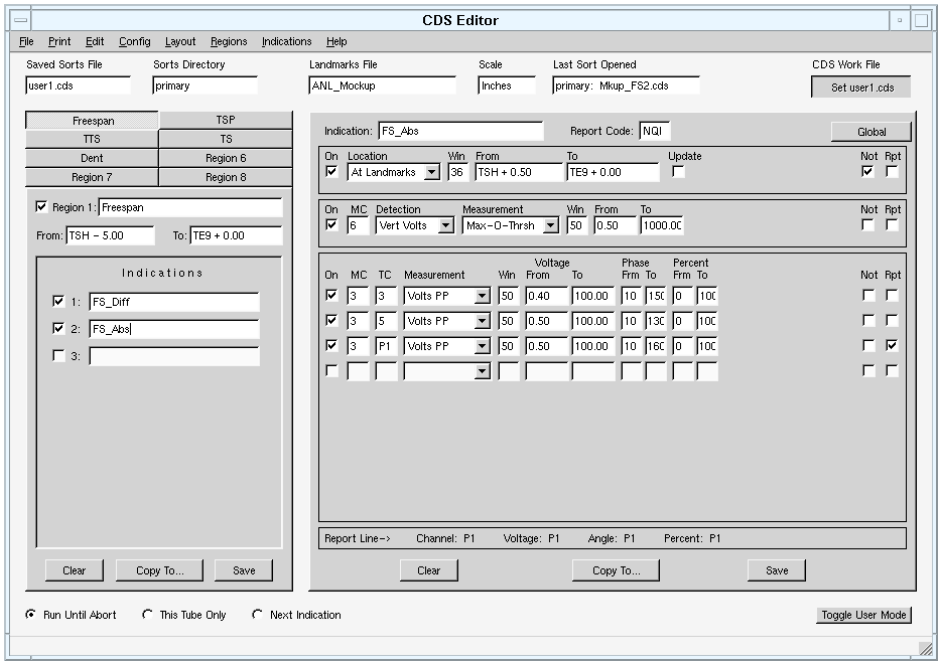

(b)

Figure 4.59 Display of the CDS editor dialog box for the setups used for screening free-span indications. Shown here are the two sorts under the *Indications* list and their associated setup parameters. The detection logic line displays (a) a differential detection channel used for the first and (b) an absolute detection channel used for the second setup, respectively.

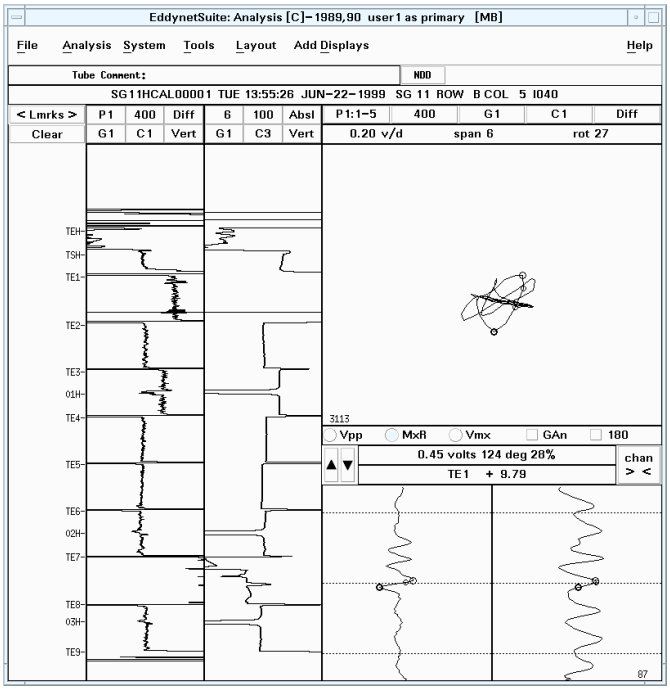

(a)

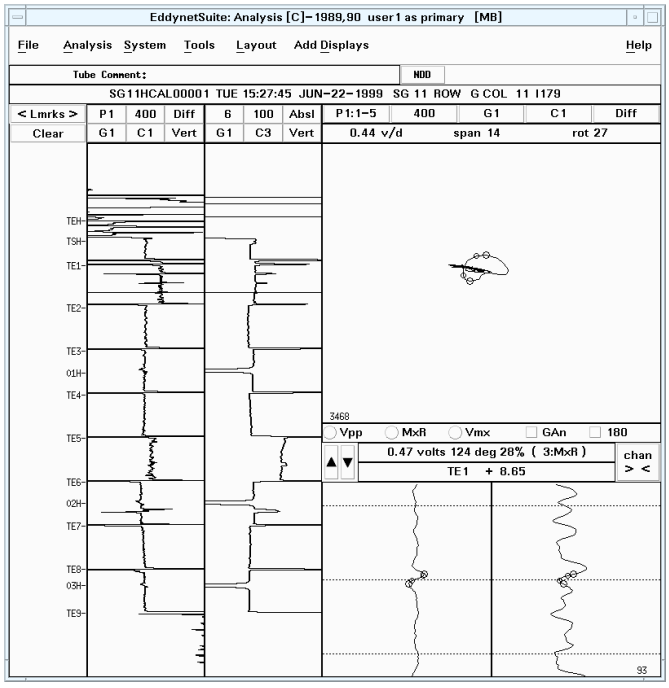

(b)

Figure 4.60 Display of data analysis results for representative signals at level-B elevation of the SG mock-up which were not reported using the CDS setup displayed in Fig. 4.59.

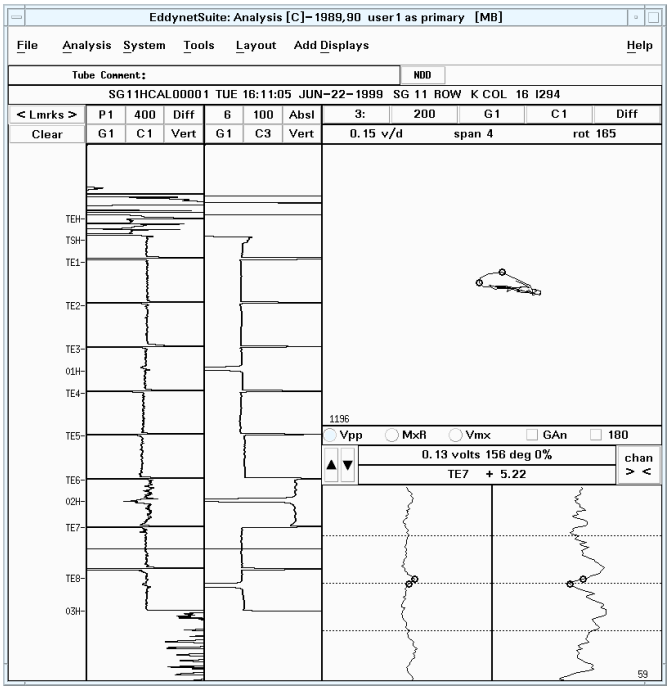

(a)

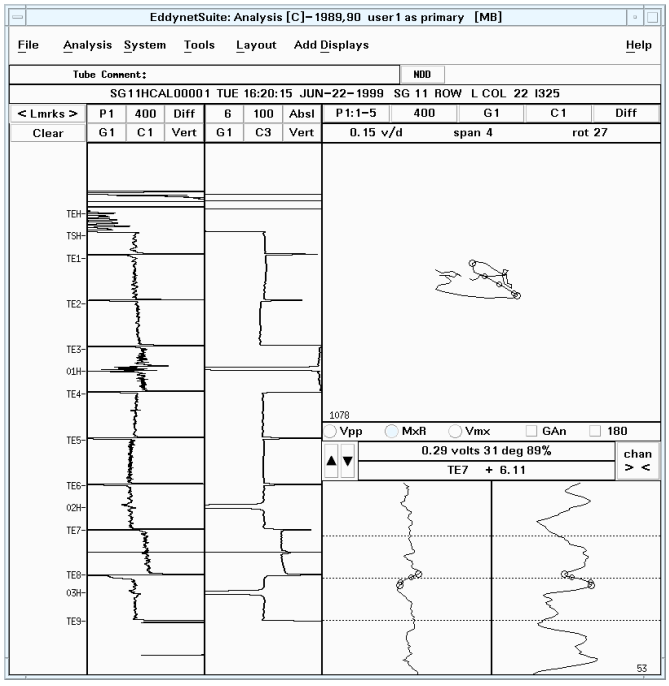

(b)

Figure 4.61 Display of data analysis results for representative signals at level-H elevation of the SG mock-up which were not reported using the CDS setup displayed in Fig. 4.59.

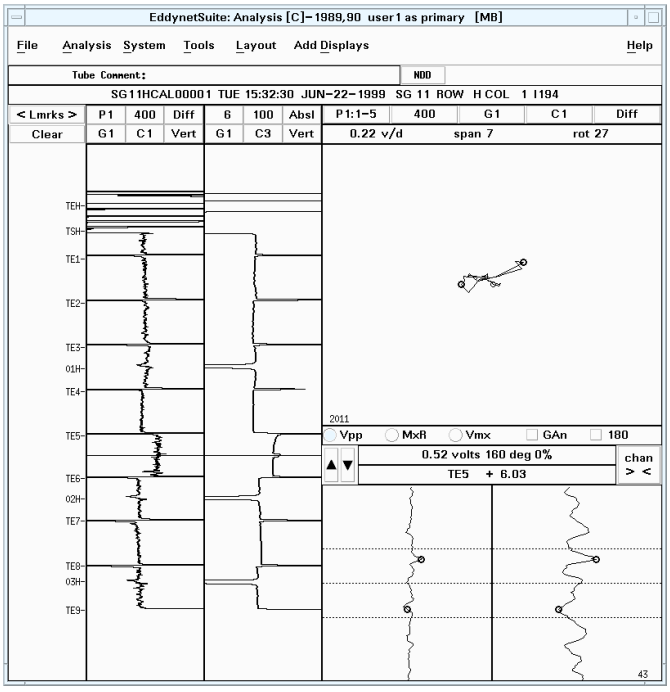

(a)

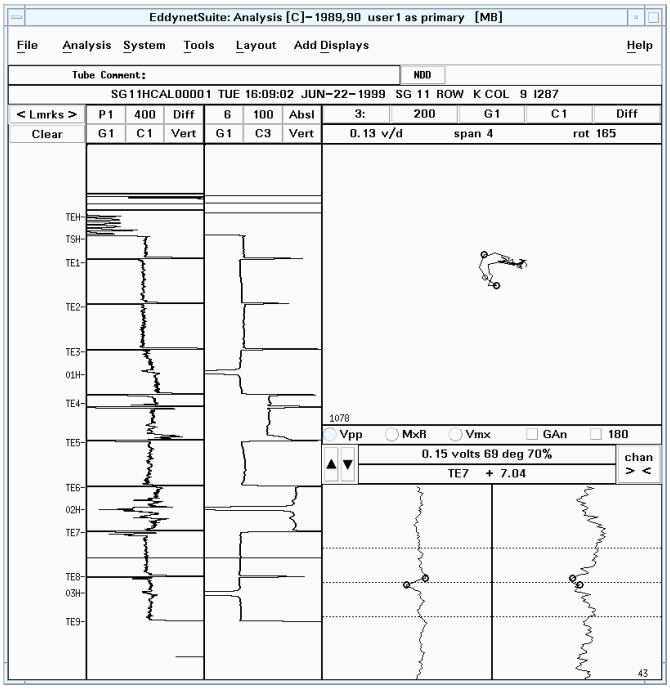

(b)

Figure 4.62 Display of data analysis results for representative signals at (a) level-F and (b) level-H of the SG mock-up which were not reported using the CDS setup displayed in Fig. 4.59.

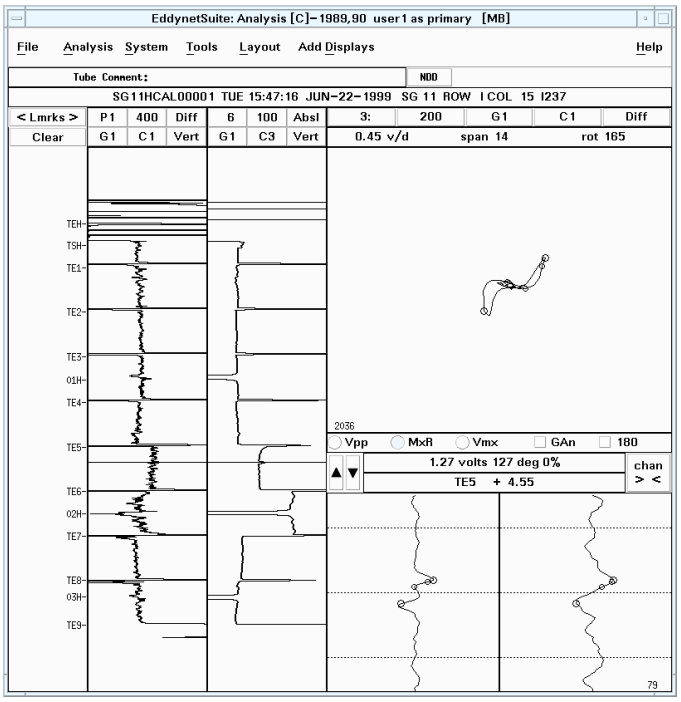

(a)

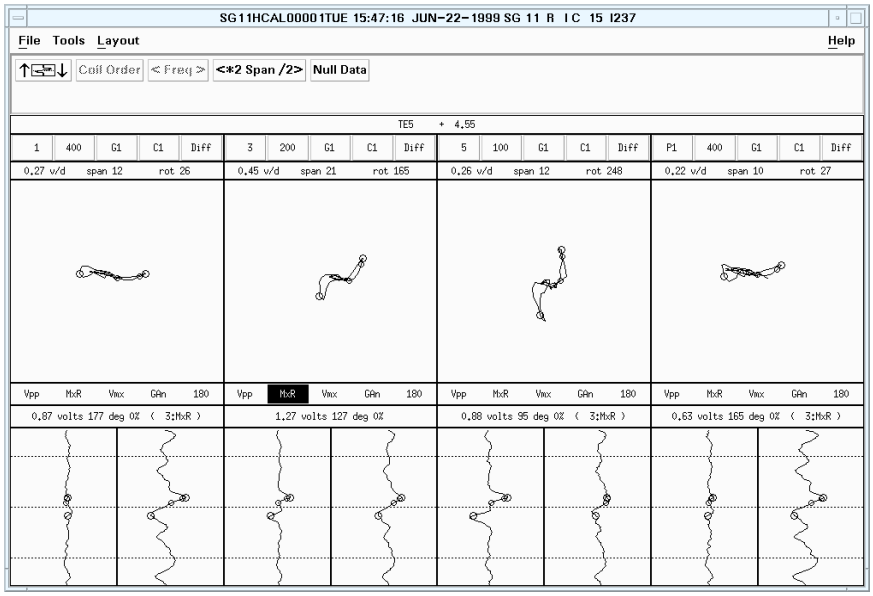

(b)

Figure 4.63 Display of data analysis results for a signal at the level-F elevation of the SG mock-up which was not reported using the CDS setups displayed in Fig. 4.59. The probe response is shown in the (a) main analysis window and (b) in multiple Lissajous window at different frequencies.

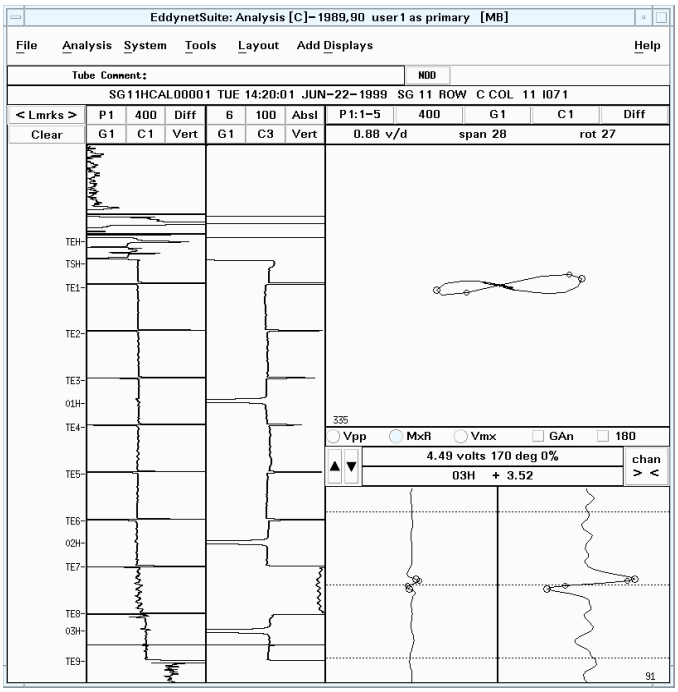

(a)

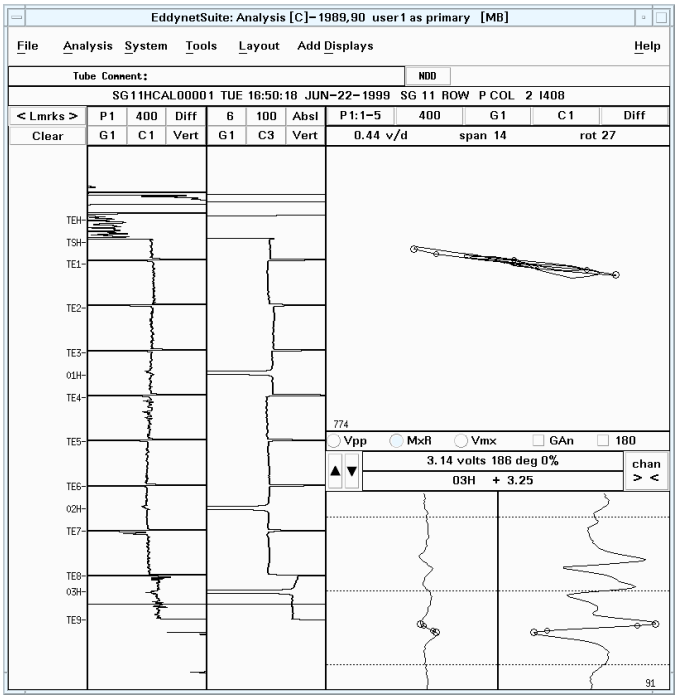

(b)

Figure 4.64 Display of data analysis results for representative signals at the level-I elevation of the SG mock-up which were not reported using the setups displayed in Fig. 4.59.

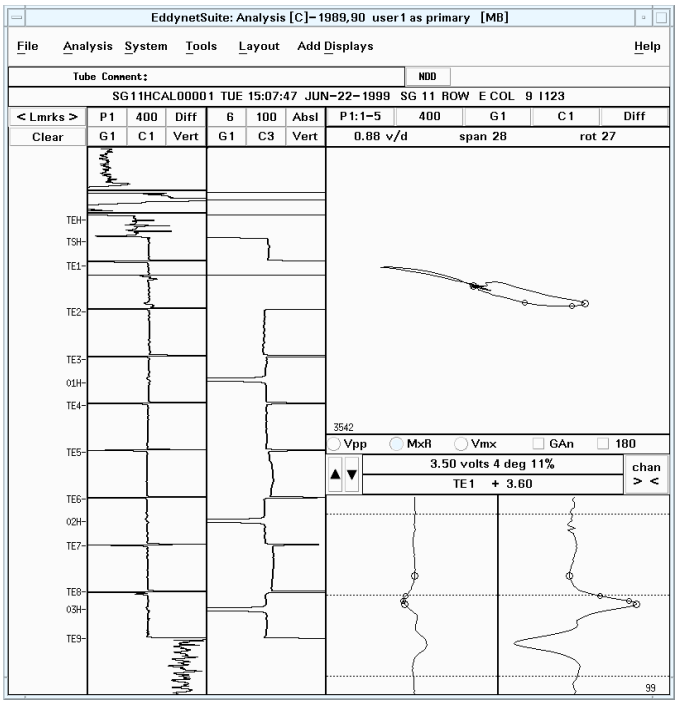

(a)

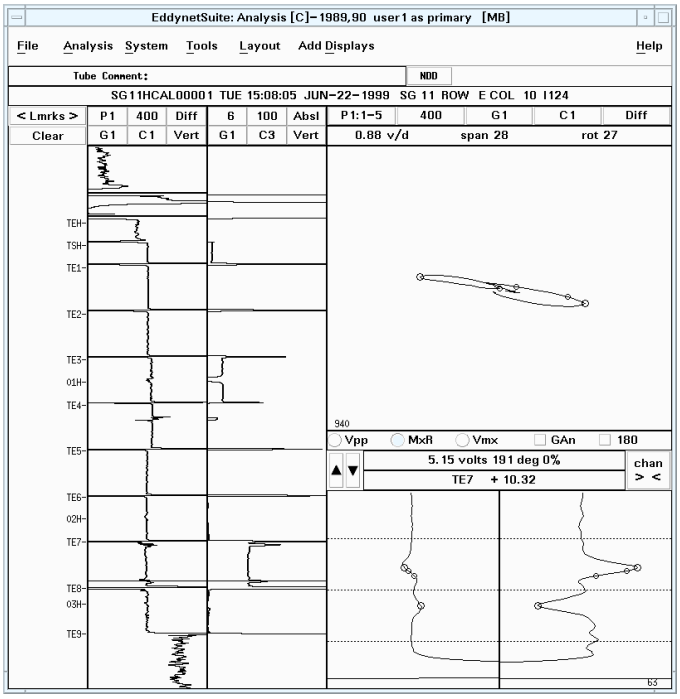

(b)

Figure 4.65 Display of data analysis results for representative signals at (a) level-B and (b) level-H elevation of the SG mock-up which were not reported using the setups displayed in Fig. 4.59.

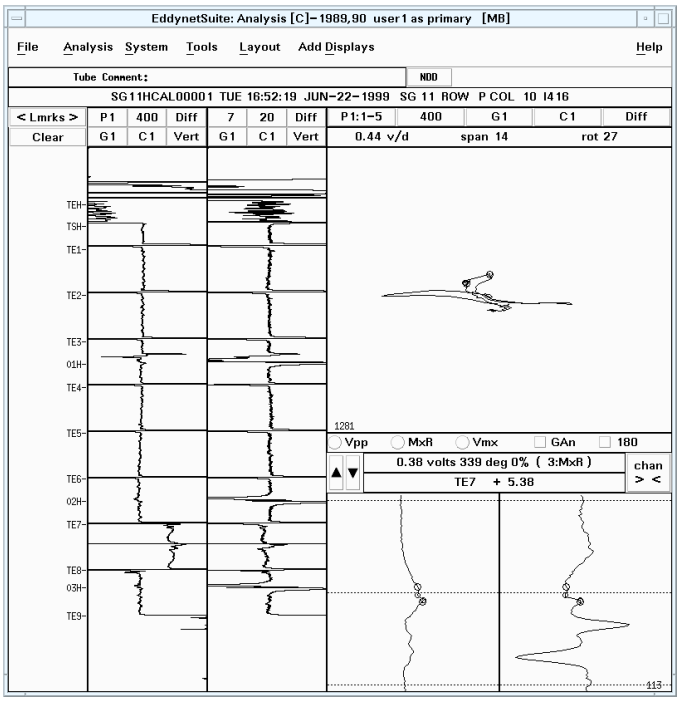

(a)

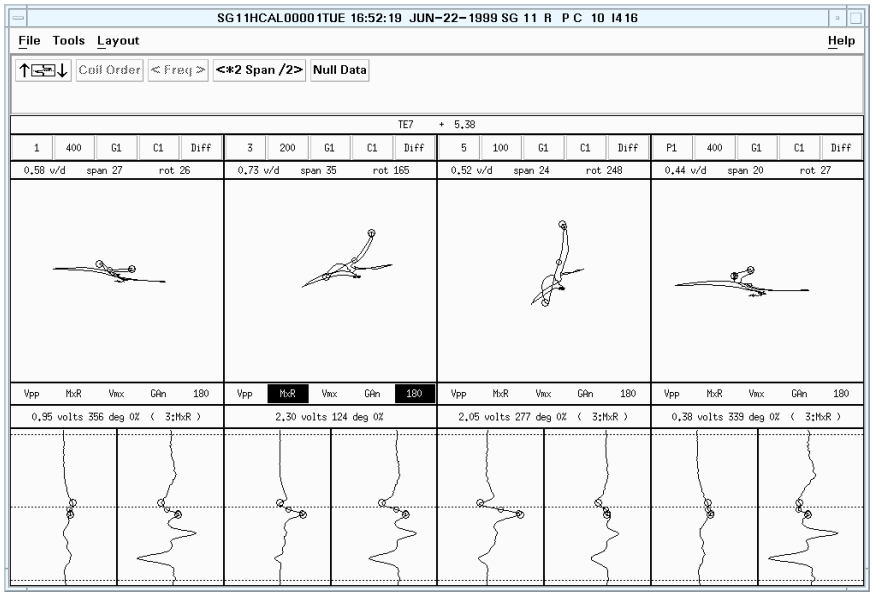

(b)

Figure 4.66 Display of data analysis results for a signal at the level-H elevation of the SG mock-up which was not reported using the CDS setups displayed in Fig. 4.59. The probe response is displayed in the (a) main analysis window and (b) in multiple Lissajous window at different frequencies.

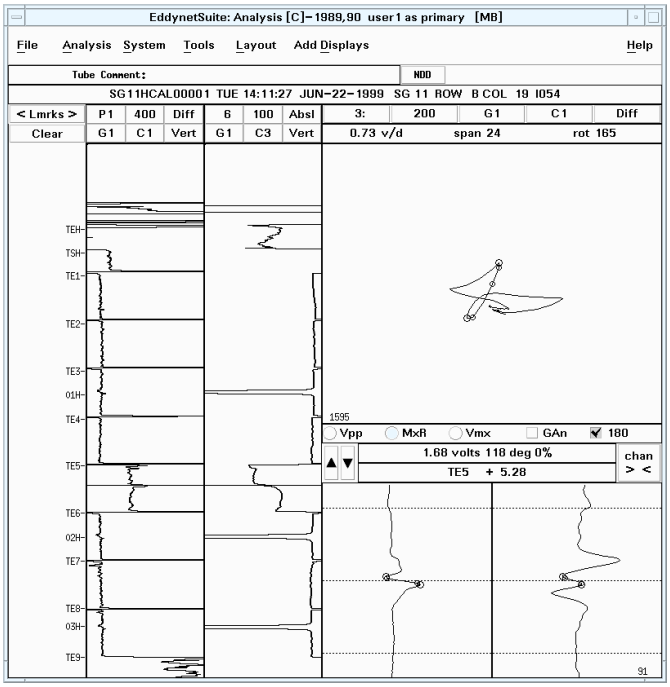

(a)

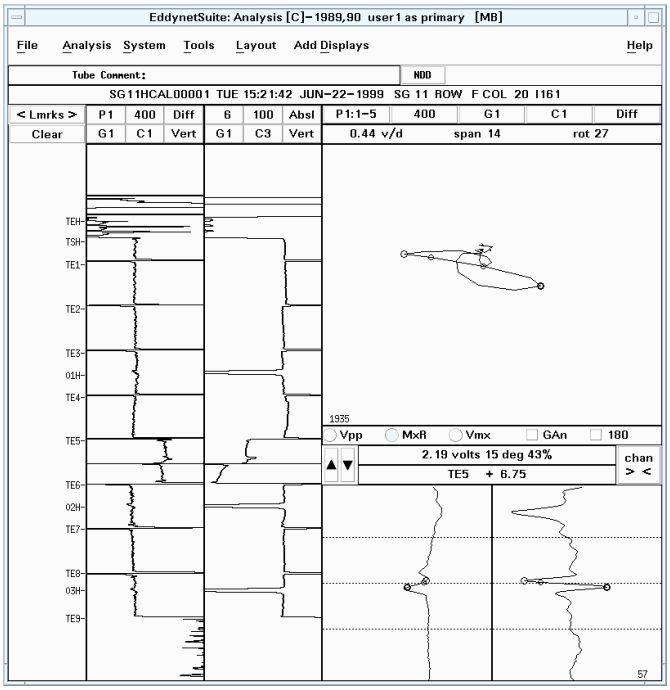

(b)

Figure 4.67 Display of data analysis results for representative signals at the level-F elevation of the SG mock-up which were not reported using the CDS setups displayed in Fig. 4.59.

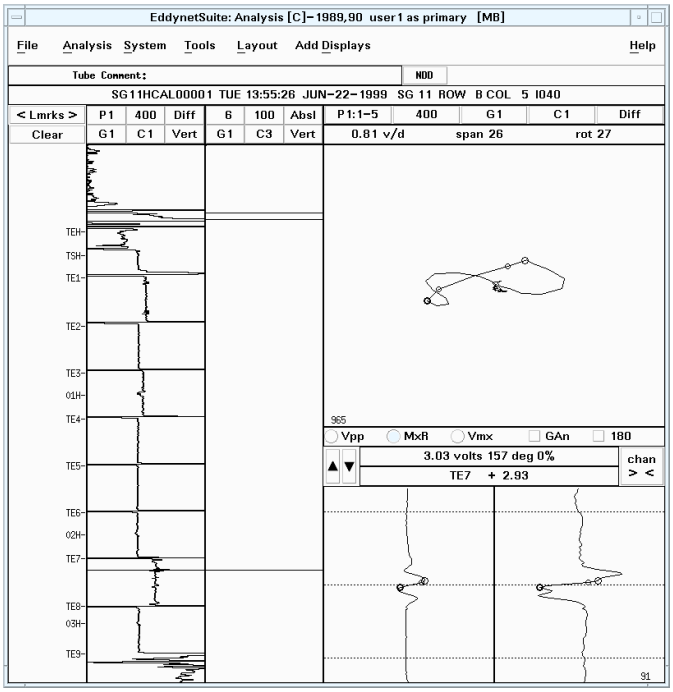

(a)

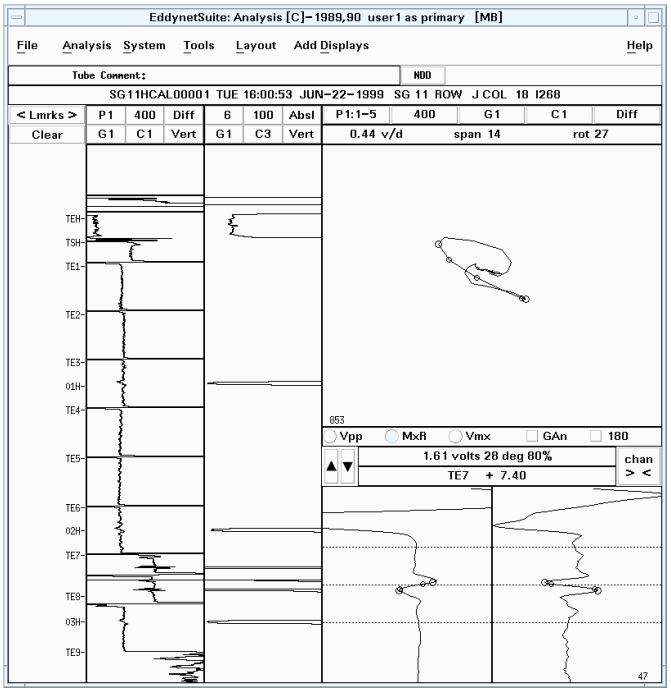

(b)

Figure 4.68 Display of data analysis results for representative signals at the level-H elevation of the SG mock-up which were not reported using the CDS setups displayed in Fig. 4.59.

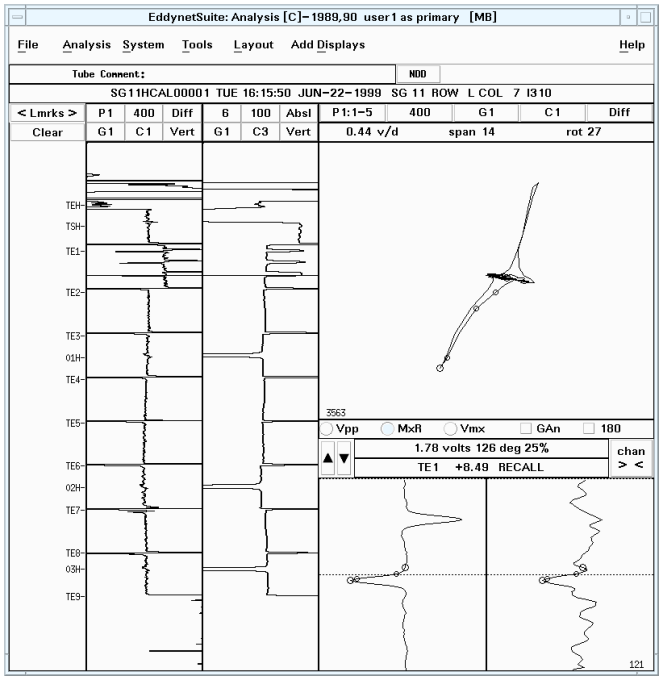

(a)

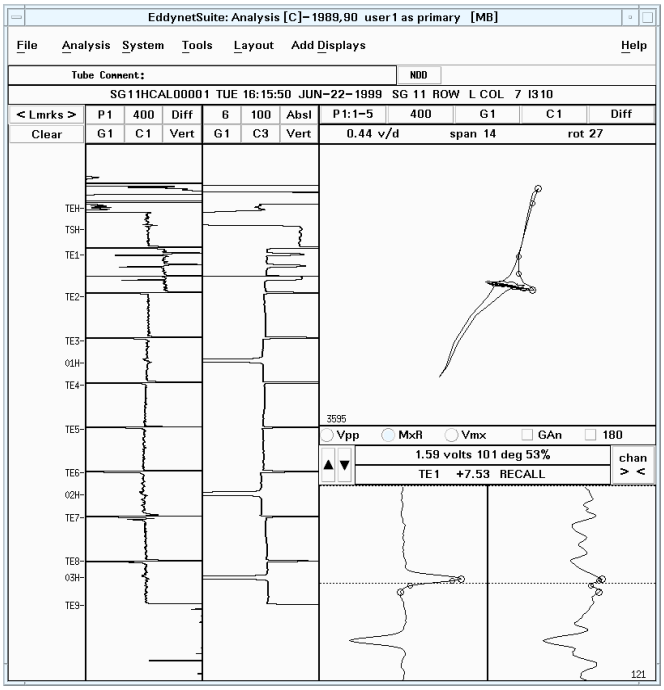

(b)

Figure 4.69 Display of representative CDS analysis results for a long axial OD flaw for two separate entries in the free-span of the SG mock-up.

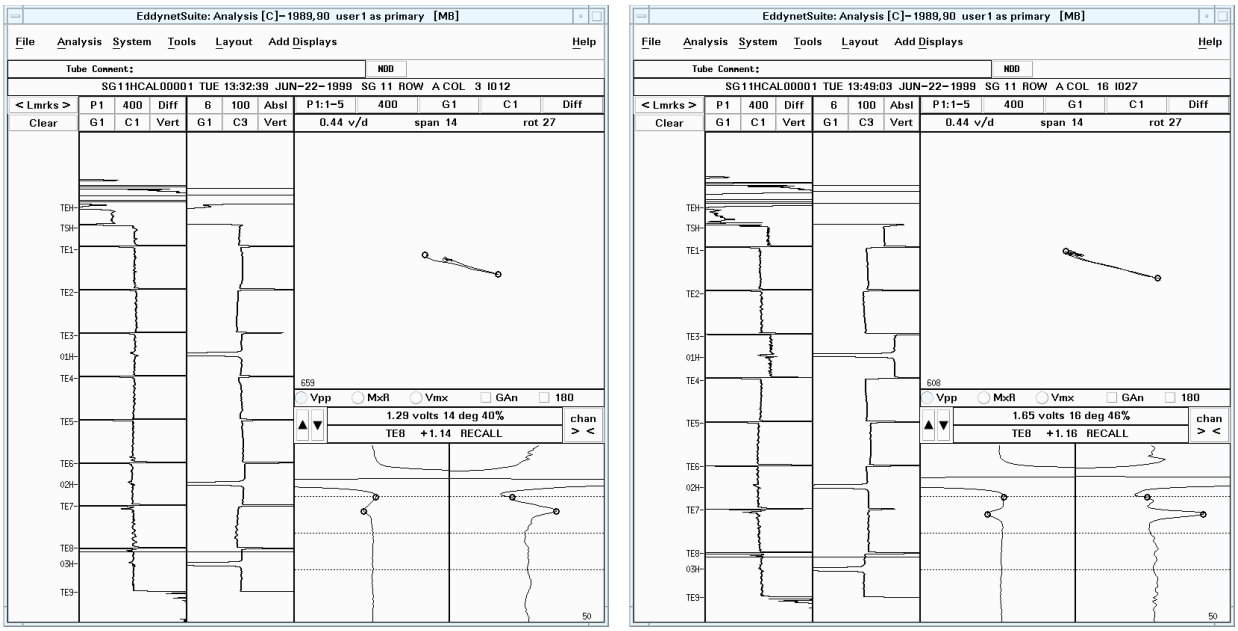

(a)

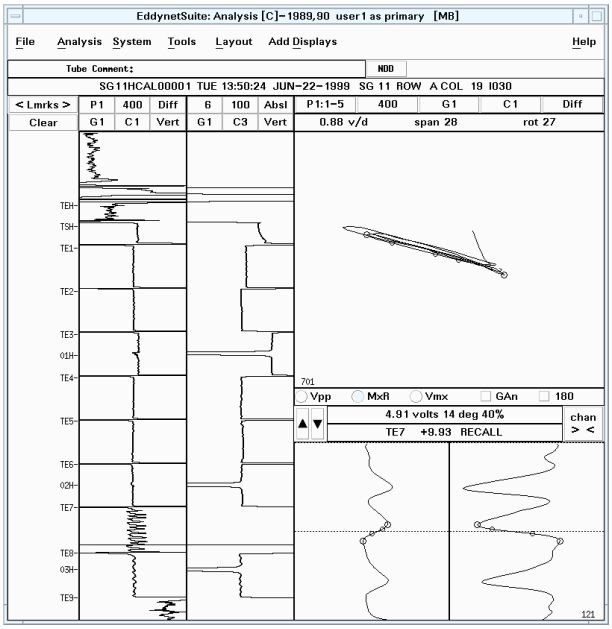

(b)

Figure 4.70 Display of the CDS analysis results associated with representative false calls in the free-span of the SG mock-up using the sort configuration of Fig. 4.59(b).

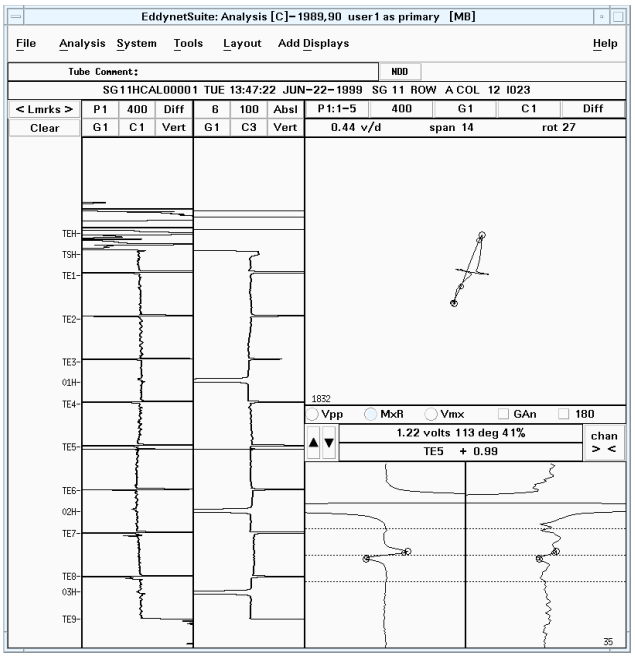

(a)

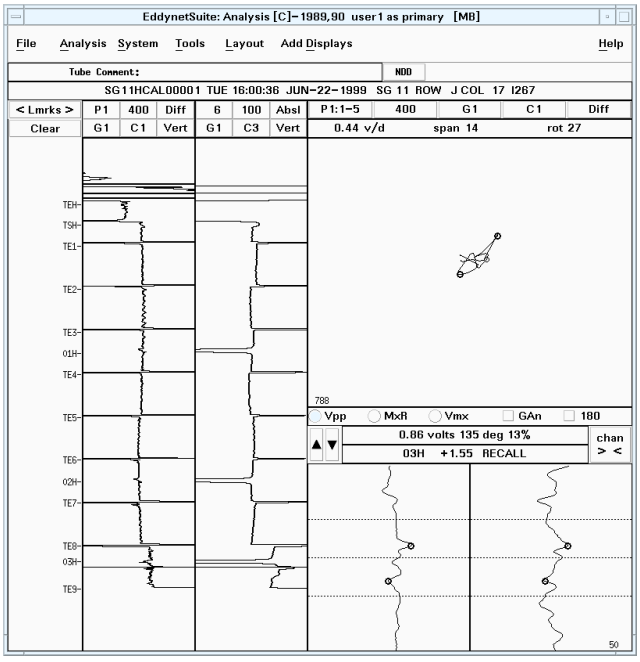

(b)

Figure 4.71 Display of data analysis results for representative signals in the free-span of the SG mock-up which were not reported using the CDS setup displayed in Fig. 4.59(a).

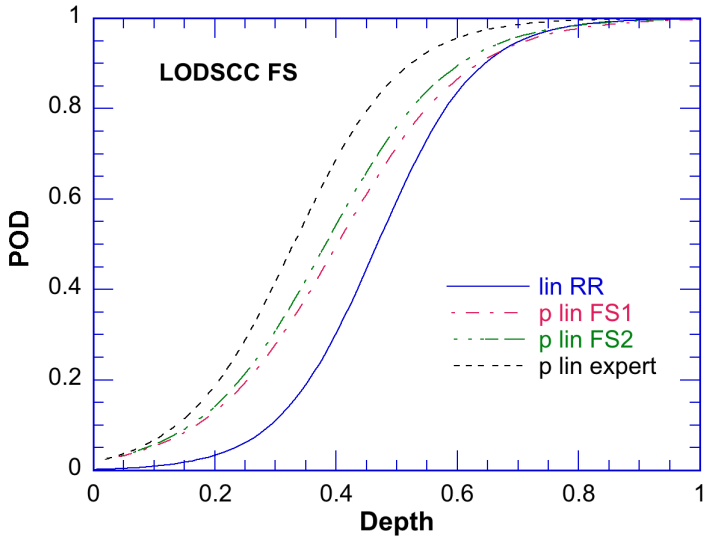

(a)

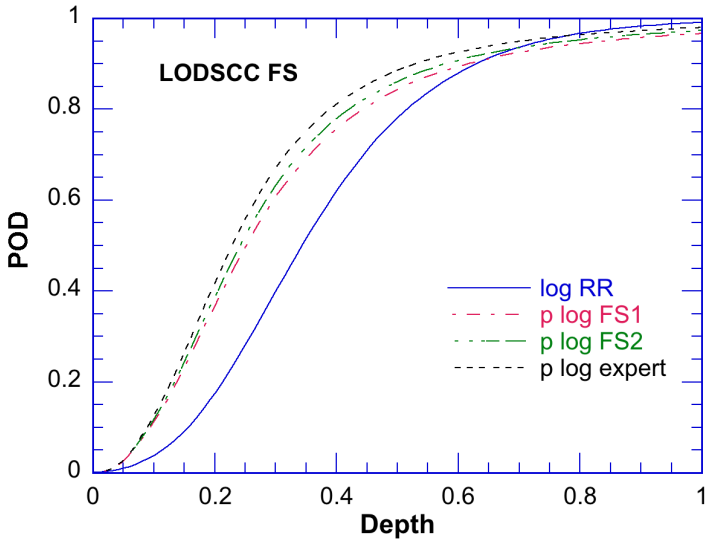

(b)

Figure 4.72 POD curves for free-span (FS) flaws identified as LODSCC using the CDS sort configurations shown in Fig. 4.59.

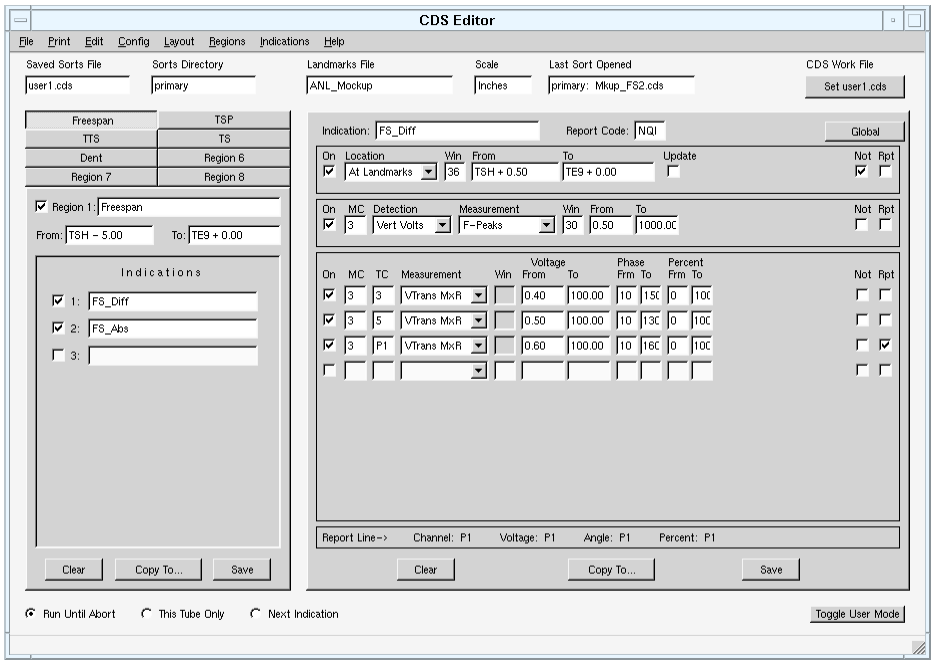

(a)

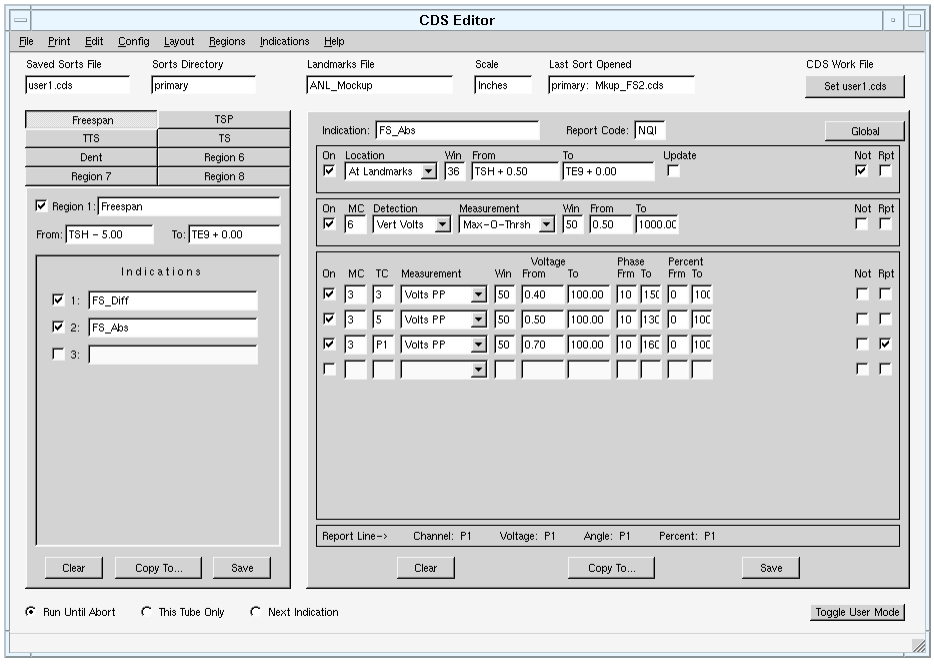

(b)

Figure 4.73 Display of the CDS editor dialog box for the modified configuration used to screen the free-span region of the SG mock-up. Shown here are the setup parameters for the sort using (a) a differential channel and (b) an absolute channel for detection.

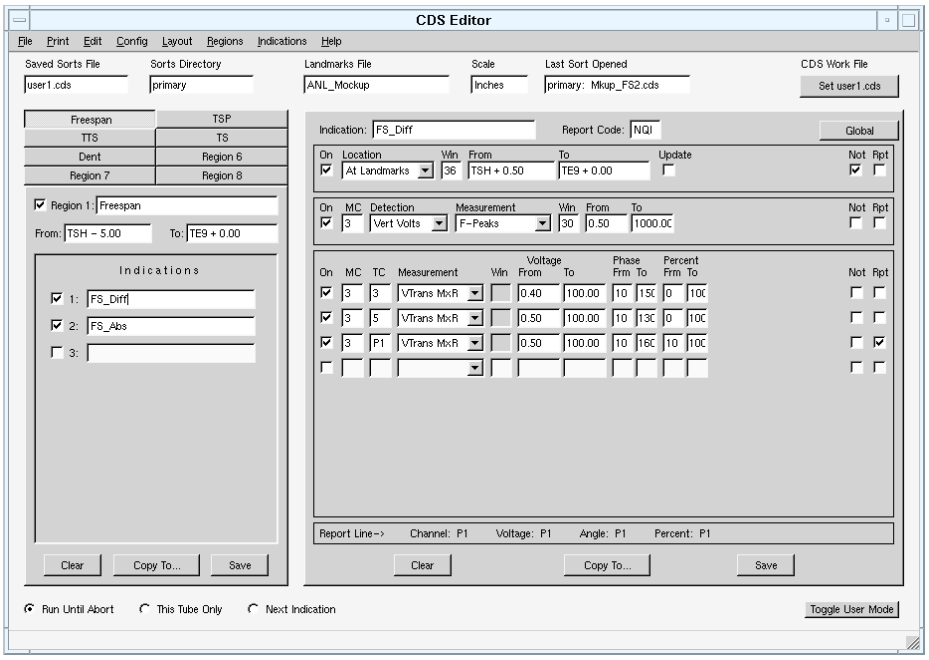

(a)

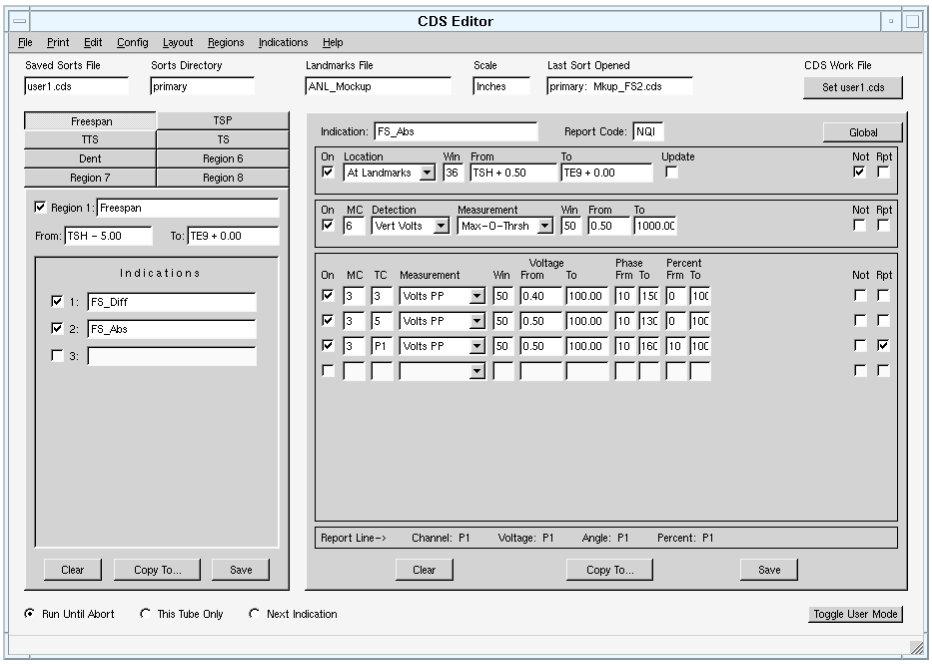

(b)

Figure 4.74 Display of the CDS editor dialog box for the modified configuration used to screen the free-span of the SG mock-up. Shown here are the setup parameters for the sort configuration using (a) a differential channel and (b) an absolute channel for detection.

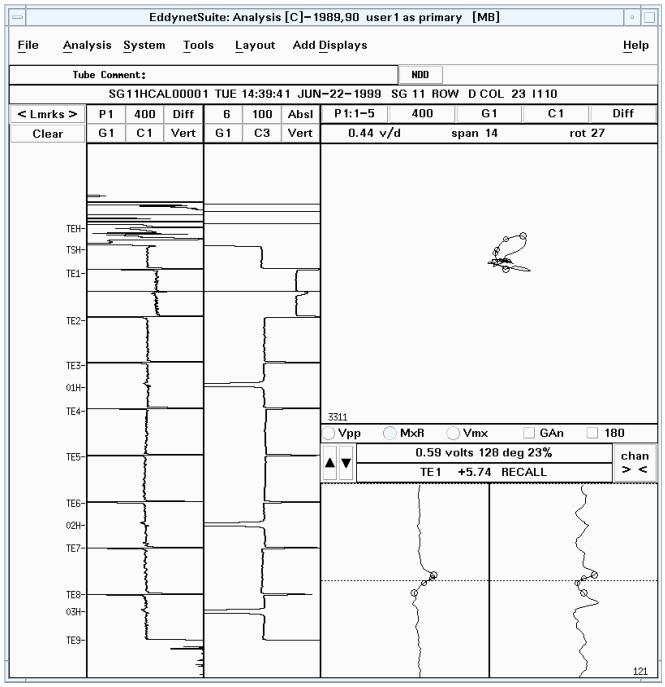

(a)

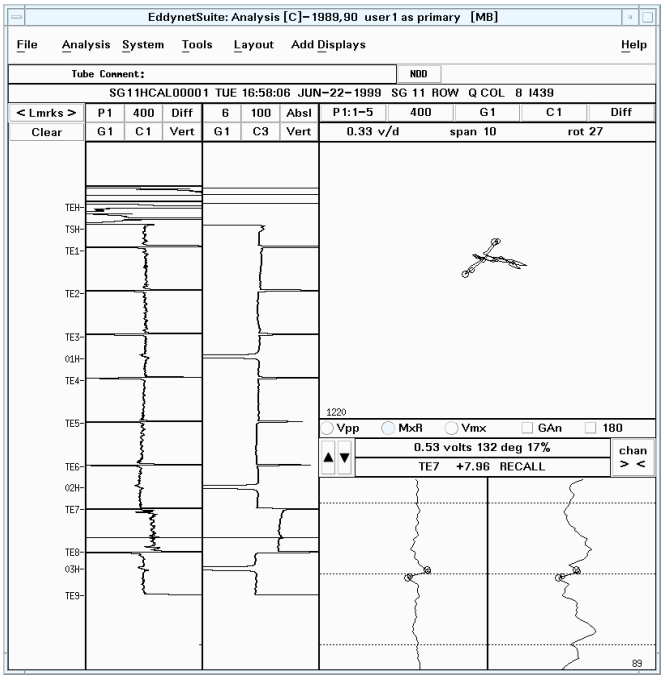

(b)

Figure 4.75 Display of CDS results for representative free-span signals. Shown here are flaws identified as axial ODSCC at (a) level-B and (b) level-H.

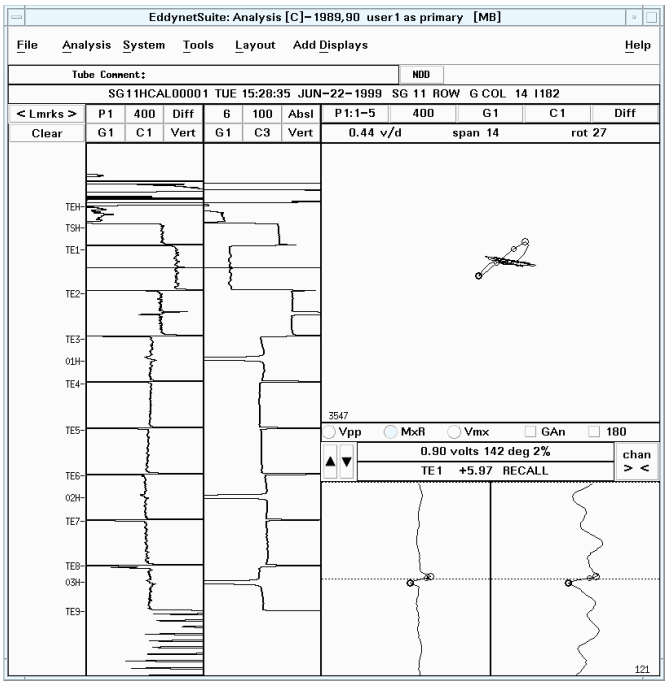

(a)

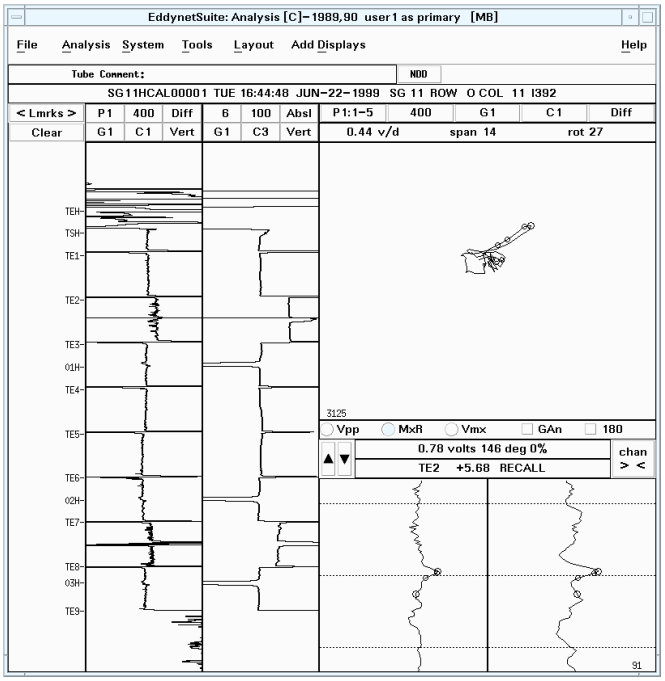

(b)

Figure 4.76 Display of CDS results for representative free-span signals. Shown here are flaws identified as (a) circumferential ODSCC at level-B and (b) axial ODSCC at level-C.

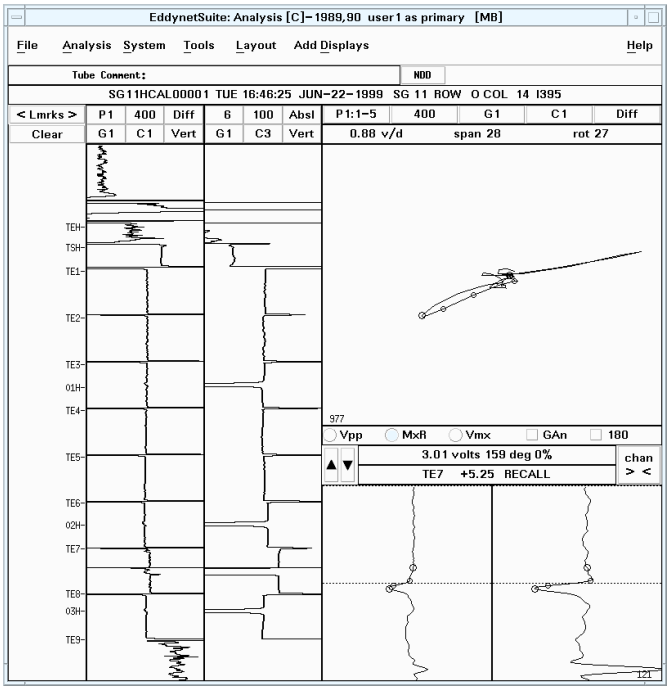

(a)

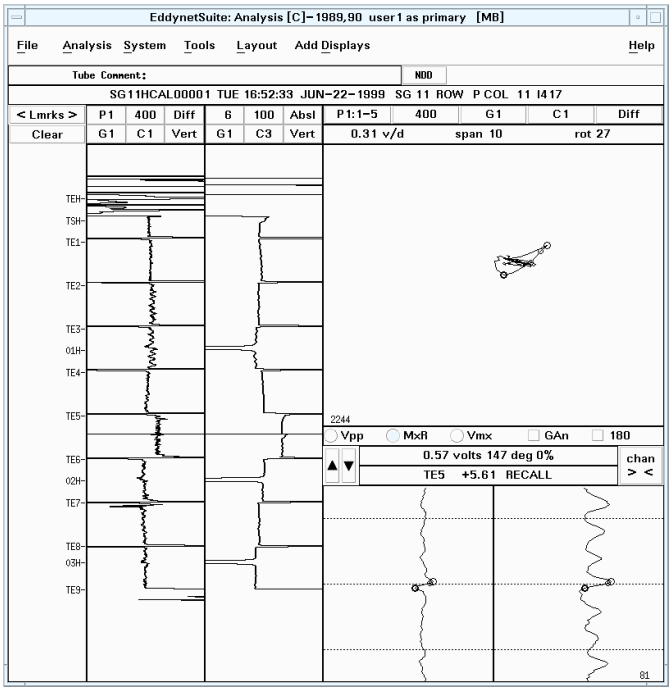

(b)

Figure 4.77 Display of CDS results for representative free-span signals. Shown here are flaws identified as axial ODSCC at (a) level-H and (b) at level-F.

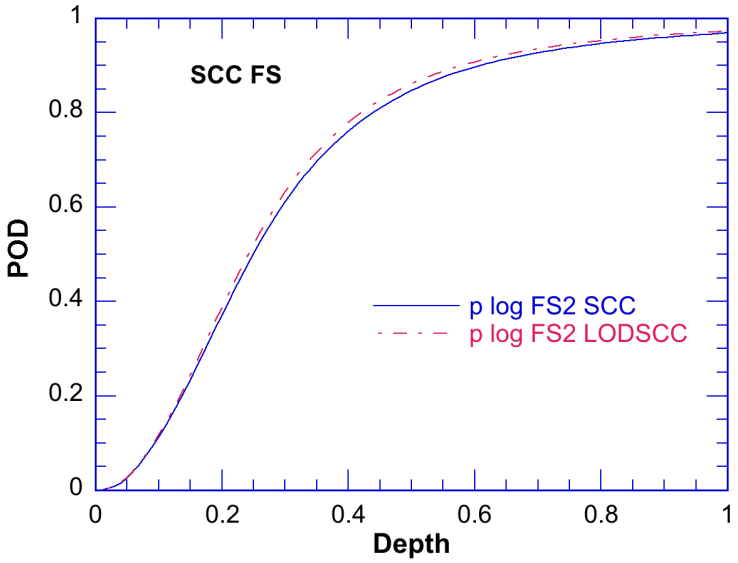

(a)

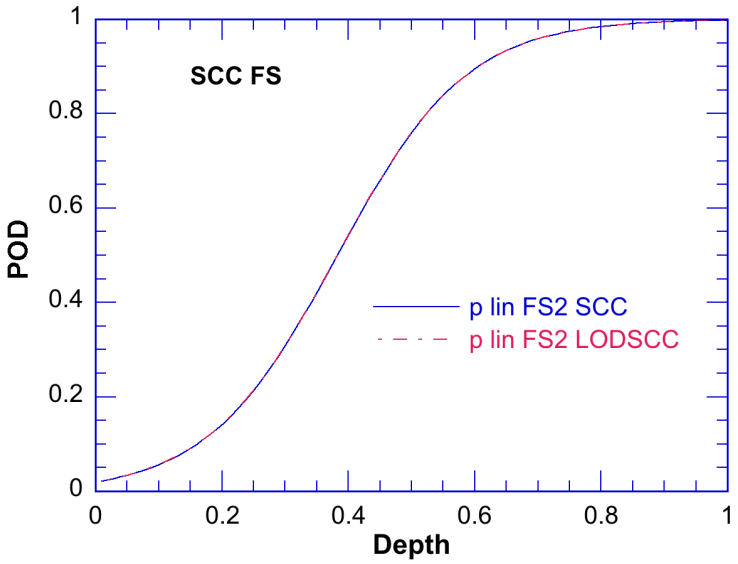

(b)

Figure 4.78 POD curves for free-span (FS) flaws identified as SCC (axial and circumferential SCC of both OD and ID origin) and LODSCC (axial ODSCC) using the optimized CDS configuration shown in Fig. 4.59.

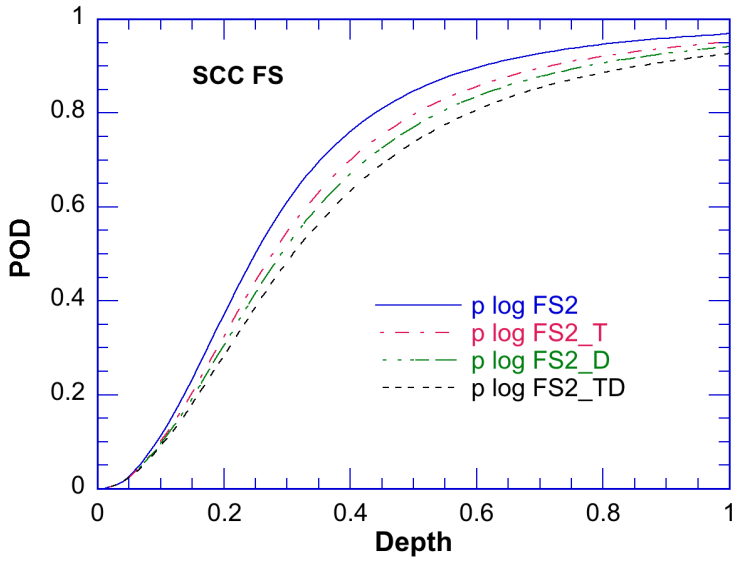

(a)

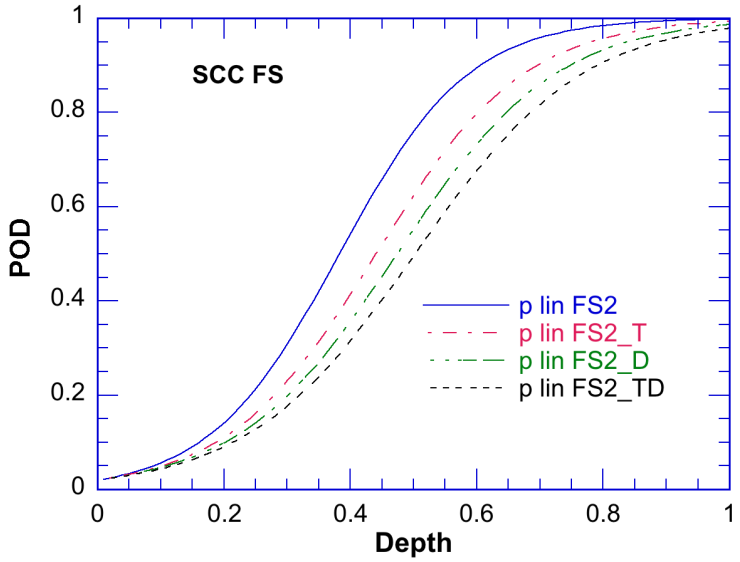

(b)

Figure 4.79 POD curves for free-span (FS) level flaws identified as SCC (axial and circumferential SCC of both OD and ID origin) using the optimized configuration shown in Fig. 4.59 (FS2) and the modified configurations shown in Figs. 4.73 (FS2_T) and 4.74 (FS2_D) for (a) linear-logistic and (b) log-logistic fits.

4.3.3 Analyses of Data for Tubesheet Elevations

Limited studies were carried out to assess the ability of automated data screening to identify flaw signals in the bobbin probe data from the tube-sheet elevation of the SG mock-up. Unlike the free-span and the TSP elevations, manual analysis of bobbin probe inspection data from TS sections was deemed unreliable due to excessive levels of noise associated with the mechanical expansion of the tubes. Therefore, data from the TS was not evaluated as part of the past round-robin exercise. Furthermore, bobbin probe techniques are not generally considered reliable for detecting and characterizing cracking in close proximity to the TS expansion transition region. Higher resolution inspection methods such as rotating probe techniques are used for more reliable examination of those regions. As such, the CDS results for the TS elevations of the SG mock-up were evaluated in a qualitative manner. The automated analysis results suggest that, in comparison with other elevations of the SG mock-up, flaws near the TTS region may be detected with comparable probability but with a significantly higher number of false calls.

The lowest level of the tube sections in the SG mock-up simulates the tube-sheet geometry. The bottom portion of each 30.5-cm (12-in.) long Alloy 600 tube section is mechanically expanded (hard rolled) into individual ~15.2-cm (6-in.) carbon steel collars. The small region near the TTS where the tube transitions from the expanded diameter to the nominal diameter simulates the expansion transition region and is located roughly in the middle of the TS-level tube sections. The majority of expansions were done at Argonne and a small subset of TS level tubes was supplied by an outside vendor. Comparison of EC inspection data between the two types of expansions suggests that on average those manufactured at Argonne have measurably higher baseline noise. The higher level of noise is attributed to the mechanical rolling process employed by the machine shop at Argonne. The manufactured flaws present in the TS level, which include both axial and circumferential cracks of ID and OD origin, are located mostly at or near the expansion transition region.

Based on expert opinion sought prior to conducting past round robin exercises, it was decided that the EC signals near the TTS (upper edge of the collar) and at the expansion transition areas of the SG mock-up are representative of those found in the field. However, based on the results from manual analysis of data with bobbin and rotating probe, it was later concluded that on average the level of noise present in the TS level of the SG mock-up was significant enough to hinder the ability of the analysts to reliably detect and characterize flaws in that region. The non-uniform geometry of the mechanically expanded portion and of the expansion transition region were determined to be the primary contributors to the relatively large number of overcalls in the TS level. Additionally, a fraction of false calls recorded by analysts were attributed to unintentional damage introduced by the mechanical expansion process and the final tube-collar assembly.

Bobbin probe data from the TS level of the SG mock-up was analyzed using the CDS software while keeping in perspective the issues discussed above. The CDS setups generated earlier based on examining the subset of tubes in the training dataset were used to assess the ability of automated data screening algorithms to detect flaw signals at the TS region of the SG mock-up. The test section was divided into two overlapping regions denoted as the TS inner region—covering the entire TS section except for a 25-mm (1-in.) zone at the top and a 25-mm (1-in.) zone at the bottom edge of the TS collar—and the TTS region—covering 25 mm (1 in.) above and 50 mm (2 in.) below the top edge of the TS collar including the expansion transition region.

The CDS setups for the two sort configurations denoted as *TS* and *TTS* under the *Regions* and *Indications* setup area of the *CDS Editor* window is shown in Figs. 4.80(a) and 4.80(b), respectively. In both setups, the detection was based on the three-frequency mix ("turbo mix™") process channel (P3) that is commonly used for simultaneous suppression of the bobbin probe response from the TS edge and the expansion transition geometry. For a 1.27-mm (0.05-in.) tube wall thickness the mix, denoted here as P3, combines the data from the 400 kHz, 200 kHz, and 100 kHz frequencies to suppress the composite probe response from the abrupt change in electrical properties (ferritic steel collar) and the tube geometry change both occurring at the upper edge of the TS. The same P3 was selected as the detection and as the measurement channel in the classification test logic line for both the *TS* and *TTS* sort configurations. In reference to Fig. 4.80(a), an additional line was included in the *TS* sort classification test logic by selecting P3 and P1 (400|100 kHz TSP suppression mix) as the measurement and test channels, respectively. The choice of channels for the detection and classification of potential flaw signals is supported by the fact that the residual signal from P3 is considered as the primary indicator of flaw signals present in close proximity to the expansion transition region while P1 is expected to provide confirmatory information about signals present within the TS and away from its edge. It is worth noting that, because P3 is used as both the measurement and the test channel in the classification logic of the TTS sort, the reported values are essentially an indicator of detection alone and may not be used for characterization purposes as no calibration curve was generated for that channel.

Representative bobbin coil data from selected tube sections in the TS level of the SG mock-up with varying levels of noise are shown next. Figures 4.81-4.89 display measurements made in test sections with different levels of noise including inside the TS, covered by the TS sort configuration, and at the expansion transition region, covered by the TTS sort configuration. In all cases the signal is shown for both P3 and P1, which are the channels used in the measurement and classification test logic of the sort setups discussed above. Figures 4.81-4.83 display three tube sections, which are representative of the range of baseline noise present in the TS-level tubes. The measured peak-to-peak values from P3 in these cases vary between 0.85v and 1.6v with the associated measurements from P1 varying between 0.1v and 5.7v. The range of variation in the baseline noise here is a good indicator of the challenge involved with selecting an appropriate amplitude threshold for detection of signals in that region. As noted before, optimization of the threshold always poses a tradeoff between the detection probability and the false call rate. Examples of measured bobbin probe signals from un-flawed expansion transitions with relatively smooth geometries are shown in Figs. 4.84-4.86. The largest value of the mix residual signal measured from P3 in those tubes is less than 2.5v. Representative expansion transitions, identified as un-flawed test sections, with significantly higher mix residual signal are shown in Figs. 4.87-4.89. These false call signals resulted from using the sort configuration as specified in Fig. 4.80(b). Once again, these examples demonstrate the challenge associated with setting of the test logic parameters for reporting of flaws at the expansion transition regions of the SG mock-up.

The CDS sort configurations displayed in Fig. 4.80 were initially used to analyze the bobbin probe data from TS sections of the SG mock-up. As noted earlier, the two overlapping sorts jointly cover the region extending approximately from 25 mm (1 in.) above the bottom edge to 25 mm (1 in.) above the top edge of the TS collar. Preliminary evaluation of the results in this case indicated that the selected data screening parameters for the TS sort configuration of Fig. 4.80(a) led to an unacceptably large false call rate in that section. As it was discussed earlier, the high false call rate was attributed mainly to non-uniform geometry of the mechanically

expanded portion of the tube. In view of the limitations of the bobbin probe technique and of the alternative characterization test logic, no further attempts were made to adjust the sort parameters that might help in reducing the number of overcalls in that region of the mock-up.

For the next test the TS sort shown in Fig. 4.80(a) was deactivated and the screening of data was limited to a short section of each tube covered by the sort configuration shown in Fig. 4.80(b). As mentioned above, this region is denoted as TTS in the *Indications* column of the CDS Editor dialog box, extending from TTS-2.0 in. to TTS+1.0 in. The elimination of the region inside the TS section from screening by CDS resulted in exclusion of a number of shallow indications in the database. Therefore, because of the bias in the statistical distribution of the remaining flaws, development of a POD curve was deemed as unreliable. As such, the CDS results for that region of the SG mock-up were evaluated only in a qualitative manner.

The analysis results based on the CDS sort parameters shown in Fig. 4.80(b) indicated that nearly all consequential indications near the TTS were detected. The false call rate—defined as the number of false calls divided by the number of unflawed test sections—of >30 percent, however, was significantly higher than those from the TSP and the free-span elevations of the SG mock-up. Figures 4.87-4.89 display representative entries for un-flawed test sections reported as flaws by CDS. The false calls in all cases were attributed to the large signal from the abrupt change in geometry at the expansion transition region. Figures 4.90-4.94 display the indications at or near the TTS, which were not reported by CDS using the setup described in Fig. 4.80(b). In Figs. 4.90-4.92, 4.94 the flaws were identified as axial IDSCC. In Fig. 4.93, the flaw was identified as circumferential IDSCC. In all those cases the small amplitude of the signal was determined to be the cause for missing the flaw. It is worth noting that, although the test logic parameters may be adjusted to detect the majority of the missed signals shown here, this in turn is expected to result in a significant increase in the number of false calls. Also, the flaw signals above the TTS that are located away from the expansion transition region may further be detected by increasing the coverage of the free-span sorts.

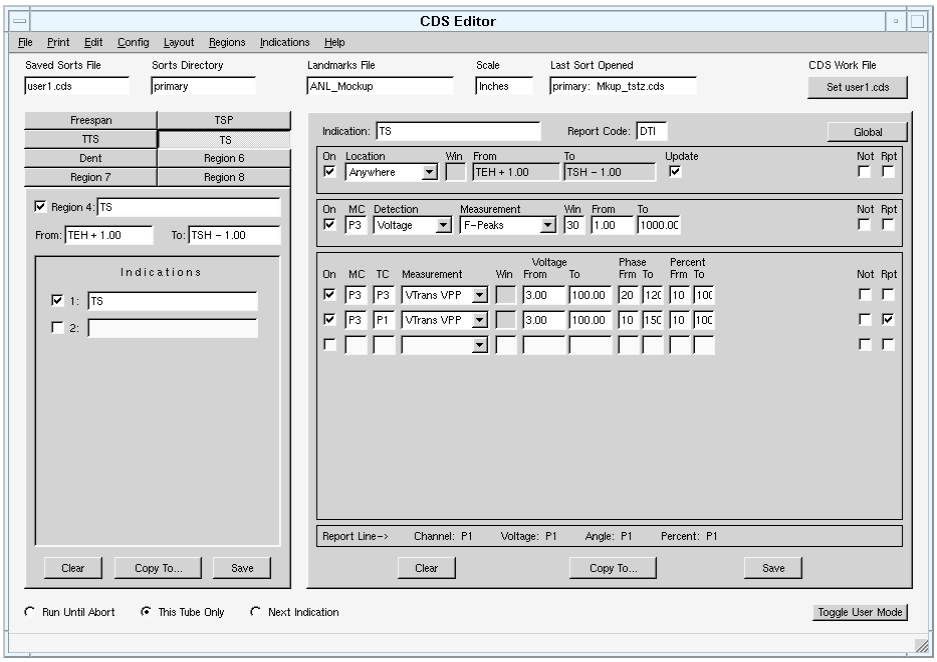

(a)

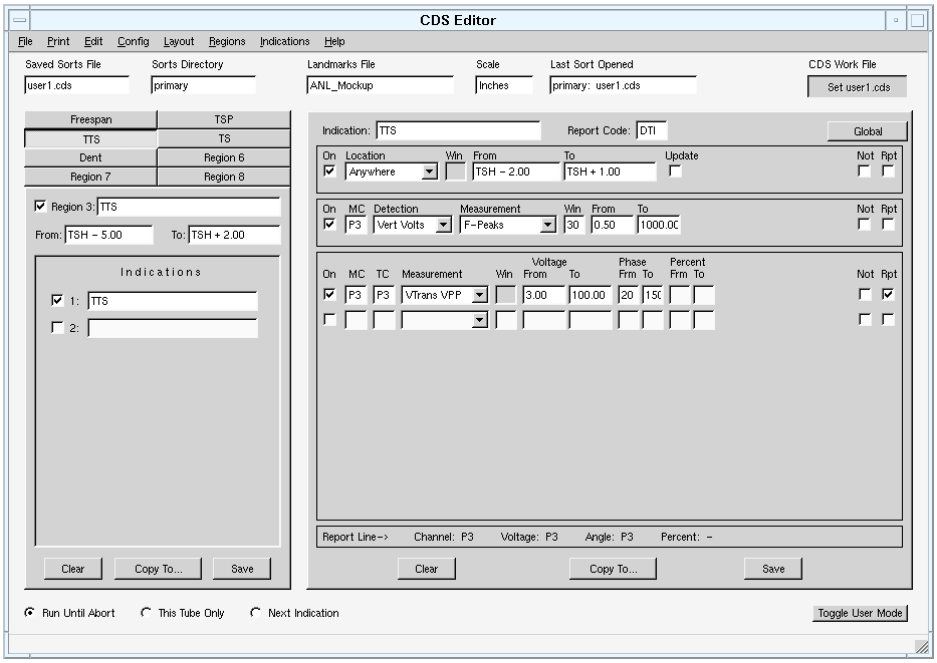

(b)

Figure 4.80 Display of the CDS editor dialog box for the setups used for screening of the tube-sheet level for (a) TS Indications and (b) TTS Indications.

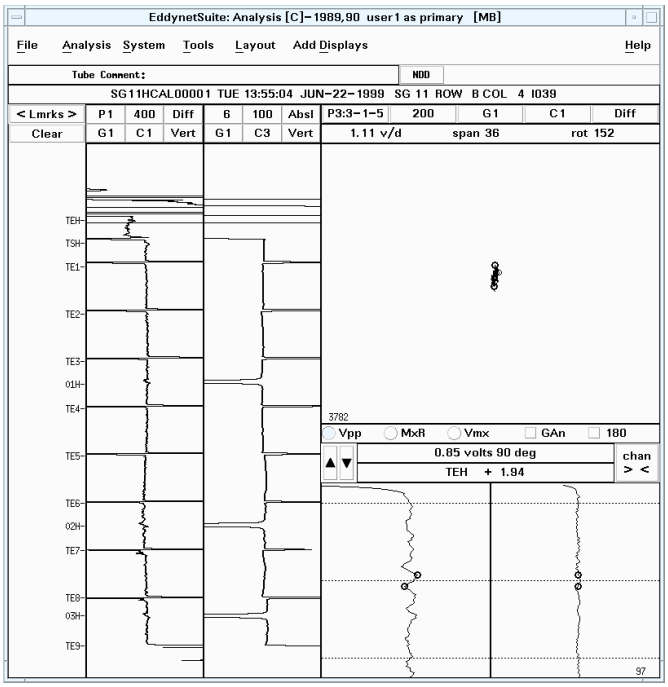

(a)

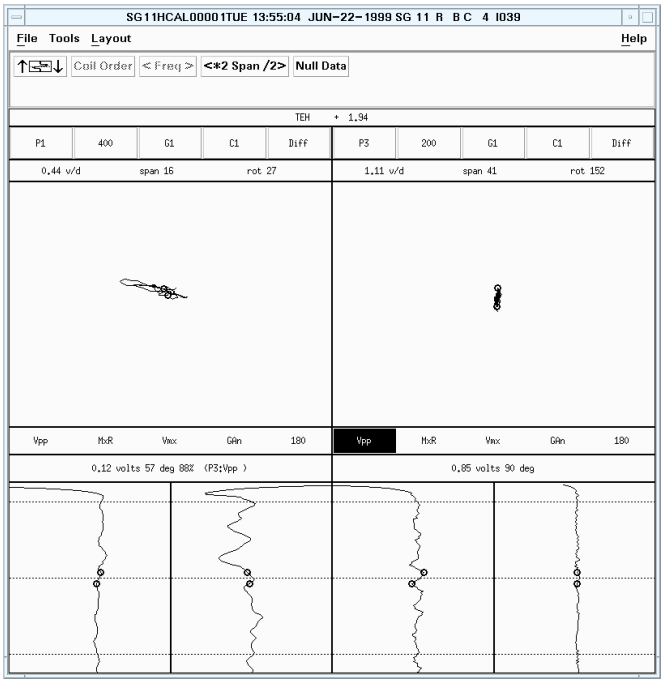

(b)

Figure 4.81 Display of bobbin coil inspection data (low baseline noise) peak-to-peak measurement of the baseline signal at an arbitrary TS location from (a) P3 in the main analysis window and (b) P1 and P3 in a multiple Lissajous display.

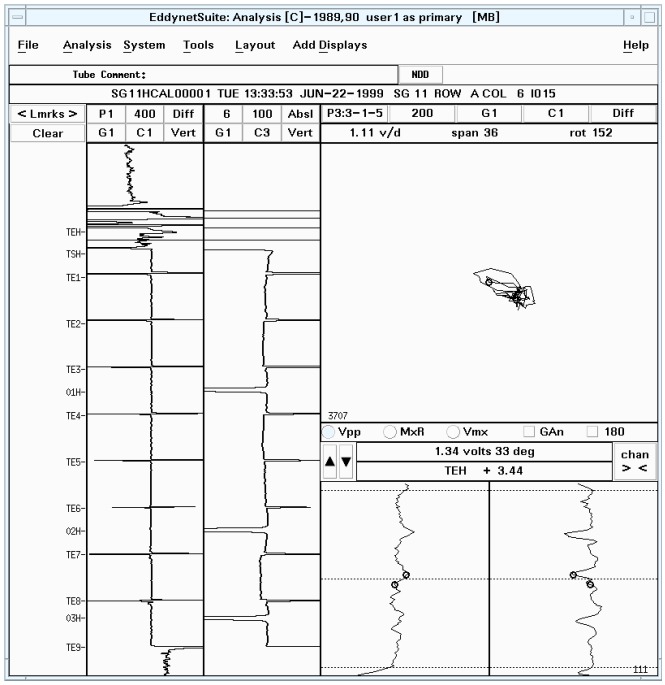

(a)

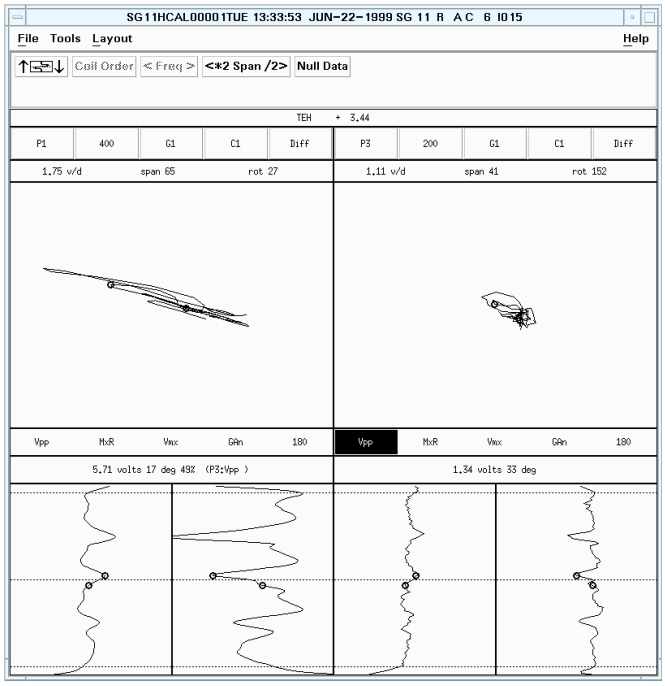

(b)

Figure 4.82 Display of bobbin coil inspection data (high baseline noise) peak-to-peak measurement of the baseline signal at an arbitrary TS location from (a) P3 in the main analysis window and (b) P1 and P3 in a multiple Lissajous display.

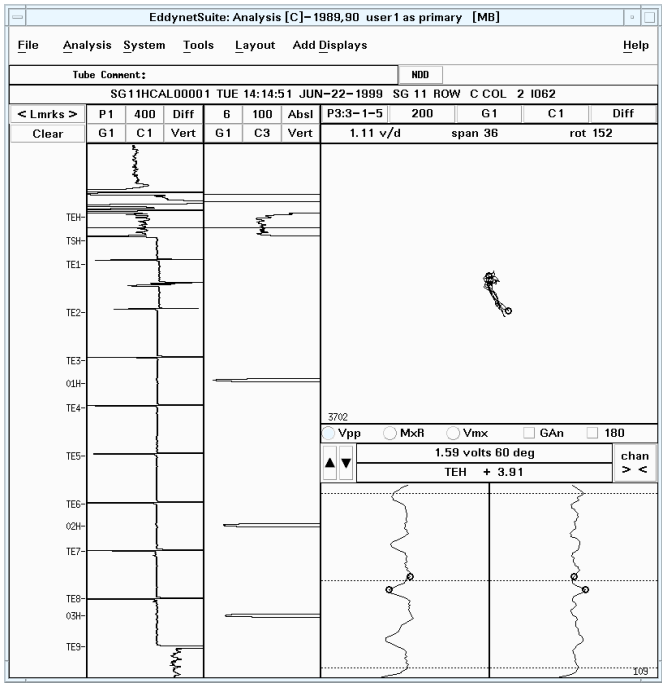

(a)

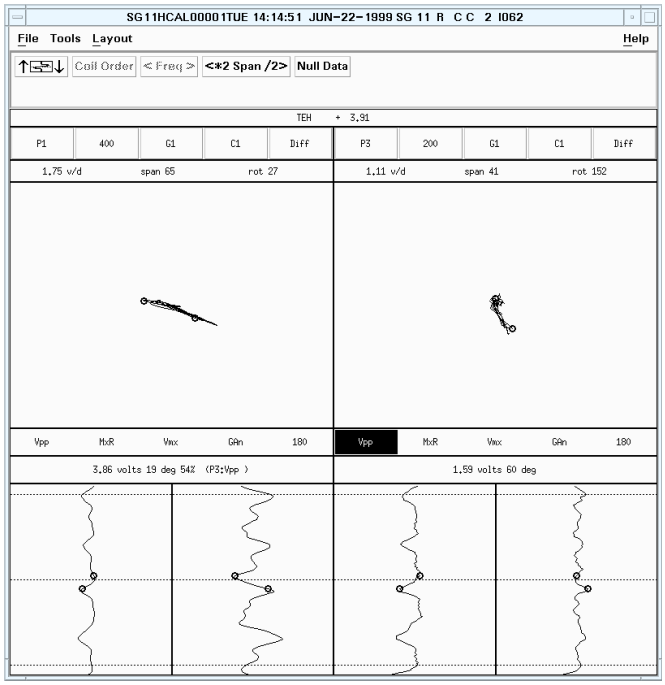

(b)

Figure 4.83 Display of bobbin coil inspection data (high baseline noise) peak-to-peak measurement of the baseline signal at an arbitrary TS location from (a) P3 in the main analysis window and (b) P1 and P3 in a multiple Lissajous display.

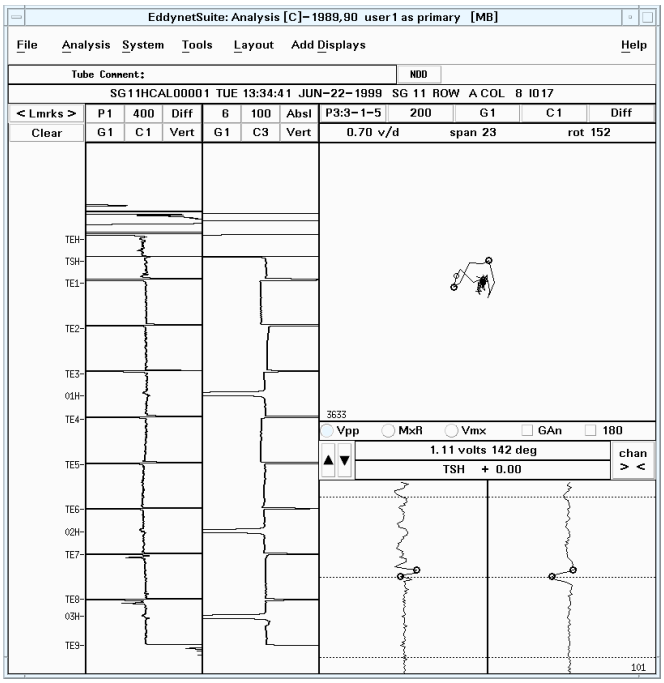

(a)

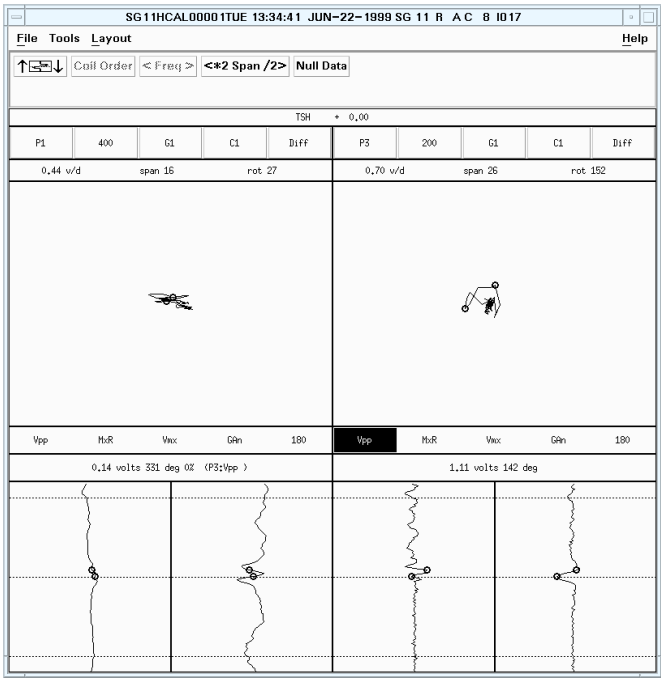

(b)

Figure 4.84 Display of bobbin coil inspection data (smooth expansion transition) peak-to-peak measurement of the residual expansion transition signal from (a) P3 in the main analysis window and (b) P1 and P3 in a multiple Lissajous display.

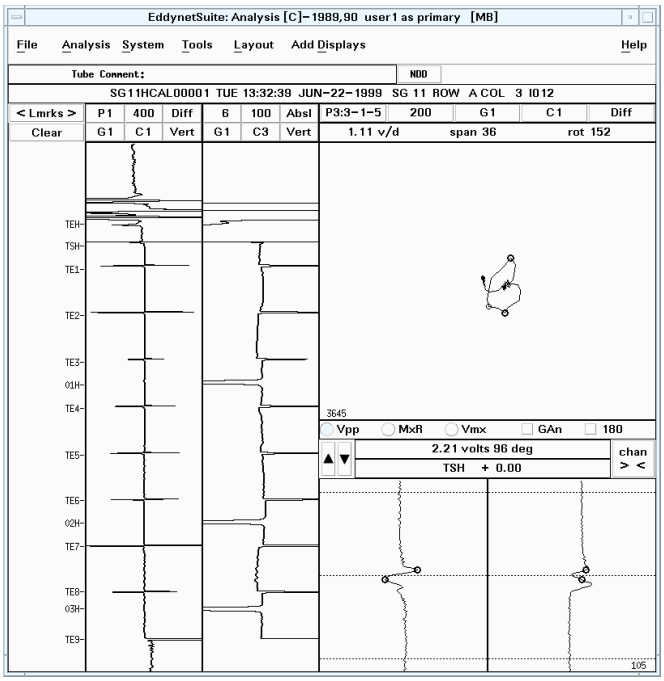

(a)

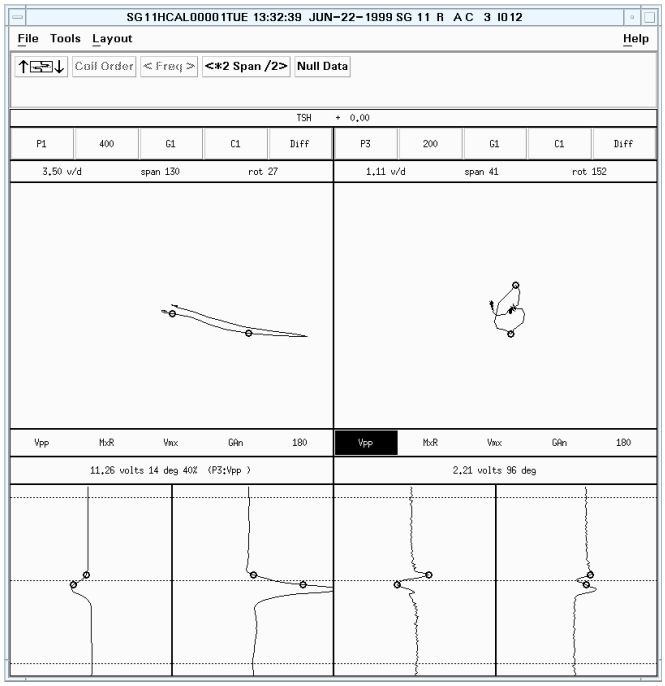

(b)

Figure 4.85 Display of bobbin coil inspection data (smooth expansion transition) peak-to-peak measurement of the residual expansion transition signal from (a) P3 in the main analysis window and (b) P1 and P3 in a multiple Lissajous display.

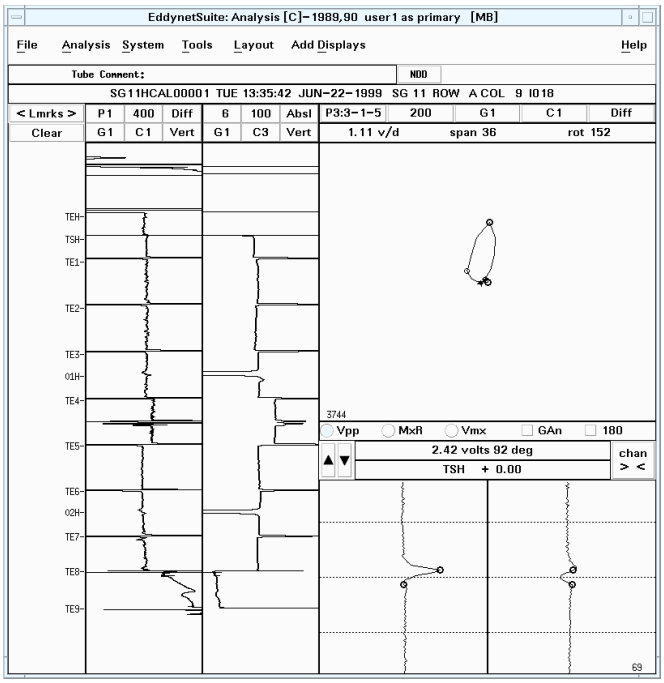

(a)

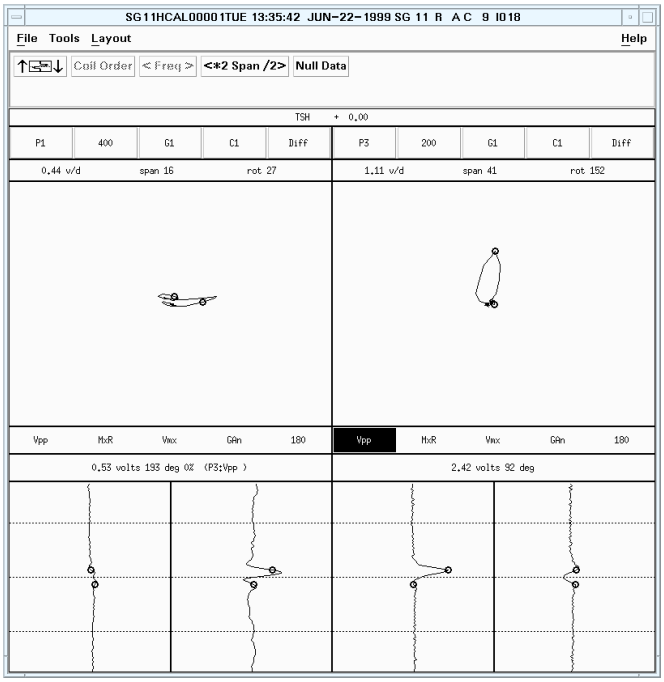

(b)

Figure 4.86 Display of bobbin coil inspection data (smooth expansion transition) peak-to-peak measurement of the residual expansion transition signal from (a) P3 in the main analysis window and (b) P1 and P3 in a multiple Lissajous display.

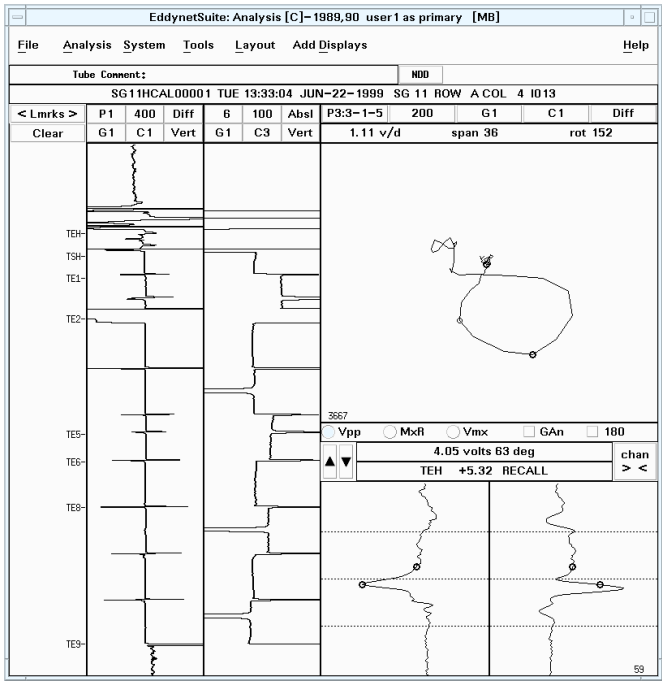

(a)

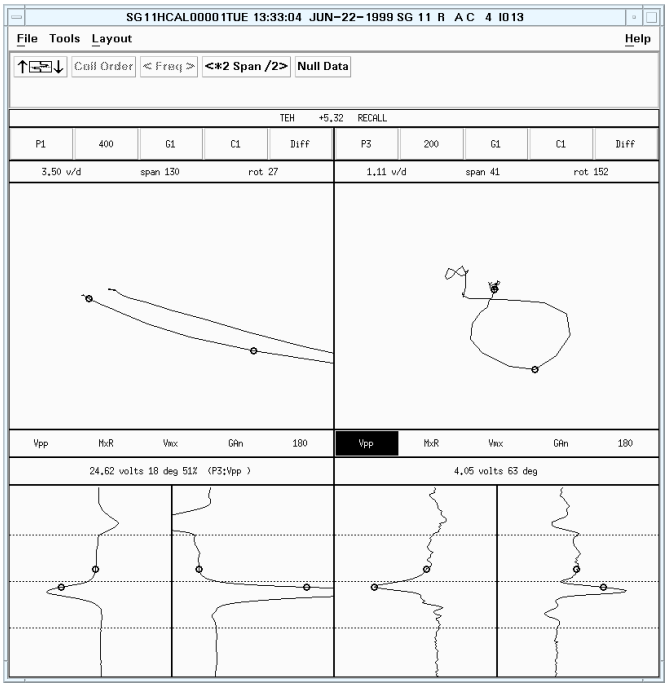

(b)

Figure 4.87 Display of CDS results from a representative TS level tube section (rough TTS expansion transition) from (a) P3 in the main analysis window and (b) P1 and P3 in a multiple Lissajous display.

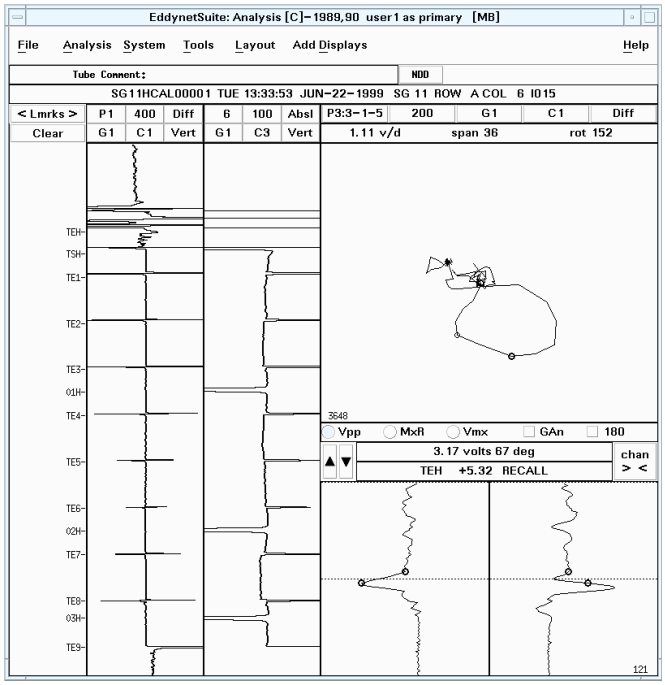

(a)

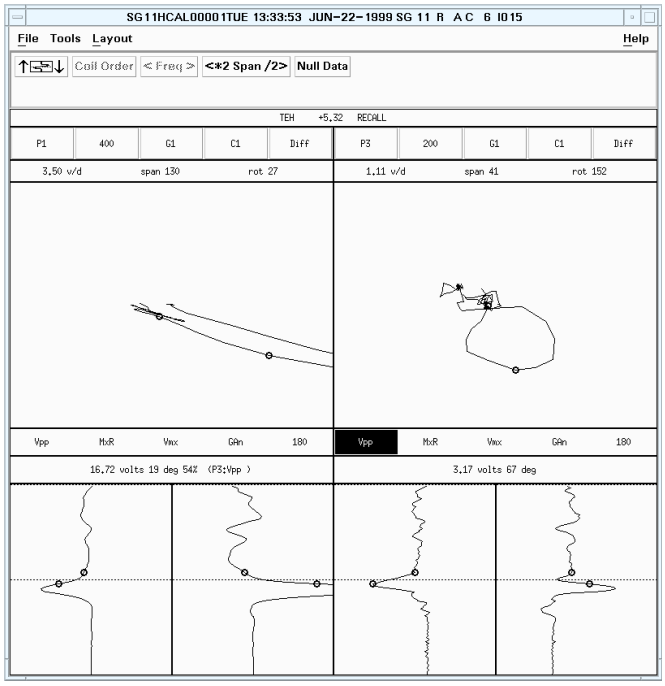

(b)

Figure 4.88 Display of CDS results from a representative TS level tube section (rough TTS expansion transition) from (a) P3 in the main analysis window and (b) P1 and P3 in a multiple Lissajous display.

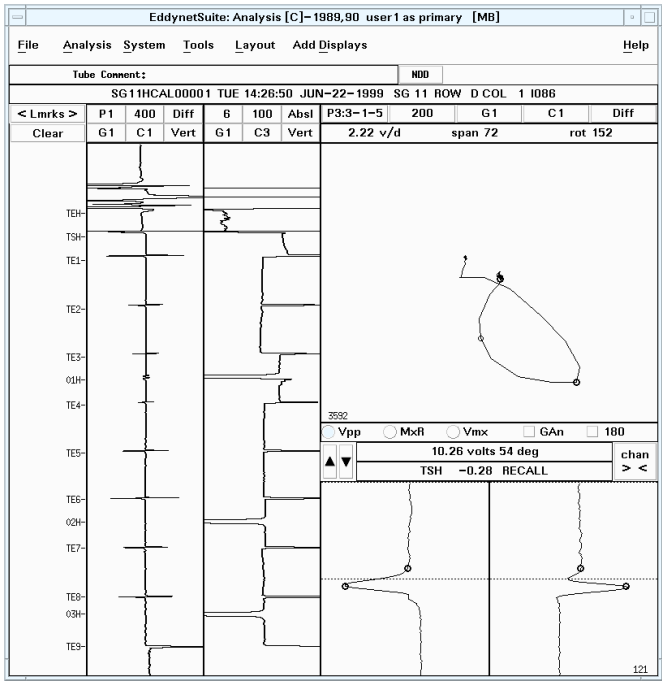

(a)

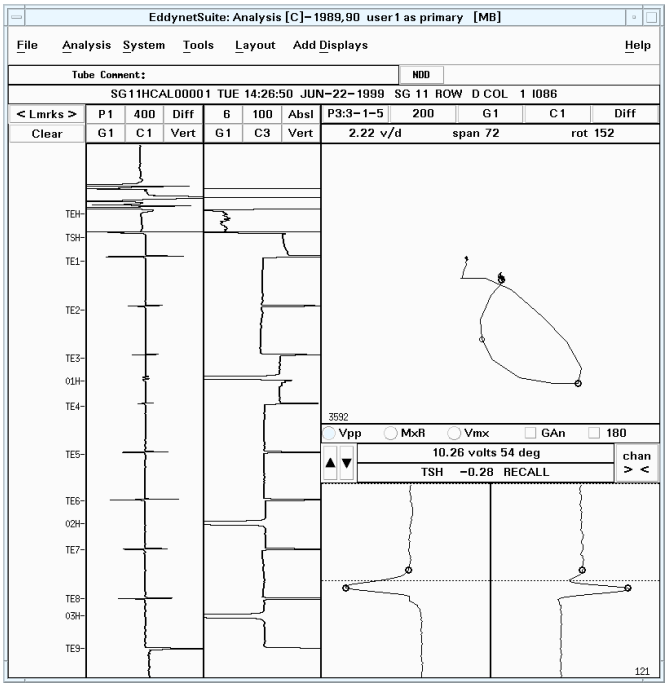

(b)

Figure 4.89 Display of CDS results from a representative TS level tube section (rough TTS expansion transition) from (a) P3 in the main analysis window and (b) P1 and P3 in a multiple Lissajous display.

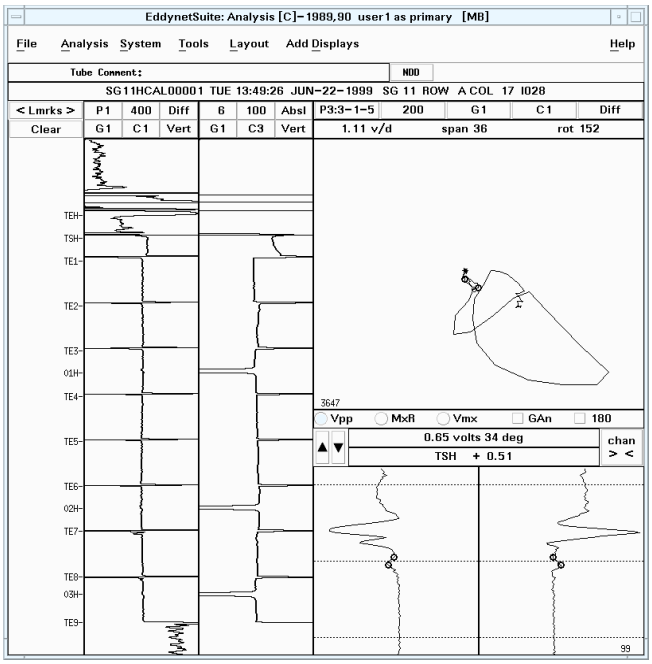

(a)

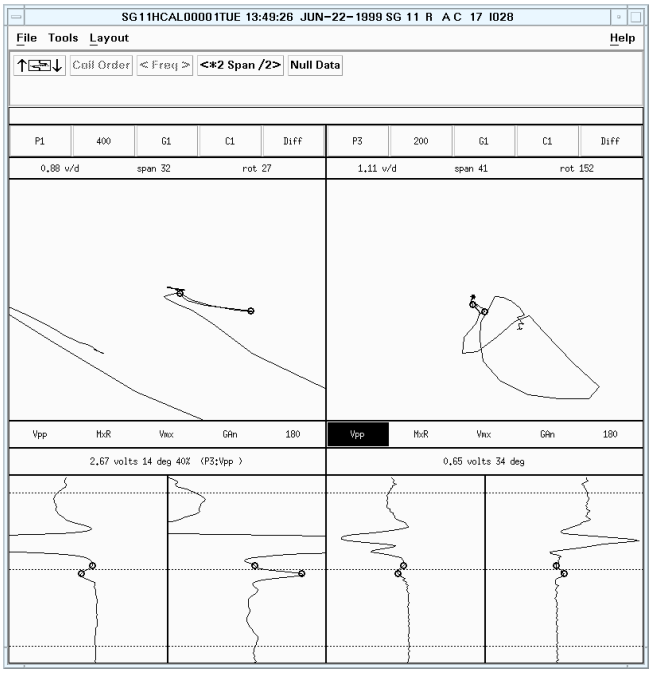

(b)

Figure 4.90 Display of manual data analysis results for a TS level tube section with a flaw near the expansion transition region in the (a) main analysis window and (b) in multiple Lissajous window at P1 and P3.

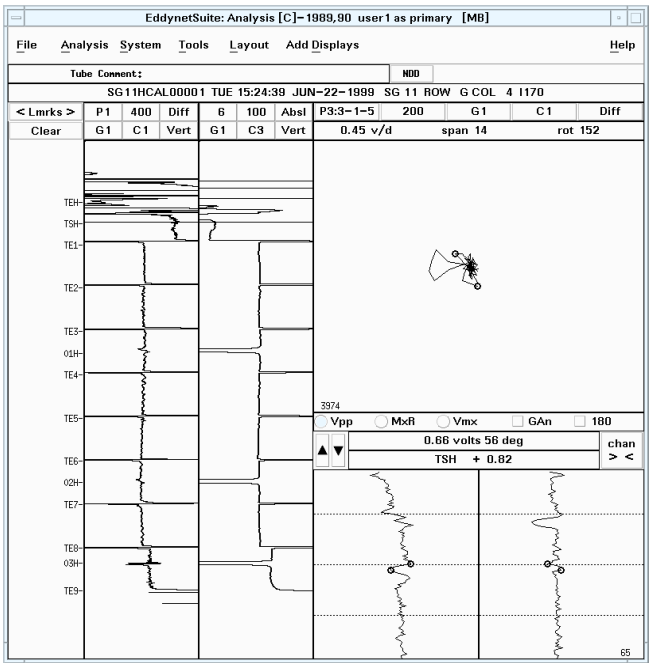

(a)

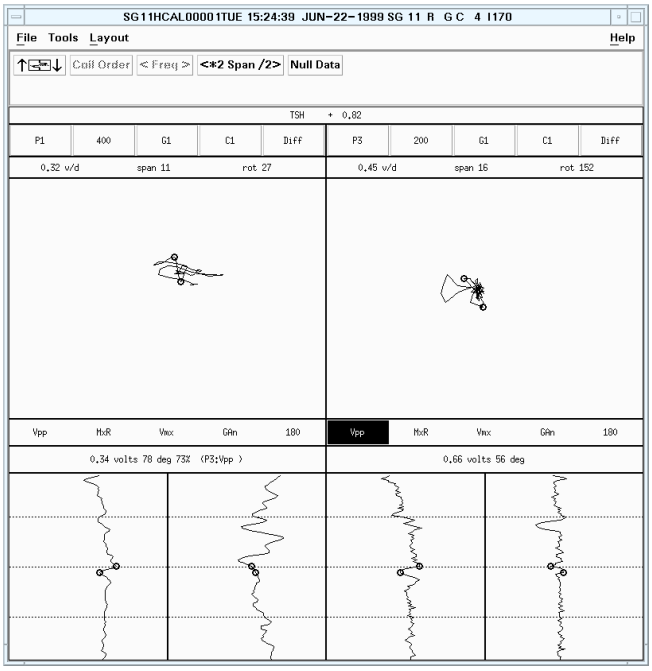

(b)

Figure 4.91 Display of manual data analysis results for a TS level tube section with a flaw near the TTS region in the (a) main analysis window and (b) in multiple Lissajous window at P1 and P3.

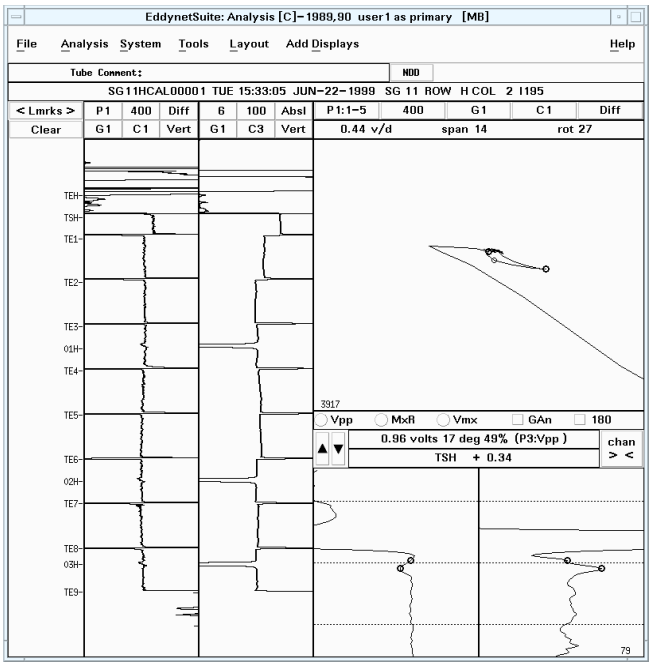

(a)

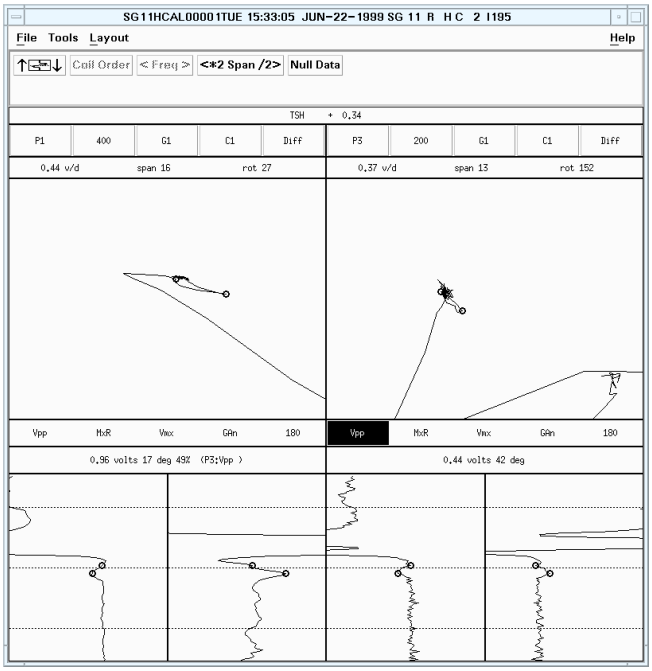

(b)

Figure 4.92 Display of manual data analysis results for a TS level tube section with a flaw near the expansion transition region in the (a) main analysis window and (b) in multiple Lissajous window at P1 and P3.

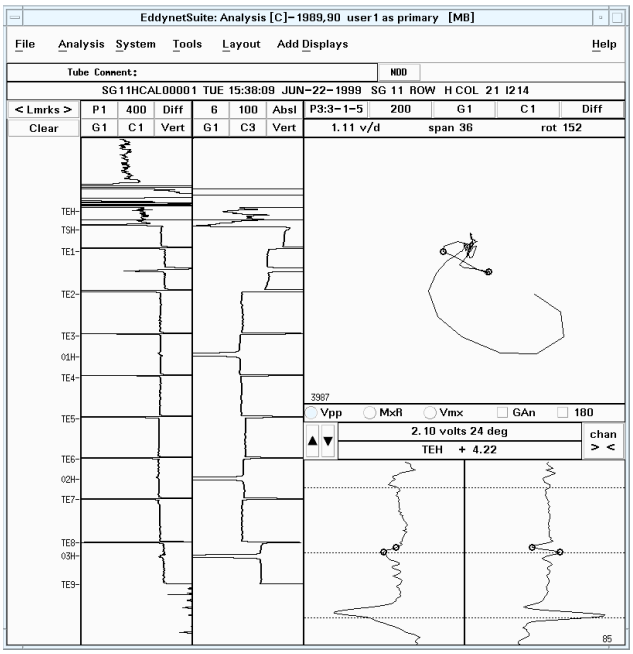

(a)

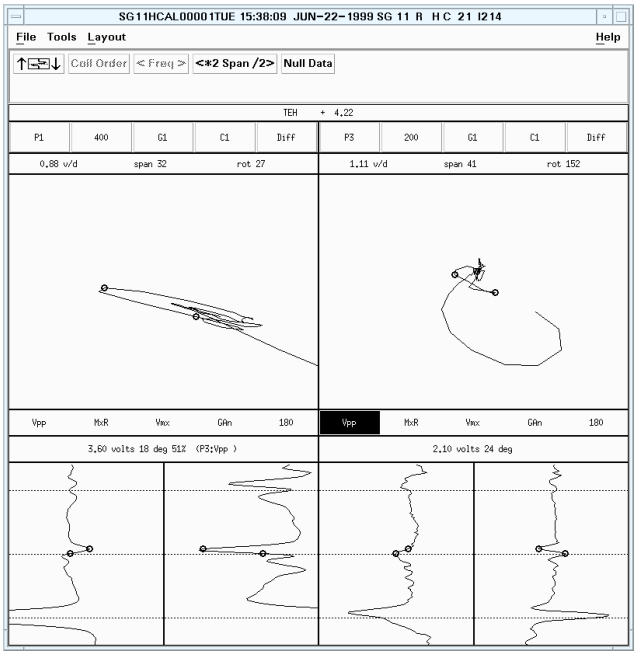

(b)

Figure 4.93 Display of manual data analysis results for a TS level tube section with a flaw below the TTS in the (a) main analysis window and (b) in multiple Lissajous window at P1 and P3.

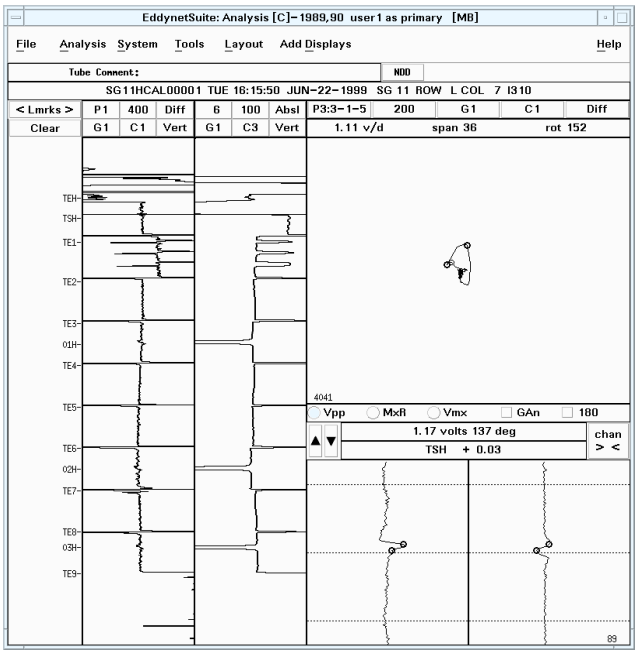

(a)

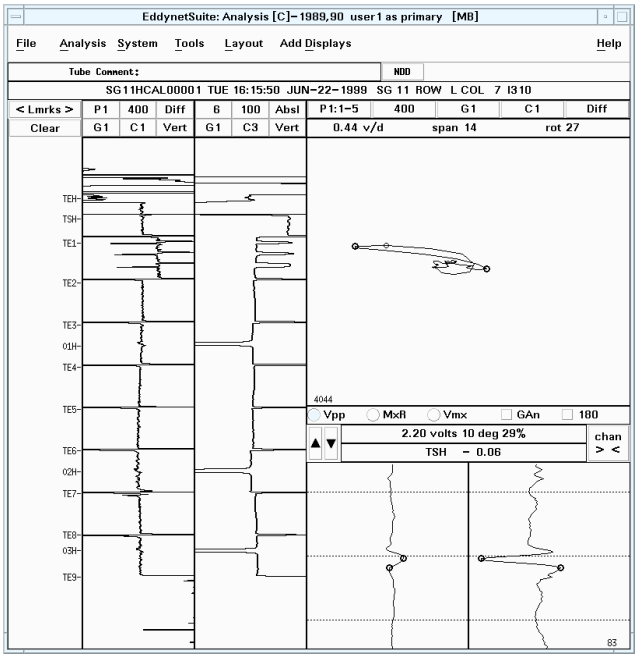

(b)

Figure 4.94 Display of manual data analysis results for a TS level tube section with a flaw below the TTS in the (a) main analysis window and (b) in multiple Lissajous window at P1 and P3.

5 SUMMARY AND CONCLUSIONS

Automated data analysis software may be employed during ISI of SG tubes as replacement for the primary, secondary, or both human analyst teams. The use of computerized data screening tools can improve the efficiency and consistency of data analysis. AA algorithms that employ threshold based detection and rule-based classification algorithms require access to a statistically significant database of representative signals to ensure reliable application. Optimization of setup parameters in general is a tradeoff between detection probability and false call rate. Better understanding of the test logic algorithms and the associated critical parameters as well as the intrinsic limitations of a particular inspection technique can help improve ISI reliability.

The results of evaluations performed at ANL on the application of industry-standard computerized data screening software to eddy current examination of SG tubes was presented. Following the initial review of the available literature, a prominent software-based tool, the Computer Data Screening (CDS™) module of the eddy current data analysis software Eddynet®Suite, from Zetec Inc., was acquired and used to automatically analyze bobbin probe data collected previously from the ANL-NRC SG tube bundle mock-up. Initially, a subset of that data was used for site-specific performance evaluations. The results of those initial tests were used to iteratively adjust the data screening parameters to further evaluate their influence on the detection and classification of signals. Alternative configurations of the screening parameters for different regions of the SG mock-up were further examined. The detection probability and false call rate were evaluated to help determine the influence of selected data screening parameters. The AA results in all cases were sorted out using Excel™ with special purpose macros generated at Argonne. The results of analyses performed on eddy current inspection data from different elevations of the SG mock-up was discussed.

Bobbin probe inspection data collected previously from all elevations (free-span, TSP, TS) of the SG mock-up were analyzed using the CDS program. Data from all free-span and TSP elevations were processed by CDS and the analysis results were subsequently used for comparative POD studies. Comparisons were made between the detection probability results based on automated analysis with that based on manual analysis of data from a previous round-robin exercise. Unlike the free-span and the TSP elevations, analysis of bobbin probe inspection data from TS sections was deemed unreliable due to excessive level of EC noise associated with the mechanical expansion of the tubes. It is worth noting that bobbin probe techniques are not generally considered reliable for detection and characterization of flaws in the TS region. As such, the CDS results for TS elevations of the SG mock-up were evaluated only in a qualitative manner. In general, the results of analyses based on bobbin probe inspection from the free-span and TSP elevations suggest that automated data screening tools can provide comparable or better detection capability than that achieved by manual analysis when comparatively higher false call rates are tolerated. The higher POD values by AA software were achieved through incorporation of multiple data screening setups for the same region of tubing. The results also suggest that, in comparison with other elevations of the SG mock-up, flaws near the TTS region may be detected with comparable probability to other elevations but with significantly higher false call rate. Some notable considerations regarding application of AA tools for SG tube examinations are summarized below.

A number of factors could affect the performance of conventional AA programs. More notable factors include inadequate or overly constrained algorithms, modification of previously qualified

setup parameters, data quality issues, influence of noise (low S/N), incomplete tube coverage, incorrect identification of support structures (landmarks), and inherent limitations of a particular NDE technique.

Intrinsic to the rule-based nature of expert system algorithms, the possibility of missing new or unexpected forms of degradation exists if representative signals are not included in the qualification database used for optimization of AA software. A comprehensive database of tubes that realistically represent the test conditions encountered during field examinations must be available to fully optimize data screening parameters. As such, direct application of screening parameters established based on a review of data in the AAPDD that are provided in generic ETSSs may not be appropriate for field implementation of AA tools. The qualification database for site-specific performance demonstrations should consist of representative tubes and the current level of EC noise present in a particular SG. The reliability of AA results could further be improved through inclusion of a larger number of potential flaw types from inactive damage mechanisms based on the operating history at plants with similar SG units. A more inclusive performance demonstration database would allow incorporation of complementary data screening algorithms to help increase the detection probability while allowing more robust optimization of data screening parameters to keep the overcall rate to a manageable number.

Automated data analysis algorithms for bobbin probe examinations are typically set to provide complete coverage of the entire tube length. Past experience with field application of AA software, however, suggests that coverage is one possible contributor to missing of relevant signals even when the detection algorithms are fully optimized. Flaw signals could be omitted if they are located within possible gaps between neighboring regions of a tube covered by separate data screening configurations. A conservative approach to ensure continuous coverage is to have some overlap between adjacent data screening regions. Additionally, the measurement window size (when applicable) should be adjusted to ensure that signals, particularly those located near the interface between two regions of interest, are properly captured. Unintentional errors associated with improper assignment of data acquisition direction (positive/negative) could potentially lead to incorrect setting of the coverage by a particular data screening configuration. It is worth noting that, availability of a visual display that would automatically provide information about the extent of coverage could help reduce the possibility of leaving gaps in the EC inspection data.

Conventional AA tools commonly employ location-dependent data analysis algorithms. Correct identification of landmarks (hot/cold leg tube ends, tube support structures, dimensional/geometry transitions, etc.) in a particular SG design is therefore critical to their proper operation. Identification and labeling of landmarks in a SG is typically performed in an automated manner. When performed automatically, the positional scaling is done based on data sampling rate obtained using the probe speed and the acquisition digitization rate **(Refs. 1, 6)**. Variations in probe speed and in turn the sampling rate could lead to small variations in axial scaling of data. This could result in small variations in locating the landmarks using the automatic landmark detection algorithm. More elaborate error checking capability could help with detecting such problems and in turn with identifying the source of discrepancy when the calculated positional information does not precisely match with the information provided in the SG landmark table. The AA process may only be allowed to continue once the landmark labels are corrected either manually or by making necessary adjustments to automatically located SG landmarks. The possibility, however, exists for AA software to process the data from a SG tube with mislabeled or omitted landmarks. This can result in improper application of location-

dependent algorithms and consequently missing of reportable signals. The same problem could also affect screening of data from SG tubes with displaced landmarks. Finally, as noted above, unintentional errors associated with improper assignment of data acquisition direction could lead to incorrect labeling of landmarks.

Although AA algorithms could be optimized to provide improved detection capability over manual analysis, the possibility exists for visually discernable signals to go undetected using automated data screening tools. Some leading factors that could result in unintended errors when using AA tools were discussed above. With stringent oversight, the automated data analysis process can help improve the reliability of ISI results. This is an important consideration when AA tools are discussed as potential replacement for both the primary and the secondary analyst team. Inclusion of manual analysis as an integral part of the ISI data analysis process can both help resolve potential discrepancies between independent AA tools and between reported redundant entries by alternative or overlapping data screening configurations of the same AA tool. Incorporation of adjustments to the measured signals by AA algorithms may also be necessary particularly when alternate repair criteria are implemented.

6 REFERENCES

1. Pressurized Water Reactor Steam Generator Examination Guidelines: Revision 7, Requirements, Electric Power Research Institute, Palo Alto, CA (2006).

2. D. S. Kupperman, S. Bakhtiari, W. J. Shack, J. Y. Park, and S. Majumdar, Eddy Current Reliability Results from the Steam Generator Mock-up Analysis Round-Robin: Revision 1, NUREG/CR–6791 Rev.1, ANL-08/30, U.S. Nuclear Regulatory Commission, Washington, DC (2009).

3. D. S. Kupperman, S. Bakhtiari, W. J. Shack, J. Y. Park, and S. Majumdar, Evaluation of Eddy Current Reliability from Steam Generator Mock–Up Round Robin, NUREG/CR-6785, ANL–01/22, U.S. Nuclear Regulatory Commission, Washington, DC (2002).

4. Computer Data Screening User Guide, Eddynet®Suite, Zetec Inc., Jan. 2008.

5. S. Bakhtiari and D. S. Kupperman, Effect on Eddy Current Qualification of Varying Parameters in Examination Technique Specification Sheets, Technical Letter Report, U.S. Nuclear Regulatory Commission, Washington, DC (2009).

6. S. Bakhtiari, D. S. Kupperman, and W. J. Shack, Assessment of Noise Level for Eddy Current Inspection of Steam Generator Tubes, NUREG/CR-6982, ANL-05/44, U.S. Nuclear Regulatory Commission, Washington, DC (2009).

NRC FORM 335
(12-2010)
NRCMD 3.7

U.S. NUCLEAR REGULATORY COMMISSION

BIBLIOGRAPHIC DATA SHEET

(See instructions on the reverse)

1. REPORT NUMBER
(Assigned by NRC, Add Vol., Supp., Rev., and Addendum Numbers, if any.)
NUREG/CR-7217

2. TITLE AND SUBTITLE
Application of Automated Analysis Software to Eddy Current Inspection Data from Steam Generator Tube Bundle Mock-up

3. DATE REPORT PUBLISHED

MONTH	YEAR
September	2016

4. FIN OR GRANT NUMBER
Y6582

5. AUTHOR(S)
Sasan Bakhtiari, William J. Shack, Thomas W. Elmer

6. TYPE OF REPORT
Technical

7. PERIOD COVERED (Inclusive Dates)

8. PERFORMING ORGANIZATION - NAME AND ADDRESS (If NRC, provide Division, Office or Region, U. S. Nuclear Regulatory Commission, and mailing address; if contractor, provide name and mailing address.)
Argonne National Laboratory
Argonne, IL 60439

9. SPONSORING ORGANIZATION - NAME AND ADDRESS (If NRC, type "Same as above", if contractor, provide NRC Division, Office or Region, U. S. Nuclear Regulatory Commission, and mailing address.)
Division of Engineering
Office of Nuclear Regulatory Research
U.S. Nuclear Regulatory Commission
Washington, DC 20555

10. SUPPLEMENTARY NOTES

11. ABSTRACT (200 words or less)
This report includes evaluation of computerized data screening software used for analyzing eddy current data obtained during steam generator inspection. Following initial review of the available literature, a software-based tool widely used by industry was acquired and used to analyze previously collected bobbin probe data. A subset of this data was used to establish screening parameters, and the results of those tests were used to iteratively adjust the screening parameters to further evaluate their influence on the detection and classification of signals. Alternative configurations of the data screening parameters for regions of the steam generator mock-up were further examined. The automated analysis software performance was evaluated based on the detection probability and false call rate. For this work, Argonne generated special-purpose algorithms to sort the data in each configuration. Some general marks are included regarding advantages and limitations of conventional automated data analysis programs for in-service inspections of steam generator tubes based on bobbin probe examinations.

12. KEY WORDS/DESCRIPTORS (List words or phrases that will assist researchers in locating the report.)
PWR
steam generator (SG)
steam generator tube
steam generator inspection
eddy current testing
nondestructive evaluation

13. AVAILABILITY STATEMENT
unlimited

14. SECURITY CLASSIFICATION
(This Page)
unclassified
(This Report)
unclassified

15. NUMBER OF PAGES

16. PRICE

Federal Recycling Program

UNITED STATES
NUCLEAR REGULATORY COMMISSION
WASHINGTON, DC 20555-0001

OFFICIAL BUSINESS

NUREG/CR-7217

Application of Automated Analysis Software to Eddy Current Inspection Data from Steam Generator Tube Bundle Mock-up

September 2016